# DEFENCE S&T TECHNICAL BULLETIN

VOL. 17 NUM. 2 YEAR 2024 eISSN 3009-1896

# CONTENTS



Ministry of Defence Malaysia

SCIENCE & TECHNOLOGY RESEARCH INSTITUTE FOR DEFENCE (STRIDE)

**Published by:**

Science & Technology Research Institute for Defence (STRIDE)
Taman Bukit Mewah Fasa 9, 43000 Kajang, Selangor, Malaysia
Email: dinesh.sathyamoorthy@stride.gov.my / mahdi.cheisa@stride.gov.my
Tel.: +603-8732 4400

The Defence S&T Technical Bulletin is published biannually.

eISSN 3009-1896

## AIMS AND SCOPE

The Defence S&T Technical Bulletin is the official journal of the Science & Technology Research Institute for Defence (STRIDE). The journal, which is indexed in, among others, Scopus, Index Corpenicus, ProQuest and EBSCO, contains manuscripts on research findings in various fields of defence science & technology. The primary purpose of this journal is to act as a channel for the publication of defence-based research work undertaken by researchers both within and outside the country.

## WRITING FOR THE DEFENCE S&T TECHNICAL BULLETIN

Contributions to the journal should be based on original research in areas related to defence science & technology. All contributions should be in English.

## PUBLICATION

The editors' decision with regard to publication of any item is final. A manuscript is accepted on the understanding that it is an original piece of work that has not been accepted for publication elsewhere.

## PRESENTATION OF MANUSCRIPTS

The format of the manuscript is as follows:

a) Page size A4
b) MS Word format
c) Single space
d) Justified
e) In Times New Roman, 11-point font
f) Should not exceed 15 pages, including references
g) Texts in charts and tables should be in 10-point font.

Please email the manuscript to:

1) Gs. Dr. Dinesh Sathyamoorthy (dinesh.sathyamoorthy@stride.gov.my)
2) Dr. Mahdi bin Che Isa (mahdi.cheisa@stride.gov.my)

The next edition of the journal (Vol. 18, Num. 1) is expected to be published in April 2025. The due date for submissions is 8 January 2025. **It is strongly iterated that authors are solely responsible for taking the necessary steps to ensure that the submitted manuscripts do not contain confidential or sensitive material.**

The template of the manuscript is as follows:

# TITLE OF MANUSCRIPT

Name(s) of author(s)

Affiliation(s)

Email:

## ABSTRACT

*Contents of abstract.*

**Keywords:** *Keyword 1; keyword 2; keyword 3; keyword 4; keyword 5.*

## 1. TOPIC 1

Paragraph 1.

Paragraph 2.

### 1.1 Sub Topic 1

Paragraph 1.

Paragraph 2.

## 2. TOPIC 2

Paragraph 1.

Paragraph 2.

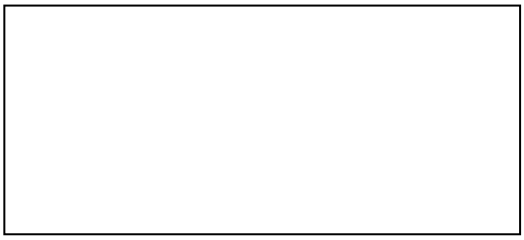

**Figure 1: Title of figure.**

**Table 1: Title of table.**

| **Content** | **Content** | **Content** |
|---|---|---|
| Content | Content | Content |
| Content | Content | Content |
| Content | Content | Content |

Equation 1 (1)
Equation 2 (2)

**REFERENCES**

Long lists of notes of bibliographical references are generally not required. The method of citing references in the text is ‘name date’ style, e.g. ‘Hanis (1993) claimed that...’, or ‘…including the lack of interoperability (Bohara *et al.*, 2003)’. End references should be in alphabetical order. The following reference style is to be adhered to:

Books

Serra, J. (1982). *Image Analysis and Mathematical Morphology*. Academic Press, London.

Book Chapters

Goodchild, M.F. & Quattrochi, D.A. (1997). Scale, multiscaling, remote sensing and GIS. *In* Quattrochi, D.A. & Goodchild, M.F. (Eds.), *Scale in Remote Sensing and GIS*. Lewis Publishers, Boca Raton, Florida, pp. 1-11.

Journals / Serials

Jang, B.K. & Chin, R.T. (1990). Analysis of thinning algorithms using mathematical morphology. *IEEE T. Pattern Anal.*, **12**: 541-550.

Online Sources

GTOPO30 (1996). *GTOPO30: Global 30 Arc Second Elevation Data Set*. Available online at: http://edcwww.cr.usgs.gov/landdaac/gtopo30/gtopo30.html (Last access date: 1 June 2009).

Unpublished Materials (e.g. theses, reports and documents)

Wood, J. (1996). *The Geomorphological Characterization of Digital Elevation Models*. PhD Thesis, Department of Geography, University of Leicester, Leicester.

# NON-DESTRUCTIVE TESTING OF SOLID PROPELLANTS: A REVIEW OF METHODS AND APPLICATIONS

Mohd Moesli Muhammad[1*], Mahdi Che Isa[1], Mohd Subhi Din Yati[1], Nik Hassanuddin Nik Yusoff[1], Azmahani Sulaiman[1], Muhammad Izzamir Firdaus Idris[1], Azmi Minal[2], Muhammad Arifin Ares[2] & Fikri Abdul Rasih[2]

[1]Marine Materials Research Group, Maritime Technology Division (BTM)
[2]Weapon Technology Division (BTP)
Science & Technology Research Institute for Defence (STRIDE), Ministry of Defence, Malaysia

[*]Email: moesli.muhammad@stride.gov.my

## ABSTRACT

*This paper discusses the complexities of non-destructive testing (NDT) for solid propellants in rocket motors, emphasising on the significance and evolution of various inspection techniques. It addresses the challenges associated with different propellant types and the inherent difficulties in defect detection. By highlighting recent advancements in digital methodologies and automated defect recognition (ADR), the study underscores the critical role of NDT in ensuring the safety and effectiveness of rocket motors, and points towards future technological trends and research needs. Given the crucial role of solid rocket motors in aerospace and defence, their inspection is paramount. Traditional methods, such as visual inspection (VI), have been essential for identifying surface defects such as cracks and debonding, though they are limited to surface anomalies. Advancements in radiographic testing, including conventional and digital radiography, have improved the detection of internal flaws such as voids, porosity, foreign objects or inclusions, and cracks. Digital radiography, utilising computed radiography (CR) and digital detector arrays (DDA), provides superior resolution and faster imaging, making it invaluable for detailed inspections. Ultrasonic testing (UT) has been instrumental, with pulse echo and through-transmission methods offering insights into internal discontinuities and bonding integrity. UT methods, particularly through-transmission, avoid contamination from couplants and are suitable for automated scanning. Shearography, using laser light to detect surface and subsurface defects, offers real-time feedback and quantitative analysis, particularly for detecting debonding and improper adhesion. Industrial computed tomography (ICT) provides high-resolution three-dimensional imaging, crucial for identifying structural abnormalities and ensuring propellant integrity, although it is challenged by high costs and operational complexity. Laser scanning thermography (LasST) generates detailed thermal maps to identify defects and material inconsistencies, making it suitable for in-line inspections during manufacturing. Recent advancements in NDT include integrating artificial intelligence (AI) and machine learning (ML) for ADR, enhancing defect detection, reducing human error, and supporting predictive maintenance. However, these technologies face challenges such as high costs, the need for specialised skills and the complexity of integration with existing methods. The future of NDT for solid propellants lies in developing cost-effective methods, standardised procedures, and portable equipment for on-site inspections. Embracing AI and ML will further automate and improve defect analysis, ensuring higher safety and performance standards for solid rocket motors.*

**Keywords:** *Non-destructive testing (NDT); solid propellants; defect detection; inspection challenges; artificial intelligence (AI) and machine learning (ML).*

## 1. INTRODUCTION

Solid propellants are energetic materials that can store substantial chemical energy, which is released through self-sustaining reactions that do not require additional oxygen. These propellants have diverse applications, including pyrotechnics, high explosives, as well as propellants for guns, missiles and rockets. They play a crucial role in rocket motor combustion, propelling missiles or rockets over specified distances and ranges. Upon ignition, the propellant's exposed surface starts to burn, sustaining combustion within a confined chamber without the need for additional oxygen. The resulting combustion gases accumulate in the chamber and, once sufficiently pressurised, are released through the nozzle, generating thrust that propels the missile forward. A notable characteristic of these propellants is their inability to be extinguished or restored once ignited. This feature is essential for the missile's functionality, ensuring continuous propulsion once launched (Elghafour *et al*., 2018; Courty *et al*., 2021).

Quality management and inspection of solid propellants are essential for ensuring their safety during storage and use. Traditionally, some inspection methods are destructive, involving the removal of rocket motors and conducting mechanical tests on small samples of the propellant. Visual inspections assess the condition of the grain, cylinder and structural integrity of the propellant. Chemical analysis is also performed to evaluate the stability of the propellant and ensure its composition remains stable without adverse reactions to the environment (Elbasuney *et al.*, 2018). Periodic inspections, including destructive testing, require dismantling missiles or rockets, rendering them unusable for these tests. Samples are typically drawn from a batch and assumed to represent the overall condition of the batch, but they may not always accurately reflect the condition of each individual missile or rocket. These destructive methods are costly, and the results, when applied to the entire batch, necessitate a large safety margin for a significant portion of the batch (Bai *et al.,* 2019).

In the high-stakes realm of aerospace and defence, maintaining the integrity of solid rocket motors is critical. Non-destructive testing (NDT) has emerged as an essential technique, offering a comprehensive view of the internal condition of these motors without compromising their structure. An important advantage of NDT is its ability to be conducted without dismantling the components, allowing for the inspection of rockets and motors that are still in service (Zhirnov *et al*., 2021). This aspect not only conserves resources but also ensures the continuous assessment of operational equipment. Far from being merely precautionary, NDT is a vital practice for identifying potential defects that could lead to catastrophic outcomes (Jin *et al*., 2022). The methodologies of NDT have evolved significantly, adapting to the complex nature of solid propellants. Each method, from ultrasonic testing to sophisticated radiography, provides unique insights crucial for ensuring that solid rocket motors meet the rigorous safety and performance standards required in their applications (Genov *et al.,* 2019).

This paper explores the complexities of NDT techniques as applied to solid rocket motor inspections. The objectives include reviewing the different types of propellants and their common defects, as well as highlighting the critical role of various NDT methods in detecting these defects. The paper also discusses on significant challenges, such as high costs, as well as environmental and handling factors, that complicate inspections. Furthermore, it highlights recent advancements in technology, including the integration of artificial intelligence (AI) and machine learning (ML), which enhanced defect detection and analysis capabilities. The paper outlines future directions for NDT, emphasising the development of more sophisticated and cost-effective methods, the establishment of standardised procedures, as well as the adoption of portable and wireless equipment for on-site inspections. By examining these critical points, this paper aims to provide a comprehensive understanding of the current landscape and future potential of NDT in ensuring the safety and reliability of solid rocket motors.

## 2. TYPE OF SOLID PROPELLANTS

Solid propellants are categorised by their composition, physical form and burning characteristics (Sutton & Biblarz, 2010). There are two main types, which are homogeneous or colloidal, and heterogeneous or composite. Homogeneous propellants, such as single-base (nitrocellulose) and double-base (nitrocellulose with nitroglycerin), are uniform in composition and often include additives for stability and performance enhancement (Lysien *et al*., 2021). These propellants are shaped using extrusion or casting methods and find use in small arms and specific rocket applications due to their predictable burning rates (Cooper & Kurowski, 2016). Heterogeneous or composite propellants consist of binder or fuel matrix (e.g., hydroxy-terminated polybutadiene and castor oil), and oxidiser particles (e.g., ammonium perchlorate), offering adaptable burning rates and high energy release for large-scale rocket applications (Yakovlev, 2018; Liu *et al*., 2023). Recent developments focus on environmentally friendly formulations, such as those based on ammonium dinitramide (ADN), addressing concerns such as toxicity and ozone depletion (Turner & Stowe, 2021).

The physical form of solid propellants significantly influences their burning behaviour. Common geometries include cylindrical, tubular, star-shaped, cruciform, multi-perforated and anchor designs (Figure 1). These shapes control the surface area exposed to combustion, thereby dictating the thrust profile. For instance, star-shaped grains provide a larger surface area, leading to higher initial thrust, which then decreases as the star points recede (Sutton & Biblarz, 2010). The burning rate of solid propellants is a crucial factor in rocket performance, controlled by both the grain geometry and chemical composition of the propellant. Typically, the burning pattern progresses from the inner surfaces outward, influenced by the grain shape. Innovations in grain design aim to achieve more controlled and efficient burning patterns, tailored to specific mission requirements (Cooper & Kurowski, 2016). The burning pattern of the grain can be categorised into three types: neutral, which maintains a constant burning surface and consistent thrust; progressive, which features an increasing burning surface and ascending thrust curve; and regressive, which has a decreasing burning surface and descending thrust curve (Dîrloman *et al*., 2020; Alexander *et al*., 2024).

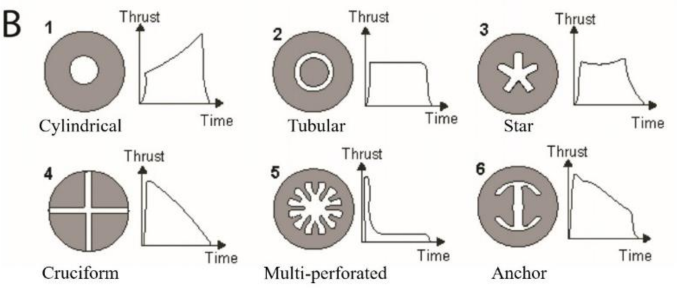


**Figure 1: Various shapes of solid propellants with the corresponding thrust patterns.**
**Source: Korompili *et al.* (2024)**

## 3. TYPES OF SOLID PROPELLENT DEFECTS

Propellant faults in solid rocket motors can significantly affect both performance and safety. These defects can notably impact the interior ballistic performance of a thruster, potentially causing the combustion chamber pressure and thrust deviation to exceed required limits. This can result in excessive burning surface and potential premature failure, which can negatively affect the thruster's performance and even lead to an explosion (Manson & Roland, 2019). The faults can be primarily categorised as grain defects and surface debonding. Grain defects are related to issues within the solid propellant, while bonding defects are linked to debonding at the propellant bonding interface and the presence of inclusions. Common flaws include voids, porosity, foreign inclusions, cracks, debonding and inadequate adhesion (Rong *et al.,* 2022).

### 3.1 Voids and Porosity

Voids and porosity play a crucial role in the performance and reliability of solid propellants, significantly impacting both combustion properties and structural strength. Voids, which are air-filled spaces within the solid propellant, can range from tiny to several millimetres in diameter. These voids may arise from various manufacturing process characteristics, such as suboptimal mixing, inadequate gas elimination and uneven solidification rates. Additionally, the inherent properties of the propellant components may lead to the formation of vacant areas. Voids can be categorised into surface and interior voids, and further classified based on size into microscopic or macroscopic. According to Li *et al*.

(2014), the presence of voids can significantly alter the rate of propellant combustion, leading to unpredictable and inefficient burning. This diminishes the resilience of the propellant grain, increasing the likelihood of fracturing and raising the danger of accidents due to unpredictable combustion patterns and heightened susceptibility to external effects. Addressing these challenges requires a comprehensive strategy focusing on improving manufacturing techniques to minimise voids, implementing stringent quality control measures for early detection, and exploring new compositions and predictive modelling methods to mitigate the adverse effects of voids on propellant performance (Ponti *et al.*, 2021).

Porosity refers to the condition of having many small pores or empty spaces within a substance, which might be filled with gas or be empty. These pores significantly impact the physical properties and combustion characteristics of the propellant. Pores in solid propellants primarily result from the production process and are influenced by factors such as mixing methods, curing conditions and compatibility of propellant constituents (binder, oxidiser, fuel, etc.). Environmental factors, including temperature and humidity during storage, can also influence porosity (Bekhouche *et al*., 2016; Mezroua *et al.*, 2016). Greater porosity can result in elevated burn rate due to increased surface area exposed to combustion. However, this can also lead to erratic and less manageable burn patterns, potentially undermining the reliability of the propulsion system. High porosity adversely affects the structural integrity of the propellant, making it more susceptible to mechanical stresses and probable fracture. In severe cases, this can result in catastrophic failure during operation (Naseem *et al*., 2019).

Understanding and managing voids and porosity are essential for maximising the efficiency of solid propellants. Effective methods involve improving manufacturing processes, implementing strict quality control measures, as well as conducting continuous research on novel materials and prediction models. These measures ensure the safe and effective utilisation of solid propellants in propulsion systems (McClain *et al*., 2019).

### 3.2 Foreign Objects or Inclusions

Foreign objects or inclusions present substantial obstacles to both performance and safety in solid propellants. Contamination or deterioration of equipment during the propellant's mixing, casting or curing stages often introduces foreign substances, including metal shards, plastic fragments or dust particles. According to Gnanaprakash *et al*. (2019), the presence of these external entities within the propellant matrix is a critical concern, as they can significantly alter combustion dynamics, leading to unpredictable changes in burn rates and pressure profiles. Moreover, these inclusions serve as stress concentration points within the propellant grain, compromising its mechanical strength and increasing the likelihood of structural failures such as cracks or fractures. This not only undermines the propellant's effectiveness but also heightens potential dangers, especially during the demanding conditions of a rocket launch. In order to mitigate these risks, the industry has implemented strict quality control protocols and adopted advanced detection techniques such as X-ray imaging and ultrasound scanning (Gupta & Khan, 2021). These techniques are designed to quickly identify and locate any foreign objects. Additionally, there is a strong focus on improving the manufacturing process to enhance environmental cleanliness and precision. Ponti *et al.* (2021) suggested that regular maintenance and inspection of production equipment can also help to prevent contamination. Managing foreign objects or inclusions is crucial in propellant manufacturing, requiring strict adherence to procedures and use of advanced technologies to ensure the reliability and safety of rocket propulsion systems.

### 3.3 Cracks

Cracks are severe flaws with significant consequences for both the functionality and safety of solid propellants. Cracks typically occur due to a combination of factors, including mechanical stresses, thermal cycling, inadequate curing during manufacturing, as well as the presence of impurities and inclusions within the propellant matrix (Li *et al.*, 2020). They range in size from microscopic fissures to larger fractures visible to the naked eye and can spread and grow over time due to operational stresses.

Cracks in a propellant grain substantially impact its combustion behaviour, resulting in higher burn rates and potential pressure instabilities in the rocket motor. This non-uniform combustion can lead to uneven propulsion, negatively affecting flight path and stability. Cracks also compromise the propellant grain's structural integrity, making it vulnerable to catastrophic failure during the high-stress conditions of rocket operation (Wu *et al*., 2022). Addressing this issue requires meticulous oversight of the manufacturing process, ensuring consistent curing, as well as minimising thermal and mechanical strains. Rong *et al.* (2022) suggested that early detection of cracks is crucial to prevent the production of low-quality solid propellants. Additionally, ongoing research focuses on developing new propellant formulations and additives to enhance material durability and reduce the likelihood of cracking. Emphasising early detection and prevention is essential for preserving the structural integrity and reliability of solid propellants, thereby ensuring the safety and effectiveness of rocket motors.

### 3.4 Debonding and Improper Adhesion

Bonding issues between solid propellant components pose significant engineering challenges in the design and optimisation of rocket motors, substantially impacting both effectiveness and safety. Bonding in rocket motors refers to the adhesion between separate layers of propellant, or between the propellant and motor casing. Establishing this bond is crucial for maintaining structural integrity and enabling efficient force transmission during rocket operation. Primary factors contributing to bonding issues include inadequate surface preparation, incompatibility between propellant and liner materials, environmental degradation, as well as defects in the propellant curing process (Hoffmann *et al*., 2020). Insufficient adhesion can lead to the formation of gaps or separations at the interface, resulting in localised areas of high temperature and uneven propulsion. This can cause deviations in the intended path or, in extreme cases, complete failure. Additionally, the presence of debonds increases the likelihood of crack formation and propagation, further undermining the structural integrity of the propellant grain, particularly under the extreme conditions experienced during launch and flight (Lei *et al*., 2022).

In order to address these bonding issues, it is essential to enhance the manufacturing process through meticulous surface preparation, careful selection of compatible materials and precise regulation of curing conditions (Liu *et. al,* 2022). Advanced diagnostic techniques, such as ultrasonic testing and radiography, can evaluate bond integrity without causing harm. Contemporary rocketry research focuses on developing new bonding agents and techniques that can withstand extreme operational conditions, aiming to improve the reliability and safety of solid rocket motors in various aerospace applications (Hoffmann *et. al.,* 2020). Incorporating rigorous quality control measures, such as NDT methods, throughout the manufacturing process is crucial for assessing adhesion quality and ensuring the safe and effective functioning of the motors (McClain *et al.*,2019).

## 4. NDT INSPECTION METHODS

As discussed in the previous section, solid propellants can experience numerous manufacturing defects and operational deteriorations. The subtle and hidden nature of these flaws necessitates the use of advanced NDT methods for detection. These techniques enable early identification and characterisation of potential defects, allowing for timely corrective actions. Technological advancements in NDT have introduced various specialised methods tailored for solid propellants, such as visual inspection, X-ray radiography, ultrasonic testing, microwave testing, shearography, computed tomography and live scanning thermography radiography. Each technique provides unique insights into the structural condition of the propellant. Employing NDT for inspecting solid propellants not only enhances the safety and reliability of rocket motors but also plays a crucial role in optimising production processes and extending the lifespan of rocket motors (Viswanathan & Suryanarayana, 2023).

### 4.1 Visual Inspection (VI)

VI is a fundamental and extensively employed NDT technique for assessing solid propellants. Figure 2 shows an example of a borescope available in the market for conducting VI for solid propellants. According to Gamdha *et al.* (2021), this approach relies on the observational skills of the inspector, supported by various tools, to evaluate the external condition and structural soundness of the propellant. VI is effective in identifying surface-related flaws such as cracks, surface erosion, inadequate bonding and foreign material inclusion (Dwivedi *et al.*, 2018).


**Figure 2: An example of a borescope available in the market for conducting VI for solid propellants. Source: Triplett (2024)**

Korompili *et al.* (2024) stated that VI can be conducted through direct observation or with the aid of inspection tools. Direct observation involves a qualified inspector directly examining the propellant surface for visible defects such as fractures, voids, surface irregularities, colour variations or other anomalies that may indicate underlying problems. They found that tool-assisted inspection is an advanced VI method that uses magnifying glasses, mirrors, videoscopes or borescopes to examine hard-to-reach areas or magnify small flaws. High-resolution cameras or video equipment are sometimes used for documentation and detailed examination, converting images into video signals for digital analysis.

The advantages of VI include its ability to easily identify surface damage and defects, operational simplicity, and high testing efficiency. It is characterised by its simplicity, cost-effectiveness and ability to yield immediate results. However, VI has limitations, including its inability to detect subsurface problems, as it can only identify surface defects. The efficacy of this approach is influenced by human factors, increasing the likelihood of errors. VI is commonly used as an initial assessment method, which can be supplemented by more sophisticated non-destructive procedures for comprehensive evaluation (Hassani & Dackermann, 2023).

### 4.2 Radiographic Testing

Radiographic testing utilises radiation absorption to penetrate materials, considering their density and thickness. The radiation source can be an X-ray tube or gamma rays emitted by radioactive isotopes such as Iridium-192 or Cobalt-60. As the radiation beam penetrates the substance, the absorbed dosage varies with the material's density and thickness. Thicker or denser areas absorb more radiation, appearing lighter on the image, while thinner or less dense areas absorb less, appearing darker. Radiographic testing can be divided into traditional and digital methods. It is a reliable technique for detecting internal flaws in solid propellants, such as voids, inclusions, cracks and porosity. This technology provides two-dimensional imagery, making it highly beneficial for routine inspections and quality control (Namboodiri *et al*., 2020).

### 4.2.1 Conventional Radiography

Conventional radiography utilises industrial film to capture images. After exposure to radiation, the film is developed in a darkroom, revealing an image that maps the internal structure of the propellant. This process provides a tangible and permanent radiographic record valuable for research and documentation. However, conventional radiography cannot provide real-time imaging. The film requires time for development in a darkroom and must be handled carefully to avoid light exposure before the image is fully developed. Remakanthan *et al.* (2015) used conventional radiography to analyse and inspect solid rocket motors. They examined large rocket motors with diameters exceeding 300 mm using a high-energy x-ray source. Two methods were employed: tangential radiography to inspect the interface between the case or insulation and the propellant grain; and normal radiography to detect flaws or cracks in the propellant grain. For this high-energy X-ray application, film as an image capture method is suitable due to its ability to absorb and handle high dose of radiation. This technique was also employed by Bikash & Kankane (2007) to estimate the location of defects in propellant grain. They used two radiographic images at different orientations and fixed a known point of a lead letter on the propellant. The dimensions of the letters were computed from the ($r$, $\theta$) values of two corners, showing close agreement with the actual dimensions and confirming the method's applicability for estimating defect locations.

### 4.2.2 Digital Radiography

Digital radiography testing surpasses conventional radiography in technological advancement. The two predominant techniques are computed radiography (CR) and digital detector array (DDA). Both utilise radiation absorption to create digital images, offering enhanced clarity and precision when examining solid propellants. High-resolution images facilitate the identification of tiny faults, crucial for ensuring the rocket motor's performance and security by identifying weaknesses that could undermine them (Economou *et al.*, 2022).

A CR system consists of a correlated readout unit and a storage phosphor imaging plate (IP). The phosphor layer in the IP absorbs energy and creates a hidden image using differential absorption patterns that correlate to the material's internal structure. A laser scans the IP in the reader, activating the phosphors to emit light proportional to the accumulated radiation energy. Photodetectors capture this light and transform it into an electrical signal (Williams *et. al.*, 2007). Bikash *et al*. (2011) compared CR and conventional radiography for a rocket engine with diameter of 225 mm and filled with composite propellant grain using a 450 kV x-ray source. The CR system used a high-density IP (HDIP) or blue plate, while MX-125 industrial film captured the image. They demonstrated CR's wide dynamic range in analysing solid propellant by capturing intricate details of the propellant grain and surfaces in a single exposure. They also used a 4 MeV linear accelerator (LINAC) X-ray source to examine solid propellant rocket motors with diameters of 540 and 740 mm.

DDA is a flat panel device that converts radiation energy into a digital image. DDA offers faster imaging capabilities, superior image resolution and decreased radiation exposure as compared to CR. It consists of a matrix of discrete detector elements or pixels that detect the incoming radiation beam penetrating the object under examination. Each pixel serves as a small-scale radiation detector that absorbs the energy. There are two mechanisms to convert radiation energy into a digital image, direct and indirect. Direct detection systems use detector material, such as amorphous selenium, which directly converts X-ray photons into an electrical charge, providing high-resolution photos. Indirect detection systems employ scintillator material to transform X-ray photons into visible light, which is then converted into an electrical signal by photodetectors, such as charge-coupled device (CCD) or complementary metal-oxide-semiconductor (CMOS). sensors. This two-step procedure is sensitive and efficient in reducing radiation exposure. The system's software processes the electrical impulses from each pixel to generate a digital image (Morigi & Albertin, 2022). Figure 3 shows a digital radiography system that can be use either a DDA or CR system.


**Figure 3: Digital radiography systems: (a) DDA (b) A CR system consisting of a reader and IP. Source: Durr NDT (2024)**

Ravindran (2006) used a flat panel detector with resolution of 400 microns to examine solid propellants measuring 10 mm in diameter, identifying flaws such as cracks, voids and irregularities within the propellant grain. Muhammad *et al*. (2023) employed DDA to examine a double-based solid propellant with diameter of 50 mm and length of 120 mm. They demonstrated that using a high-energy X-ray source and increasing the frame integration number enhanced the signal-to-noise ratio (SNR). The frame integration number amalgamates several images into a single average image, reducing the impact of random variations and resulting in improved image quality. Enhanced radiation energy improves signal penetration through the object while reducing scattering effects (Figure 4).

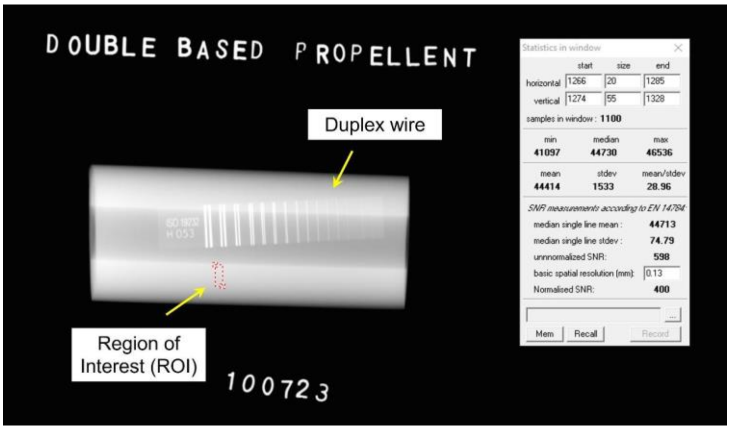


**Figure 4: Digital radiography image of a propellant taken at 80 kV with a frame integration number of 8. Source: Muhammad *et al.* (2023).**

### 4.2.3 Safety and Hazard Management of Radiation Exposure

Safety in controlling ionising radiation exposure is paramount in both traditional and digital radiography. Film processing for conventional radiography requires the use of hazardous chemicals and higher radiation doses, necessitating significant safety measures such as thorough shielding, personal protective equipment and careful handling of chemical reagents. While digital radiography requires lower radiation doses and eliminates chemical processing hazards, strict safety protocols remain essential. This includes adherence to safety regulations to protect operators, routine equipment maintenance, and continuous radiation level monitoring. In Malaysia, the Atomic Energy Licensing Board (AELB) enforces the regulation regarding the licensing and supervision of atomic energy use, including radiographic equipment and radiation safety, under the Atomic Energy Licensing Act 1984. This act ensures that all radiographic practices comply with stringent safety and regulatory standards. Training in radiation safety, adherence to regulatory standards and use of dosimetry to monitor exposure are crucial for maintaining a safe radiography workplace. Despite advancements in digital radiography technology, the fundamental principles of radiographic safety, which prioritise mitigating radiation threats and rigorous adherence to safety criteria, remain unchanged (Government of Malaysia, 2011).

## 4.3 Ultrasonic Testing (UT)

UT employs a transducer to generate high-frequency ultrasonic sound waves that penetrate materials. These sound waves travel through materials at velocities determined by their acoustic properties, specifically density and elastic modulus. In a homogeneous, defect-free material, the waves propagate uniformly and continuously. UT is particularly useful in examining solid rocket motors to detect issues with propellant coating layers and interface debonding (Li *et al*., 2015). The two primary types of UT are pulse echo and through-transmission. Pulse echo uses a single transducer, while through transmission utilises two transducers (Kurabayashi *et al.*, 2010).

### 4.3.1 Pulse Echo

Pulse echo employs ultrasonic pulses directed into the propellant. When these pulses encounter boundaries or discontinuities, such as defects, within the material, they are reflected back to the transducer. The time it takes for the echoes to return is measured to determine the location and size of the defect (Nudurupati, 2021). The strength of the echo provides insights into the nature of the defect. This method requires a couplant to act as a medium between the transducer and the solid propellant, ensuring effective transmission of ultrasonic waves. Without the couplant, the air gap between the transducer and propellant surface would significantly reflect and scatter the ultrasonic waves, impeding their entry into the material. Different materials have varying acoustic impedances, which define the resistance an ultrasound wave encounters as it travels through a medium. The couplant helps match the acoustic impedance between the transducer (typically piezoelectric material) and the solid propellant, minimising energy loss at the interface. The couplant also displaces air from the surface interface, preventing the reflection and absorption of sound waves in air gaps, which would otherwise lead to poor signal quality and false indications. It provides a consistent medium through that ultrasound waves can travel, ensuring uniform signal strength and clarity, which is crucial for accurate defect detection and characterisation in solid propellants (Smith & Doe, 2020).

### 4.3.2 Through Transmission

Through transmission utilises two transducers, one acting as a transmitter and the other as a receiver. In this non-contact method, ultrasonic waves are transmitted by one transducer and received by the other through the test material. This approach has been stated by Tiwari & Raisutis (2016) that is superior to the contact method, which requires a couplant as a medium, leading to time-consuming and unstable acoustic coupling when the transducer moves on the test surface. Additionally, it prevents secondary contamination on the test material's surface since no couplant is applied. Kurabayashi *et al*. (2010) suggested that using air as a medium in the non-contact method is effective for inspecting solid propellants. They reported that this method is better suited for automatic scanning as it avoids contaminating the solid propellant with couplant. However, the significantly lower acoustic impedance of air compared to other materials poses a challenge, causing acoustic damping. Another study by Huan *et al*. (2022) on solid propellant quality using ultrasonic testing found that air coupling yielded stable signals, good reproducibility and signal amplitude unaffected by coupling pressure. The transducer used in their study was made from special materials capable of transmitting ultrasonic waves at different frequencies. They recommended that the thickness of the solid propellant inspected using this through transmission method should be limited to up to 100 mm (Figure 5).

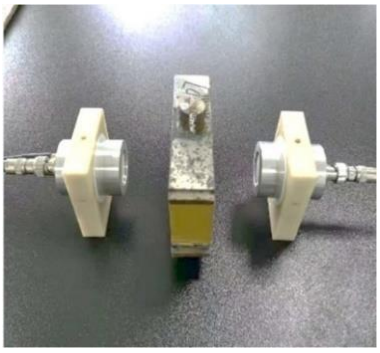

**Figure 5: Application of ultrasonic trough transmission for solid propellant examination at a laboratory scale.**
**(Source: Huan *et al.*, 2022)**

### 4.4 Shearography

Shearography employs a laser light source to coherently illuminate an object, forming a speckle pattern when light of the same wavelength and phase reflects off an uneven surface. This pattern results from the stochastic interference between reflected light waves. The speckle pattern of an object is captured when it is not subjected to any external force. After applying external stress, such as thermal, mechanical or vacuum stress, another speckle pattern is recorded to capture the resulting deformations. By comparing these patterns, shearography can identify and measure surface and subsurface abnormalities such as delaminations, cavities, cracks and inclusions (Tao *et al.*, 2022).

Shearography is highly beneficial for examining solid propellants because it can accurately identify surface and subsurface defects with great sensitivity. Detecting areas of high-stress concentration helps forecast potential failure locations in propellant materials. Shearography can also be performed in real time, providing instant feedback and enabling quick assessment during manufacturing or maintenance inspections. This method is essential for assessing adhesive strength at the interface between distinct propellant layers and is extremely effective in identifying small imperfections that might be overlooked by other methods. Studies by Wang et al. (2021) and Liu *et al*. (2022) demonstrated that shearography can detect debonding defects with a minimum diameter of 2 mm. Figure 5 shows phase maps of solid propellants containing debonding defects measuring 2, 3 and 4 mm respectively. Shearography offers numerous benefits, including its non-contact nature, ensuring safety when handling dangerous or fragile materials, its capacity to identify even the tiniest flaws, as well as its ability to produce accurate quantitative data. However, the method has several drawbacks, such as its complex nature, the need for expert interpretation of results, as well as potential restrictions on analysing certain types of materials or geometries (Sun *et al.,* 2019).

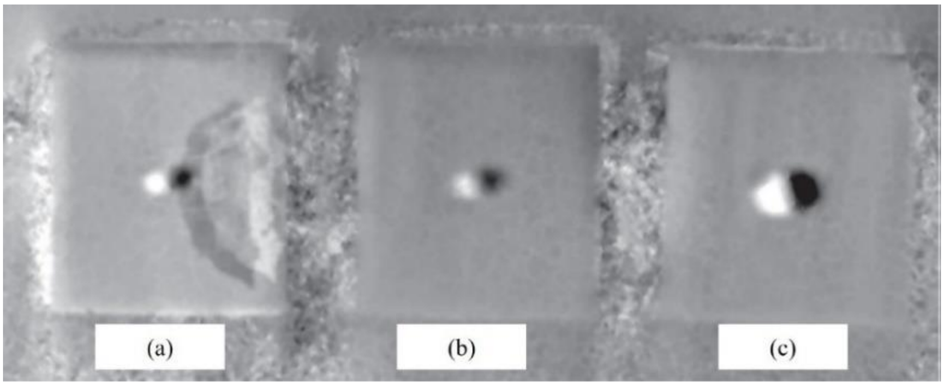


**Figure 6: Phase maps of the solid propellants with debonding defects of (a) 2 mm, (b) 3 mm and (c) 4 mm.**
**(Source: Liu *et al.*, 2022)**

## 4.5 Industrial Computed Tomography (ICT)

ICT is an advanced NDT method used for examining solid rocket motors. It relies on X-ray absorption to provide accurate geometric data from cross-sectional images of both external and internal structures. An ICT system comprises an X-ray source, a rotary table, an X-ray detector, a workstation for processing and software for 3D image construction and data analysis. ICT utilises emitted photons to project a radiation beam through an object from various angles, generating cross-sectional images after a full revolution (Figure 7). As the radiation beam traverses the object, part of it is absorbed, while the remainder is scattered or transmitted. The detector collects the photons that pass through the object, which are then visualised by the computer, allowing for a complete reconstruction of the scanned object. The scattered and absorbed X-rays undergo attenuation, decreasing radiation intensity and preventing them from reaching the detector. This method is highly regarded for its numerous advantages, including high-resolution imaging, crucial for identifying tiny structural abnormalities and flaws, ensuring the dependability and safety of the propellants. ICT's non-invasive characteristic preserves the structural integrity of the propellant, enabling multiple inspections over time (Dai *et al*., 2022).


**Figure 7: An example of an ICT system that is available in the market.**
**(Source: Visiconsult, 2024)**

A distinct advantage of ICT is its capacity to generate three-dimensional analyses, providing a comprehensive view of the propellant's internal structure, which is crucial for evaluating the material's integrity and performance. It excels in analysing materials by differentiating them according to their X-ray attenuation coefficients, allowing for the evaluation of propellant mixture uniformity and the identification of any foreign materials. Moreover, sophisticated ICT systems are equipped with automated defect recognition algorithms, enhancing the efficiency and precision of the inspection process. ICT is highly effective at identifying a wide range of flaws in solid propellants, including void formations that can significantly impact combustion rates and overall performance, as well as the detection of cracks and fissures that may expand under pressure, leading to structural collapse (Ravindran *et al*., 2008; Fan & Tan, 2013). Additionally, it effectively identifies changes in density, ensuring uniform propellant function, and evaluates the strength of connections when propellants are combined with other substances (Muralidhar *et al*., 2009).

Despite its significant benefits, ICT is not without limitations and challenges. One major issue is the substantial financial cost involved in purchasing and maintaining the equipment, making it a significant investment for many organisations. The high operational expenses are further exacerbated by the need for skilled personnel with expertise in ICT operation and data interpretation. Additionally, the thoroughness of ICT scanning and data reconstruction processes can be time-consuming, leading to longer inspection cycles as compared to other NDT methods. This can be a significant challenge in high-volume production environments where fast throughput is crucial. Furthermore, although ICT offers exceptional precision and thoroughness, its resolution constraints may occasionally hinder the identification of extremely subtle flaws, particularly in materials with low X-ray contrast (Dakak *et al*., 2022). Managing the large amounts of data generated by ICT scans also poses a challenge, requiring robust computational resources and sophisticated software for storage, processing and analysis, which can result in higher operational complexity and cost. Moreover, as radiation safety in ICT systems is comparable to other conventional and digital systems, it involves implementing strict protective measures and maintaining controlled operating environments to minimise X-ray exposure. These precautions could complicate the setup and use of ICT systems. Comprehensive shielding and safety protocols to protect operators and other personnel from radiation exposure can increase operational and infrastructure complexity (Inoue, 2023).

### 4.6 Laser Scanning Thermography (LaaST)

LasST is a thermal imaging technique that detects and analyses potential defects that could undermine the integrity of solid propellants. LasST's advanced scanning abilities offer detailed thermal maps crucial for identifying even the tiniest defects or variations in composition, which can lead to significant performance problems or catastrophic failure. As the line-shaped heat source moves across the propellant's surface, the infrared camera detects and records the thermal reaction, capturing small differences that could indicate inclusions, voids, cracks or areas with uneven density. These imperfections affect the material’s thermal conductivity and heat storage capacity, resulting in abnormal thermal behaviour observable in the recorded data (Xie *et al*., 2024).

Rong *et al*. (2022) demonstrated LasST's ability to detect multiple orientations of surface and hidden cracks in solid propellant (Figure 8). Additionally, it can detect adhesion defects in the cladding layer (Wang *et al*., 2021). The real-time monitoring capability of LasST is well-suited to the production and quality control processes of solid propellants, allowing for swift scanning of extensive surfaces, making it ideal for in-line inspection. This ensures that any irregularities are promptly identified during manufacturing, minimising risks and reducing the probability of defects in the final product. This feature is particularly advantageous given the rigorous safety and reliability standards mandated in the aerospace sector. Furthermore, LasST's ability to detect changes in thermal properties can be utilised to evaluate the uniformity of the propellant mixture. Uneven distribution of the binder or oxidiser within the propellant can be identified by meticulously analysing the thermal images, as such inhomogeneities can negatively impact the burn rate and overall effectiveness of the propellant. This capability assists in examining completed propellant grains and offers valuable input during the propellant mixing and casting processes (Kakami *et al*., 2008).

However, applying LasST in solid propellant inspection is not without challenges. The complex geometry of some propellant grains, combined with the inherently heterogeneous composition of the material, can complicate the interpretation of thermal data. Advanced data processing algorithms and a thorough understanding of the material's thermal behaviour are essential to accurately identify and characterise defects. Additionally, the presence of highly energetic materials necessitates stringent safety protocols during inspection to prevent any risk of ignition by the heat source (Buchanan, *et al*., 2019).

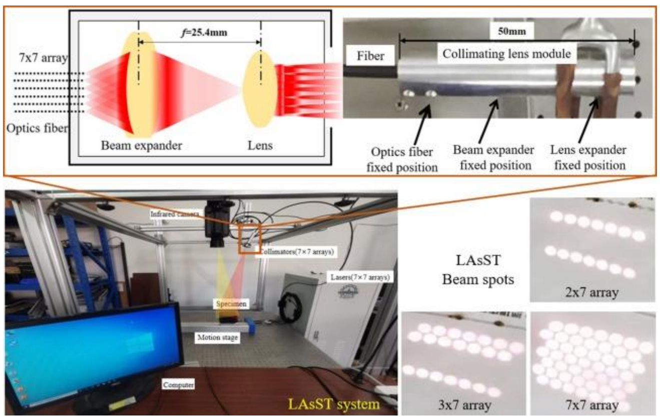


**Figure 8: Schematic diagram of LasST.**
**(Source: Rong *et al.*, 2022)**

## 5. COMPARISON OF NDT INSPECTION METHODS

Solid propellant inspection is crucial for ensuring the reliability and safety of rocket motors, given the complex and heterogeneous nature of these materials. This paper explores various NDT methods, including VI, radiographic testing, UT, shearography, ICT and LaaST. Each method offers distinct advantages and limitations, and is employed to detect and characterise internal defects and material inconsistencies that could compromise the integrity and performance of solid propellants. Collectively, these techniques provide a comprehensive evaluation framework for solid propellant inspection. A summary of these techniques, highlighting their benefits and drawbacks, is presented in Table 1.

**Table 1: Summary of NDT methods with their advantages and limitations.**

| NDT Method | Type of Defects Identified | Advantages | Limitations | References |
|---|---|---|---|---|
| Visual Inspection (VI) | ▪ Surface-related flaws: Cracks, surface erosion, debonding and inclusion. | ▪ Simple.<br>▪ Cost-effective.<br>▪ Immediate results.<br>▪ Easily identifies surface damage and faults.<br>▪ High level of testing effectiveness. | ▪ Cannot detect subsurface defects.<br>▪ Relies heavily on the skill and observation abilities.<br>▪ Human errors are more likely. | ▪ Korompili *et al*. (2024) |
| Conventional Radiography | ▪ Internal flaws: Debonding, inclusions, cracks, voids and porosity. | ▪ Provides a permanent radiographic record.<br>▪ Suitable for high-energy X-ray applications.<br>▪ Can inspect large rocket motors.<br>▪ Capable of estimating defect locations using multiple images. | ▪ Inability to provide real-time imaging.<br>▪ Requires time for development in a darkroom.<br>▪ High radiation dosage required.<br>▪ Usage of dangerous chemicals for film processing. | ▪ Bikash & Kankane (2007)<br>▪ Remakanthan *et al.* (2015) |
| Digital Radiography: Computed Radiography (CR) | ▪ Internal flaws: Debonding, inclusions, cracks, voids and porosity. | ▪ Wide dynamic range.<br>▪ High-resolution images.<br>▪ Suitable for analysing solid propellants.<br>▪ Capable of detailed inspection in a single exposure.<br>▪ Can utilise high-energy X-ray sources for large propellant grains. | ▪ Expensive technology.<br>▪ Requires careful handling and processing.<br>▪ Sensitive to radiation levels and environmental conditions.<br>▪ Regular maintenance needed.<br>▪ Regulatory compliance necessary.<br>▪ Continuous radiation level monitoring required. | ▪ Bikash *et al.* (2011) |
| Digital Radiography: Digital Detector Array (DDA) | ▪ Internal flaws: Debonding, inclusions, cracks, voids and porosity. | ▪ Superior image resolution.<br>▪ Faster imaging capabilities.<br>▪ Decreased radiation exposure.<br>▪ Effective for detecting small defects.<br>▪ Capable of direct and indirect radiation detection.<br>▪ Image averaging improves image quality. | ▪ Expensive technology.<br>▪ Requires complex calibration and setup.<br>▪ High sensitivity to environmental conditions.<br>▪ Regular maintenance needed.<br>▪ Requires high-energy X-ray sources for optimal results.<br>▪ Regulatory compliance necessary. | ▪ Ravindran (2006)<br>▪ Muhammad *et al.* (2023) |

| | | | | |
|---|---|---|---|---|
| | | | ▪ Continuous radiation level monitoring needed. | |
| Ultrasonic Testing (UT): Pulse Echo | ▪ Defects such as boundaries and discontinuities within the material. | ▪ Can determine location and size of defects.<br>▪ Provides insights into the nature of the defect.<br>▪ Contact method ensures effective transmission of ultrasonic waves. | ▪ Requires couplant for effective transmission.<br>▪ Couplant displacement necessary to avoid reflection and absorption of sound waves in air gaps.<br>▪ Potential for poor signal quality and false indications if not properly coupled. | ▪ Nudurupati (2021) |
| Ultrasonic Testing (UT): Through Transmission | ▪ Defects such as boundaries and discontinuities within the material. | ▪ Allows for automatic scanning.<br>▪ Stable signals with good reproducibility.<br>▪ No couplant needed, thus avoiding contamination. | ▪ Lower acoustic impedance of air as compared to other materials can cause acoustic damping.<br>▪ Limited effectiveness for solid propellants thicker than 100 mm.<br>▪ Potential challenges in maintaining stable acoustic coupling when using air as a medium. | ▪ Kurabayashi *et al.* (2010)<br>▪ Huan *et al.* (2022) |
| Shearography | ▪ Surface and subsurface abnormalities such as delaminations, cavities, cracks, and inclusions. | ▪ High sensitivity in identifying small flaws.<br>▪ Real-time feedback.<br>▪ Accurate quantitative data.<br>▪ Effective for detecting small imperfections and assessing adhesive strength. | ▪ Complex equipment<br>▪ Requires expert interpretation of results<br>▪ Potential restrictions on analysing certain materials or geometries. | ▪ Wang *et al.* (2021)<br>▪ Tao *et al.* (2022)<br>▪ Liu *et al.* (2022) |
| Industrial Computed Tomography (ICT) | ▪ Internal voids, cracks, inclusions and density changes. | ▪ High-resolution imaging for identifying tiny structural abnormalities.<br>▪ Enables multiple inspections over time.<br>▪ Generates three-dimensional analyses to provide comprehensive internal views.<br>▪ Differentiates materials based on X-ray attenuation coefficients.<br>▪ Automated defect recognition algorithms enhance efficiency and precision. Evaluates uniformity and foreign material presence in propellant mixture. | ▪ High financial cost for equipment procurement and maintenance.<br>▪ Requires skilled personnel for operation and data interpretation.<br>▪ Time-consuming scanning and data reconstruction processes.<br>▪ Longer inspection cycles as compared to other methods.<br>▪ Requires robust computational resources and sophisticated software for data management.<br>▪ Complex setup and operation due to radiation safety measures. | ▪ Ravindran *et al.* (2008)<br>▪ Muralidhar *et al.* (2009)<br>▪ Fan & Tan (2013)<br>▪ Dai *et al.* (2022)<br>▪ Dakak *et al.* (2022) |

| | | | | |
|---|---|---|---|---|
| Line Array Scanning Thermography (LasST) | ▪ Internal defects, material inconsistencies, inclusions, voids, cracks, and areas of inconsistent density in solid propellants. | ▪ High-resolution and rapid scanning capabilities.<br>▪ Provides detailed thermal map.<br>▪ Suitable for in-line inspection.<br>▪ Real-time monitoring.<br>▪ Detects minute defects.<br>▪ Helps assess homogeneity of propellant mixture. | ▪ Complex geometry and heterogeneous composition can complicate thermal data interpretation.<br>▪ Requires advanced data processing algorithms and thorough understanding of thermal behaviour.<br>▪ Stringent safety protocols needed due to highly energetic materials. | ▪ Wang *et al.* (2021)<br>▪ Rong *et al.* (2022)<br>▪ Xie *et al*. (2024) |

## 6. CHALLENGES IN SOLID PROPELLENT INSPECTION

The inspection of solid propellants poses several challenges, each rooted in the intricate nature of propellant grains, diversity of composition materials, limitations of NDT instruments, cost considerations and other relevant factors. One significant challenge lies in the inherent complexity of propellant grains, whereby these grains often exhibit intricate geometries and internal structures, making it challenging to detect subtle defects or irregularities that may impact performance or safety. The diverse formulations and configurations of propellant grains necessitate sophisticated inspection techniques capable of comprehensively evaluating their structural integrity. The complexity of solid propellant composition is also significant as they consist of various chemical components, including oxidisers, fuels, binders and stabilisers. This complex composition presents significant challenges in inspection as defects or inconsistencies in any component can lead to catastrophic failures. Detecting such flaws requires sophisticated analysis techniques (Cooper & Kurowski, 2016).

These challenges are further exacerbated when considering hypersonic missiles, which utilise very high energetic materials. The extreme conditions these missiles endure, including high velocities and temperatures, demand an even higher level of scrutiny in propellant inspection. The reliability and safety of hypersonic missiles depend on the flawless performance of their solid propellants, making the detection of minute defects and material inconsistencies critical. Advanced NDT methods, integrated with AI and ML, can enhance the detection capabilities for such high-stakes applications. These technologies enable the identification of defects that traditional methods might miss, ensuring that the high energetic materials used in hypersonic missiles maintain their integrity under extreme operational conditions. Consequently, the development and implementation of these advanced inspection techniques are vital for the continued advancement and safety of hypersonic missile technology (Gupta *et al*., 2021).

Moreover, ageing and environmental exposure cause significant physical and chemical changes in solid propellants, impacting their performance and stability. These effects, accelerated by factors such as temperature, humidity and mechanical stress, necessitate advanced monitoring and maintenance strategies to ensure long-term reliability and safety in defence applications (Hasanoğlu, 2008; Hamza *et al*., 2021; Deswandri *et al*., 2023). In Malaysia's tropical climate, characterised by frequent rainfall and high humidity, these ageing processes are further exacerbated. The region's environmental conditions lead to increased moisture absorption and accelerated degradation of propellant materials, resulting in higher risks of cracks and mechanical failures (Li *et al*., 2019; Tang, 2019). Consequently, specific strategies tailored to Malaysia's unique climate are essential for maintaining propellant integrity.

Limitations in NDT instruments represent a pivotal challenge in the inspection process. The conventional instruments employed for inspecting solid propellants may face constraints in terms of resolution, sensitivity, or the ability to penetrate dense or opaque materials. These limitations can hinder the accurate detection of subtle defects, internal inconsistencies and other critical anomalies that could compromise the performance and safety of the propellant (Goose *et al*., 2011). Moreover, traditional NDT methods may not effectively address the complex geometries and diverse compositions of solid propellant grains, further complicating the inspection process. Overcoming these limitations requires the development and implementation of state-of-the-art NDT technologies, including those integrated with AI, to enhance detection capabilities, and provide more accurate and reliable results. Advanced technologies such as high-frequency ultrasonics, digital radiography and terahertz imaging, when combined with AI-driven data analytics, can significantly improve the resolution and sensitivity of inspections, enabling the identification of minute defects that were previously undetectable (Choi *et al*., 2023).

Additionally, the skill and experience of NDT operators play a crucial role in ensuring reliable inspections. Interpreting NDT data is often subjective and requires high level of expertise. Experienced operators can distinguish between true defect signals, and false positives or background noise, reducing the risk of misdiagnosis. They can also assess the significance of detected defects in the context of the material's operational environment. In addition, skilled operators possess the technical expertise needed to set up and calibrate sophisticated equipment accurately, interpret complex data and troubleshoot issues during inspections (Silva *et al*., 2023). Their ability to adapt to advanced technologies further enhances the accuracy and efficiency of inspections. Continuous training and certification can ensure that operators remain proficient and up-to-date with the latest industry standards and technological advancements. However, the cost to purchase advanced NDT equipment and to train operators can be substantial. High-quality NDT instruments are often expensive and their sophisticated nature requires comprehensive training programmes to ensure operators can use them effectively (Gupta *et al*., 2021). Nonetheless, investing in both the technology and continuous development of operator skills is essential to maintain the reliability and safety of solid propellants in defence and aerospace applications.

## 7. RECENT ADVANCEMENTS AND FUTURE DIRECTIONS IN SOLID PROPELLANT INSPECTION

The integration of AI has significantly influenced recent advancements in NDT inspection methods for solid propellants (Hoffmann *et al*., 2020). These advancements are transforming the field of propellant inspection, bringing about increased levels of precision, efficiency and dependability. Automated defect recognition (ADR) systems are becoming increasingly prominent in the field of solid propellant inspection (Gamdha *et al*., 2021). These AI-powered systems are mainly used to analyse X-ray radiographs of solid propellants. AI algorithms, particularly deep learning models, excel at detecting and categorising subtle abnormalities and flaws in propellant grains that may be overlooked by conventional techniques. Automated systems offer not only substantial increase in speed but also decrease in the probability of human error, thereby guaranteeing a more dependable quality control process (Remakanthan *et al.*, 2015; Hu *et al*., 2023).

Huang *et al*. (2021) applied ML techniques to identify anomalies in solid propellants. The study employed a dataset of physicochemical properties and stability parameters to predict critical properties of high energy density materials (HEDMs) with high accuracy using models such as XGBoost, AdaBoost and random forest. The results emphasise the efficacy of ML in identifying crucial factors that impact the trade-off between performance and stability. Additionally, they offer recommendations for the most advantageous design of HEDMs. Regarding solid propellant inspection, comparable ML techniques can be utilised to examine and forecast the stability and performance of solid propellant grains. By incorporating data obtained from X-ray inspections, these models have the ability to enhance the identification of flaws and abnormalities, thereby improving the dependability and security of solid propellant development (Williams *et al.,* 2020).

Another significant trend is the utilisation of synthetic radiographic data, which is facilitated by ray tracing-based radiographic simulations (Li *et al*., 2014). This methodology facilitates the automatic identification of abnormalities in X-ray images by deep learning algorithms. Hena *et al*. (2024)

proposed that synthetic data generation techniques play a crucial role in training AI models, particularly in situations where genuine faulty samples are scarce or not accessible for training. Furthermore, the incorporation of AI in NDT techniques for solid propellants extends beyond the scope of identifying defects. It also encompasses predictive maintenance and life cycle assessment. For example, AI models have the ability to forecast the process of ageing and deterioration of propellants by analysing both historical and real-time data. This capability assists in proactive maintenance and guarantees safety (Gamdha *et. al*., 2021).

The future of NDT for structural composites is poised for significant advancements driven by emerging sensing technologies and sophisticated data processing techniques. These developments have profound implications for the inspection of solid propellants, where similar challenges in detecting subtle defects and ensuring material integrity exist. Data-driven approaches, including deep learning and physics-informed ML, promise to improve the accuracy and reliability of defect detection in propellants. Furthermore, advanced sensing technologies, such as frequency modulated continuous wave (FMCW) radar, offer non-contact and real-time capabilities resilient to environmental interferences, making them ideal for inspecting solid propellants in diverse conditions (Wibowo & Zulkifli, 2019; Guillet *et al*., 2024). The implementation of digital twin systems can also facilitate detailed monitoring and predictive maintenance strategies for solid propellant storage and usage. Advanced non-contact methods, such as digital image correlation (DIC) and infrared thermography, are increasingly prevalent, offering high-resolution monitoring crucial for assessing the integrity of solid propellants (Zaba *et al*., 2021). Breakthroughs in UT and integration of internet of things (IoT) devices further enhance real-time monitoring and data collection, promoting continuous health monitoring of propellant grains. Application-specific innovations, tailored to the unique demands of sectors such as defence and aerospace, are set to address specific inspection challenges, ensuring the reliability and safety of solid propellants (Almutairi *et al*., 2024). These advancements collectively herald a new era in NDT, marked by enhanced accuracy, efficiency and comprehensive monitoring capabilities, which is crucial for maintaining the integrity and performance of solid propellants in various high-stakes applications.

## 8. CONCLUSION

NDT techniques are pivotal in the inspection of solid propellants, ensuring their safety and reliability. The evolution from traditional methods such as VI and conventional radiography to advanced techniques such as digital radiography, UT, shearography and LasST highlights significant progress in the field. These advancements enhance defect detection capabilities, providing more accurate and real-time data crucial for maintaining the integrity of rocket motors. Future trends indicate a move towards integrating AI and ML to further automate and improve defect analysis, ensuring even higher levels of safety and performance for solid propellants.

## ACKNOWLEDGEMENT

The authors would like to thank the officers and staff from the various laboratories at the Maritime Technology Division (BTM) and Weapon Technology Division (BTP), Science & Technology Research Institute for Defence (STRIDE), Ministry of Defence, Malaysia, for their technical support during the writing process

## REFERENCES

Alexander, Y.R., Rathi, N. & Ramakrishna, P. A. (2024). Development of high burn rate propellant and testing in miniature rocket motor for control applications. *FirePhysChem*, **4**:107-113.

Almutairi, R., Bergami, G.,& Morgan, G. (2024). Advancements and challenges in IoT simulators: A comprehensive review. *Sensors*, **24**:1511.

Bai, S., Cheng, Z. & Guo, B. (2019). Maintenance optimisation model with sequential inspection based

on real-time reliability evaluation for long-term storage systems. *Processes*, **7**:1-22.
Bekhouche, S., Trache, D., Abdelaziz, A., Chelouche, S. & Tarchoun, A.F. (2024). Towards understanding the effect of temperature and humidity on the safety and performance of tracer pyrotechnic composition. *FirePhysChem*, **2**:111-124.
Bikash, G. & Kankane, D.K. (2008). Estimation of location of defects in propellant grain. *NDT & E Int.***41**:125-128.
Bikash, G., Patil, D.P., Kasar, A.H. & Kankane, D.K, (2011). Radiographic inspection of solid propellant using Computer Radiography (CR) system with 450 kV x-ray source. *Proc. Natl. Semin. Exhib. Non-Destr. Eval*, 8-10 December, India, pp 259-263.
Buchanan, R.C., Frost, M., Hawkins, T.W., McCaffrey, A.K. & Rutherford, G. (2019). Laser diagnostics for solid rocket propellants and explosives. *Proc. IEEE RAPID 2019*, Miramar Beach, FL, USA, August 19-21, 2019 pp. 1-4.
Choi, J.B., Nguyen, P.C.H., Sen, O., Udaykumar, H.S. & Baek, S. (2023). Artificial intelligence approaches for energetic materials by design: State of the art, challenges, and future directions. *Propell. Explos. Pyrotech*., **48**:1-24.
Courty, L., Gillard, P., Ehrhardt, J. & Baschung, B. (2021). Experimental determination of ignition and combustion characteristics of insensitive gun propellants based on RDX and nitrocellulose. *Combust. Flame*, **229**:111402.
Dai, J.; Li, T.; Xuan, Z. & Feng, Z. 2022. Automated defect analysis system for industrial computerized tomography images of solid rocket motor grains based on YOLO-V4 model. *Electron.* **11**:1-14.
Dakak, A.R., Bouvet, P., Gueye, L., Nguyen, D., Autret, A., Fayard, B. & Kaftandjian, V. (2022). Automation of non-destructive evaluation of casting parts based on computed tomography and machine learning. *In Proc. iCT 2022, 12th Conf. Ind. Comput. Tomogr*., February 27 - March 2, 2023, Fürth, Germany, pp. 1-12.
Deswandri, D., Tyas, R.L., Intaningrum, D., Putro, I.E., Riyadl, A., Junianto, I.D., Meliana, A., Andiarti, R. & Hakim, A.N. (2023). Risk assessment of solid propellant rocket motor using a combination of HAZOP and FMEA methods. *J. Adv. Res. Fluid Mech. Therm. Sci.*, **110**:63-78.
Dîrloman, F.-M., Ţigănescu, T. V., Rotariu, T., Ungureanu, M.-I. & Zecheru, T. (2020). Eco-oxidizers for composite propellants: Ammonium nitrate and ammonium dinitramide. *J. Mil. Technol*., **3**:31-36.
Durr NDT (2024). *Computed Radiography*. Durr NDT, Bietigheim-Bissingen, Germany.
Dwivedi, S.K., Vishwakarma, M., & Soni, A. (2018). Advances and researches on non-destructive testing: A review. *Proc. 7$^{th}$ Int. Conf. Mater. Process. Charact*. (ICMPC 2017), December 2017, Hyderabad, India, pp. 3690-3698.
Elbasuney, S., Fahd, A., Mostafa, H.E., Mostafa, S.F. & Sadek, R. (2018). Chemical stability, thermal behaviour, and shelf-life assessment of extruded modified double-base propellants. *Def. Technol*., **14**:70-76.
Elghafour, A.M.A., Radwan, M., Fahd, A., Mostafa, H.E. & Elbasuney, S. (2018). Novel approach to quantify the chemical stability and shelf life of modified double-base propellants. *Def. Technol*., **14**:720-724.
Economou, G., Kandarakis, I., Panagiotakis, G. & Vlachos, I. (2022). Principles & functions of conventional & digital X-rays imaging systems in diagnosis. *Paripex Indian J. Res.*, **11**: 57-61.
Fan, J.W. & Tan, F.T. (2013). Analysis of major defects and non-destructive testing methods for solid rocket motor. *Appl. Mech. Mater*., **365–366**:618–622.
Gamdha, D., Unnikrishnakurup, S., Rose, K.J.J., Surekha, M., Purushothaman, P., Gose, K. & Balasubramaniam, K. (2021). Automated defect recognition on x-ray radiographs of solid propellant using deep learning based on convolutional neural networks. *J. Nondestruct Eval*, **40**: 17-13.
Genov, B., Nedelchev, D., Mihovski, M. & Mirchev, Y. (2019). Comprehensive approach for service life assessment of solid-propellant rocket motors. *Int. J. NDT Days*, **2**: 467-474.
Ghose, B., Patil, D.P., Kasar, A.H. & Kankane, D.K. (2011). Radiographic inspection of solid propellant using computer radiography (CR) system with 450 kV X-ray source. *Proc. Natl. Semin. Exhib. Non-Destruct. Eval.*, 8-10 December, India, pp 1-5.
Gnanaprakash, K., Chakravarthy, S.R. & Sarathi, R. (2017). Combustion mechanism of composite solid propellant sandwiches containing nano-aluminium. *Combust. Flame*, **182**:64-75.

Government of Malaysia (2011). *Atomic Energy Licensing Act 1984 (Act 304)*. Government of Malaysia, Malaysia.

Guillet, J.-P., Fauquet, F. & Rioult, J. (2024). Augmented reality terahertz (AR-THz) sensing and imaging with frequency-modulated continuous-wave radar. *J. Infrared Millim. Terahertz Waves*, **45**:123-135.

Gupta, M. & Khan, M. (2021). Advances in applications of Non-Destructive Testing (NDT): A review. *Adv. Mater. Process. Technol.*, **8**:2286-2307.

Gupta, R., Mitchell, D., Blanche, J., Harper, S., Tang, W., Pancholi, K., Baines, L., Bucknall, D.G. & Flynn, D. (2021). A review of sensing technologies for non-destructive evaluation of structural composite materials. *J. Compos. Sci*., **5**:1-29.

Hamza, N., Yerra, J., Murthy, H. & Ramakrishna, P. A. (2021). Ageing studies on AP/HTPB based composites solid propellants. *Energ. Mater. Front.*, **2**:111-124.

Hasanoğlu, M. S. (2008). Storage reliability analysis of solid rocket propellants. *M.S. Thesis*, Middle East Technical University, Türkiye.

Hassani, S. & Dackermann, U. (2023). A systematic review of advanced sensor technologies for non-destructive testing and structural health monitoring. *Sens.*, **23**:1-83.

Hena, B., Wei, Z., Perron, L., Castanedo, C.I. & Maldague, X. (2024). Towards enhancing automated defect recognition in digital X-ray radiography: Synthesizing training data through X-ray intensity distribution modeling for deep learning algorithms. *Inf.*, **15**:16-36.

Hoffmann, L.F.S., Bizarria, F.C.P. & Bizarria, J.W.P. (2020). Detection of liner surface defects in solid rocket motors using multilayer perceptron neural networks. *Polym. Test*., **88**:1-11.

Hu, H., Li, S., Huang, J., Liu, B. & Che, C. (2023). Casting product image data for quality inspection with Xception and data augmentation. *J. Theory Pract. Eng. Sci.*, **3**:6-16.

Huang, X., Li, C., Tan, K., Wen, Y., Guo, F., Sun, C.Q., Gozin, M. & Zhang, L. (2021). Applying machine learning to balance performance and stability of high energy density materials. *iScience*, **24**:1-16.

Huang, L., Jian, L. & Bojun, L. (2022). Experimental research on ultrasonic A-scan testing technology of composite solid propellant. *J. Phys. Conf. Ser.*, **2338**:1-6.

Inoue, Y. (2023). Radiation dose management in computed tomography: Introduction to the practice at a single facility. *Tomogr*., **9**: 955–966

Jin, B., Xu, H., Yang, S., Lei, X., Ding, Y. & Liu, P. (2022). Digital in-line holography of condensed phase particles in solid rocket motor plume. *Front. Phys*., **9**: 1-7.

Kakami, A., Hiyamizu, R., Shuzenji, K. & Tachibana, T. (2008). Laser-assisted combustion of solid propellants at low pressures. *J. Propuls. Power*, **24**: 1355–1360.

Korompili, G., Mußbach, G. & Riziotis, C. (2024). Structural health monitoring of solid rocket motors: from destructive testing to perspectives of photonic-based sensing. *Instrum*., **8**:1-21.

Kurabayashi, H., Minato, M. & Sato, E. (2010). ultrasonic inspection method for solid rocket motor. *Proc. 7th Int. Conf. NDE Struct. Integr. Nucl. Pressur. Comp*, 12-15 May 2009, Yokohama, Japan. pp 1-7.

Lei, M., Ren, S., Chen, E., Zhang, Z., Xiao, J., Wen, L. & Hou, X. (2022). Correlation between solid propellant failure and interface debonding in solid rocket motors. *Polym. Test.*, **115**: 107755.

Li, Y., Yang, W. & Ying, S. (2014). The effects of porous structure on the burning characteristics of foamed NC-based gun propellants. *Propell. Explos. Pyrotech*., **39**:852-858.

Li, C., Lu, G.-E., Jiang, J., Ge, Q. & Wang, S. (2015). Review on the test method of adhesive failure in solid rocket motor. *Proc. Natl. Seminar & Exhib. Non-Destruct. Eval*., 8-10 December 2015, China, pp. 675-681.

Li, J., Xu, Z., Ai, C. & Wang, X. (2019). A review of studies on temperature field changes of solid rocket engines under different environments. *IOP Conf. Ser. Earth Environ. Sci.*, **300**: 042106.

Li, H., Liang, D., Yu, M., Liu, J., Wang, Y., Pang, A., Tang, G. & Huang, X. (2020). Study on dehydrogenation and oxidation kinetics mechanisms of micron α-AlH3 in an oxidative atmosphere. *Int. J. Hydrogen Energy*, **45**:24958-24967.

Liu, B., Wang, S., Zham, M., Wang, H., Zhang, G. & Qiwei, J. (2022). Optical nondestructive evaluation for minor debonding defects and interfacial adhesive strength of solid propellant. *Measurement*, **194**:1-6.

Liu, J., Yang, D., Li, S., Bai, C., Tu, C., Zhu, F., Xin, W., Li, G. & Luo, Y. (2023). Synthesis and

characterization of hydroxyl-terminated polybutadiene modified low temperature adaptive self-matting waterborne polyurethane. *RSC Adv*., **13**:7020-7029.
Lysien, K., Stolarczyk, A. & Jarosz, T. (2021). Solid propellant formulations: A review of recent progress and utilized components. *Mater*., **14**: 6657.
Mason, B.P. & Roland, C.M. (2019). Solid propellants. *Rubber Chem. Technol.*, **92**: 1-24.
McClain, M.S., Gunduz, I.E. & Son, S.F. (2019). Additive manufacturing of ammonium perchlorate composite propellant with high solids loadings. *Proc. Combust. Inst.*, **37**: 3135-3142.
Mezroua, A., Khimeche, K., Lefebvre, M.H., Benziane, M. & Trache, D. (2013). The influence of porosity of ammonium perchlorate (AP) on the thermomechanical and thermal properties of the AP/polyvinylchloride (PVC) composite propellants. *J. Therm. Anal. Calorim*., **115**:635-646.
Morigi, M.P. & Albertin, F. (2022). X-ray digital radiography and computed tomography. *J. Imaging*, **8**: 119.
Muhammad, M.M., Azmahani, S., Subhi, D.Y., Hassanuddin, N.H.N & Mahdi, C.I (2023). Image quality digital industrial radiography on solid propellant using digital detector array. *Defence S&T Bull.*, **16**:98-104.
Muralidhar, C., Lukose, S.N., Subramanian, M.P., Reddy, M.V. & Joshi, J.R. (2009). Evaluation Evaluation of Internal details in Rocket Motors using Computed Tomography. *Proc. Nat. Sem. Non-Destructive Eval.*, 7-8 December 2009, Hydreabad, India, pp 79-80.
Namboodiri, G. N., Moideenkutty, K. K., Remakanthan, S., Kumar, B. N., Nagarajan, K., Nallaperumal, M., Kumar, L.M. & Jayaprakash, J. (2020). Detection and characterisation of interface defects in solid rocket motor by radiography inspection. *NDT Int.*, **9**:1-8.
Naseem, H., Yerra, J., Murthy, H. & Ramakrishna, P.A. (2021). Ageing studies on AP/HTPB based composites solid propellants. *Energ. Mater. Front***.**, **2**: 111–124.
Novo (2024). *Novo Portable Radiography*. Grand Blanc, USA.
Nudurupati, A.K. (2021). Non-destructive ultrasonic testing of solid rocket motor casing. *Res. J. Eng. Sci*., **12**:1-8.
Ponti, F., Mini, S., Fadigati, L., Ravaglioli, V., Annovazzi, A. & Garreffa, V. (2021). Effects of inclusions on the performance of a solid rocket motor. *Acta Astronaut*.,**189**: 283-297.
Ravindran, V.R., Sreelakshmi, C. & Vibinkumar, S. (2008). Digital radiography-based 3D-CT imaging for the NDE of solid rocket propellant systems. *Insight: Nondestruct. Test. Cond. Mon.*, **50**:564–568.
Ravindran, V.R. (2006). Digital radiography using flat panel detector for the non-destructive evaluation of space vehicle components. *Proc. Nat. Sem. Non-Destructive Eval.*, 7-8 December 2006, Hydreabad, India, pp 410-415.
Remakanthan, S., Moideenkutty, K.K., Gunasekaran, R., Cherian, T & Thomas C.R. (2015). Analysis of defects in solid rocket motors using x-ray radiography. *Nat. Sem. Exhib. Non-Destructive Eval. 2014 (NDE 2014)*, 4-6 December 2014, Pune, India.
Rong, X., Zhao, J., Yue, Z., Wang, F., Liu, J., Zhong, Y., Qiang, G., Sun, J., Wei, J., Wang, Y., Chen, M. & Yue, H. (2022). Rapid detection for the surface and hidden crack of solid propellant motor charge using laser arrays scanning thermography (LasST). *Infrared Phys. Tech.*, **125**:1-10.
Silva, M.I., Malitckii, E., Santos, T.G. & Vilaça, P. (2023). Review of conventional and advanced non-destructive testing techniques for detection and characterization of small-scale defects . *Prog. Mater. Sci*., **138**: 101155.
Smith, J. & Doe, A. (2020). Water-based couplants for general-purpose use for UT applications. *J. Sci. Ind. Res.*, **59**: 935-939.
Sun, F., Wang, Y., Yan, P., Zhao, Q. & Yang, L. (2019). The application of SLM in shearography detecting system. *Opt. Lasers Eng.*, **114**: 90-94.
Tang, K.H.D. (2019). Climate change in Malaysia: Trends, contributors, impacts, mitigation and adaptations. *Sci. Total Environ.*, **650**:1858-1871.
Tao, N., Anisimov, A.G. & Groves, R.M. (2022). Shearography non-destructive testing of thick GFRP laminates: Numerical and experimental study on defect detection with thermal loading. *Compos. Struct***.**, **282**:1-12.
Tiwari, K.A. & Raisutis, R. (2016). Comparative analysis of non-contact ultrasonic methods for defect estimation of composites in remote areas. *Proc. CBU Int. Conf. Proc.*, 23-25 March 2016, Prague, Czech Republic, pp. 846-851.

Triplett (2024). *High Definition Boroscope Inspection Camera (Dual Camera)*. Triplett Test Equipment & Tools, US.

Visiconsult (2024) *Visiconsult XRH222 CT Scanner.* Visiconsult, Stockelsdorf, Germany.

Viswanathan, K. & Suryanarayana, P.V. (2023). Non-destructive evaluation of solid rockets and missiles systems. *Proc. Natl. Semin. Exhib. Non-Destr. Eval*., December 2023, New Delhi, India, pp. 1-10.

Wang, F., Liu, J., Song, P., Gong, J., Peng, W., Liu, G., Chen, M. & Wang, Y. (2021). Multimodal optical excitation pulsed thermography: Enhanced recognize debonding defects of the solid propellant rocket motor cladding layer. *Mech. Syst. Signal Pr.*, **163**:101864.

Wibowo, T.P. & Zulkifli, F.Y. (2019). Design of FMCW ground penetrating radar for concrete inspection at ISM band 2.4–2.5 GHz. *Proc. 2019 IEEE Asia-Pac. Microw. Conf. (APMC)*, 13 December 2019, Depok, West Java, Indonesia, pp. 1232-1234.

Williams, M.B., Krupinski, E.A., Strauss, K.J., Breeden, W.K., Rzeszotarski, M.S., Applegate, K., Wyatt, M., Bjork, S. & Seibert, J. A. (2007). Digital radiography image quality: Image acquisition. *J. Am. Coll. Radiol.*, **4**: 371-388.

Williams, A., Himschoot, A., Saafir, M., Gatlin, M., Pendleton, D. & Alvord, D. (2020). A machine learning approach for solid rocket motor data analysis and virtual sensor development. *Proc. AIAA Propuls. Energy 2020 Forum*, August 24-28, 2020, New Orleans, LA, USA, pp. 1-10.

Wu, C., Fu, X. & Li, H. (2022). Research progress on crack propagation behavior of solid propellant. *Adv. Eng. Technol. Res*., **3**: 878-885.

Xie, L., Lian, Y., Du, F., Wang, Y. & Lu, Z. (2024). Optical methods of laser ultrasonic testing technology in the industrial and engineering applications: A review. *Opt. Laser Technol*., **176**: 110876.

Żaba, K., Trzepieciński, T., Puchlerska, S., Noga, P. & Balcerzak, M. (2021). Coupled thermomechanical response measurement of deformation of nickel-based superalloys using full-field digital image correlation and infrared thermography. *Mater.*, **14**: 2163.

Zhirnov, A.A., Stepanov, K.V., Sazonkin, S.G., Choban, T.V., Koshelev, K.I., Chernutsky, A.O., Pnev, A.B., Novikov, A.O. & Yagodnikov, D.A. (2021). Study of intra-chamber processes in solid rocket motors by fiber optic sensors. *Sens.*, **21**:7836.

# FAILURE ANALYSIS ON LUGLESS JOINING SHACKLES OF A NAVAL SHIP

Muhammad Azrain Mohammad, Mohd Moesli Muhammad*, Mohd Subhi Din Yati, Abdul Rauf Abdul Manap, Azmahani Sulaiman, Nik Hassanuddin Nik Yusoff, Muhammad Izzamir Firdaus Idris, Mohammad Syafiq Mohammad Rafi & Mahdi Che Isa

Maritime Technology Division (BTM),
Science & Technology Research Institute for Defence (STRIDE), Malaysia

*Corresponding author: moesli.muhammad@stride.gov.my

**ABSTRACT**

*Lugless joining shackles (LJS) are foundational elements in the structures of various heavy-duty industrial applications. Despite their widespread use and importance, the failure of LJS during their operations is scarcely reported, indicating that this issue is yet to be fully explored. Hence, this study investigates the underlying causes of these failures through a combination of fractographic analysis and X-ray digital radiography. The analysis reveals the presence of internal voids and cavities, particularly concentrated at the connection area of the shackle halves. These defects, likely originating from manufacturing inconsistencies, acted as stress concentrators, leading to localised stress amplification, crack initiation, and eventual structural failure under operational loads. These findings highlight the crucial need for stringent quality control in the manufacturing process to prevent the occurrence of such defects. Ensuring the homogeneity and integrity of shackle materials is essential for maintaining the structural reliability of LJS, especially in demanding maritime environments.*

**Keywords:** *Lugless joining shackles (LJS); failure analysis; fractographic analysis; X-ray digital radiography; voids and cavities.*

## 1. INTRODUCTION

Lugless joining shackles (LJS), commonly known as kenter shackles, are critical integral components used in a wide array of industrial and maritime operations, serving as crucial links in lifting, rigging and load-securing systems. These shackles are designed to connect and secure chains, ropes, or cables, and thus play a vital role in ensuring the safe transfer of loads (Kim *et al.*, 2010; Pauw *et al.*, 2013; The Royal Navy, 2023). Their importance cannot be overstated, given their ubiquitous utilisation in industries ranging from construction, shipping, mining and offshore drilling (Cochet *et al.*, 2016, 2019). In maritime applications, LJS are used in mooring systems, towing operations and cargo handling (Mcmaster *et al.*, 2010; Spong *et al.*, 2022). Additionally, in construction and mining, they aid in lifting heavy components and material handling systems respectively (Kang & Huang, 2007; Butterfield, 2024).

LJS are typically constructed from materials such as nickel, alloy and stainless-steel, and consist of specific components that include a pair of shackle halves (usually U-shaped or bow-shaped), a lead pellet, a metal spile / taper pin and a stud, as shown in Figure 1. These shackles are engineered to withstand significant tensile and shear forces, making them indispensable in applications where reliability and durability are paramount (Pauw *et al.*, 2013; Nair *et al.*, 2024; Tunçel *et al.*, 2024).

In order to ensure the safe use of LJS, stringent standards and regulations from organisations such as the American Society for Testing and Materials (ASTM) and International Organization for Standardization (ISO) have been established, outlining specifications for material properties, manufacturing processes, and load capacities. The relevant ASTM standards are ASTM A952/A952M-

02: Standard Specification for Forged Grade 80 and Grade 100 Alloy Steel Lifting Components and Welded Attachment Links (ASTM, 2022a), and ASTM F1145-05: Standard Specification for Turnbuckles, Swaged, Welded, Forged (ASTM, 2022b). Meanwhile, the relevant ISO standards are ISO 18279: Imperfections in Brazed Joints (ISO, 2023), ISO 2415: Forged Shackles for General Lifting Purposes – Dee Shackles and Bow Shackles (ISO, 2022), and ISO 16857: Ships and Marine Technology – Loose Gear of Lifting Appliances on Ships – Shackles (ISO, 2013). Compliance with these standards is crucial to prevent failures that could result in catastrophic accidents.

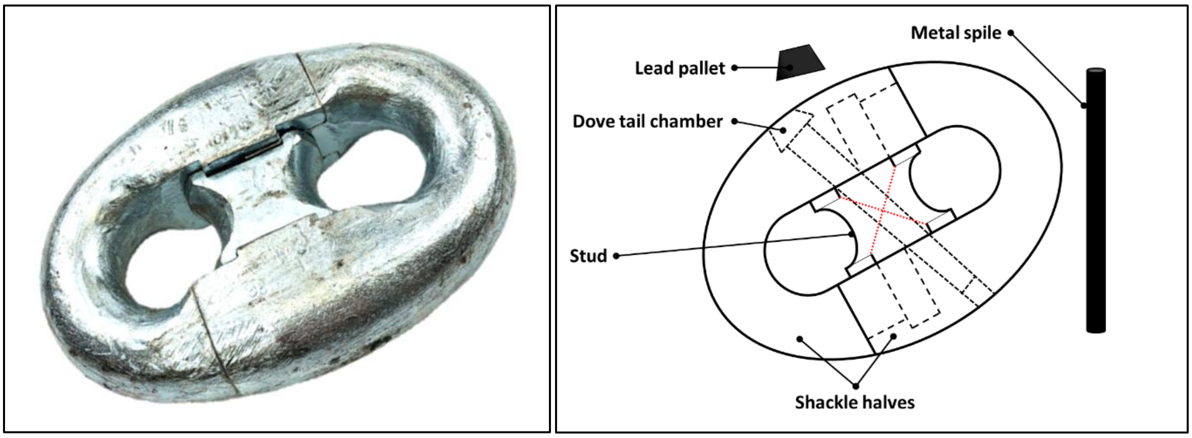


**(a)** **(b)**

**Figure 1: (a) Typical commercially available LJS (Source: Wescovan, 2024). (b) Schematic diagram of main components of LJS: shackle halves, a lead pellet, a metal spile and a stud.**

Due to their widespread use and importance, failures of LJS can cause severe consequences, including injuries, fatalities and substantial financial losses (Wang *et al.*, 2019; Rezende *et al.*, 2021; Rezende *et al.*, 2024). However, research on failure analysis of LJS is limited, highlighting a gap in scientific understanding within this area. In view of this, further studies are required to comprehensively analyse the causes of LJS failures during operations to enhance safety and prevent accidents. To this end, this paper presents a systematic study that has been specifically conducted on the inner structure of failed LJS during operations.

## 2. METHODOLOGY

### 2.1 LJS Properties and Sample Preparation

In this study, several LJS that failed during operations in a local naval ship were examined. They are made from austenitic stainless-steel grade 304. Prior to testing, the shackles were cleaned with an industrial solvent to remove any surface contaminants and then air-dried. The samples were inspected for any visible defects and measurements were taken to confirm adherence to specific dimensions. All the samples had length of 88.90 mm, height of 225.14 mm and weight of 1.15 kg. The obtained samples were categorised as follow: (1) broken LJS (failed sample during operation); (2) utilised LJS (used sample without any damage); and (3) as-received LJS (new sample). They were labelled as SA and SB (broken samples), SC (utilised sample) and SD (new sample) as shown in Figure 2.

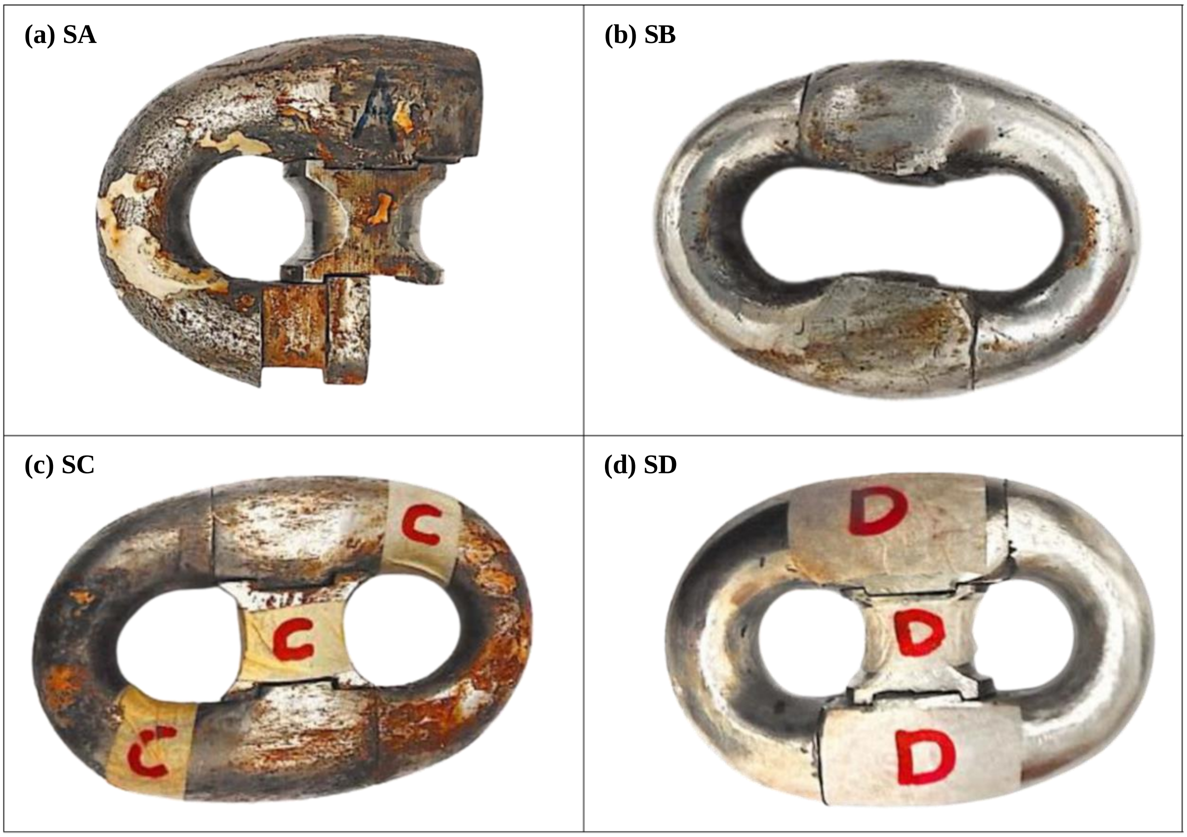


**Figure 2: Tested LJS samples: (a) and (b) Broken LJS samples that failed during operation, labelled as SA and SB respectively. (c) Utilised LJS sample without any damage during operation, labelled as SC. (d) As-received LJS sample, labelled as SD.**

## 2.2 Material Inspection

### 2.2.2 Fractographic Analysis

Fractographic analysis is a critical technique used in material science to examine fracture surfaces of materials to understand the causes and mechanisms of failure (Carroll & Lisin, 2024). In this study, the analysis was specifically applied to the LJS samples. The procedure for conducting fractographic analysis involves several key steps, including cleaning, preparation, examination and documentation of the fractured surfaces.

The first step in the process is the preparation of the samples, which started with thorough cleaning to remove any contaminants that might interfere with the analysis. The fracture surfaces of the LJS samples were initially cleaned using a sodium hydroxide (NaOH) solution. This step was essential for removing oily residues that could obscure important fracture features, as NaOH is effective in breaking down and removing organic residues. Following the NaOH treatment, the samples were rinsed with ethanol, a common cleaning solvent that evaporates quickly and leaves no residue, ensuring that the fracture surfaces are free from contaminants. After cleaning, the samples were air-dried at room temperature of approximately 25°C, under ambient relative humidity of 60%. The drying process is crucial to prevent any moisture from altering the fracture surface features. Once dried, the samples were stored in a desiccator cabinet, which provides a low-humidity environment essential for preserving the integrity of the fracture surfaces, and preventing atmospheric corrosion or contamination.

Fractographic analysis was carried out by first examining the fracture surfaces through visual inspection, where the entire fracture surface was viewed with the naked eye or through a low magnification optical microscope. During this phase, the fracture surfaces were photographed and documented at various magnifications to capture the overall appearance of the fracture and any significant features observable without high magnification. This macroscopic examination facilitated in identifying key fracture features such as the location of crack initiation sites, crack propagation paths and the overall mode of failure. Crack initiation sites are areas where the fracture process begins, with identification of these sites being crucial for understanding the root cause of failure. Propagation paths, which are the routes taken by the crack as it spreads through the material, provide valuable information about the loading conditions and the material's resistance to crack growth. The mode of failure, whether brittle, ductile or fatigue, can be inferred from the fracture surface features, offering critical insights into the failure mechanism and guiding subsequent material or design improvements (Carroll & Lisin, 2024).

### 2.2.2 X-Ray Digital Radiography

In order to investigate and evaluate the internal structures of the LJS samples, digital radiography was performed using an X-ray machine (Yxlon XPO EVO 225D) as the X-ray source and a digital detector array (DDA) (NOVO DR NV22WNSR03) to convert the X-ray images into digital format. The profile radiography technique was employed, allowing for real-time evaluation and analysis of the captured digital images. The arrangement of the X-ray source, sample and DDA is illustrated in Figure 3.

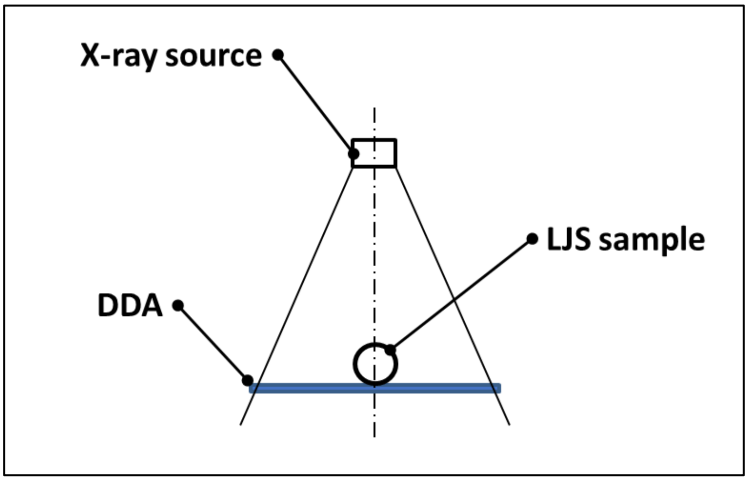


**Figure 3: Arrangement of the X-ray source, LJS sample and DDA.**

## 3. RESULTS

As shown in Figure 4(a), fractographic examination of the fracture surface for sample SA (marked by the red circle) revealed a hollow structure located at the centre of the shackle's halved surface. Additionally, grunting surfaces were also observed adjacent to the hollow structure, highlighted by the red arrows. Further inspection indicated that this hollow structure is interconnected with cavities, as indicated in Figure 4(b). Similar findings were observed for sample SB.

In order to gain a deeper insight into this specific issue, internal structure analysis was conducted using X-ray digital radiography. The results discovered the presence of anomalies within the structures for samples SA, SB and SC. As depicted in Figures 5(a)–(c), noticeable colour contrasts in the digital radiographic images signified the presence of voids or empty spaces within the internal structures of these samples, as indicated by the yellow arrows. Conversely, no defects were observed in sample SD, as shown in Figure 5(d). From the acquired images, it can be inferred that samples SA and SB exhibited the most significant damage, with larger voids as compared to sample SC. Notably, these voids were predominantly concentrated at the connection areas of the shackle halves.

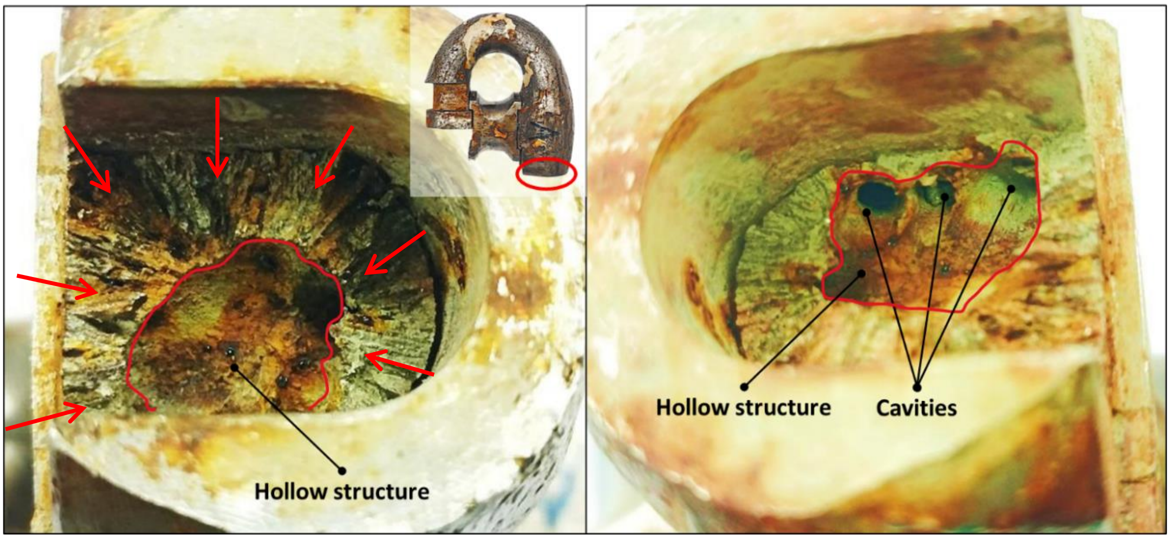


**(a)** **(b)**

**Figure 4: Fractographic analysis of fracture surface for sample SA: (a) A hollow structure was found, with the centre area showing apparent grunting surfaces at the vicinity of the hollow zone. (b) Formation of cavities that are interconnected to the hollow structure.**

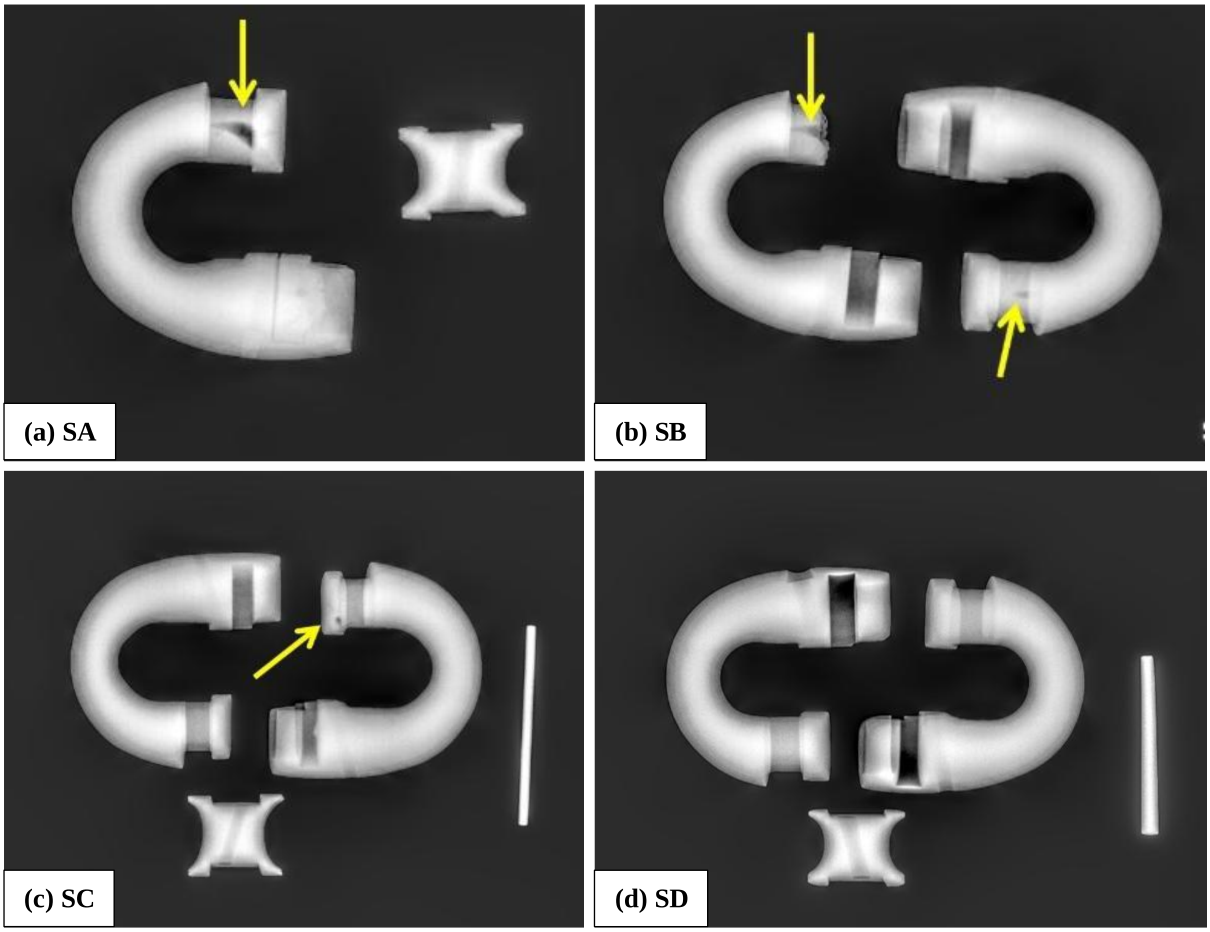


**Figure 5: Digital radiographic images of the LJS samples: (a) and (b) Voids can be observed in both samples SA and SB. However, the void within sample SA was noticeably slightly larger as compared to sample SB. (c) Relatively small void found in sample SC. (d) No anomality was found within sample SD.**

## 4. DISCUSSION

The failure of LJS samples SA and SB, as investigated in this study, can largely be attributed to the presence of internal voids and cavities within the shackle material. These defects, especially when located in critical load-bearing regions such as the connection areas of shackle halves, play a significant role in compromising the structural integrity of the LJS. These defects act primarily as stress concentrators, amplifying localised stress when the shackles are subjected to operational loads. This phenomenon can significantly increase the localised stress beyond the material's yield strength, leading to plastic deformation and initiation of crack formation at these sites. Once a crack is initiated, the cyclic nature of the loads commonly encountered in marine environments can cause the crack to propagate. Over time, the crack can grow to a critical size, which reduces the effective cross-sectional area of the material that can carry the load, thereby lowering the overall load-bearing capacity of the shackle (Pauw *et al.,* 2013; Lee *et al.,* 2018; Sachan *et al.,* 2020).

The detection of these defects via fractographic analysis and confirmation by X-ray digital radiography suggests that the manufacturing process may have been inadequate in ensuring the homogeneity and integrity of the shackle material. Possible causes include improper casting or forging techniques, insufficient control over material composition, as well as inadequate quality control during manufacturing. For instance, during the casting process, improper cooling rates can lead to the formation of voids or porosities within the metal. Additionally, inadequate material mixing or contamination could result in non-uniformities, leading to the formation of cavities. These defects are particularly detrimental in high stress regions of LJS where they can severely compromise the mechanical properties of the material (Zerbst *et al*., 2019; Liu *et al.,* 2022).

The concentration of voids at the connection areas of the shackle halves is particularly concerning. This region is subjected to high tensile and bending stresses during operations, making it a critical point of potential failure. The presence of these defects in such a critical region likely accelerated the initiation and propagation of cracks, ultimately leading to premature failure of the shackles under operational loads (Davis *et al.,* 2017, Dwivedi *et al.,* 2024).

Concisely, it can be deduced that the failure of the LJS samples on the naval ship in this study is likely due to the presence of manufacturing defects in the form of voids and cavities, particularly in the critical connection areas of the shackle halves. These defects compromised the structural integrity of the shackles, leading to stress concentration, crack initiation and eventual failure under load. This analysis underscores the importance of stringent quality control measures in the manufacturing process to prevent the occurrence of such defects, thereby ensuring the reliability and safety of critical components in demanding operational environments (Wang *et al.,* 2020).

## 5. CONCLUSION

In summary, a systematic study on the failure analysis of LJS during operations on a naval ship has been presented, which can be attributed to the presence of internal voids and cavities within the shackle structures, particularly concentrated at the connection areas of the shackle halves. This conclusion is supported by the findings from both fractographic analysis and X-ray digital radiography, which revealed significant internal defects that are likely to have compromised the mechanical integrity of the shackles. In addition, this study has indirectly highlighted the significant impact of LJS manufacturing process on the structural integrity, which is crucial for preventing future failures.

## ACKNOWLEDGEMENT

The authors would like to thank the officers and staff from the various laboratories at the Maritime Technology Division (BTM), Science & Technology Research Institute for Defence (STRIDE), Ministry of Defence, Malaysia for their technical support during the investigation works.

## REFERENCES


ASTM (American Society for Testing and Materials) (2022a). *Standard Specification for Forged Grade 80 and Grade 100 Alloy Steel Lifting Components and Welded Attachment Links*. American Society for Testing and Materials *(*ASTM), Pennsylvania, US.

ASTM (American Society for Testing and Materials) (2022b). *Standard Specification for Turnbuckles, Swaged, Welded, Forged*. American Society for Testing and Materials *(*ASTM), Pennsylvania, US.

Butterfield, T. (2024). *Automating Assembly on Construction Sites*. University of Cambridge, UK.

Carroll, M. & Lisin, M. (2024). Examination of fracture surfaces. *In* Schroeder, C.J., Parrington, R.J., Maciejewski, J.O. & Lane, J.L. (Eds.), *Fractography.* ASM International, Almere, Netherlands, pp. 1-22.

Cochet, J., Thuillier, S., Decultot, N. & Manach, P.Y. (2019). Investigation of the key process parameters in the hot forming of a shackle. *Int. J. Adv. Manuf. Technol.*, **105**: 3209-3219.

Cochet, J., Thuillier, S., Manach, P.Y. & Decultot, N. (2016). Thermo-mechanical forming of a large sling shackle. *Int. J. Adv. Manuf. Technol.*, **86**:1573-1591.

Davis, T., Healy, D., Bubeck, A. & Walker, R. (2017). Stress concentrations around voids in three dimensions: The roots of failure. *J. Struct. Geol.*, **102**: 193-207.

Dwivedi, A.K., Khan, I.A. & Chattopadhyay, J. (2024). Effect of shape and distribution of secondary voids on ductile crack path. *Procedia Struct. Integr.*, **60**: 286-297.

ISO (International Organization for Standardization). (2013). *Ships and Marine Technology – Loose Gear of Lifting Appliances on Ships – Shackles*. International Organization for Standardization (ISO), Geneva, Switzerland.

ISO (International Organization for Standardization). (2022). *Forged Shackles for General Lifting Purposes – Dee Shackles and Bow Shackles*. International Organization for Standardization (ISO), Geneva, Switzerland.

ISO (International Organization for Standardization). (2023). *Imperfections in Brazed Joints.* International Organization for Standardization (ISO), Geneva, Switzerland.

Kang, S. & Hwang, I. (2007). Design and implementation of miniaturized auto shackle using duplex RF transmission. *J. Korean Inst. Commun. Inf. Sci*. **32**: 1050-1056.

Kim, T.G., Lee, S.B. & Lee, H.C. (2010). A case study on engineering failure analysis of link chain. *Saf. Health Work*, **1**: 43-50.

Lee, S., Jeon, I. & Baek, D.C. (2018). Deviation based fault detection method for shackles under variable loading. *J. Mech. Sci. Technol.*, **32**: 753-760.

Liu, Z., Lei, Y., Zhang, X., Kang, Z. & Zhang, J. (2022). Effect mechanism and simulation of voids on hygrothermal performances of composites. *Polym.*, **14**: 1-18.

McMaster, F.J., Abadin, J., Waldhart, C., Lee, Y.D., Das, S. & Greiner, B. (2010). Fit-for-service assessment of deepwater in-service low toughness mooring shackles. *Proc. Offshore Technol. Conf.*, May 2010, Houston, Texas, US, pp. 1-12.

Nair, A., Dhaigude, M., Yao, A., Chen, Y., Jaiswal, V. & Shavandi, M. (2024). Setting the stage for a novel mooring chain integrity and design assessment practice: The partial SCF and hot-spot SN curve approach. *Offshore Technol. Conf.*, May 2024, Houston, Texas, US, pp. D011S013R002.

Pauw, J., Sukumaran, J., Perez Delgado, Y., Rodriguez, V. & DeBaets, P. (2013). Effect of hardness in shackle chain wear under harsh environmental conditions. *Wear*, **306**: 131-137.

Rezende, F. A., Simão, M. L., Gomes, R. S., Videiro, P. M. & Sagrilo, L. V. (2021). Fatigue reliability-based inspection planning methodology for corroded mooring chain links. *Int. Conf. Offshore Mech. Arctic Eng.*, June 2024, Virtual, Online, pp. V002T02A019.

Rezende, F.A., Videiro, P.M., Sagrilo, L.V. & Oliveira, M.C. (2024). Reliability-based fatigue inspection planning for mooring chains of floating systems. *Relia. Eng. Sys. Safety*, **242**: 109775.

Sachan, A. & Choo, Y.S. (2020). Mooring chain strength tests and ductile failure modeling using micromechanics and phenomenology-based failure models. *Ocean Eng*, **195**: 106663.

Spong, R., Garrity, R., Thompson, C., Yan, X., Gabrielsen, Ø., L'Hostis, D., Heyl, C., Minnebo, J., Naciri, M., Roberts, C. & Byatt, D. (2022). Mooring integrity issues and lessons learned

database-deepstar® project 20401. *Proc. Offshore Tech. Conf*., May 2022, Houston, Texas, US, pp. 1-15.
The Royal Navy. (2023). *Admiralty Manual of Seamanship, 13th Ed.* The Nautical Institute, UK.
Tunçel, A. L., Sezer, S. I., Elidolu, G., Uflaz, E., Akyuz, E. & Arslan, O. (2024). A rule-based Bayesian network modelling under evidential reasoning theory for risk analysis of anchoring operation in maritime transportation. *Ocean Eng*, **292**: 116521.
Wang, S., Zhang, X., Kwan, T., Ma, K., Li, Z., Baker, D.A., Izadparast, A., Farrow, G.H., Potts, A.E., Nair, A., Prabhu, M.L., Vargas, P.M., Perez, I.M., Luo, M. & Fontaine, E. (2019). Assessing fatigue life of corroded mooring chains through advanced analysis. *Offshore Tech. Conf*., May 2019, Houston, Texas, US, pp. D011S014R001.
Wang, Z., Xie, M., Li, Y., Zhang, W., Yang, C., Kollo, L., Eckert, J. & Prashanth, K.G. (2020). Premature failure of an additively manufactured material. *NPG Asia Mater*., **12**: 1-10
Wescovan. (2024). 7/8 inch GR3 ABS galvanized kenter links - ProCraft rigging. Available online at: https://wescovan.com/marine-stud-link-chain/kenter-links/78-inch-gr3-abs-galvanized-kenter-links (Last access date: 7 August 2024).
Zerbst, U., Madia, M., Klinger, C., Bettge, D. & Murakami, Y. (2019). Defects as a root cause of fatigue failure of metallic components. III: Cavities, dents, corrosion pits, scratches. *Eng. Fail. Anal*., **97**: 759-776.

# COMPARISON ON HUMAN VIBRATION EXPOSURE BETWEEN WHEELED AND TRACKED ARMOURED VEHICLES IN MALAYSIAN TROPICAL ENVIRONMENT

Fadzli Ibrahim*, Ezza Nur Adzlilliya Azali & Shamsul Akmar Ab Aziz

Mechanical & Aerospace Technology Division, Science and Technology Research Institute for Defence (STRIDE), Ministry of Defence, Malaysia

*E-mail: fadzli.ibrahim@stride.gov.my

**ABSTRACT**

*Personnel who are assigned to driving for long periods of time can be exposed to whole-body vibration (WBV) and hand-arm vibration (HAV) directly to the body through the driver's seat and steering wheel. This paper will evaluate the comparison of WBV and HAV exposure for military vehicle drivers for wheeled and tracked armoured vehicles in Malaysian tropical environments. The study is performed on a Malaysian highway with tarmac road surface for different speed ranges. The results show that tracked vehicles contribute to higher WBV and HAV exposure as compared to wheeled vehicles especially when the vehicle is moving. These readings do not exceed the daily exposure limit values set by the European Directive Physical Agent (Vibration) 2002/44/EC. However, for tracked vehicles, the daily exposure action values are exceeded during cruising, indicating that an action plan must be implemented to prevent the exposure from exceeding the exposure limit values.*

**Keywords**: *Human comfort; armoured vehicles whole-body vibration (WBV); hand-arm vibration (HAV); tropical environment.*

## 1. INTRODUCTION

In human vibration, the human body acts as a mechanical structure to allow vibration to spread until the mechanical coupling is lost and the vibration is no longer propagating. According to the European Directive Physical Agent (Vibration) 2002/44/EC (EU-OSHA, 2002), human vibration can be classified as either hand-arm vibration (HAV) or whole-body vibration (WBV) where HAV is vibration that is transmitted to the human hand-arm system and can cause deficits in sensory perception, reduced muscle strength in forearms and tendonitis in wrist, elbows, or shoulders (Dong *et al*., 2021) while WBV is vibration that is transmitted to the whole body and can cause hyperventilation syndrome, cramps, mental fatigue and affect biodynamic response of the spine (Marieke *et al*., 2021)

Human vibration occurs in a moving vehicle when ground vibration is generated from the engine, and the interaction between tyres and road surface transmits from the components in-contact, such as car seat, steering-wheel and floor, to the human body (Krylov *et al*., 2007; Wang *et al.*, 2020). In the idle condition, the source of vibration is commonly from the engine (Shen *et al*., 2020). Normally, the car seat is the component with the widest contact area with the passenger and hence directly influences driving comfortability due to vibration exposure (Luo *et al*., 2023). This vibration is dependent on several factors such as type and particularities of the road, suspension type, as well as type of vehicle and load (Voicu *et al*., 2023). In addition, the posture of the driver also contributes to the level of vibration exposure (Raffler *et al*., 2016).

In military settings, vibration exposure is critical considering heavy-duty vehicle design with massive loads and mounts for equipment, operation of military vehicles in adverse environmental conditions, as well as posture of the personnel during the operation that sometimes requires standing and being unfastened. Zafer & Aybar (2022) found that the main source of vibration in tracked armoured vehicles is the running gear system, which includes moving tracks, sprockets, support rollers and idler wheels. As military vehicle vibrations are amplified by these factors, prolonged exposure to excessive vibrations can reduce the fatigue life of parts and components, leading to operational unreliability (Kashyzadeh *et al.*, 2015; Li *et al.*, 2022). In some cases, it will aggravate the vibration, such as worn-out engine mounting due to friction-vibration effects (Jaiswal, 2014). In regards to human vibration, Katu *et al.* (2003) found that personnel exposed to such vibration are prone to increased discomfort, while Mohammad *et al*. (2016) established that vibration poses risks to safety and health, including head, lumbar and organ pain, as well as fatigue. These factors contribute to decrease in personnel attention, thus affecting performance during operations (Park *et al.*, 2019).

In tropical countries, vibration levels in military vehicles are important to be assessed considering the high possibility of adverse vibration levels due to vehicle design requirements and road surface irregularities. Malaysia, as a tropical country with a variety of landforms, provides challenges to military vehicle manufacturers in ensuring that the comfort level of the driver and crew is at the optimum level (King *et al.* 1998, 2006; Aziz & Ibrahim 2022). The design requirements of military vehicles also emphasise on heavy duty and off-road usage that will intensify vibration levels, such as the usage of tracks instead of wheels in armoured vehicles (Zafer & Aybar, 2022). These inevitable contributing factors highlight the need to test vehicles to ensure that precautions and countermeasures can be taken. The assessment of vibration levels in vehicles can be carried out in accordance with ISO 2631-1: 1997 for WBV (ISO, 1997) and ISO 5349-1 for HAV (ISO, 2001). In addition, the European Directive 2002/44/EC (EU-OSHA, 2002) provides a guideline on requirements for WBV and HAV.

Various assessments and studies have been conducted for WBV and HAV in vehicles. Khan *et al.* (2010) found that differences in road surfaces has significant impact on WBV readings in the vehicle cabin. It was demonstrated that rough road conditions exhibit higher WBV readings as compared to smoother tarmacs. Wang (2010) explained that different types of vehicles and engine configurations produce different vibration exposures to the driver. Aziz *et al*. (2014) conducted a study on HAV for steering wheels of three-tonne trucks used by the Malaysian Army (MA). They investigated the speed-vibration relationship under various road conditions, noting that vibration levels increased with speed. This finding is valid for asphalt, bumpy and Belgian road surfaces, but not for block road surfaces, where vibration is inversely proportional to speed (Yoo *et al*., 2011; Aziz *et al.*, 2017). Given that road surface irregularity is a major contributing factor to vibration, the dynamic nature of tyres plays a significant role to counter the issue. While Stosiak *et al.* (2023) found high levels of vibration for different types military vehicle applications, Zafer & Aybar (2022) noted that the severity of vibrations encountered in armoured track vehicles is much higher as compared to those in wheeled vehicles.

There are two types of armoured vehicles used by the Malaysian Armed Forces (MAF), which are wheeled armoured vehicles that are primarily deployed in all-terrain conditions, and tracked armoured vehicles that are mainly utilised for off-road operations. This study aims to establish a database focusing on MAF vehicles, specifically concerning human vibration in Malaysia's tropical environment. Conducted by the Science & Technology Research Institute for Defence (STRIDE), the study involved comprehensive tests on several MAF vehicles during their evaluation and acceptance phases as part of the procurement process. In order to ensure relevance to current military vehicle technologies, the data collection focused on vehicles from the year 2020 onwards. This study specifically focuses on human vibration tests, encompassing WBV and HAV. Its objective is to analyse the patterns of vibration exposure within the cabins of military vehicles during idling and cruising. Subsequently, it aims to assess human vibration levels for compliance with international standards, considering Malaysia's weather and topography.

## 2. RESEARCH METHODOLOGY

This study was conducted on a Malaysian highway with a tarmac road surface. This is due to the fact the test procedure only applies to paved roads and there is no specific method for unpaved roads. All the tests were conducted while the vehicle was idle as well as cruising at multiple speed ranges, i.e., 60-100 km/h for armoured wheeled vehicles and 20-50 km/h for armoured tracked vehicles. The speed selection was based on engine power and the maximum speed allowed for heavy vehicles on Malaysian highways under the Road Transport Act 1987.

### 2.1 Whole-Body Vibration (WBV)

The measurement of WBV in the cabin was performed using a seat pad containing a tri-axial piezoelectric accelerometer that was connected to a SVANTEK SV 106A vibration analyser, which logged the total vibration level in each axis. Calibration of the accelerometer was performed prior to all data collections using a vibration calibrator with calibration reference acceleration level of 10 $m/s^2$ and calibration reference frequency of 159.2 Hz, which is the point in the calibration with the lowest uncertainty and the response is flat (SVANTEK, 2015). At these calibration reference values, the measurement uncertainty is the lowest and the response is flat.

The procedure for the measurement and assessment of human exposure to WBV is specified in ISO (1997), while compliance with daily exposure limits is based on EU-OSHA (2002). Exposure to individual sources of constant WBV was calculated from the magnitude of the vibration, expressed as acceleration in $m/s^2$, and the duration of exposure. The daily vibration exposure, A(8) is the amount of vibration to which a driver or crew is exposed during a working day, normalised to an 8 h reference period. A(8) can be calculated using the following equation:

$$A(8) = a_w \sqrt{\frac{T}{T_0}} \qquad (1)$$

where $\boldsymbol{a_w}$ is the vibration magnitude (in $m/s^2$) on the axis that was measured, $T$ is the actual duration of exposure to $\boldsymbol{a_w}$ in hours, and $T_o$ is the reference duration of 8 h.

### 2.2 Hand-Arm Vibration (HAV)

Human exposure to HAV was assessed based on ISO (2017), while compliance with daily exposure limits was based on EU-OSHA (2002), with daily exposure action value of 2.5 $m/s^2$ and daily exposure limit of 5 $m/s^2$. The measurement was performed at the interface between the driver's hands and steering wheel. The calibrated hand-arm accelerometer was connected to the vibration analyser and a transducer was mounted on hand-arm measurement adapters positioned close to the usual hand grip position.

All three axes were used for frequency weighting when determining the overall HAV value. The three frequency weighted acceleration components, denoted as $a_{hx}$, $a_{hy}$ and $a_{hz}$, were combined to give the total HAV value, $a_h$ ($m/s^2$). The root sum of the three components with the weighting factor of $k$ =1.0 for each axis can be calculated using the following equation:

$$a_h = \sqrt{(k\,a_{hx})^2 + (k\,a_{hy})^2 + (k\,a_{hz})^2} \qquad (2)$$

The daily vibration exposure is standardised to a reference period of 8 h:

$$A(8) = a_h \sqrt{\frac{T}{T_0}} \tag{3}$$

where $T$ is the actual duration of exposure to the vibration magnitude $a_h$ in hours and $T_0$ is the reference duration of 8 h.

## 3. RESULTS AND DISCUSSION

### 3.1 Whole-Body Vibration (WBV)

Figure 1 shows the average WBV values for wheeled and tracked armoured vehicles under different conditions: idle, at cruising speeds of 20-30 and 40-50 km/h for tracked vehicles, and at cruising speeds of 60-100 km/h for wheeled vehicles. In general, it is found that tracked vehicles have higher WBV as compared to wheeled armoured vehicles. This is as tracked armoured vehicles consist of running gear systems that predominantly contribute to higher vibration levels, especially while driving, as compared to wheeled armoured vehicles. This is consistent with the findings observed in Zafer & Aybar (2022), which suggested that running gear systems are the main source of vibration in tracked armoured vehicles. For wheeled vehicles, the graph shows that WBV increases with vehicle speed, with the WBV values at the idle condition and cruising speed of 60-100 km/h being 0.05 and 0.37 $m/s^2$ respectively. These WBV values are considered as benign, as it is well below the daily exposure action value of 0.5 $m/s^2$ and the daily exposure limit value of 1.15 $m/s^2$ (EU-OSHA, 2002).

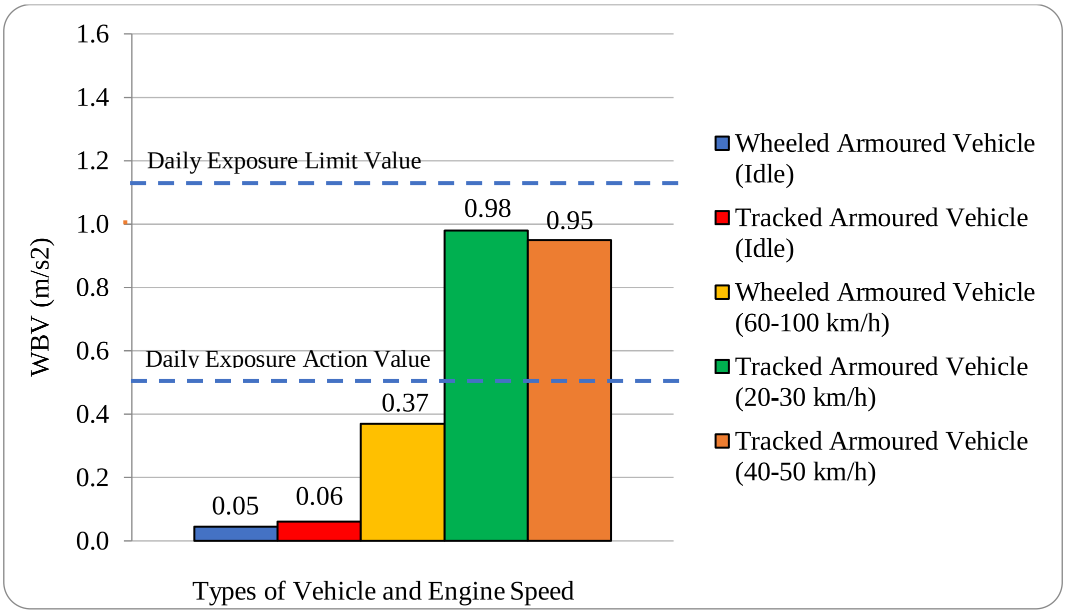


**Figure 1: WBV for different types of evaluated vehicles.**

In contrast, for tracked vehicles, inconsistency is found in the relationship between WBV and vehicle speed. At the idle condition, WBV is 0.06 $m/s^2$ and increases up to 0.98 $m/s^2$ for cruising speed of 20-30 km/h. At cruising speed of 40-50 km/h, WBV drops to 0.95 $m/s^2$. This indicates that WBV is indirectly proportional to speed when the vehicle is travelling at cruising speed. This is as for the tensioning systems of idler pulleys, higher vehicle speed leads to lower tension of the chains. This contributes to increase in slippage, which minimises frictional vibrations between the parts of the suspension system (Balamurugan *et al.*, 2017). Consequently, WBV decreases with increasing speed.

For the tracked vehicle, at cruising speeds of 20-30 and 40-50 km/h, while the WBV values are below the daily exposure limit value, they exceed the daily exposure action value, indicating that an action plan must be implemented to prevent the exposure from exceeding the exposure limit values (EU-OSHA, 2002).

### 3.2 Hand-Armed Vibration (HAV)

Figure 2 shows the average HAV values for wheeled and tracked armoured vehicles under different conditions: idle, at cruising speed of 20-30 and 40-50 km/h for tracked vehicles, and at cruising speed of 60-100 km/h for wheeled vehicles. Based on the graph, the HAV values for both types of vehicles increase with increasing speed, with tracked vehicles having higher HAV values as compared to wheeled vehicles, except when idling. A comparable result was reported by Aziz *et al.* (2015), where a regression model was used to observe the relationship between vehicle speed and HAV exposure. Similar to WBV, the pattern of HAV from wheeled vehicles shows that HAV increases relative to vehicle speed, with HAV increasing from 0.26 $m/s^2$ at idle to 0.60 $m/s^2$ at cruising speed of 60-100 km/h. Both values are well below the daily exposure action value of 2.5 $m/s^2$ and the daily exposure limit value of 5 $m/s^2$.

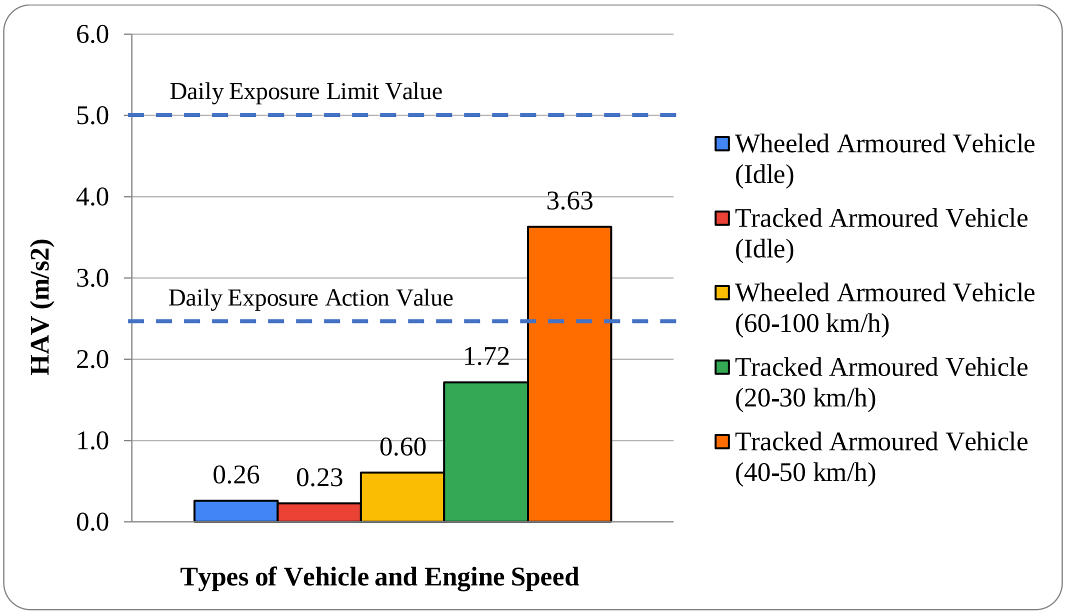


**Figure 2: HAV for different types of evaluated vehicles.**

The same pattern can also be observed for armoured tracked vehicles. However, the HAV values during cruising are significantly higher, with the values for cruising at speeds of 20-30 km/h and 40-50 km/h being 1.72 and 3.63 $m/s^2$ respectively. At speed of 40-50 km/h, while the HAV value are below the daily exposure limit value, it exceeds the daily exposure action value.

## 4. CONCLUSION

WBV and HAV in military vehicles are largely influenced by vehicle design, in particular the components that come into contact with the road while driving, while when in the idle condition, the source of vibration is mainly from the engine. Both the WBV and HAV results show that vibration levels are higher while cruising than when idling, due to additional contributing factors such as tyre-road interaction. It is also found that tracked armoured vehicles contribute to higher WBV and HAV exposure as compared to wheeled armoured vehicles especially when the vehicle is moving. Normally, most studies show that human vibrations are proportional to increase in speed. However, in this study, this was not the case for the WBV of tracked armoured vehicles due to the mechanism of the tensioning systems of idler pulleys.

The WBV and HAV values for both types of vehicles do not exceed the daily exposure limit values specified in the European Directive 2002/44/EC. However, for the tracked vehicle, the daily action limit values are exceeded, indicating that an action plan must be implemented to prevent the exposure from exceeding the exposure limit values. Among the steps that should taken include proper and regular maintenance of the vehicles and machineries to minimise vibrations caused by mechanical issues. Wheels and tracks also should also be well balanced and aligned to reduce vibration. In addition, personal protective equipment, such as anti-vibration gloves and vibration-absorbing seat cushions, can be used to reduce the effect of vibration on personnel.

In this study, the WBV and HAV of armoured wheeled vehicles and armoured tracked vehicles were measured at different cruising speeds, as wheeled and tracked vehicles can generally reach different maximum speeds due to different operational requirements and vehicle designs. Therefore, the comparison of the vibration data for both vehicle types is not a direct comparison. Nonetheless, the data generally provides an overview of the WBV and HAV patterns for both vehicle types.

## REFERENCES


Aziz, S.A.A., Nuawi, M.Z. & Nor, M.J.M. & Daruis D.D.I (2014). Determination of dominant axis for hand arm vibration (HAV) n Malaysian army three-tonne truck steering wheels. *Aus. J. Basic Appl. Sci.*, **8**: 14-16.

Aziz, S.A.A., Nuawi, M.Z. & Nor, M.J.M. (2015). New regression model for predicting hand-arm vibration (HAV) of Malaysian Army (MA) three-tonne truck steering wheels. *J. Occup. Health.* **57**: 513-520.

Aziz, S.A.A., Nuawi, M.Z. & Nor, M.J.M. (2017). Monitoring of hand-arm vibration. *Int. J. Acoust. Vib.*, **22**: 34-43.

Aziz, S.A.A. & Ibrahim. F. (2022). Study on braking efficiency of military armoured vehicles in Malaysian tropical environment. *Defence S&T Tech. Bull.*, **15**: 28–33.

Aziz, S.A.A., Nuawi, M.Z. & Nor, M.J.M. (2016). Predicting whole-body vibration (WBV) exposure of Malaysian Army three-tonne truck drivers using integrated kurtosis-based algorithm for Z-notch. filter technique 3D (I-Kaz 3D). *Int. J. Ind. Ergon.*, **52**: 59–68.

Balamurugan, S. & Srinivasan, R. (2017). Tracked vehicle performance evaluation using multi body dynamics. *Defence Sci J.*, **67**: 476-480.

Dong, R. G., Wu, J. Z., Xu, X. S., Welcome, D. E., & Krajnak, K. (2021). A review of hand–arm vibration studies conducted by US NIOSH since 2000. *Vib*, **4**: 482-528.

EU-OSHA (European Agency for Safety and Health at Work) (2002). *Directive 2002/44/EC: On the Minimum Health and Safety Requirements Regarding the Exposure of Workers to the Risks Arising from Physical Agents (Vibration)*. European Agency for Safety and Health at Work (EU-OSHA), Bilbao, Spain.

ISO (International Organization for Standardization) (1997). *ISO 2631-1:1997: Mechanical Vibration and Shock — Evaluation of Human Exposure to Whole-Body Vibration — Part 1: General Requirements.* International Organization for Standardization (ISO), Geneva, Switzerland.

ISO (International Organization for Standardization) (2001). *ISO 5349-1:2001: Mechanical Vibration — Measurement and Evaluation of Human Exposure to Hand-Transmitted Vibration — Part 1: General Requirements*. International Organization for Standardization (ISO), Geneva, Switzerland.

Jaiswal, S., Singh, A. & Kashinakunti, G. (2014). *Numerical Failure Investigation for Feasibility of Advanced Composite Automotive Engine Mounts Subjected to Dynamic Loads* (No. 2014-28-0028). SAE International, Warrendale, Pennsylvania, US.

Kashyzadeh, R.K., Ghorabi, M.J.O.A. & Arghavan, A. (2015). Fatigue life prediction of package of suspension automotive under random vibration based on road roughness. *Med. J. Model. Simul,*. **4**, 37-50.

Katu, U. S., Desavale, R. G. & Kanai, R. A. (2003). Effect of vehicle vibration on human body – RIT experience. *Proc. 11$^{th}$ Nat. Conf. Mach. Mech*., 18-19 December 2003, New Delhi, India.

Khan, M.K.J., Gani. A., Aziz, S.A.A. & Hassan, A.H., (2010). Determination of whole-body vibration (WBV) of main battle tank (MBT) PT-91M. *Defence S&T Tech. Bull.*, **3**: 29–35.

King, W.C., Harmon, R., Juvik, J., Hendrickx, J.M.H. & Palka, E.J. (2006). *A Technical Analysis of Suriname for Tropical Testing of Army Materiel and Systems*. United States Army Research Office, North Carolina, US.

King,W.C., Harmon, R., Bullard,T., Dement,W., Doe, W., Evans, J., Larsen, M.C., Lawrence, W., McDonald, K. & Morrill, V. (1998). *A Technical Analysis to Identify Ideal Geographic Locations for Tropical Testing of Army Materiel and Systems*. United States Army Research Office, North Carolina, US.

Krajnak, K. (2018). Health effects associated with occupational exposure to hand-arm or whole-body vibration, *J. Toxicol. Env. Heal B,* **21**: 320–334.

Krylov, V. V., McNuff, J. & Pickup, S. (2007). Theoretical prediction of ground vibrations from heavy military vehicles. *Proc. 11$^{th}$ Nat. Conf. on Acoust.*, 2-7 September 2007. Madrid, Spain,

Li, F., Wu, H., Liu, C., Wu, P. & Zeng, J. (2022). Vibration fatigue analysis of high-speed railway vehicle carbody under shaking condition. *Vehicle Syst. Dyn.*, **60**: 1867-1887.

Luo, Q., He, Y., Zhang, Z. & Gao, K (2013). Transmission of vertical vibration through a seat cushion at the seat pan: Effect of foam physical properties during different excitation magnitudes. *J. Low. Freq. Noise V.A*., **43**: 144-155.

Mansfield, N. (2017). Vibration and shock in vehicles: new challenges, new methods, new solutions. *1$^{st}$ Intl. Comfort Cong.*, 7-8 June 2017, Salerno, Italy

Marieke J. G. V. H., Rittweger, J., Judex, S., Sañudo, B., Seixas, A., Fuermaier, A. B., & Van Der Zee, E. A. (2021). Reporting guidelines for whole-body vibration studies in humans, animals and cell cultures: A consensus statement from an international group of experts. *Biol.*, **10**: 965.

Mohammad, A., Walaa, A., Hani, E., Mohammad, O., Mohammed, B. & Andrew, G. S. (2016). Effect of mechanical vibrations on human body. *World J. Mech*, **6**: 273-304

Mohammadian, F., Nasiri, P., Giahi, O., Rezvani, Z., Kangavari, M., Rafieepour, A. (2015). Effects of noise and whole-body vibration on individual's mental performance, *Int. J. Occup. Hyg*., **7**: 209–214.

Nakashima, A. M. (2005). Whole-body vibration in military vehicles: a literature review. *Can. Acoust.* , **33**: 35-40.

Park, D. J., Choi, M. G., Song, J. T., Ahn, S. J. & Jeong, W. B. (2019). Attention decrease of drivers exposed to vibration from military vehicles when driving in terrain conditions. *Int. J. Ind. Ergonom..*, **72**: 363-371.

Raffler, N., Ellegast, R., Kraus, T., & Ochsmann, E. (2016). Factors affecting the perception of whole-body vibration of occupational drivers: an analysis of posture and manual materials handling and musculoskeletal disorders. *Ergon.*, **59**, 48-60.

Shen, H. M., Tang, P., Bian, F., Wu, X. W., Zhao, W. J., & Hu, L. L. (2020). An experimental study of vehicle 1st order vibration improvement at engine idle. *Int. J. Acoust. Vib*., **25**: 542-548.

Stosiak, M., Karpenko, M., Prentkovskis, O., Deptuła, A. & Skačkauskas, P. (2023). Research of vibrations effect on hydraulic valves in military vehicles. *Defence Tech.*, **30**: 111-125.

SVANTEK. (2015). *SVANTEK User Manual: SV 110 Portable Vibration Calibrator.* SVANTEK, Warsaw, Poland.

Voicu, D., Stoica, R. M., Vilău, R., Marinescu, M., Digulescu, A., Despina-Stoian, C. & Popescu, F. (2023). Frequency analysis of vibrations in terms of human exposure while driving military armoured personnel carriers and logistic transportation vehicles. *Elec.*, **12**, 3152-3170.

Wang, X. (2010). *Vehicle Noise and Vibration Refinement*. Woodhead Publishing Limited, UK.

Wang, X., Osvalder, A., Höstmad, P., and Johansson, I. (2020). *Human Response to Vibrations and Its Contribution to the Overall Ride Comfort in Automotive Vehicles - A Literature Review* (No. 2020-01-1085). SAE International, Warrendale, Pennsylvania, US.

Yoo, W. S., Na, S. D. & Kim, M. S. (2011). Relationship between subjective and objective evaluations of steering wheel vibration. *J. Mech. Sci. Tech.*, **25**: 1695-1701.

Zafer, N. & Aybar, U. (2022). Vibration Analysis and Optimization of a Tracked Armored Vehicle. *J. Vib. Eng. Tech.*, **11**: 3177-3184.

# A REVIEW OF DECONTAMINATION TECHNIQUES FOR ORGANOPHOSPHATE COMPOUNDS: CURRENT METHODS AND FUTURE DIRECTIONS

Nur Shazwani Abdul Latif[1*], Wan Md Zin Wan Yunus[2], Hafizah Ariff[1], Alinda Samsuri[1], Rauda A. Mohamed[3], Nurnadia Andenan[4], Noor Azilah Mohd Kasim[5], Ong Keat Khim[5] & Victor Feizal Abd Shattar Knight[6]

[1]Centre for Tropicalisation, Defence Research Institute, Universiti Pertahanan Nasional Malaysia (UPNM), Malaysia
[2]Faculty of Defence Science and Technology, Universiti Pertahanan Nasional Malaysia (UPNM), Malaysia
[3]School of Applied Sciences, Nilai University, Malaysia
[4]Centre for Research and Innovative Management, Universiti Pertahanan Nasional Malaysia (UPNM), Malaysia
[5]Centre for Defence Foundation Studies, Universiti Pertahanan Nasional Malaysia (UPNM), Malaysia
[6] Research Centre for Chemical Defence, Universiti Pertahanan Nasional Malaysia (UPNM), Malaysia

[*]Email: shazwani@upnm.edu.my

## ABSTRACT

*Organophosphates (OPs) have been utilised as pesticides in agricultural contexts for many years. Nevertheless, due to their high levels of toxicity, these substances are also illicitly produced into hazardous chemical weapons, posing a threat to both humans and the environment. As a result of its impact on public safety and overall welfare, this subject has gained international attention. Improper handling or intentional self-harm can result in the penetration of toxic compounds through the skin, leading to acute toxicity that can potentially progress to fatality. Therefore, in such critical situations, implementing a rapid and effective method of decontamination for these compounds is to reduce the risk of intoxication. There are a number of methods for decontaminating OPs, including physical, chemical and biological methods. However, no single method is universally effective, and there are still challenges in developing effective decontaminating agents against OPs. Therefore, given the availability of various decontamination agents, this paper will discuss on recent advances in the development of decontaminating agents for OPs and their effectiveness on OP compounds with highlights of future strategies to develop decontaminating agents that are safe, reliable and efficient to be used under various circumstances.*

**Keywords:** *Organophosphate (OP) compounds; OP poisoning; decontamination agents; degradation; neutralisation.*

## 1. INTRODUCTION

Organophosphate (OP) chemicals have been widely used around the world for many years, particularly in agriculture, where they are used as pesticides to protect crops. OP pesticides have become widely used worldwide, which accounts for 45% of total global market usage (Mali *et al.*, 2023). Although these pesticides have numerous benefits, the major concern is that these compounds are highly toxic to both humans and the environment due to their ability to inhibit acetylcholinesterase enzyme. This could eventually lead to acetylcholine accumulation at synapses in both the central and peripheral nervous systems, which results in serious health problems (Ganie *et al.*, 2022). Kamaruzaman *et al.* (2020) found that agricultural insecticides, particularly OPs, are the second most common type of pesticides involved in pesticide poisoning incidents, accounting for 34% of incidents and ranking in the top 40% of OP poisoning cases. Furthermore, 20% of all suicides globally involve deliberate ingestion of pesticides, with the majority of incidents occurring in developing countries (Pathak *et al.*, 2022). The data suggests that pesticide poisoning incidents involving OP pesticides are common, hence, it is crucial to develop and implement effective strategies to minimise the use and impact of these pesticides, as well as ensuring the safety of those who handle them.

In the late 1930s, during World War II, due to the high toxicity effect of OP compounds, the German army created neurotoxins from OPs (Gupta, 2020). These neurotoxin agents were developed as chemical nerve agents to be used as chemical weapons in wars. These chemical nerve agents are extremely toxic, which can be disseminated in liquid, gas or aerosol form (Ganesan *et al.*, 2010). Despite being banned by the Chemical Weapons Convention, OPs are still synthesised on a large scale and used during military crises and terrorist attacks. In fact, the rate of their production and use seems to have increased in recent years. Stockpiles of these chemical weapons are still available since the synthesis routes of different nerve agents have been published in open literature (Worek & Thiermann, 2013; Collina, 2013; Worek *et al.*, 2020). In fact, due to their readily available raw materials, relative inexpensiveness, ease of production and extreme toxicity effects, small terrorist groups can use them to cause mass casualties (Ganesan *et al.*, 2010; Valiveti *et al.*, 2015). There have been recent incidents of chemical warfare agents causing public fatalities, such as the Sarin attacks in Japan (1994 and 1995), VX assassination in Kuala Lumpur, Malaysia (2017), and Novichok poisoning in Salisbury, United Kingdom (2018) (Picard *et al.*, 2019).

OP poisoning is a severe toxicity caused by exposure through ingestion, inhalation and dermal absorption of OP compounds commonly present in pesticides and chemical warfare agents (Roby *et al*., 2018; Bhadesiya *et al*., 2020). The high toxicity of OPs can be life-threatening as the compounds ease in skin permeation, with the clinical signs of sweating, salivation, diarrhoea, muscle tremors and confusion rapidly appearing, with the acute effects progressing swiftly, potentially resulting in death if not treated instantly (Kassa *et al.*, 2015; Robb & Baker, 2022). The onset of symptoms is influenced by various factors such as the amount of agent absorbed through the skin, which is dependent on exposure area, agent concentration and exposure conditions (Thors *et al.*, 2020). Determining an effective antidote for OP poisoning remains a challenge, with no optimum solution discovered to date (Bušić *et al.*, 2016). In cases of both external and internal exposure to OPs, prompt measures can significantly reduce the extent and severity of exposure. At the moment, clinically, administration of atropine and oxime injection such as 2-pralidoxime (2-PAM) is essential to reactivate acetylcholinesterase and restore the patient to normal condition (Alnoaimi, 2024). Nevertheless, immediate application of decontamination procedure is essential to mitigate the risk of exacerbating the condition prior to poisoning. Magnano *et al.* (2021) found that the most effective method of reducing the risk of intoxication is through rapid skin decontamination. Ideally, the decontamination agent used should be quick and easy to apply, efficient, environmentally safe and cost effective, as per Federal Drug Administration (FDA) guidelines for various classes of chemical agents (Clarkson & Gordon, 2020).

Therefore, this paper comprehensively discusses the efficiency of various conventional decontaminating agents in the remediation of OP compounds, covering chemical, biological and physical methods. Additionally, it also explores current advances to the decontamination methods and future perspectives, to enhance decontamination efficiency and sustainability. By reviewing the current state and future directions of OP decontamination, this paper aims to contribute to mitigating OP exposure risks and promoting safer remediation strategies.

## 2. METHODS FOR DECONTAMINATION

Effective decontaminating agents play a vital role in mitigating the harmful effects of exposure to OPs. The decontaminating agents work by neutralising or removing the contaminants from surfaces preventing from further absorption of the toxic compounds into the body system. The currently utilised approaches for decontaminating OPs can be categorised into three main groups, which are physical, chemical and biological (Jacquet *et al.*, 2016; Ore *et al.*, 2023), as illustrated in Figure 1.

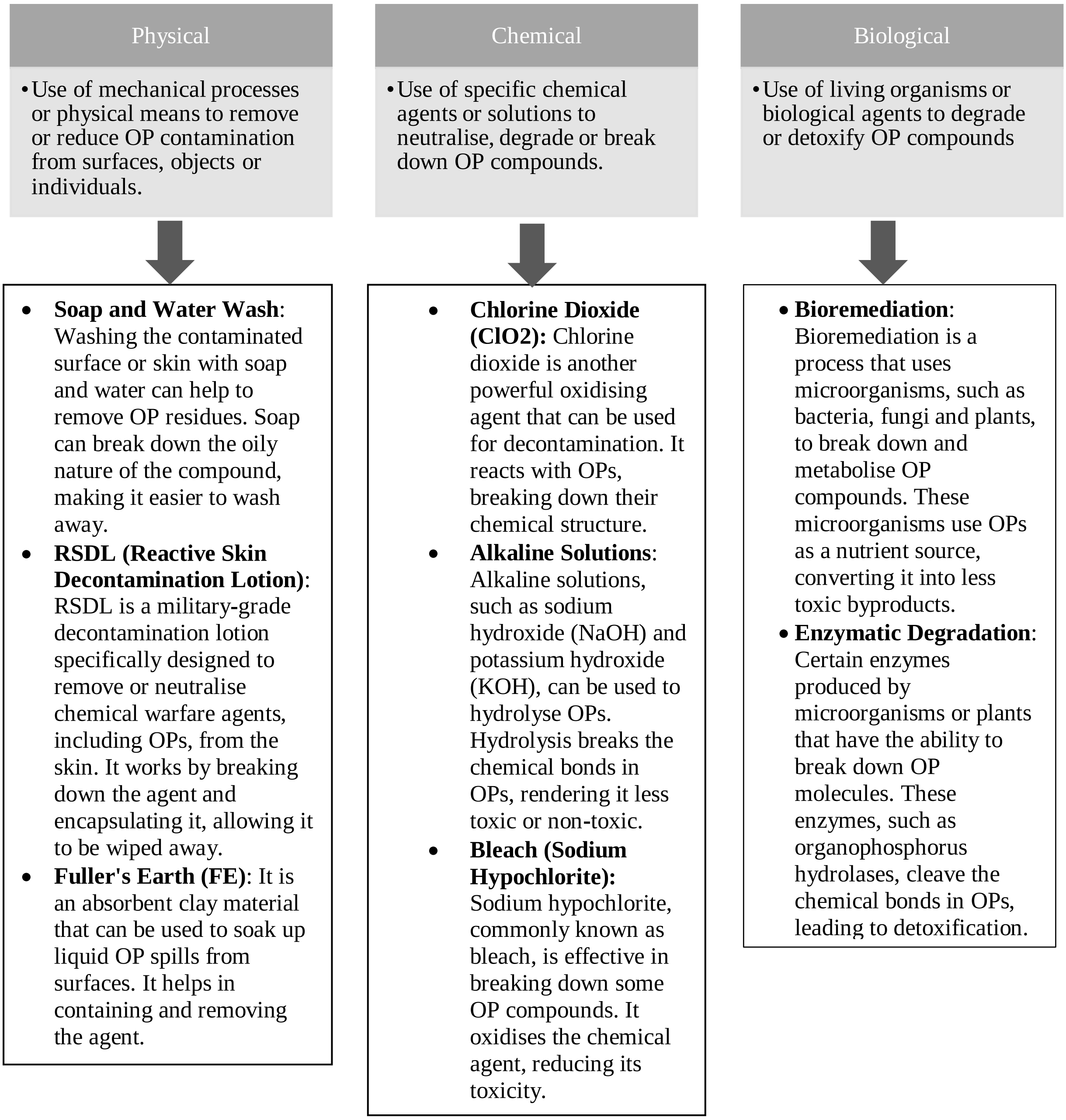


**Figure 1: Types of decontamination agents.**

## 2.1 Physical Decontamination

Physical decontamination is the first phase of elimination or decomposition of toxic and dangerous substances into harmless products from individuals, equipment and the environment (Eid *et al.*, 2020). During the initial moments of exposure, immediate and effective decontamination steps are crucial to prevent OPs from further absorbing into the skin. At this early stage of contamination, it is essential to physically remove the contaminant within minutes of exposure (Dachir *et al.*, 2021).

Physical decontamination against OP compounds focuses on the physical removal or destruction of these chemicals from surfaces, objects or the human body. One of the most common physical decontamination methods used against OPs is thorough washing or rinsing with copious amounts of water or with additional specialised decontamination additive solutions including soaps and detergents

(Amend *et al.*, 2020). The most cost-effective and environmentally safe options for decontamination are water-only and soapy water hydrolysis (Schwartz *et al.*, 2012; Lin *et al.*, 2017). This mechanism of water decontamination exploits the inherent reactivity of water molecules to break down the chemical structure of OP compounds, rendering them less harmful (Zhang *et al*., 2022). It is a cost-effective and environmentally safe method that can be readily applied in various decontamination scenarios. Additionally, the use of detergents or soaps aids in breaking down and emulsifying the compounds, further enhancing their removal (Mijaljica *et al.*, 2022). However, Forsberg (2020) found that skin decontamination using soapy water can result in dramatically increased penetration rate for OPs. This is due to the wash-in effect that occurs when the soapy water solution does not adequately penetrate or interact with OP residue, resulting in incomplete decontamination (Chiang *et al*., 2021). This can leave behind traces of OP compounds, which can pose continued risks of exposure and potential harm.

Another commonly applied physical decontamination method is reactive skin decontamination lotion (RSDL), available in lotion or gel form. It effectively removes and neutralises a wide range of chemical contaminants by binding to and absorbing harmful substances on the skin's surface, thereby minimising their absorption into the body. Schwartz *et al.* (2012) found that RSDL is particularly effective against OPs, including VX, as compared to 1% soapy water. Its compact size and portability make it convenient for diverse scenarios, including military operations, industrial accidents or chemical spills. However, RSDL is primarily intended for intact skin and may not be suitable for open wounds or sensitive areas due to potential irritation or adverse reactions (Connolly *et al*., 2020). Furthermore, Magnano *et al*., (2021) found that while RSDL's is effective in removing toxins even when applied up to 60 min after contact, but it loses effectiveness at 90 and 120 min. Therefore, situations involving extensive contamination or more resilient chemical agents may require additional and more thorough decontamination procedures.

Fuller’s earth (FE) is a naturally occurring clay material known for its excellent absorbing and purifying properties. For centuries, it has been used in the wool fulling process to cleanse wool by removing oils, dirt and impurities. Besides its traditional role in textile processing, FE is valued for its cost-effectiveness and availability. Composed of layers with high ion exchange capacities, FE facilitates interaction with OPs, making it ideal for decontaminating and purifying OPs (Danoy *et al*., 2022). FE suspension has proven to be a rapid and reliable method for skin decontamination as compared to free powder form and water solutions (Roul *et al.*, 2020; Danoy *et al*., 2022; Robb & Baker, 2022). However, due to its powerful oil-absorbing properties, excessive use of FE may cause dryness and irritation to the skin. Therefore, it may not be suitable as a primary skin decontamination tool, especially for those with sensitive skin. Another critical consideration in decontamination is ensuring the safety of the surrounding area affected by contamination. While FE effectively captures and contains contaminants due to its high adsorption capacity, it lacks degradation properties (Thors *et al*., 2017a). This limitation means that while FE can remove harmful substances from the immediate environment, it cannot break them down (Magnano *et al.*, 2021). Consequently, the risk to the surrounding contaminated area and individuals nearby remains unresolved. Therefore, additional measures must be implemented to mitigate the persistent threat and ensure comprehensive safety.

## 2.2 Chemical Decontamination

Chemical decontamination refers to the use of specific chemical agents that can break down or neutralise the toxic properties of OPs. One of the commonly employed techniques is the use of oxidising agents such as chlorine bleach or chlorine dioxide, and hydrogen peroxide that can chemically react with OPs, converting them into less toxic derivatives (Roul *et al*., 2020). Hydrogen peroxide-based decontamination solutions can effectively decontaminate chemical warfare agents, such as VX (O-ethyl-S-(2-diisopropylaminoethyl-methylphosphothiolate) and Soman (GD), via perhydrolysis to their non-toxic phosphonates and HD by oxidation to its non-vesicant sulfoxide (Wagner, 2010; Zhao *et al*., 2020; Dong *et al*., 2021;). However, using hydrogen peroxide for decontaminating OPs may have limitations and potential risks, including incomplete decontamination, production of toxic byproducts, as well as skin and eye irritation (Oudejans *et al.*, 2020; Yang & Liu, 2021). Careful consideration of its effectiveness and safety is necessary in the decontamination process.

Another method used for skin decontamination is a 0.5% solution of household bleach containing sodium or calcium hypochlorite, followed by thorough rinsing with water (Clarkson & Gordon, 2020). Historically, these bleaching powders were the primary decontaminants used to neutralise chemical nerve agents. However, these chemicals may not be suitable for skin decontamination due to their moderate toxicity and potential adverse effects, including temporary redness, skin irritation and allergic reactions. Consequently, safer and more effective alternatives have been sought for decontamination purposes. Another chemical decontamination method commonly employed involves the use of alkalis or acids, such as sodium hydroxide (Vakhitova *et al.*, 2019). Sodium hydroxide reacts with OPs, breaking them down into phosphonic acids. Although most OP pesticides and nerve agents are rapidly neutralised at pH levels between 10 and 13 (Lockridge *et al*., 2019), this method is unfavourable due to the significant risk of chemical burns to the skin and eyes caused by the highly alkaline pH of the chemicals used (Clarkson & Gordon, 2020).

Furthermore, to combat a broad spectrum of OP compounds, U.S. and NATO forces have adopted commercially available products such as Decontamination Solution 2 (DS2), BX-24 and Decontamination Formulation DF-200, which have proven to be highly effective (Thakur *et al*., 2019). Unfortunately, these agents are considered unsafe due to their corrosive nature and generation of hazardous waste (Xu *et al.*, 2021). Therefore, there is an urgent demand for decontamination strategies that are non-toxic, non-corrosive and environmentally friendly.

## 2.3 Biological Decontamination

Biological decontamination is an innovative approach that utilises living organisms or biological agents to neutralise and degrade OPs. This method harnesses the natural capabilities of certain microorganisms or enzymes to break down and eliminate these toxic substances, offering a promising solution for managing organophosphate contamination. This approach is easy to use, environmentally friendly and cost-effective (Huang *et al.*, 2021).

Biological decontamination methods involve introducing specific microorganisms, such as bacteria or fungi, that possess the ability to degrade OPs. Several studies have showed that microbial enzymes (such as esterase enzymes from Pseudomonas sp. C11 and hydrolase enzyme from Arthrobacter sp. HM01) are directly use to remediate pesticides (OPs, pyrethroids and carbamide) in the environment (Mali *et al.*, 2023). Among the several IP degrading enzymes, the best characterised is the bacterial enzyme phosphotriesterase (PTE) (Dyguda-Kazimierowicz *et al.*,2014).

As compared to the previous physical and chemical decontamination strategies, one of the advantages of biological decontamination is its specificity and selectivity. Hydrolase, phosphotriesterase, and phosphatase enzymes from microorganisms target the P–O alkyl and aryl bonds of OPs and hydrolyse it (Kumar *et al*., 2018). Moreover, biological decontamination is often considered as an environmentally friendly approach (Pathak *et al.*, 2022). It takes advantage of natural processes and avoids the use of harsh chemicals or high-energy treatments. This reduces the potential negative impact on ecosystems and minimises the generation of hazardous by-products during the decontamination process (Javaid *et al.*, 2016).

## 2.4 Summary of Studies Conducted

Based on the literature, numerous studies have been conducted to evaluate the efficacy of different decontamination agents against different OP compounds. Table 1 summarises the studies conducted over the last five years.

**Table 1: Summary of studies conducted on the efficacy of decontamination agents against various OP compounds.**

| Authors | Decontaminants | Agents | Type of study | Findings |
|---|---|---|---|---|
| **Physical Decontamination** | | | | |
| Fentabil *et al.* (2020) | RSDL | Parathion and aldicarb pesticide | In vivo | This study assessed the efficacy of the RSDL against parathion and aldicarb pesticide dermal exposure in a guinea pig model and found that animals exposed to 749 mg/kg of Parathion died within 24 h without RSDL decontamination. RSDL-treated animals showed only mild signs of neurotoxicity. |
| Gebremedhin *et al.* (2020) | RSDL | Riot control agents (RCAs) | In vitro | RSDL lotion was found to be effective in degrading RCAs at certain molar ratios and reaction times. |
| Cao *et al.* (2018) | Dermal Decontamination Gel (DDGel) and RSDL | Diisopropyl methylphosphonate (DIMP) | In vitro | DDGel was found to be more effective in decontaminating the skin surface even as late as 90 min after skin exposure to the simulants. Both decontaminants removed more than 90% recovery dose of DIMP from the skin as compared to control group. |
| Thors *et al.* (2020) | RSDL | VX | In vitro | A slightly extended procedure for RSDL-decontamination is recommended for improved efficacy. The study found that prolonged skin contact time of RSDL is important for efficient decontamination of VX. The paper also highlights the importance of using low water content procedures for skin decontamination of nerve agents. |
| Danoy *et al.* (2022) | FE | Paraoxon | In vitro and In vivo | In presence of FE suspensions, disappearance of paraoxon from the stratum corneum was observed. Water potentiates the absorbing capacities of FE powder making FE aqueous suspensions as a safe tool for OP skin decontamination. |

| | | | | |
|---|---|---|---|---|
| **Chemical Decontamination** | | | | |
| Redy Keisar *et al*. (2021) | Hydrogel contains polyvinyl alcohol, borax and sodium perborate (NaBO3) | Sarin (GB), VX, and sulfur mustard (HD) | In vitro | This gel instantly forms and effectively sticks when sprayed on various matrices contaminated with the contaminants. It efficiently detoxifies GB, VX and HD to provide nontoxic products. |
| Kim & Lee (2020) | Montmorillonite-based acid-activated clay (AACL) | VX | In vitro | With optimised weight ratio of AACL to VX (40: 1), 99.6% of VX is chemically decontaminated within 10 min. AACL also shows good adsorption capacity for CWAs. |
| Qi *et al.* (2023) | Sodium percarbonate (SPC) complexed with 1-acetylguanidine (ACG) | HD and VX | In vitro | HD molecule was oxidised while VX molecule was oxidised and nucleophilic substituted after treated with SPC/ACG solution. 99% decontamination was achieved when the molar ratio of active oxygen to CWAs ((O)/(CWAs)) was at least 3 for HD and 7 for VX. |
| **Biological Decontamination** | | | | |
| Jacquet *et al*. (2021) | OPNA-degrading enzymes | G- agents, V- agents and Novichok agent | In vitro | Two enzymes (GG1 and GG2 engineered from Brevundimonas diminuta PTE (P0A434) can degrade most of these molecules (Cyclosarin, Sarin, Soman, Tabun and VX) at high concentrations (25 mM) in less than 5 min. The enzyme-based solutions can decontaminate 97.6% and 99.4% of 10 g·m2 of Soman- and VX-contaminated surfaces respectively, and also can degrade ethyl-paraoxon. |
| Moon *et al*. (2019) | Organophosphorus hydrolase | Methyl parathion | In vitro | 100% hydrolysis of methyl parathion into para- nitrophenol was observed after 24 h. |
| Bigley & Raushel (2019) | Bacterial enzyme phosphotriesterase (PTE) | GB | In vitro | Hydrolysis of organophosphates by PTE via direct nucleophilic attack of a hydroxide on the phosphorus centre and cleave the phosphorus oxygen bond. |
| Soares, Birolli, Ferreira & Porto (2021) | Marine-derived fungi *Aspergillus sydowii* CBMAI 935 | Chlorpyrifos, methyl parathion and profenofos | In vitro | Biodegradation of chlorpyrifos, methyl parathion and profenofos |

## 3. CHALLENGES OF DECONTAMINATION AGENTS

Decontaminating OPs remains a significant challenge due to the various limitations associated with existing decontamination methods. Physical, chemical and biological approaches often fail to effectively neutralise these toxic compounds. Due to the nature and wide variety of contaminants, each with unique characteristics and contamination mechanisms, there is no single approach that can be applied in all circumstances of contamination (Khan *et al*., 2013; Wong *et al*., 2020).

Physical decontamination is commonly associated with secondary contamination as it only physically removes the toxic compound. If the contaminants are embedded deeply in porous materials or adhere strongly to surfaces, contaminants still retain their harmful effects and can pose a threat if the decontaminated material is not disposed of safely. Moreover, the application of physical methods commonly requires a significant amount of water to rinse and remove chemicals from skin and hair, in which it can cause huge quantities of contaminated wastewater with additional economic burden for the industry and environment (Collins *et al*., 2021; Dallagi *et al*., 2023).

Chemical and biological methods also present substantial challenges. Chemical decontamination, utilising agents such as bleach and hydrogen peroxide may leave toxic residues, and excess usage have been associated with respiratory damage and increased risk of developing asthma (Dewey *et al.*, 2022). Additionally, the effectiveness of chemical agents can be compromised by the presence of interfering substances, such as organic matter, which can react with the decontaminants and reduce their efficacy (Cristale *et al*., 2017).

The efficacy of biological methods, which employ microorganisms or enzymes to degrade OPs, can vary significantly based on environmental conditions such as temperature and pH. These methods are often time-consuming, making them less viable for rapid response situations of decontamination (Pashirova *et al*., 2024). Moreover, the introduction of microorganisms into the environment raises concerns about potential ecological disruptions and unintended spread of non-native species (Sarker *et al*., 2024). Thus, the development of universally effective decontaminating agents against OPs remains a complex and multifaceted challenge, necessitating a combination of approaches tailored to specific contamination contexts.

## 4. RECENT ADVANCES AND FUTURE RECOMMENDATIONS

The success of decontamination depends not only on the decontaminating agent but also on the decontamination protocol, including the amount, concentration and application method (Dachir *et al*., 2020). Different outcomes were observed in studies with the same decontaminating agents but different protocols, as was demonstrated in the study by Taysse *et al.* (2017). Furthermore, the timing of decontamination application and duration of contact with the skin are also important factors. Thors *et al.* (2017b) found that early decontamination is crucial for preventing penetration of toxic compounds into the skin. Therefore, these factors should be included as important parameters in developing effective methods to decontaminate OPs.

To date, no single approach has been successfully reported as a universal decontamination agent. However, recent advancements have introduced innovative and more efficient approaches to OP decontamination, enhancing both effectiveness and safety as compared to conventional methods. The advancements summarised in Table 2 represent a significant leap forward in the field of OP decontamination, offering diverse and innovative solutions.

**Table 2: Recent advances in decontamination agents.**

| Agent | Mechanism of action | Advantages | References |
|---|---|---|---|
| Activated carbon from agricultural waste | Adsorbs OP compounds | Cost-effective, sustainable, easy to operate and eco-friendly | Ore *et al*. (2023) |
| Bioremediation / Engineered biocatalytic systems | OP degrading enzymes (PTE/OPH) | High catalytic activity to rapidly degrade / detoxify hazardous pesticides in the environment, and highly stable in harsh environmental conditions | Mali *et al*. (2023); Jaiswal *et al*. (2024) |
| Nanoparticles / nanomaterials | Oxidations and adsorption | High surface area, highly efficient and less reaction time | Boulkhessaim *et al*. (2022) |
| Photocatalytic | Oxidation and degradation | Economical, fast and efficient | Lakshmi *et al*. (2020); Fawad Ahmad (2022); Emmanuel *et al*., (2024) |
| Hydrogel-based systems | Perhydrolysis and oxidation | Universal decontamination abilities, mild nature and easy application | Redy Keisar *et al.* (2021) |

Future research in the field of OP decontamination should prioritise the development of multi-functional materials that not only adsorb OPs effectively but also possess degradation properties, providing a more comprehensive solution by both capturing and breaking down harmful substances. Modern approaches that involve the use of gels or polymeric films / coatings with addition of nanoparticles possess benefits to the decontamination strategy (Ginghină *et al*., 2022). In addition, innovations in nanotechnology hold significant promise, with nanoparticle-based adsorbents and catalysts potentially enhancing the efficiency and speed of OP removal (Hosseini & Salari, 2021; Boulkhessaim *et al.*, 2022). Exploring and engineering microorganisms or enzymes for biodegradation could also offer sustainable and eco-friendly decontamination methods, warranting optimisation for practical applications (Sheng *et al.*, 2022). Hybrid systems that integrate physical, chemical and biological decontamination approaches should be investigated to maximise efficiency and safety. Furthermore, advancements in real-time monitoring and control systems, including advanced sensors, could facilitate early detection and efficient management of contamination (Umapathi *et al.*, 2022). Addressing these areas will significantly advance the field, leading to safer and more effective methods for OP removal and improved protection of public health and the environment.

## 6. CONCLUSION

In conclusion, physical chemical and biological decontamination methods offer valuable approaches to mitigate the risks associated with OPs. Physical methods remove or contain the contamination, chemical methods neutralise or break down the compounds, and biological methods harness the natural capabilities of microorganisms or enzymes. Given the diverse nature and characteristics of contaminants, these conventional methods alone are often insufficient for comprehensive decontamination. Therefore, by advancing technologies, integrating these methods, and developing innovative agents, more effective and environmentally sustainable decontamination strategies can be developed to safeguard human health and mitigate the ecological impact of organophosphate contamination.

## ACKNOWLEDGEMENT

This work was supported by the Ministry of Higher Education (MOHE) through the Fundamental Research Grant Scheme (FRGS/1/2024/STG04/UPNM/01/1) and the National Defence University of Malaysia (UPNM) Short Term Grant (UPNM/2022/GPJP/SG/10).

## REFERENCES

Alnoaimi, M.M. (2024). Nerve-agent mass casualty incidents. In *Ciottone's Disaster Medicine* (3rd Eds.). Elsevier, pp. 679–685.

Amend, N., Niessen, K.V., Seeger, T., Wille, T., Worek, F. & Thiermann, H. (2020). Diagnostics and treatment of nerve agent poisoning—current status and future developments. *Ann. N. Y. Acad. Sci.*, **1479**: 13–28.

Bhadesiya, C.M., Chaudhary, G.R., Patel, T., Patel, V.A., Anikar, M. & Gajjar, P.J. (2020). Clinical management of organophosphate poisoning in an Indian spectacled cobra (Naja naja; Linnaeus, 1758). *Int. J. Cur.r Microbiol. App.l Sci.,* **9**: 2356–2360.

Bigley, A.N. & Raushel, F M. (2019). The evolution of phosphotriesterase for decontamination and detoxification of organophosphorus chemical warfare agents. *Chem. Biol. Interact.,* **308**: 80–88.

Boulkhessaim, S., Gacem, A., Khan, S.H., Amari, A., Yadav, V.K., Harharah, H. N., Elkhaleefa, A.M., Yadav, K.K., Rather, S., Ahn, H.-J., & Jeon, B.-H. (2022). Emerging trends in the remediation of persistent organic pollutants using nanomaterials and related processes: A Review. *Nanomaterials,* **12**: 2148.

Bušić, V., Katalinić, M., Šinko, G., Kovarik, Z. & Gašo-Sokač, D. (2016). Pyridoxal oxime derivative potency to reactivate cholinesterases inhibited by organophosphorus compounds. *Toxicol. Lett.,* **262**: 114–122.

Chiang, C., Kashetsky, N., Feschuk, A., Burli, A., Law, R. & Maibach, H. (2021). Efficacy of water-based skin decontamination of occupational chemicals using in vitro human skin models: A systematic review. *J Toxicol Environ Health B*, **24**: 337–353.

Cao, Y., Hui, X., Elmahdy, A. & Maibach, H. (2018). In vitro human skin permeation and decontamination of diisopropyl methylphosphonate (DIMP) using Dermal Decontamination Gel (DDGel) and Reactive Skin Decontamination Lotion (RSDL) at different timepoints. *Toxicol. Lett.*, ***299***: 118–123.

Clarkson, E.D. & Gordon, R.K. (2020). Rapid decontamination of chemical warfare agents from skin. In *Handbook of Toxicology of Chemical Warfare Agents*, Elsevier, pp.: 1233–1247).

Collina, T.Z. (2013). *The Chemical Weapons Convention (CWC) at a Glance*. Available online at: http://www.armscontrol.org/factsheets/cwcglance (Last access date: 1 August 2024).

Collins, S., James, T., Carter, H., Symons, C., Southworth, F., Foxall, K., Marczylo, T., & Amlôt, R. (2021). Mass casualty decontamination for chemical incidents: Research outcomes and future priorities. *Int. J. Environ. Res. Public Health,* **18**: 3079.

Connolly, J.M., Stevenson, R.S., Railer, R.F., Clark, O.E., Whitten, K.A., Lee-Stubbs, R.B. & Anderson, D.R. (2020). Impairment of wound healing by reactive skin decontamination lotion (RSDL ® ) in a Göttingen minipig ® model. *Cutan. Ocul. Toxicol.*, **39**: 143–157.

Cristale, J., Dantas, R.F., De Luca, A., Sans, C., Esplugas, S. & Lacorte, S. (2017). Role of oxygen and DOM in sunlight induced photodegradation of organophosphorous flame retardants in river water. *J. Hazard. Mater.*, **323**: 242–249.

D. Schwartz, M.,G. Hurst, C.,A. Kirk, M., J.D. Reedy, S. & H. Braue, E. (2012). Reactive Skin Decontamination Lotion (RSDL) for the decontamination of chemical warfare agent (CWA) dermal exposure. *Curr. Pharm. Biotechnol.*, **13**: 1971–1979.

Dachir, S., Cohen, M., Buch, H. & Kadar, T. (2021). Skin decontamination efficacy of sulfur mustard and VX in the pig model: A comparison between Fuller's earth and RSDL. *Chem. Biol. Interact.*, **336**: 109393.

Dachir, S., Fishbine, E., Meshulam, Y., Buch, H., Allon, N. & Kadar, T. (2020). Fuller's Earth: Old and faithful skin decontaminant against toxic agents. In Zhu, Z. & Maibach, H.I (Ed.), *Skin Decontamination*. Springer, Berlin, Germany, pp. 101–119.

Dallagi, H., Jha, P.K., Faille, C., Le-Bail, A., Rawson, A. & Benezech, T. (2023). Removal of biocontamination in the food industry using physical methods; An overview. *Food Control*, **148**: 109645.

Danoy, A., Durmaz, K., Paoletti, M., Vachez, L., Roul, A., Sohier, J. & Verrier, B. (2022). Aqueous suspensions of Fuller's earth potentiate the adsorption capacities of paraoxon and improve skin decontamination properties. *J. Hazard. Mater.,* **425:** 127714.

Dewey, H.M., Jones, J.M., Keating, M.R. & Budhathoki-Uprety, J. (2022). Increased use of disinfectants during the covid-19 pandemic and its potential impacts on health and safety. *ACS Chem. Health Safe.*, **29:** 27–38.

Dong, J., Sun, X., Zhen, N., Li, Z., Liu, D., Zou, B., Dai, Q., Chi, Y., Chen, S-L, Poblet, J.M., & Hu, C. (2021). Oxidative detoxification of nerve agent VX simulant by polyoxoniobate: Experimental and theoretical insights. *J. Catal.*, **394:** 83–93.

Dyguda-Kazimierowicz, E., Roszak, S. & Sokalski, W.A. (2014). Alkaline hydrolysis of organophosphorus pesticides: The dependence of the reaction mechanism on the incoming group conformation. *J. Phys. Chem. B*, **118:** 7277–7289.

Eid, A., Giovanni, D. D., Galatas, I., Fayçal, J., Karkalic, R., Gloria, A. & Carestia, M. (2020). Mass decontamination of vulnerable groups following an urban CBRN incident. *Biomedicine & Prevention,* **1:**1-5.

Emmanuel, S.S., Idris, M.O., Olawoyin, C.O., Adesibikan, A.A., Aliyu, A.A. & Suleiman, A.I. (2024). Biosynthesized metallic nanoarchitecture for photocatalytic degradation of emerging organochlorine and organophosphate pollutants: A review. *Chemistry Select,* **9**: 1-24.

Fawad Ahmad, M.M. (2022). A critical review of photocatalytic degradation of organophosphorus pesticide "parathion" by different mixed metal oxides. *Adv. J. Chem. Sect. A,* **5**: 284–310.

Fentabil, M., Gebremedhin, M., Barry, J., Mikler, J., & Cochrane, L. (2020). In vivo efficacy of the Reactive Skin Decontamination Lotion (RSDL®) kit against organophosphate and carbamate pesticides. *Chem. Biol. Interact.,* **318:** 108980.

Forsberg, E., Öberg, L., Artursson, E., Wigenstam, E., Bucht, A., & Thors, L. (2020). Decontamination efficacy of soapy water and water washing following exposure of toxic chemicals on human skin. *Cutan. Ocul. Toxicol.,* **39:** 134–142.

Ganesan, K., Raza, S.K., & Vijayaraghavan, R. (2010). Chemical warfare agents. *J. Pharm. Bioallied Sci.*, **2:** 166–178.

Ganie, S.Y., Javaid, D., Hajam, Y.A., & Reshi, M.S. (2022). Mechanisms and treatment strategies of organophosphate pesticide induced neurotoxicity in humans: A critical appraisal. *Toxicology*, **472**: 153181.

Gebremedhin, M., Fentabil, M., Cochrane, L., Lau, V., Toth, D., & Barry, J. (2020). In vitro decontamination efficacy of the RSDL® (Reactive Skin Decontamination Lotion Kit) lotion component against riot control agents: Capsaicin, Mace™ (CN) and CS. *Toxicol. Lett.,* **332**: 36–41.

Ginghină, R.E., Toader, G., Bratu, A.E., & Stoian, I.-A. (2022). Emerging technologies and solutions for chemical warfare agents decontamination. *Int. Conf. Knowl. Based Organ.,* **28**: 39–43.

Gupta, R.C. (2020). Neurotoxicity of organophosphate nerve agents. In *Advances in Neurotoxicology,* Academic Press, pp. 79-112.

Hosseini, H., & Salari M. (2021). Application of nanoparticle technology in water and wastewater treatment: A mini review. *J. Adv. Appl. NanoBio Tech.*, **2**: 86–92.

Huang, Y., Zhang, W., Pang, S., Chen, J., Bhatt, P., Mishra, S., & Chen, S. (2021). Insights into the microbial degradation and catalytic mechanisms of chlorpyrifos. *Environ. Res.,* **194**: 110660.

Jacquet, P., Daudé, D., Bzdrenga, J., Masson, P., Elias, M., & Chabrière, E. (2016). Current and emerging strategies for organophosphate decontamination: special focus on hyperstable enzymes. *Environ. Sci. Pollut. Res.,* **23**: 8200–8218.

Jacquet, P., Rémy, B., Bross, R.P.T., van Grol, M., Gaucher, F., Chabrière, E., & Daudé, D. (2021). Enzymatic decontamination of G-Type, V-Type and Novichok nerve agents. *Int. J. Mol. Sci.,* **22**: 8152.

Jaiswal, S., Singh, B., Dhingra, I., Joshi, A., & Kodgire, P. (2024). Bioremediation and bioscavenging for elimination of organophosphorus threats: An approach using enzymatic advancements. *Environ. Res.*, **252**: 118888.

Javaid, M.K., Ashiq, M., & Tahir, M. (2016). Potential of biological agents in decontamination of agricultural soil. *Scientifica*, **2016:** 1–9.

Kamaruzaman, N.A., Leong, Y.H., Jaafar, M.H., Mohamed Khan, H.R., Abdul Rani, N.A., Razali, M.F., & Abdul Majid, M.I. (2020). Epidemiology and risk factors of pesticide poisoning in Malaysia: A retrospective analysis by the National Poison Centre (NPC) from 2006 to 2015. *BMJ Open*, **10**: e036048.

Kassa, J., Misik, J., & Karasova, J.Z. (2015). Neuroprotective efficacy of newly developed oximes in comparison with currently available oximes in tabun-poisoned rats. *J. Appl. Biomed.*, **13**: 39–46.

Khan, A., Kotta, S., Ansari, S., Ali, J., & Sharma, R. (2013). Recent advances in decontamination of chemical warfare agents. *Def. Sci. J.*, **63**: 487–496.

Kim, S.D., & Lee, Y.H. (2020). Decontamination of VX with acid-activated clay. *ACS Chem. Health Safe.*, **27:** 280–287.

Kumar, S., Kaushik, G., Dar, M.A., Nimesh, S., Lopez-Chuken, U.J., & Villareal-Chiu, J.F. (2018). Microbial degradation of organophosphate pesticides: A review. *Pedosphere*, **28**:190–208.

Lakshmi, K., Varadharajan, V., & Kadirvelu, K.G. (2020). Photocatalytic decontamination of organic pollutants using advanced materials. In *Modern Age Waste Water Problems*. Springer, Berlin, Germany, , pp. 195–212.

Lin, P.-I.D., Wu, C.-F., Kou, H.-S., Huang, T.-Y., Shiea, J., & Wu, M.-T. (2017). Removal of diethylhexyl phthalate from hands by handwashing: Evidence from experimental N-of-1 and crossover designs. *Sci. Rep.*, **7**: 454.

Lockridge, O., Verdier, L., & Schopfer, L.M. (2019). Half-life of chlorpyrifos oxon and other organophosphorus esters in aqueous solution. *Chem. Biol. Interact.*, **311**: 108788.

Magnano, G.C., Rui, F., & Larese Filon, F. (2021). Skin decontamination procedures against potential hazards substances exposure. *Chem. Biol. Interact.*, **344**: 109481.

Mali, H., Shah, C., Raghunandan, B.H., Prajapati, A.S., Patel, D.H., Trivedi, U., & Subramanian, R.B. (2023). Organophosphate pesticides an emerging environmental contaminant: Pollution, toxicity, bioremediation progress, and remaining challenges. *J. Enviro.n Sci.*, **127**: 234–250.

Mijaljica, D., Spada, F., & Harrison, I.P. (2022). Skin cleansing without or with compromise: Soaps and syndets. *Molecules*, **27:** 2010.

Moon, Y., Jafry, A.T., Kang, S.B., Seo, J.Y., Baek, K.-Y., Kim, E.-J.,Pan, J.-G., Choi, J.-Y., Kim, H.-J., Lee, K.H., Jeong, K., Bae, S.W., Shin, S., Lee, J., & Lee, Y. (2019). Organophosphorus hydrolase-poly-β-cyclodextrin as a stable self-decontaminating bio-catalytic material for sorption and degradation of organophosphate pesticide. *J. Hazard. Mater.*, **365**: 261–269.

Ore, O.T., Adeola, A.O., Bayode, A.A., Adedipe, D.T., & Nomngongo, P.N. (2023). Organophosphate pesticide residues in environmental and biological matrices: Occurrence, distribution and potential remedial approaches. *Environ. Toxicol. Chem.*, **5**: 9–23.

Oudejans, L., Mysz, A., Gibb Snyder, E., Wyrzykowska-Ceradini, B., Nardin, J., Tabor, D., Starr, J., Stout, D., & Lemieux, P. (2020). Remediating indoor pesticide contamination from improper pest control treatments: Persistence and decontamination studies. *J. Hazard. Mater.*, **397**: 122743.

Pashirova, T., Salah-Tazdaït, R., Tazdaït, D., & Masson, P. (2024). Applications of microbial organophosphate-degrading enzymes to detoxification of organophosphorous compounds for medical countermeasures against poisoning and environmental remediation. *Int. J. Mol. Sci.,* **25**: 7822.

Pathak, V.M., Verma, V.K., Rawat, B.S., Kaur, B., Babu, N., Sharma, A., & Cunill, J.M. (2022). Current status of pesticide effects on environment, human health and it's eco-friendly management as bioremediation: A comprehensive review. *Front. Microbiol.*, **13:** 962619.

Picard, B., Chataigner, I., Maddaluno, J., & Legros, J. (2019). Introduction to chemical warfare agents, relevant simulants and modern neutralisation methods. *Org. Biomol. Chem.*, **17:** 6528–6537.

Qi, L., Xiao, B., Kong, L., Xu, Y., Yang, J., & Zuo, G. (2023). Decontamination of mustard sulfur and

VX by sodium percarbonate complexed with 1-acetylguanidine as a novel activator. *Water Sci. Technol.,* **87**: 336–346.

Redy Keisar, O., Nahum, V., Yehezkel, L., Marcovitch, I., Columbus, I., Fridkin, G., & Chen, R. (2021). Active and strippable PVA/Borax/$NaBO_3$ hydrogel for effective containment and decontamination of chemical warfare agents. *ACS Omega*, **6**: 5359–5367.

Robb, E.L. & Baker, M.B. (2022). *Organophosphate Toxicity*. StatPearls Publishing; Treasure Island.

Roby, K.A.C., Srinivas, B., Sandeep, B., Reddy, S.N., Yadav, M.A., & Harinadha Baba, K. (2018). A prospective observational study and survival pattern of organo phosphorous poisoning patients with intensive care treatment in a tertiary care hospital. *Int. J. Basic Clin. Pharmacol.*, **7**: 1889-1894.

Roul, A., Le, C.-A.-K., Gustin, M.-P., Clavaud, E., Verrier, B., Pirot, F., & Falson, F. (2020). Comparison of four different Fuller's Earth formulations in skin decontamination. In *Skin Decontamination,* Springer, Berlin, Germany, , pp. 121–139.

Sarker, A., Shin, W.S., Masud, M. A. A., Nandi, R., & Islam, T. (2024). A critical review of sustainable pesticide remediation in contaminated sites: Research challenges and mechanistic insights. *Environ. Pollut.,* **341**: 122940.

Sheng, Y., Benmati, M., Guendouzi, S., Benmati, H., Yuan, Y., Song, J., Xia, C., & Berkani, M. (2022). Latest eco-friendly approaches for pesticides decontamination using microorganisms and consortia microalgae: A comprehensive insights, challenges, and perspectives. *Chemosphere*, **308**: 136183.

Soares, P.R.S., Birolli, W.G., Ferreira, I.M., & Porto, A.L.M. (2021). Biodegradation pathway of the organophosphate pesticides chlorpyrifos, methyl parathion and profenofos by the marine-derived fungus Aspergillus sydowii CBMAI 935 and its potential for methylation reactions of phenolic compounds. *Mar. Pollut. Bull.*, **166**: 112185.

Taysse, L., Daulon, S., Delamanche, S., Bellier, B., & Breton, P. (2007). Skin decontamination of mustards and organophosphates: comparative efficiency of RSDL and Fuller's earth in domestic swine. *Hum. Exp. Toxicol.,* **26**: 135–141.

Thakur, M., Medintz, I.L., & Walper, S.A. (2019). Enzymatic bioremediation of organophosphate compounds—progress and remaining challenges. *Front. Bioeng. Biotechnol.,* **7:** 289.

Thors, L., Koch, M., Wigenstam, E., Koch, B., Hägglund, L., & Bucht, A. (2017a). Comparison of skin decontamination efficacy of commercial decontamination products following exposure to VX on human skin. *Chem. Biol. Interact.,* **273:** 82–89.

Thors, L., Lindberg, S., Johansson, S., Koch, B., Koch, M., Hägglund, L., & Bucht, A. (2017b). RSDL decontamination of human skin contaminated with the nerve agent VX. *Toxicol. Lett.,* **269:** 47–54.

Thors, L., Wigenstam, E., Qvarnström, J., Hägglund, L., & Bucht, A. (2020). Improved skin decontamination efficacy for the nerve agent VX. *Chem. Biol. Interact.*, **325**: 109135.

Umapathi, R., Park, B., Sonwal, S., Rani, G. M., Cho, Y., & Huh, Y.S. (2022). Advances in optical-sensing strategies for the on-site detection of pesticides in agricultural foods. *Trends Food Sci. Technol.,* **119:** 69–89.

Vakhitova, L., Bessarabov, V., Taran, N., Kuzmina, G., Derypapa, V., Zagoriy, G., & Popov, A. (2019). Development of chemical methods for individual decontamination of organophosphorus compounds. *EasternEuropean J. Enterp. Technol.,* **2:** 6–14.

Valiveti, A.K., Bhalerao, U.M., Acharya, J., Karade, H.N., Gundapu, R., Halve, A.K., & Kaushik, M.P. (2015). Synthesis and in vitro kinetic study of novel mono-pyridinium oximes as reactivators of organophosphorus (OP) inhibited human acetylcholinesterase (hAChE). *Chem. Biol. Interact.,* **237**: 125–132.

Wagner, G.W. (2010). Hydrogen peroxide-based decontamination of chemical warfare agents. *Main Group Chemistry,* **9**: 257–263.

Wong, P.T., Tang, S., Cannon, J., Yang, K., Harrison, R., Ruge, M., J.O'Konek, J., & Choi, S.K. (2020). Shielded α-nucleophile nanoreactor for topical decontamination of reactive organophosphate. *ACS Appl. Mater. Interfaces,* **12**: 33500–33515.

Worek, F. & Thiermann, H. (2013). The value of novel oximes for treatment of poisoning by organophosphorus compounds. *Pharmacol. Ther.,* **139**: 249–259.

Worek, F., Thiermann, H., & Wille, T. (2020). Organophosphorus compounds and oximes: A critical

review. *Arch. Toxicol.*, **94**: 2275–2292.
Xu, W., Zhao, S., Zhang, W., Wu, H., Guang, C., & Mu, W. (2021). Recent advances and future prospective of organophosphorus-degrading enzymes: identification, modification, and application. *Crit. Rev. Biotechnol.*, **41**:1096–1113.
Yang, X.-Y., & Liu, H.-Y. (2021). Hydrogen peroxide is a risk factor for occupational chemical poisoning. *Chin. Med. J.*, **134**: 881–882.
Zhang, Q., Wang, Y., Zhang, C., Yao, Y., Wang, L., & Sun, H. (2022). A review of organophosphate esters in soil: Implications for the potential source, transfer, and transformation mechanism. *Environ. Res.*, **204:** 112122.
Zhao, S., Zhu, Y., Xi, H., Han, M., Li, D., Li, Y., & Zhao, H. (2020). Detoxification of mustard gas, nerve agents and simulants by peroxomolybdate in aqueous H2O2 solution: Reactive oxygen species and mechanisms. *J. Environ. Chem. Eng.*, **8:** 104221.

# A REVIEW OF TOXICITY EFFECTS OF COLOURED SMOKE BOMBS AND RISK MITIGATION EFFORTS

Nurnadia Andenan[1]*, Wan Md Zin Wan Yunus[2], Mohd Norfaiz Norrrahim[3], Victor Feizal Knight Abd. Shattar[3], Nur Shazwani Abdul Latif[4], Hafizah Ariff[4], Ruwaida Jamian[5], Nor Afizah Salleh[6], Noor Farahana Abdul Rahman[7], Zuraidah Salleh[7] & Khairol Amali Ahmad[1]

[1]Centre for Research and Innovative Management, National Defence University of Malaysia, (UPNM), Malaysia
[2]Faculty of Defence Science and Technology, National Defence University of Malaysia (UPNM), Malaysia
[3]Research Centre for Chemical Defence (CHEMDEF), Defence Research Institute, National Defence University of Malaysia (UPNM), Malaysia
[4]Centre for Tropicalisation (CENTROP), Defence Research Institute, National Defence University of Malaysia (UPNM), Malaysia
[5]Malaysian Japan International Institute of Technology (MJIIT), Universiti Teknologi Malaysia (UTM), Malaysia
[6]Science and Technology Research Institute for Defence (STRIDE), Ministry of Defence, Malaysia
[7]High Energy Material Research Laboratory (HEMREL), School of Mechanical Engineering, College of Engineering, Universiti Teknologi MARA (UiTM), Malaysia

*Email: nurnadia@upnm.edu.my

## ABSTRACT

*Smoke bombs are a type of pyrotechnic device used in military operations, search and rescue, crowd control, and training exercises. Early smoke bombs produced black or white smoke, but coloured smoke bombs have become more versatile and widespread. However, concerns about the toxicity and carcinogenic potential of the dyes and carrier materials used to create these vivid colours have been raised. To this end, studies have been conducted to improve the safety and performance of coloured smoke bombs. Alternative carrier materials, such as ammonium perchlorate, have been explored. Efforts have also been made to improve the consistency of dye dispersion and overall burn characteristics of smoke bombs. Despite these efforts, there is still uncertainty regarding the toxicological effects of coloured smoke bombs. Many of the dyes and carrier materials used in these devices have been shown to have toxic or carcinogenic properties in laboratory studies. Additionally, several cases of smoke bomb-related illnesses and injuries have been reported, particularly among military personnel. This paper provides a review of the chemistry, physiology and military applications of colour smoke bombs and their components, as well as an evaluation of the latest research on the potential health risks associated with their use. Some of the most notable cases of toxicity associated with smoke bombs are highlighted, and the implications of these findings for the safety and future development of pyrotechnic technology are discussed.*

**Keywords:** *Smoke bombs; coloured smoke; dyes; oxidisers; toxicity*.

## 1. INTRODUCTION

Smoke bombs have been used for various purposes, from military training exercises to signalling and special effects for movies. Smoke bombs have traditionally produced white or black smoke. White smoke has been considered as the superior choice for many years due to its high visibility and less obscuring effect as compared to black smoke (Danali *et al.*, 2010). The pyrotechnic mixture used to produce white smoke can vary, with some formulations containing zinc oxide and hexachloroethane (HC) that produce dense, bright white smoke when ignited. White phosphorus is also commonly used to produce white smoke in particular for military operations due to its high brightness and long duration.

However, it has sparked controversy due to its potential health hazards, including severe burns and toxicity (Aviv *et al.,* 2017).

The development of coloured smoke bombs in recent years has expanded their utility, particularly in military applications. Coloured smoke bombs produce smoke in various colours, making them useful for marking unit flanks, positions of lead elements, locations of targets, drop zones, tactical landing areas and medical evacuation landing sites (NRC, 1997; Gluck *et al.*, 2016). In addition to their military applications, coloured smoke bombs are used in various civilian settings, such as for signalling during search and rescue operations, and as part of pyrotechnic displays in movies and concerts.

Coloured smoke bombs contain various chemicals responsible for producing the desired colour. Typically, the chemicals used in coloured smoke bombs combine oxidisers, dyes and fuel, as follows (Stoenescu, 2014; Istiqamah *et al.,* 2024):

- **Oxidisers**
  Used to provide the oxygen necessary for combustion. Common oxidisers in coloured smoke bombs include potassium chlorate, sodium nitrate and ammonium nitrate.

- **Dyes**
  Usually added to the mixture to produce the desired colour. Different dyes produce different colours; for example, potassium perchlorate combined with strontium nitrate produces red, while barium chloride combined with sodium bicarbonate produces green.

- **Fuel**
  Used to sustain combustion and produce smoke. Common fuel sources used in coloured smoke bombs include sucrose, lactose and dextrin.

The development of coloured smoke bombs has brought new challenges and concerns about their potential health effects (Stoenescu, 2014). Some of the most common health effects of exposure to coloured smoke include respiratory and skin irritation (NRC, 1997; Cao *et al.* 2016). Long-term exposure to some of the dyes and carrier materials used in coloured smoke bombs has also been associated with higher risk of cancer (Stoenescu, 2014). In order to better understand the potential health effects of coloured smoke bombs, we have compiled a list of common dyes used in these devices and their associated health effects, as presented in Table 1. It shows that some of the dyes used in coloured smoke bombs can have serious health effects, including acute inhalation toxicity, carcinogecity and skin sensitisation. In addition, the carrier materials used to disperse the dyes can also be toxic, further increasing the potential health risks. As a result, efforts have been made to develop safer coloured smoke bombs, such as using alternative carrier materials or nanotechnology to disperse the dyes more efficiently (Zeman *et al.,* 2022). By understanding the potential health risks associated with coloured smoke bombs, we can work towards making these devices safer for use in a range of applications.

**Table 1: Dyes used in coloured smoke bombs and their potential health effects (Dilger *et al.*, 2022).**

| Dye | Health effects |
|---|---|
| Disperse Red 9 | Acute inhalation toxicity, carcinogenicity, genotoxicity mutagenicity and skin sensitisation. |
| Solvent Green 3 | Acute inhalation toxicity, carcinogenicity, genotoxicity mutagenicity and endocrine disruption. |
| Chlorinated Vat Yellow 4 | Acute oral toxicity and endocrine disruption |
| Solvent Blue 35 | Acute inhalation toxicity, carcinogenicity and genotoxicity mutagenicity. |

This paper aimed to provide a review of the toxicity and carcinogenicity of the dyes and carrier materials used in coloured smoke bombs and current efforts to mitigate these risks. By examining the history of smoke bombs and their initial applications, development of coloured smoke bombs, possible health consequences that could arise from exposure to these devices, as well as different types of coloured smoke bombs and their applications, better understanding can be gained on the risks associated with its usage. Through this review, we hope to raise awareness about the potential dangers of coloured smoke bombs and encourage further research into safer alternatives that can be used in both military and civilian applications.

## 2. CHEMISTRY OF COLOURED SMOKE BOMBS

Coloured smoke bombs typically consist of a few essential components: an oxidiser, with potassium chlorate ($KClO_3$) often chosen; a fuel derived from lactose or sucrose; an organic dye; and various additives designed to enhance combustion and improve the composition's processing characteristics (Faber *et al.,* 2013; Tang *et al.,* 2023). $KClO_3$ has seen widespread usage as an oxidiser in pyrotechnics for an extended period due to its ease of ignition, oxygen-rich properties and cost-effectiveness (Hosseini *et al.,* 2005; Ouyang *et al.,* 2011).

### 2.1 Mechanism of Coloured Smoke Bombs

Additionally, it is crucial that the chosen oxidisers exhibit low hygroscopicity, possess proper particle size and have acceptable heat of decomposition (Srinivasan, 2017). The ignition temperature for a mixture of $KClO_3$ and sucrose can drop to as low as 180 °C (Hosseini *et al.*, 2005). It is important to know its decomposition temperature to avoid accidental ignition or explosive reactions. The oxidiser's role is paramount as it furnishes the necessary oxygen for fuel combustion (Babar & Malik, 2014). This combustion process causes the dye to evaporate and be expelled from the device, where it condenses in the atmosphere, forming an aerosol composed of minute particles that give the smoke its distinctive colour (Hemmila *et al.,* 2007). The binary reaction between chlorate and lactose can take a different path depending on the amount of oxygen available, as shown in Equation 1 (Ellern, 1968; Eslami & Hosseini, 2010):

$$4KClO_3 + C_{12}H_{22}O_{11} \longrightarrow 4KCl + 12CO + 11H_2O \quad \Delta H = -2.9 \text{ kJ/g} \qquad (1)$$
$$8KClO_3 + C_{12}H_{22}O_{11} \longrightarrow 8KCl + 12CO_2 + 11H_2O \quad \Delta H = -4.2 \text{ kJ/g}$$

A previous study by Lee *et al.* (2001) highlighted potassium perchlorate ($KClO_4$) as a potent oxidising agent known to decompose at elevated temperatures, producing oxygen as one of its major byproducts. In order to investigate the thermal properties of $KClO_4$ with varying particle sizes ranging from 44 to 150µm, the researchers employed differential scanning calorimetry (DSC), differential thermal analysis (DTA) and thermogravimetry (TG). Their findings revealed that the DSC curves of $KClO_4$ with varying particle sizes exhibited endothermic peak at 308 °C and melting point at 608 °C. Notably, smaller particle sizes of $KClO_4$ displayed a shifted initial decomposition temperature to lower levels. Furthermore, the thermal behaviour of pyrotechnic mixtures underwent scrutiny using TG and DTA, revealing that $KClO_3$ + sucrose has a notably low ignition temperature, rendering it more prone to manufacturing hazards and self-ignition when compared to $KClO_4$ + sucrose. Consequently, incorporating $KClO_4$ into a mixture with sucrose enhances stability and elevates the ignition temperature, which is attributed to $KClO_4$'s superior stability over $KClO_3$. Additionally, the inclusion of stabilisers such as sodium bicarbonate, which undergoes endothermic decomposition, leads to reduced reaction temperatures and extended reaction times, resulting in slower and more sustained release of smoke (Tabacof & Calado, 2017). Moreover, a cooling agent should be introduced to prevent excessive decomposition of the dye (Istikamah *et al.,* 2024).

Hosseini *et al.* (2005) found similar thermal behaviours for sucrose, $KClO_3$, $KClO_4$, as well as mixtures of $KClO_3$ + sucrose and $KClO_4$ + sucrose, which are sometimes employed as pyrotechnic compositions in military applications. As summarised in Table 2, the findings indicate that the ignition temperatures for $KClO_3$ and $KClO_4$ alone are 472 and 592 °C respectively. In contrast, pure sucrose exhibits decomposition at a much lower temperature, at approximately 180 °C. Furthermore, substituting $KClO_3$ with $KClO_4$ as the oxidiser for sucrose results in decrease of the mixture's sensitivity. Significantly, the ignition temperature for combination of $KClO_3$ and sucrose can drop to as low as 180 °C. On the other hand, substituting $KClO_3$ with $KClO_4$ increases the ignition temperature to approximately 410 °C, creating a safer threshold that prevents accidental activation due to factors such as static electricity. Besides using $KClO_3$ and $KClO_4$ as oxidisers, a recent study by Istikamah *et al.* (2024) used potassium nitrate ($KNO_3$) as oxidiser in the formulation. The study indicates that the optimal ratio of smoke signal composition determines the longest burn period, best ignition time and greatest colour output. The findings also showed that a ratio of 50 wt% $KNO_3$, 20 wt% $MgCO_3$ and 30 wt% sugar produced the best-looking coloured smoke signal, with the consistent colour opacity and thickness of the smoke, and ignition and burn times of 5 and 120 s respectively.

**Table 2: Summary of DTA-TG results (Hosseini *et al.*, 2005).**

| Component | Composition (by mass) | Transition Temperature (ºC) | | |
|---|---|---|---|---|
| | | Fusion | Ignition | T* |
| Sucrose | 100 | 180 | Decomposes | 180-300 |
| $KClO_3$ | 100 | 356 | 472 | 475-500 |
| $KClO_4$ | 100 | 590 | 592 | 592-600 |
| $KClO_3$+ sucrose | 74/26 | 180 | 180 | 180-220 |
| $KClO_4$+ sucrose | 71/29 | 410 | 410 | 410-500 |

## 2.2 Coloured Smoke Dyes

Various dyes have historically been utilised in coloured smoke mixtures. However, many of these dyes are currently under scrutiny due to concerns about their potential carcinogenicity and other health hazards (Stoenescu, 2014; Zeman *et al.*, 2022). Some dyes from the anthraquinone group have been identified as toxic and carcinogenic substances (Sendelbach, 1989). Most anthraquinone dyes that exhibit positive responses in the Ames mutagenicity test contain hydroxyl, nitro and amino functional groups (Sigman *et al.*, 2008). These dyes are also known to act as primary irritants and potent sensitisers. Organic dyes were previously employed in coloured smoke bombs for the formulation of the colours of yellow, green, red and violet, but due to safety concerns associated with their smoke formulations and combustion byproducts, new organic dyes have been introduced as replacements to achieve the same colours. Table 3 provides the old and new smoke colour formulations, and their respective dye components.

It is well-established that a coloured smoke bomb's formulation includes a dye that condenses to create an aerosol of minuscule particles, imparting the characteristic colour to the smoke. Effective coloured smoke compositions necessitate molecules with low toxicity, including minimal carcinogenicity. These molecules should readily sublime without undergoing decomposition at the reaction temperature to produce high-quality coloured smoke (Stoenescu, 2014). Previous research has also highlighted the importance of the thermal stability of dyes to prevent molecular decomposition and maintain colour purity (Dilger *et al.*, 2022). However, it is important to note that some of these dyes have been identified as toxic and carcinogenic substances, posing risks to both health and the environment. This longstanding concern, particularly regarding environmental and safety aspects, persists as military personnel who work with these smokes may be exposed to potential health hazards. Tragic accidents resulting from excessive inhalation of such smoke have been documented (Huang *et al.*, 2008). Furthermore, limited attention has been directed toward analysing the potentially hazardous combustion byproducts generated by these devices (Perkins *et al.*, 2022).

**Table 3: The smoke colour formulations with their dye components (NRC, 1999).**

| Smoke Colour | Old Organic Dyes | Current Organic Dyes |
|---|---|---|
| Yellow | Vat Yellow 4 and benzanthrone | Solvent Yellow 33 |
| Green | Vat Yellow 4 and benzanthrone and Solvent Green 3 | Solvent Yellow 33 and Solvent Green 3 |
| Red | Disperse Red 9 | Solvent Red 1 and Disperse Red 11 |
| Violet | Disperse Red 9 and 1,4-diamino-2,3-dihydroanthraquinone | - |

The materials that exhibit optimal performance in coloured smoke share several common properties, such as volatility and chemical stability. For a dye to be suitable, it must go through phase change into gaseous state upon heating without experiencing significant decomposition. Low molecular weight dyes (those weighing less than 400 grams/mol) are typically preferred, as volatility generally decreases with increasing molecular weight (Stoenescu, 2014). Salts are generally unsuitable for this purpose, as ionic species tend to have low volatility due to the strong inter-ionic attractions present within their crystalline lattice. Consequently, functional groups such as —COO— (carboxylate ions) and —NR3+ (substituted ammonium salts) should be avoided. Moreover, oxygen-rich functional groups such as NO and —SOH should also be excluded from consideration. These groups are prone to releasing oxygen at the typical reaction temperatures of smoke compositions, potentially leading to the oxidative decomposition of dye molecules. Although groups such as NH and —NHR (amines) are used, caution is essential as potentially hazardous oxidative coupling reactions can occur in oxygen-rich environments (Stoenescu, 2014). Chunlong *et al.* (1993) conducted research on the relationship between functional groups and thermal stability in dyes, concluding that functional groups such as $–CONH_2$, -CN, $-NO_2$, -CL, and $–OCH_3$ enhance the thermal stability of dyes.

The volatilisation of organic dyes within smoke devices takes place through the thermal interaction of the fuel and oxidiser. In order to be deemed suitable, an organic dye must rapidly volatilise at temperatures of around 400 - 500 ºC with minimal decomposition, resulting in smoke characterised by a specific colour and sufficient stability in the air (Chin & Borer, 1983). Excessive temperatures can lead to the decomposition of dye molecules, compromising the colour quality and volume of the generated smoke (Stoenescu, 2014). While a low ignition temperature is essential, the smoke-generating composition must remain stable during manufacturing and storage across the expected range of ambient temperatures. The colour of pyrotechnics arises from volatilised materials in the flame zone, emitting atomic spectra, molecular spectra, chemiluminescent radiation and incandescence from entrained condensed phases (Ambekar *et al.*, 2017). The oxidative reaction must generate sufficient heat to vaporise the dye and enough gas to disperse the dye for the desired colour effect. The literature suggests that the amount of hazardous dyes can be minimised while achieving an identical colour impression. However, each coloured smoke dye possesses a unique enthalpy of sublimation, which significantly influences the performance and behaviour of a coloured smoke formulation. Consequently, each dye requires its optimised formulation to achieve burn time and colour feature requirements (Gluck *et al.*, 2018). Furthermore, a low burning temperature is essential to prevent the decomposition of the dye, typically an organic compound (Tabacof & Calado, 2017).

## 3. TOXICITY STUDIES OF DYE IN COLOURED SMOKE BOMBS

The investigation into the inhalation toxicity of anthraquinone dyes remains relatively limited. Some earlier studies have tried to assess the harmful emissions of various coloured smoke devices. Hemmila *et al.* (2007) conducted experiments that revealed evidence of acute toxicity in four coloured smokes when assessed using the Trypan Blue exclusion method, involving the exposure of human bronchial epithelial cells to these smokes in vitro. The order of acute toxicity appears to be orange > violet ~ yellow > red. Historically, older M18 coloured smoke grenades contained dyes based on anthraquinone combined with sulphur, potassium chlorate and sodium bicarbonate. However, due to concerns regarding health and toxicity implications, these smoke compositions are no longer in production, as they are suspected of releasing hazardous sulphur dioxide ($SO_2$) during combustion (Gluck *et al.*, 2018). Researchers have considered sugar (lactose / sucrose) as a less toxic alternative to replace the previously used sulphur containing formulations. Compared to sulfoxides produced in the past, combustion products derived from sugar now only contain harmless $H_2O$ and $CO_2$ (Sabatini, 2014).

Disperse Red 9 has been categorised with a toxicity rating of 1 when inhaled or ingested. This rating is attributed to slightly toxic substances, with effects that are generally temporary and cease upon discontinuation of exposure (Perkins *et al.*, 2022). When subjected to combustion, this dye undergoes oxidative and pyrolytic reactions, generating various reaction by-products. At the combustion state, Disperse Red 9 [1-(methyl-amino) anthraquinone] primarily transforms into 1-aminoanthraquinone and 2-aminoanthraquinone (Buchanan *et al.*, 1983). Notably, 2-aminoanthraquinone has been identified as carcinogenic in rat and mouse bioassays (NCI, 1987). Additionally, Hemmila *et al.* (2007) observed weak genotoxicity in red smoke at high concentration levels. Disperse Red 9 has been substituted in contemporary formulations with a blend of Solvent Red 1 and Disperse Red 11 (Springer *et al.*, 2008).

In response to the known toxicity concerns associated with Disperse Blue 180, efforts have been made to develop more environmentally friendly compositions that do not rely on anthraquinone-based dyes. Marss *et al.* (1989) conducted studies to evaluate potential health risks arising from continuous exposure to pyrotechnic compositions containing Disperse Blue 180. Their findings revealed various inflammatory changes in the lungs of mice, rats and guinea pigs exposed to the test material for 1 h per day, five days a week for over 42 weeks at different concentrations within a static chamber. A statistically substantial increase in the incidence of alveologenic carcinoma was observed in the high-dose group of mice. A previous study by Ledgard (2007) also found similar blue smoke formulations comprising of potassium chlorate (32.1 wt%), rice starch (2.9 wt%), milk sugar (26.2 wt%) and CuPc (38.8 wt%). However, a formulation containing potassium chlorate (20.0 wt%), magnesium carbonate (2.0 wt%), lactose (18.0 wt%) and CuPc (60.0 wt-%) resulted in the decomposition of the dye and production of gray soot on a 2 g scale. Even after experimenting with different oxidisers such as ammonium nitrate and ammonium dinitramide, no coloured smoke was detected. Consequently, the dye was used on Moretti's Solvent Yellow 33 system, with varying amounts of 5-amino-1H-tetrazole (5-AT) to enhance efficiency (Moretti *et al.*, 2013). Maintaining the combustion temperature below 350 ºC is important, as this is the dye's self-ignition point (Eslami & Hosseini, 2010). Fuels such as boron and azodicarbonamide generate excessively high temperatures, and for that reason, are unsuitable for these low-temperature formulations (Ojha & Karmakar, 2018; Guo *et al.*, 2023).

Previously, both toxic yellow dyes, benzanthrone and Vat Yellow 4, were used in the U.S. Army's M194 yellow smoke hand-held signal. However, the M194 yellow smoke production was halted in the early 1980s, partly due to concerns of the risks that these two dyes pose to health and the environment (Moretti *et al.*, 2012). To this end, an alternative yellow smoke formulation was developed in response to these toxicity issues and the need for continued production, incorporating the non-toxic dye Solvent Yellow 33. This environmentally friendly replacement dye has found extensive industrial use and has also been safely employed in signalling devices. Similarly, for green smoke formulations, an anthraquinone-based dye was effectively substituted with more environmentally benign dyes, Copper (II) Phthalocyanine (CuPc) and Solvent Yellow 33 (SY 33), as reported by Gluck *et al.* (2018). The authors also suggested that these formulations are promising alternatives to the existing M18 green smoke formulation. In addition, Moretti *et al.* (2014) validated a yellow smoke formulation based on environmentally friendly dye using Solvent Yellow 33 as an alternative to the current formula specified for the M194 yellow smoke hand-held signal.

## 4. RECENT PROGRESS TO OVERCOME ISSUES RELATED WITH COLOURED SMOKE BOMBS

There are significant challenges for the evolving emphasis on safer and more environmentally friendly materials, as well as the aim of maintaining or enhancing existing performance benchmarks. In addressing these challenges, several objectives for improved smoke bombs have emerged, including the development of formulations with heightened efficiency and reduced sensitivity levels, as well as research into nano-scale smoke bombs, as well as the replacement of hygroscopic and toxic ingredients (Danali *et al.,* 2010). Developing time delay pyrotechnic elements is also important to enhancing new fuses, which enable precise timing in igniting or activating explosives (Mojsilovic *et al.*, 2022). Consequently, there is crucial demand for new and enhanced compositions for coloured smoke bombs that predominantly excludes toxic or irritant materials while ensuring effective smoke production (Perkins *et al*., 2022).

Considering the potential health concerns associated with the current use of anthraquinone dyes, exploration into alternative materials is underway. An attractive option involves the utilisation of organic dyes with a diketopyrrolopyrrole (DPP) structure, which has been deemed as toxicologically safe for substitution in pyrotechnic compositions. What makes this material particularly intriguing is its distinctive chemical attributes, diverging from the typical structures relying on anthraquinones or azo-compounds. The functional studies presented here have demonstrated that DPP exhibits the potential to generate a more efficient red smoke cloud as compared to conventional anthraquinone dyes, as illustrated in Figure 1 (Zeman *et al*., 2022).

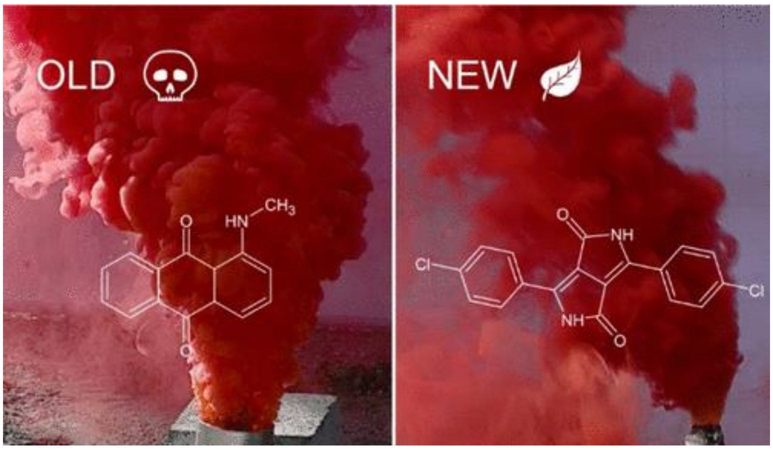


**(a)** **(b)**

**Figure 1: Smoke generated by the (a) Disperse Red 9 and (b) diketopyrrolopyrrole (DPP).**

In manufacturing smoke bombs, mechanical effects such as friction and impact are unavoidable and ever-present. The pyrotechnic materials are typically subjected to three types of investigations to determine the safety and security measures needed in handling the compositions, which are impact sensitivity, friction sensitivity and vacuum stability tests (Pulpea *et al*., 2023). Previous studies by Srinivasan (2017) and Monogarov *et al.* (2023) emphasised the significance of impact sensitivity, which is crucial for determining the safest impact energy threshold that prevents unintended ignition. In addition, mechanical sensitivity measurement is important for ensuring safety during handling and usage. It is also essential to consider the potential consequence of excessive moisture absorption by agents, which can affect emission performance. When moisture is absorbed, the composition of coloured smoke bombs tends to clump together, and excessive humidity may even lead to agent decomposition (Han *et al.,* 2019). Additionally, the analysis of particulate matter emitted from smoke bombs is a crucial aspect. Carrico *et al.* (2018) emphasised how important particulate material, mainly fine fraction, influences atmospheric chemistry and optics. Particulate matter with aerodynamic diameter of less than 2.5 µm (PM 2.5) is a specific parameter of interest due to its implications for health, atmospheric visibility and climate. Reategui-Inga *et al.* (2024) reported on air quality damages due to concentrations of particulate matter (PM 2.5 and PM 10) in short periods.

Han *et al.* (2019) also presented a novel formula for an environmentally friendly method for unpacking fireworks powder that yields lower PM 2.5 and PM 10 levels after combustion. This improvement can be attributed to the elimination of sulphur from the new formula, thereby reducing the production of

$SO_2$. Beyond considering the formulation's ingredient toxicity profile, it is paramount to detect potential harmful combustion byproducts and their particle sizes. Particles smaller than 2 µm can deeply penetrate lung alveoli upon inhalation. In a study by Hemmila *et al.* (2007), it was observed that the particles from yellow and red smokes were mostly spherical and smaller than 1 mm in diameter, as depicted in Figure 2. Some of these particles were interconnected, forming chains of several micrometres in length. Orange smoke contained rounded particles and needles, spherical particles smaller than 1 mm in diameter, and needle lengths below 2 mm. Very long chains of these particles were discovered on the filter. As for violet smoke, its particles appeared to be predominantly spherical.

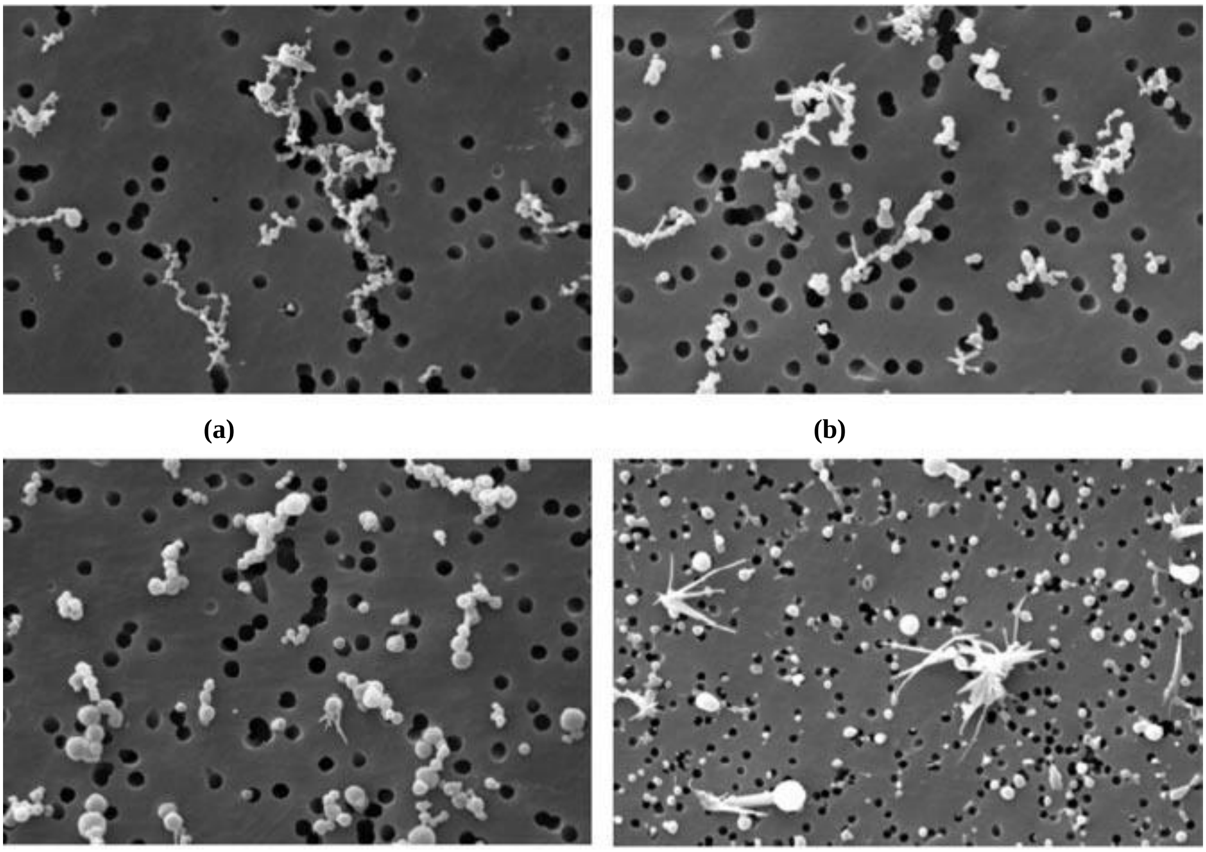


**Figure 2: Particles of (a) orange, (b) yellow, (c) red and (d) violet smokes (Source: Hemmila *et al.* 2007).**

With growing concern on environmental pollution, the world is increasingly recognising the importance of analysing the combustion products of smoke devices. Many of the existing formulations today have evolved through extensive trial and error processes in the past. However, there is still no acceptable chlorine-free oxidiser available to substitute potassium chlorate in low-temperature smoke formulations (Gluck, 2018). The issue of toxicity stemming from the use of chlorine-containing compounds warrants further investigation and discussion. Previous studies have also pointed to the contamination of groundwater and surface water by perchlorate, particularly in the vicinity of manufacturing and display sites, with the full extent of health and ecological impacts still awaiting comprehensive assessment (Sijimol & Mohan, 2014). Additionally, it is worth noting that carbon monoxide has been found among the combustion products of coloured smoke (Hemmila *et al.*, 2007). Future research should explore the potential role of carbon monoxide in reducing the toxicity of this smoke. In addition, in order to ensure a thorough evaluation, new strategies should be developed for characterising aerosols produced by mixtures (Rabha & Saikia, 2020).

The safety, reliability and performance of smoke bombs have garnered increasing attention for military technologies. Shi & Wang (2018) conducted a study exploring how ambient temperature, packing conditions, size and heating rate affect the safety of pyrotechnic smoke bombs during storage and transportation. Their findings indicate that thermal hazards associated with pyrotechnics increase as ambient temperature rises. Ignition temperature is a crucial characteristic influencing the efficiency of pyrotechnic mixtures for smoke dye. Low-temperature igniting pyrotechnics may create dangerous problems, including uncontrollable and accidental self-ignition, while high-temperature variants may cause the breakdown of dye components at ignition temperature (Eslami & Hosseini, 2010). Notably, the inherent ignition temperature of pyrotechnics remains unaffected by packing conditions and size. Selvakumar *et al.* (2013) highlighted that that explosivity hinges not only on chemical composition but also on factors such as shape, particle size, physical form, selection of oxidizers and fuel, fuel-to-oxidizer ratio, degree of mixing, moisture content, chemical purity, presence of additives, local pressure, as well as packing density. The authors analysed the ballistic behaviour of gunpowder and flash powder of firework chemicals with varying particle sizes in a closed vessel in order to determine the maximum pressure upon ignition. They also noted that nanoparticle-sized powders exhibited increased specific surface areas, facilitating easier ignition and higher burn rates. These nanopowders were synthesised through wet milling in a ball mill using toluene as the wetting agent. The evaluation of smoke bomb safety through thermal analysis has been widely adopted to investigate the ignition behaviour of colour smoke bomb mixtures, a critical factor influencing colour smoke safety (Brown *et al.,* 2003; Tuukkanen *et al.,* 2005; Gluck *et al.,* 2018).

An additional challenge in the search for an ideal smoke-generating composition involves the creation of solid residue during the combustion of conventional smoke-producing compositions. The residue, which is the byproduct of the reaction, contributes to the generation of waste materials such as slag and solid clinkers (Stoenescu, 2014). These will cause the solid materials to accumulate within the core of a pyrotechnic smoke-producing munition and obstruct the escape of gas-phase dye molecules into the environment. This obstruction can lead to deflagration, which poses the risk of causing harm to bystanders or resulting in only restricted emission of coloured smoke. Küblböck *et al*. (2020) reported that combustion products, which are potassium chlorate in combination with organic material, lead to carcinogenic polychlorinated compounds, which can be prevented using "nitrogen-rich-only" smokes. However, further evaluation of the toxicity of these combustion products is necessary to address health concerns (Küblböck *et al*., 2020). In addition, by understanding the chemical composition of smoke and its reaction products, potential toxicity effects can be easily assessed to evaluate any potential toxicity effects, which can result in safer formulations with better efficacy (Fedick *et al*., 2023). Therefore, future research endeavours should address these issues and enhance the formulations.

## 5. CONCLUSION

This paper presented an overview of smoke bombs, particularly for effective composition improvement of coloured smoke bomb formulations. Current formulations face challenges due to the presence of chlorine-based oxidisers, which are associated with toxic byproducts and environmental contamination. Efforts to identify chlorine-free alternatives and understand the role of carbon monoxide in reducing toxicity are crucial. There may be other possible candidate compounds, which could further improve the effectiveness of smoke mixtures. For these future compounds, the dye content should be modified or enhanced to ensure less toxic, unique and vivid colour impressions. Research into alternative materials, such as diketopyrrolopyrrole (DPP) dyes, shows promise in offering safer and more effective colour options as compared to traditional anthraquinone dyes. The toxicity of these combustion products should also be further evaluated to satisfy health aspects. Future research should also focus on creating compositions that minimise harmful byproducts while ensuring effective smoke production. The evaluation of residue formation, potential for carcinogenic byproducts, and overall toxicity of new formulations will be vital for developing safer and more efficient smoke bombs. Addressing these issues will contribute to enhanced safety and environmental responsibility in smoke bomb technology.

## ACKNOWLEDGEMENT

This research was funded by Ministry of Education, Malaysia, under the grant UPNM/2018/CHEMDEF/ST/1 and UPNM/2022/GPJP/SG/8. The authors acknowledge the encouragement, support, and constructive suggestions of Prof. Emeritus Dato' Dr. Wan Md Zin Wan Yunus and the active participation of the colleagues of the Centre of Tropicalisation (CENTROP).

## REFERENCE

Ambekar, A., Kim, M., & Yoh, J.Y. (2017). Characterization of display pyrotechnic propellants: Coloured light. *Appl. Therm. Eng.*, **110**: 1066-1074.

Aviv, U., Kornhaber, R., Harats, M., & Haik, J. (2017). The burning issue of white phosphorus: A case report and review of the literature. *Disaster Mil. Med.*, **3**: 1-5.

Babar, Z., & Malik. A.Q. (2014). Synthesis of micro porous barium nitrate with improved ignition reliability as a reliable pyrotechnic oxidant. *J. Saudi Chem. Soc.*, **18**: 707-711.

Brown, S.D., Charsley, E.L., Goodall, S.J., Laye, P.G., Rooney, J.J., & Griffiths, T.T. (2003). Studies on the ageing of a magnesium potassium nitrate pyrotechnic composition using isothermal heat flow calorimetry and thermal analysis techniques. *Thermochim. Acta,* **401**: 53-61.

Buchanan, M.V., Rubin, I.B., & Moneyhun, J.H. (1983). Compositional changes in red and violet smoke mixes after combustion. United States. Available online at: https://www.osti.gov/biblio/6344118.

Cao, L., Zhang, X.G., Wang, J.G., Wang, H.B., Chen, Y.B., Zhao, D.H., Shi, W.F., & Xie, L.X. (2016). Pulmonary function test findings in patients with acute inhalation injury caused by smoke bombs. *J. Thorac. Dis.*, **8**:3160-3167.

Carrico, C.M., Gomez, S.L., Dubey, M.K., & Aiken, A.C. (2018). Low hygroscopicity of ambient fresh carbonaceous aerosols from pyrotechnics smoke. *Atmos. Environ.*,**178**:101–108.

Chin, A., & Borer, L. (1983). Identification of combustion products from coloured smokes containing organic dyes. *Propellants, Explos. Pyrotech.*, **8**: 112-118.

Chunlong, Z., Nianchun, M., & Liyun, L. (1993). An investigation of the thermal stability of some yellow and red azo pigments. *Dyes Pigm.*, **23**: 13-23.

Danali, S.M., Palaiah, R.S., & Raha, K.C. (2010). Developments in pyrotechnics. *Def. Sci. J.*, **60**: 152-158.

Dilger, J.M., Martin, T.M., Wilkins, B.P., Bohrer, B.C., Thoreson, K.M., & Fedic, P.W (2022). Detection and toxicity modeling of anthraquinone dyes and chlorinated side products from a coloured smoke pyrotechnic reaction. *Chemosphere*, **287**: 131845

Ellern, H. (1968). Military and civillian pyrotechnics. Chemical Publishing Company Inc., New York.

Eslami, A., & Hosseini, S.G. (2010). Improving safety performance of lactose-fueled binary pyrotechnic systems of smoke dyes. *J. Therm. Anal. Calorim*., **104**: 671–678.

Faber, P., Drewnick, F., Veres, P.R., Williams, J., & Borrmann, S. (2013). Antropogenic sources of aerosol particles in football stadium: Real time characterization of emissions from cigarette smoking, cooking, hand flares, and colour smoke bombs by high resolution aerosol mass spectrometry. *Atmospheric Environ.*, **77**: 1043-1051.

Gluck, J. (2018). *Development and Characterization of Environmentally Benign Light and Smoke Producing Pyrotechnical Formulations*. PhD Thesis, University Munchen, Trostberg, Deutschland.

Gluck, J., Klapötke, T.M., Rusan, M., & Shaw, A.P. (2016). improved efficiency by adding 5-aminotetrazole to anthraquinone-free new blue and green coloured pyrotechnical smoke formulations. *Propellants, Explos. Pyrotech.*, **42**: 131-141.

Gluck, J., Klapötke, T.M., & Küblböck, T. (2018). 5-amino-1h-tetrazole-based multi-coloured smoke signals applying the concept of fuel mixes. *New J. Chem.*,**42**: 10670-10675.

Guo, R.-L, Liu, S.-H., & Lu, Y.-M. (2023). Investigation of how pressure influences the thermal decomposition behavior of azodicarbonamide. J. Loss Prev. Process. Ind., 83: 105062.

Han, Z., Jiang, Q., Du, Z., Hoon, H.H., Yu, Y., Zhang, Y., Gong, L., & Sun, Y. (2019). A novel environmental friendly and safe unpacking powder without magnesium, aluminium and sulphur for fireworks. *J. Hazard. Mater*., **373**: 835-843.

Hemmila, M., Hihkio, M., & Linnainmaa, K. (2007). Evaluation of the acute toxicity and genotoxicity of orange, red, violet and yellow pyrotechnic smoke in vitro. *Propellants, Explos. Pyrotech*., **32**: 415-422.

Hosseini, S.G., Pourmortazavi, S.M., & Hajimirsadeghi, S.S. (2005). Thermal decomposition of pyrotechnic mixtures containing sucrose with either potassium chlorate or potassium perchlorate. *Combust. Flame.*, **141**: 322–326.

Huang, K.-L., Chen, C.-W., Chu, S.-J., Perng, W.-C., & Wu, C.-P. (2008). Systemic inflammation caused by white smoke inhalation in a combat exercise. *Chest*, **133:** 722–728.

Istikamah, S., Zuraidah, S., Mecktin, M., Ahmad Hussein, A.H., & Noor Farahana, A.R. (2024). Synthesis of smoke signal with potassium nitrate (KNO3) as the oxidizer. *AIP Conf. Proc.*, **3014:** 070002

Küblböck, T., Angé, G., Bikelytė, G., Pokorná, J., Skácel, R., & Klapötke, T. M. (2020). Guanidinium 5,5′-azotetrazolate: A colourful chameleon for halogen-free smoke signals. *Angew. Chem. Int. Ed.*, **59**: 12326-12330.

Ledgard, J. (2007). *The Preparatory of Black Powder and Pyrotechnics, Version 1.4,* Jared Ledgard, Seattle.

Lee, J.-S., Hsu, C.-K., & Jaw, K.-S. (2001). The thermal properties of KClO4 with different particle size. *Thermochim. Acta*, **367-368**: 381–385.

Marrs, T.C., Colgrave, H.F., Rice, P., Edginton, J.A.G., & Morris, B. (1989). The repeated dose toxicity of a smoke containing Disperse Blue 180, an anthraquinone dye mixture, *J. Hazard. Mater*., **21**: 73-88.

Mojsilović, J., Petković-Cvetković, J., Kostić, D., Nešić, J., Ilić, J., & Krstović, M. (2022). Design of suitable pyrotechnic delay composition with widely used components. *International Scientific Conference on Defensive Technologies*, Belgrade, Serbia.

Monogarov, K.A., Meerov, D.B., Fomenkov, I.V., & Pivkina, A.N. (2023). Energy transferred to energetic materials during impact test at reaction threshold: Look back to go forward. *FirePhysChem*, **3**: 255–262.

Moretti, J.D., Sabatini, J.J., Shaw, A.P., & Chen, G. (2012). *Environmentally Sustainable Yellow Smoke Formulations for Use in the M194 Hand Held Signal*. U.S. Army RDECOM-ARDEC, Arsenal.

Moretti, J.D., Sabatini, J.J., Shaw, A.P., Chen, G., Gilbert, R.A., & Oyler, K.D. (2013). Prototype Scale development of an environmentally benign yellow smoke hand-held signal formulation based on Solvent Yellow 33. *ACS Sustain. Chem. Eng.*, **1**: 673–678.

Moretti, J.D., Sabatini, J.J., Shaw, A.P., & Gilbert, R.J. (2014). Promising properties and system demonstration of an environmentally benign yellow smoke formulation for hand-held signals. *ACS Sustain. Chem. Eng*., **2**:1325-1330.

NCI (National Cancer Institute). (1987). *Bioassay of 2-Aminoanthraquinone for Possible Carcinogenicity*, National Institute of Health, Bethesda, Maryland, USA.

NRC (National Research Council). (1997). *Toxicity of Military Smokes and Obscurants: Volume 1.* The National Academies Press, Washington, DC.

NRC (National Research Council). (1999). *Toxicity of Military Smokes and Obscurants: Volume 3.* The National Academies Press, Washington, DC.

Ojha, P.K., & Karmakar, S. (2018). Boron for liquid fuel Engines-A review on synthesis, dispersion stability in liquid fuel, and combustion aspects. Prog. Aerosp. Sci., 100: 18-45.

Ouyang, D., Pan, G., Guan, H., Zhu, C., & Chen, Xin. (2011). Effect of different additives on the thermal properties and combustion characteristics of pyrotechnic mixtures containing the KCIO4/Mg-Al alloy. *Thermochim. Acta*. **513**: 119-123.

Perkins, E.J., To, K.T., St Mary, L., Laber, C.H., Bednar, A.J., Truong, L., Tanguay, R.L., & Garcia-Reyero, N. (2022). Developmental, behavioral and transcriptomic changes in zebrafish embryos after smoke dye exposure. *Toxics*,**10**: 210.

Pulpea, B.G., Nuță, C-V., Pulpea, D., Rotariu, A., Trană, E., Toader, G., Rotariu, T., Dîrloman, F., Șomoiag, P., & Ungureanu, M.I. (2023). Characterization of pyrotechnic composition used in tracer ammunitions. *Sci. Bull., Series B*, **85**:185-198.

Rabha, S., & Saikia, B.K. (2020). Advanced micro- and nanoscale characterization techniques for carbonaceous aerosols. In *Handbook of Nanomaterials in Analytical Chemistry*. Elsevier, pp. 449–472.

Reategui-Inga, M., Valdiviezo, W.A., Lu, J.K.G., Durand, R.P., Coaguila-Rodriguez, P., Reategui-Inga, R., Casas, G.V., Álvarez-Tolentino, D., & Cueva, A.F.C. (2024). PM2.5 and PM10 airborne concentrations resulting from fireworks during festivities: A systematic review. *Int. J. Sustain. Dev. Plan*., **19**: 1307-1318.

Sabatini, J.J. (2014). Advances toward the development of "green" pyrotechnics. *In* Brinck, T., *Green Energetic Materials*, John Wiley & Sons, Ltd, pp. 63-102.

Selvakumar, N., Azhagurajan, A., Sheikmohamed, P., & Suresh, A. (2013). Ballistic behaviour of gun powder and flash powder for firework chemicals as a function of particle sizes. *Measurement*, **46**: 3202–3210.

Sendelbach, L.E. (1989). A review of the toxicity and carcinogenity of antraquinone derivatives. *Toxicology*, **57**:227-240.

Shi, X. J., & Wang, L.Q. (2018). Thermal self ignition simulation of pyrotechnic composite in different conditions. *J. Therm. Anal. Calorim.*,**134**:2349-2358.

Sigman C.C., Papa, P.A., Doeltz, M.K., Perry, L.R., Twhigg, A.M., & Helmes C.T. (2008). A study of anthraquinone dyes for the selection of candidates for carcinogen bioassay. *J. Environ. Sci. Health A*, **20**:427-484.

Sijimol, M.R., & Mohan M. (2014). Environmental impacts of perchlorate with special reference to fireworks—A review. *Environ. Monit. Assess.*, **186**: 7203–7210.

Stoenescu, L. (2014). *Coloured Pyrotechnic Smoke-Producing Composition.* US PATENT, US20140238258A1

Springer, M.L, Rush, T., Beardsley, H.M., Watts, K., & Bergmann, J. (2008). *Demonstration of the replacement of the dyes and sulfur in the m18 red and violet smoke grenades*, Final Technical Report, Aberdeen.

Srinivasan, K. (2017). Eco friendly fireworks for atom bomb (Local name of cracker bomb). *J. Adv. Sci. Res.*, **1**: 2454-3225.

Tabacof, A., & Calado, V.M.d.(2017). Thermogravimetric analysis and differential scanning calorimetry for investigating the stability of yellow smoke powders. *J. Therm. Anal. Calorim.*, **128**: 387-398.

Tang, J-S., Liu, F-F., & Zhu, C-G. (2023). Thermal decomposition and combustion behavior of potassium perchlorate catalyzed by LaFeO3. *Energetic Materials Frontiers*, **4**: 44-48.

Tuukkanen, I. M., Brown, S.D., Charsley, E.L., Goodall, S.J., Laye, P.G., Rooney, J.J., Griffiths, T.T., & Lemmetyinen, H. (2005). A study of the influence of the fuel to oxidant ratio on the ageing of magnesium-strontium nitrate pyrotechnic compositions using isothermal microcalorimetry and thermal analysis techniques. *Thermochim. Acta*, **426**: 115-121.

Zeman, O., Pelikan, V., & Pachman, J. (2022). Diketopyrrolopyrrole─A greener alternative for pyrotechnic smoke compositions. *ACS Sustain. Chem. Eng.*, **10**: 4788-4791.

# EVALUATING THE EFFECT OF BACKGROUND MUSIC TEMPO ON MANUAL HAND DEXTERITY

Tan Wai Yee[1], Nur Hamizah Nazaruddin[1], Brinnell Caszo[2] & Justin Gnanou[2*]

[1]School of Pharmacy
[2]School of Medicine
International Medical University, Malaysia

[*]Email: justingnanou@gmail.com

## ABSTRACT

*Manual hand dexterity involves highly coordinated hand motions for completion of specific tasks, which is crucial for various military activities such as hand-to-hand combat and practical drills. This response is usually a learned behaviour and can be influenced by the body's physiological responses to external stimuli such as background music. In this study, the effect of background music tempo on manual hand dexterity was investigated. A total of 50 male subjects aged 18 to 26 years were administered a manual hand dexterity test with a Purdue Pegboard under three conditions: no background music, slow-tempo classical music and fast-tempo classical music. The order of the music conditions was determined randomly. Mean dexterity values for no music, slow-tempo classical music and fast-tempo classical music were 51.34 ± 6.26, 50.30 ± 6.34 and 52.32 ± 6.82 respectively. Repeated measures ANOVA followed by post-hoc analysis for Bonferroni correction showed no statistically significant differences between the three music conditions, indicating that manual hand dexterity is not affected by different types of background music. The main finding of this study is that listening to slow- and fast-tempo music did not have statistically significant effect on manual dexterity scores among the subjects. This indicates that other factors such as familiarisation, rhythmic auditory stimulation and sufficient time are needed concurrently for the effects to be prominent.*

**Keywords:** *Manual hand dexterity; background music; tempo; Purdue Pegboard; statistical significance.*

## 1. INTRODUCTION

Hand dexterity is an important physical function required to carry out various military training exercises such as acquiring higher level of skills in combative training, such as hand-to-hand combat, judo and karate. This requires acquisition skills such as mobility and flexibility along with dexterity (Wąsik *et al.*, 2022). Other than self-defence and forms of combat involving hands, dexterity of one's hand is also important for practical drills, such as obstacle courses, which requires good hand motor skills in the execution of climbing and jumping the various obstacles, parallel cables and pillars (Terlizzi *et al*., 2022). The same function could also be useful in other military activities, such as throwing grenades, applicative swimming and skiing (Stănciulescu, 2023).

Dexterity represents highly coordinated, flexible and defined movements that allow for the completion of various tasks (Sobinov & Bensmaia, 2021). Flexibility involves the ability to train new movements in muscles until they become muscle memories. For the hands, this translates into the ability to conform to specific shapes to hold things with the right amount of strength and force (Sobinov & Bensmaia, 2021). Several tests have been developed to evaluate hand dexterity, including hand features such as grip shape and dexterity stages. Nevertheless, there are still limitations to these tests as they are unable to grasp the complexity of the hands' functions. The Purdue Pegboard test is one of the tests used to assess one's ability to elicit more controlled finger and hand movements through small objects, pins, washers and collars. It measures articulated finger and hand manipulation, which emphasises reliability and validity (Sanchez, 2016).

Hand dexterity though is an innate skill, can be improved by training as well as by understanding the factors that has an effect of hand dexterity. Studies have shown, hand dexterity can be improved by background music. An example of this effect is the improved performance of e-sports players, where the games' repeated beats and background music makes it easier for the players to manipulate their fingers to be more harmonised and coordinated (Shah & Oberoi, 2021). In the medical field, it has been shown that background music enhances surgeons' hand performances during surgeries, resulting in better post-surgical outcomes (Rogers *et al*., 2019; Han *et al*., 2022; Co *et al*., 2022). Both these examples illustrate the effect of background music on hand dexterity in performing fine coordinated motor actions. This effect is explained by the fact that listening to music modifies one's behavioural responses (Warren, 2008). However, there is a lack of studies on the effects of different types of background music on hand dexterity.

Background music seems to affect working performances both positively and negatively (Taheri *et al*., 2022). For instance, surgeons are known to work with self-selected playlists during surgeries because this aids their attention and operative skills. Self-selected playlists boost one's attention span and strengthen one's hand dexterity, eventually producing fine-tuned hand motions and speed. Some surgeons have reported that self-selected playlists buffer undesirable background noise, reducing distraction levels during surgeries. These distractions could increase their cognitive and mental burdens, affecting their capability for dissecting information during work. Background music also acts as an anxiolytic with its soothing effect. On the other hand, other surgeons prefer working in silence because they regard background music as a source of distraction. They have claimed that background music has detrimental effect on their attention span (Rogers *et al*., 2019).

The type of music also has varying effects on hand dexterity and fine hand movements. Lyrical music is known to affect one's performance negatively, with the lyrics posing as a distraction (de Witte *et al*., 2020; Souza & Leal Barbosa, 2023). On the other hand, instrumental and classical music, which lacks lyrics, tends to be less distracting. This type of music may help individuals concentrate better and avoid forming biased opinions about the effects of background music on their performance. Essentially, it could lead to more objective assessments of how music affects their work (Huang & Shih, 2011). Music tempo may also influence performance. Generally, fast-tempo music has 120 or more beats per minute (BPM), while slow-tempo music has between 40 to 60 BPM. It is hypothesised that fast-tempo music excites movements, while slow-tempo music relaxes movements, thus influencing hand dexterity (Woo & Song, 2022).

The objective of this study is to investigate the effects of listening to slow- and fast-tempo instrumental classical music and compare it with the effect of not listening to any music while performing tests of manual hand dexterity. This would help to understand the effect of background music on improving hand dexterity and thus can be useful in developing strategies in improving skills that require good hand dexterity.

## 2. METHODOLOGY

A total of 50 male university students (18-26 years) were recruited for this study. Participants with hand injuries, history of arthritis and neck strain, hand deformities, oedematous, vascular or inflammatory hand conditions, as well as neurodegenerative diseases were excluded from this study. Informed consent was obtained prior to the start of the experimental protocol detailing the project's purpose, procedures and potential risks. Clear instructions were given and repeated on the day of the experiment to ensure the participants' full comprehension. Ethical approval was obtained from the Joint Research and Ethics Review Committee of the university.

## 2.1 Experimental Protocol

Manual hand dexterity was measured using the Purdue Pegboard test (Fabrication Enterprises Inc, USA). Participants were briefed about the test protocol before the start of the experiment. This test was conducted in four segments. Segments 1 and 2 required the participants to insert pins using each hand individually for 30 s time periods. Segment 3 required the participants to insert pins with both hands simultaneously for 30 s time periods. Segment 4 required the participants to build small assemblies involving pins, collars and washers with both hands simultaneously for 1 min time periods. Five scores were obtained from the four segments: 1) right (R) hand (30 s); 2) left (L) hand (30 s); 3) both hands (30 s); 4) right + left + both hands; and 5) assembly (60 s). The total score (R + L + score for both hands + assembly, i.e., combined score) was taken to represent the overall dexterity function.

This test was conducted under three conditions; no music, slow-tempo classical music and fast-tempo classical music with short breaks in between. The slow-tempo classical music played was String Quartet No. 16, Op. 135 by Beethoven, while the fast-tempo classical music played was Symphony No. 35, IV. Presto by Mozart. The entire experiment was conducted in a standardised room, where each session took 1 h. The participants were asked to complete the tasks while wearing a set of headphones.

## 2.2 Statistical Analysis

The data collected was expressed through means and standard deviation. Repeated measures ANOVA with post-hoc analysis of Bonferroni correction was conducted to compare the mean dexterity scores of each music condition using the SPSS (v29) statistical package. A *p*-value of less than or equal to 0.05 was taken as statistically significant.

# 3. RESULTS

The participants' mean physical traits are expressed in Table 1, including their age, weight, height and calculated body mass index (BMI). Right-handed participants accounted for 94% of the total, while the remaining 6% were left-handed, with none reporting ambidexterity.

**Table 1: Participants physical traits.**

| Subjects' Traits | Age (years) | Weight (kg) | Height (m) | BMI (kg/m$^2$) |
|---|---|---|---|---|
| Mean | 21.66 ± 1.98 | 66.77 ± 10.50 | 1.72 ± 0.06 | 22.49 ± 3.18 |

The scoring procedure of the Purdue Pegboard test is the score combination of Segments 1, 2 and 3, titled 'total scores'. These total scores represent manual hand dexterity. The mean dexterity scores calculated from the total scores under the three background music conditions are shown in Table 2. Repeated measures ANOVA analysis showed a $F$-statistic value of 2.33 and $p$-value of 0.10 (Table 3), indicating that the mean scores between the groups are not statistically significant. Post-hoc analysis for Bonferroni correction to study multiple comparisons between the groups also showed no significant difference ($p > 0.01667$, with the corrected significance level being 0.05/3 group pairs) (Table 4).

**Table 2: Mean hand dexterity scores using the Purdue Pegboard Test.**

| | No music | Slow-tempo music | Fast-tempo music |
|---|---|---|---|
| Mean dexterity score | 51.34 ± 6.26 | 50.30 ± 6.34 | 52.32 ± 6.82 |

**Table 3: Repeated measures ANOVA test.**

| | Degree of freedom | Sum of square (SS) | Mean square (MS) | *F*-statistic ($df_1$, $df_2$) | *p*-value |
|---|---|---|---|---|---|
| Interaction between groups | 2 | 102.04 | 51.02 | 2.33 (2.98) | 0.10 |

**Table 4: Post-hoc analysis for Bonferroni correction.**

| Group Pairs | Difference between pairs | *F*-statistic | Critical value | *p*-value |
|---|---|---|---|---|
| No music - Slow music | 1.04 | 1.58 | 6.14 | 0.21 |
| No music - Fast music | 0.98 | 0.80 | 6.14 | 0.38 |
| Slow music - Fast music | 2.02 | 5.50 | 6.14 | 0.02 |

## 4. DISCUSSION

Previous studies have found that music-supported therapies (MST), whereby music is integrated into therapy for patients with impaired gross and fine motor skills, have better outcomes alongside rehabilitation (Hatampour *et al*., 2011; Maktoufi *et al*., 2015). It was found that repetitive motion while coordinating with the music's rhythm and beats fine tunes the fingers' neuromuscular function by strengthening their muscles and stimulating inhibited motions (Kimoto *et al*., 2019; Huang *et al*., 2021; Yang *et al*., 2022). Huang & Shih (2011) found that playing musical instruments affects the physical aspects of hand movements, whereby the rhythmic auditory stimuli initiate recovery pathways within the patients' damaged hemispheres, refining the hemispheres' cerebral functions. This mechanism triggers a self-repair system within the central nervous system known as neuroplasticity, whereby the construction of new synapses and increased blood flow to damaged areas occurs (Huang *et al*., 2021). A similar result was found in a study conducted by Friedman *et al*. (2014) on stroke patients, with a glove designed for hand rehabilitation therapy, specifically to train patients' grasping ability and thumb-finger locomotion. This therapy involved an interactive musical video game, stimulating repetitive finger muscle motions following the music's rhythm and beats. With MST, persistent hand movements and rhythmic auditory stimuli both appear to play a role to stimulate one's full potential in hand motions. Additionally, these therapies were conducted in a four to eight-week course, where the time given was believed to play a role in restoring their hand dexterity. While repetitive performance of the task had positive influence on dexterity, the skill may have been enhanced by the auditory effect of music rhythms and beats.

Contrary to this, in our study, there was no significant differences between the mean scores for all groups (no music, slow-tempo and fast-tempo), indicating that background music has no effect on manual hand dexterity. This could be attributed to the fact that only rhythmic auditory stimulation was present as well as no extensive repetitions of hand movements were involved since the participants only had to conduct the Purdue Pegboard test three times. Each test also took about 2 minutes, which is not ample for neuroplasticity and finger manipulation to take place fully. These factors could be the reason for the lack of the insignificant differences seen in our study.

Another aspect of background music that has been studied is the tempo of the music. The brain processes music specifically through Heschl's gyrus with its surroundings handling complex musical components. Ley-Flores *et al*. (2022) proved that these interpreted musical components trigger certain bodily responses when they are projected physically, emotionally and mentally. These responses explain the musical tempo differences inflicted on one's body. Musical tempos have larger effect on the cardiovascular system where fast-tempo music causes increased minute ventilation, blood pressure, heart rate and mid-cerebral artery flow, while slow-tempo music causes the opposite effect (Haluk & Turchian, 2009; Kulinski *et al*., 2022). Fast-tempo music is an excitatory component and is often used as a working companion as it increases productivity (Haluk & Turchian, 2009). On the other hand, slow-tempo music is a soothing component, which calms down an individual physically and emotionally by reducing cortisol levels. Therefore, it is illustrated as a relaxing tool for stress and anxiety (Ley-Flores *et al*., 2022). The differences can be observed among athletes, where fast-tempo music is used for energising, while slow-tempo music is used for calming purposes. Oftentimes, they perform better when warmed up under the influence of fast-tempo music (Haluk & Turchian, 2009).

However, in our study, we did not find any statistical difference between slow- and fast-tempo music, indicating that background music may not have much effect on manual hand dexterity. Instead, repeated finger movements and ample duration of time are still required to exert an effect on manual hand dexterity (Olafsdottir *et al*., 2008; Blázquez-Fernández *et al*., 2024).

## 5. CONCLUSION

Based on the findings of this study, the effect of background music on manual hand dexterity remains ambiguous. However, previous studies have suggested that extensive repetition of finger motions, rhythmic auditory stimulation and long durations are required to affect manual hand dexterity. These factors have been taken into consideration as a guideline when using music in treatment and rehabilitation of stroke patients. The same strategy can also be used as a training tool within military training to improve hand dexterity.

## REFERENCES

Blázquez-Fernández, A., López-Hazas-Jiménez, G., Fernández-Vázquez, D., Navarro-López, V., Fernández-González, P., Marcos-Antón, S., Molina-Rueda, F., & Cano-de-la-Cuerda, R. (2024). Effects of the powerball® system on muscle strength, coordination, fatigue, functionality and quality of life in people with multiple sclerosis. A randomized clinical trial. *J. Neuroeng. Rehabil*., **21**: 33.

Co, M., Fong, S.M. & Lau, Y.C.C. (2022). Effect of background music in the operating room on surgical outcomes: A prospective single-blinded case-control study. *J. Am. Coll. Sur.*, **235:** 447–453.

de Witte, M., Spruit, A., van Hooren, S., Moonen, X. & Stams, G. J. (2020). Effects of music interventions on stress-related outcomes: a systematic review and two meta-analyses. *Health Psychol. Rev.*, **14**: 294–324.

Friedman, N., Chan, V., Reinkensmeyer, A.N., Beroukhim, A., Zambrano, G.J., Bachman, M. & Reinkensmeyer, D.J. (2014). Retraining and assessing hand movement after stroke using the MusicGlove: comparison with conventional hand therapy and isometric grip training. *J. Neuroeng. Rehabil.*, **11**: 76.

Haluk, K., & Turchian, C. (2009). The effects of music on athletic performance. *"Ovidius" Univ. Ann. Ser. Phys. Educ. Sport. Sci., Mov. Health.*, **9**: 44.

Han, Y., Zheng, B., Zhao, L., Hu, J., Zhang, C., Xiao, R., Wang, C. & Pu, D. (2022). Impact of background music on the performance of laparoscopy teams. *BMC Med. Educ.*, **22**: 439.

Hatampour, R., Zadehmohammadi, A., Masoumizadeh, F., & Masoud, S. (2011). The effects of music therapy on sensory motor functions of multiple handicapped People: Case study. *Procedia. Soc. Behav. Sci.*, **30**: 1124–1126.

Huang, R.H. & Shih, Y.N. (2011). Effects of background music on concentration of workers. *Work*, **38**: 383–387.

Huang, W. H., Dou, Z. L., Jin, H. M., Cui, Y., Li, X., & Zeng, Q. (2021). The Effectiveness of Music Therapy on Hand Function in Patients with Stroke: A Systematic Review of Randomized Controlled Trials. *Front. Neurol.*, **12**: 641023.

Kimoto, Y., Oku, T., & Furuya, S. (2019). Neuromuscular and biomechanical functions subserving finger dexterity in musicians. *Sci. Rep-UK.*, **9**: 12224.

Kulinski, J., Ofori, E. K., Visotcky, A., Smith, A., Sparapani, R., & Fleg, J. L. (2022). Effects of music on the cardiovascular system. *Trends Cardiovas. Med.*, **32**: 390–398.

Ley-Flores, J., Alshami, E., Singh, A., Bevilacqua, F., Bianchi-Berthouze, N., Deroy, O., & Tajadura-Jiménez, A. (2022). Effects of pitch and musical sounds on body-representations when moving with sound. *Sci. Rep-UK.*, **12**: 2676.

Maktoufi, R., Ghotbi. N., & Nakhostin, A. N. (2015). The Effects of Listening to Persian Music on the Hand Dexterity and Depression in a Patient with Stroke: A Case Report. *J. Rehab. Sci. Res.*, **2**: 68-70.

Olafsdottir, H. B., Zatsiorsky, V. M., & Latash, M. L. (2008). The effects of strength training on finger strength and hand dexterity in healthy elderly individuals. *J. Appl. Physiol.*, **105**: 1166–1178.

Rogers, C. M., Palmerton, H., Saway, B., Tomlinson, D., & Simonds, G. (2019). Effect of Various OR Noise on Fine Motor Skills, Cognition, and Mood. *Sur. Res. Pract.*, **2019**: *5*372174.

Sanchez, V. (2016). Development of a dexterity assessment method. Doctor of Philosophy [Internet]. https://api.semanticscholar.org/CorpusID:114159447

Shah, H., & Oberoi, M. (2021). Effect of video game music on hand dexterity performance in Young Adults. *Int. J. Cur. Res. Rev.*, **13**: 39–42.

Sobinov, A. R., & Bensmaia, S. J. (2021). The neural mechanisms of manual dexterity. *Nat. Rev. Neurosci.*, **22**: 741–757.

Souza, A. S., & Leal Barbosa, L. C. (2023). Should We Turn off the Music? Music with Lyrics Interferes with Cognitive Tasks. *J. Cogn.*, **6**: 24.

Stănciulescu, R. (2023). Dexterity, Mobility and Flexibility, Essential Components in the Development of the Military Students' Motor Skills. *Int. Con. KBO.*, **29**: 242-246.

Taheri, S., Razeghi, M., Choobineh, A., Kazemi, R., Rasipisheh, P., & Vali, M. (2022). Investigating the effect of background music on cognitive and skill performance: A cross-sectional study. *Work*, **71**: 871–879.

Terlizzi, B., Abrams, T. C., Sacko, R. S., Hand, A. F., Silvey, K., & Stodden, D. F. (2022). The Relationship Between Functional Motor Competence and Performance on the Army Combat Fitness Test in Army Reserve Officer Training Corps Cadets. *Mil. Med.*, **537**: 1–8.

Warren J. (2008). How does the brain process music? *Clin. Med.*, **8**: 32–36.
Wąsik, J., Bajkowski, D., Shan, G., Podstawski, R., & Cynarski, W.J. (2022). The Influence of the Practiced Karate Style on the Dexterity and Strength of the Hand. *App. Sci.*, **12**: 3811.
Woo, H. S., & Song, C. S. (2022). Comparison of Hand Dexterity According to Selected Thermal and Auditory Stimuli. *Int. J. Environ. Res. Public Health*, **20**: 765.
Yang, S., Suh, J. H., Kwon, S., & Chang, M. C. (2022). The effect of neurologic music therapy in patients with cerebral palsy: A systematic narrative review. *Front. Neurol.* **13**: 852277.

# DESIGN AND SIMULATION OF RF FILTERS FOR MITIGATING CO-LOCATION INTERFERENCE IN MILITARY GROUND VEHICLE TACTICAL RADIOS

Muhammad Ramdhan Mohd. Suhaili*, Amirah Sakinah Mohd Rozlan, Ahmad Faridz Abd.Ghafar & Ibrahim Tahir

Electromagnetic Compatibility (EMC) Branch, Instrumentation and Electronics Technology Division (BTIE), Science & Technology Research Institute for Defence (STRIDE), Malaysia

*Email: ramdhan@stride.gov.my

## ABSTRACT

*This paper presents the design and simulation of radio frequency (RF) filters to mitigate co-location interference between high-frequency (HF) and very high-frequency (VHF) tactical radios used in military ground vehicles with minimal insertion loss. The interference occurs due to the proximity of the HF and VHF radio antennas, with HF signals distorting the VHF radio signals and vice versa. In order to minimise the interference, low- and high-pass filters are designed and simulated to achieve steep roll-off, low passband ripple and complete rejection in the stop-band region. The Advanced Design System (ADS) simulator is used in the filter design, which starts with preliminary studies to choose the best method for designing the RF filter based on military communication system specifications. This includes selecting the insertion loss method, filter topology and passband ripple. Based on this, the RF filter implements a Chebyshev type 1 design with passband ripple of 0.15 dB and passive lumped elements. Therefore, 19th-order Chebyshev low- and high-pass filters are designed and simulated using ADS. From the simulation, a low-pass filter with a cut-off frequency of 29.73 MHz at -3.00 dB was designed. This filter exhibits a sharp suppression of about -114.83 dB in the stop-band at 40 MHz and a return loss of -14.7 dB. Similarly, a high-pass filter with cut-off frequency of 29.27 MHz at -3.00 dB was designed. This filter also shows a sharp suppression of about -114.82 dB in the stop-band at 21.76 MHz and has return loss of -14.7 dB, making it effective for eliminating co-location interference.*

**Keywords:** *Co-location interference; high frequency (HF) and very high frequency (VHF); low- and high-pass filter; insertion loss method; Chebyshev.*

## 1. INTRODUCTION

Communication is a crucial element of military operations and missions. Thus, the development of various radio technologies, such as narrowband radios, broadband radios and radio relays, has enabled radio communication devices at both stationary and mobile command posts for voice and data transmission services. One of the key challenges faced by those responsible for organising these radio communication systems is ensuring the internal compatibility of the system by suppressing internal interference. In this respect, the most difficult problem is frequency planning for radios located at the same site. When multiple radio frequency (RF) transmitting and receiving systems are installed in close proximity, the issue of co-location antenna interference can often arise. The physical closeness of the various antennas can result in undesirable interactions and coupling between the RF signals, leading to interference that degrades the performance and reliability of the communication systems (Polak, 2020; Umer *et al.*, 2020; Murthy & Reddy, 2022).

In the modern warfare era, most military ground assets are equipped with high-frequency (HF) and very high-frequency (VHF) tactical radios as their communication systems. These subsystems offer different advantages depending on the communication needs (Chan *et al.*, 2021). Figure 1 shows the block diagram for HF and VHF radio communication systems that are currently used in Malaysia's military ground assets such as Gempita and Adnan. VHF radios have frequency range of 30 to 300 MHz, while HF radios have frequency range of 3 to 30 MHz. As electrically short antennas, such as whip and dipole antennas are shorter than a quarter-wavelength, auto tuning unit (ATU) is often required to effectively match the antenna's impedance to the impedance of the transmitter or transmission line (Carr, 2001). The positioning of HF and VHF radio antennas on military ground vehicles is close to each other due to the limited antenna installation space available, which increases the risk of co-location interference (Karlsson *et al.*, 2013). This interference can be observed when HF radio signals penetrate the VHF frequency path, distorting the VHF radio signals. This is particularly evident when HF and VHF radios are used simultaneously (Sarris *et al.*, 2002).

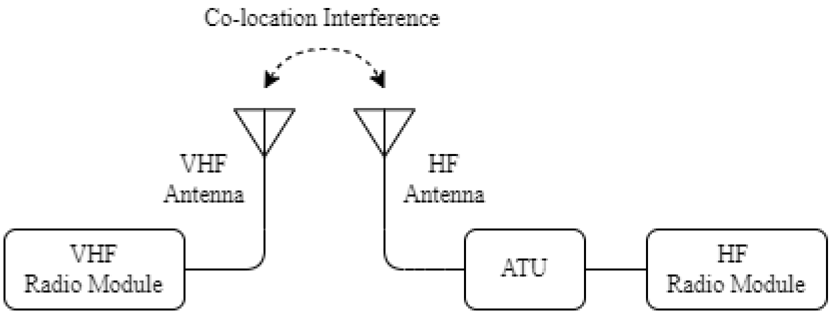


**Figure 1: Block diagram for a communication system in military ground vehicles.**

The use of RF filters can reduce the effects of co-location interference. RF filters are designed to selectively pass or reject specific frequency bands, allowing for efficient signal transmission and reception while attenuating unwanted signals or interference. The use of low- and high-pass filters can minimise the effects of co-location interference on HF and VHF radio signals respectively. A low-pass filter allows signals with frequencies below a certain cut-off frequency to pass through while attenuating or blocking higher-frequency signals. On the other hand, a high-pass filter allows signals with frequencies above a certain cut-off frequency to pass through, while attenuating or blocking lower-frequency components (Pozar *et al.*, 2012; Yang *et al.*, 2023).

In this paper, low- and high-pass filters are designed and simulated. The design starts with preliminary studies to choose the best method for designing the RF filter based on military communication system specifications. This includes selecting the insertion loss method, filter topology and pass-band ripple. Based on this, the RF filter design implements a Chebyshev type 1 design with pass-band ripple of 0.15 dB and passive lumped elements.

## 2. DESIGN REQUIREMENTS

The design requirements of low- and high-pass filters are based on existing military communication system specifications. Table 1 shows the design requirements for both filters.

**Table 1: RF filter design requirements.**

| Requirements | Low Pass Filter | High Pass Filter |
|---|---|---|
| Cut-off Frequency | 29.5 MHz | 29.5 MHz |
| Stopband Attenuation | -113 dBm | -113 dBm |
| Power Transmit | 150 W | 50 W |
| Design Technique | Passive | Passive |
| Design Type | Lumped elements | Lumped elements |
| Impedance | 50 Ω | 50 Ω |

Due to limited power supply in military vehicles, a passive filter design technique is employed for power conservation. This technique will benefit the existing installation system because no additional modifications are needed. Lumped element filters are passive electronic circuits composed of discrete inductors, capacitors and resistors. These filters are designed to selectively pass or attenuate signals based on their frequency, fulfilling specific filtering requirements in various applications (Bharathy *et al.*, 2020; Zedníček, 2023). Lumped elements offer significant advantages in RF applications, characterised by their compact size and cost-effectiveness as compared to micro-strip filters in low-frequency bands. They excel in handling high RF power levels while maintaining a stable stop-band response (Chen, 2013). They are particularly effective for frequencies ranging from low frequency up to 500 MHz, making them suitable for filters designed to cover frequencies up to a maximum of 300 MHz. This characteristic makes them ideal for a wide range of RF filtering applications where space and cost considerations are critical (Salama *et al.*, 2022).

Figure 2 shows the proposed improvement of the communication system. For the VHF communication system, a high-pass filter is proposed to be placed between the VHF radio and antenna. For the HF communication system, a low-pass filter will be installed between the HF radio and ATU.

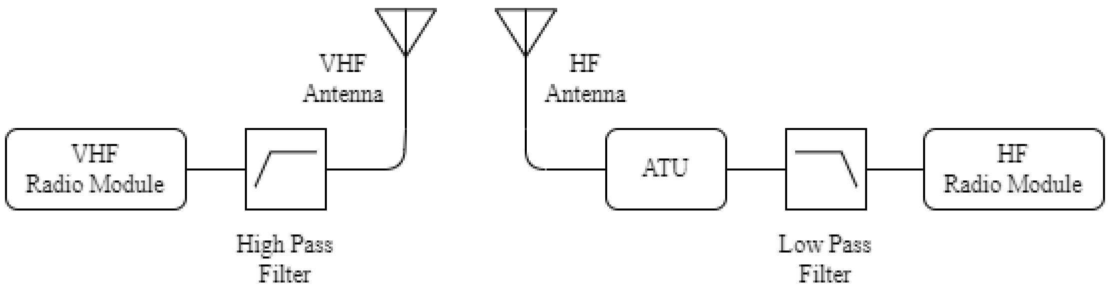


**Figure 2: Block diagram for improved communication system in military ground vehicles.**

## 3. PRELIMINARY STUDY

A preliminary study was conducted to select an appropriate design methodology to ensure that the filter effectively eliminates co-location interference. The designed filter aims to achieve two key objectives: steep roll-off and low pass-band ripple. Steep roll-off is a gradient of transition from the passband to the stop band, while pass-band ripple is a ripple that occurs at the pass-band region before the cut-off frequency. These specifications are crucial for enhancing the filter's performance in preventing unwanted frequency components and maintaining signal integrity within the desired pass-band (Tomar & Parihar, 2023). Designing a high-pass filter from a low-pass filter is a common technique in filter design. This is usually achieved through a transformation that inverts the frequency response of the low-pass filter. The process involves replacing the elements of the low-pass filter (inductors and capacitors) with their high-pass equivalents. Therefore, all the preliminary studies are conducted for low-pass filters.

### 3.1 Insertion Loss Method Selection

In this paper, the insertion loss method is employed for the filter design. It is a widely adopted approach in filter design and enables the creation of filters with predetermined power transmission ratios. This method operates under the assumption of a lossless filter structure, theoretically implying a unity reflection power ratio within the stop-band. This characteristic designates these filters as reflective filters, as the input power ratio in the stop-band is reflected to the input port. However, it has been observed that the reflected power can negatively impact the overall system performance when a reflective filter is not appropriately integrated with adjacent circuits (Lee *et al*., 2019).

Three types of filters that will be considered to create the low-pass filter, which are ~~are~~ Butterworth, Chebyshev and Bessel. The most crucial parameter is a steeper roll-off transition with the minimum number of filter orders. Figure 3 shows that Chebyshev filters boast the steepest transition from passband to stop-band, providing the most abrupt cut-off among the three topologies. On the other hand, Butterworth filters have a more gradual transition (Laghari *et al*., 2014), while Bessel filters prioritise a linear phase response over transition band sharpness, resulting in the most gradual transition. Based on this, for this study, Chebyshev filters are well-suited when steep transitions from passband to stop-band are priorities (Langhammer *et al*., 2023).

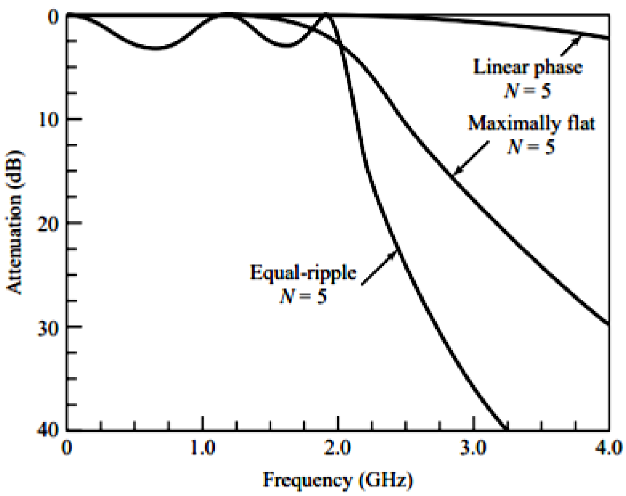


**Figure 3: S[2,1] responses for Butterworth (maximally flat), Chebyshev (equal-ripple) and Bessel (linear phase) low-pass filters (Source: Pozar *et al.*, 2012).**

S[2,1] is one of the important parameters for designing RF filters. It shows the power loss as it passes through the RF filter, revealing how effectively the RF filter allows desired frequencies while blocking unwanted ones. A low S[2,1] value indicates low insertion loss and high filter efficiency (Kiouach *et al*., 2023).

### 3.2 Filter Design Topology

In filter design, π and T topologies represent different configurations of passive components used to create RF filters with specific frequency responses. The π topology of the low-pass filter features two series capacitors with a shunt inductor connected between them to the ground. Conversely, the T topology of the low-pass filter consists of two series inductors with a shunt capacitor connected between them to the ground. The choice of filter topology is crucial, as it directly impacts the low-pass filter's frequency response (Adamczyk & Timmerman, 2024).

For this preliminary study, simulations are conducted using the Advance Design System (ADS) software for 3rd order Chebyshev low-pass filter with both π and T topologies. Figure 4 presents the comparison of the S[2,1] response for both topologies. It is observed that the π topology outperforms the T topology in the roll-off transition from passband to stop-band. The insertion loss of the π topology filter at 1.52 MHz is approximately -15.55 dB, while the T topology filter exhibits a value of -11.02 dB at the same frequency. This indicates that the π topology has a steeper roll-off as compared to the T topology. Thus, the π topology for the Chebyshev low-pass filter meets the design objective of achieving a steep roll-off transition from passband to stop-band.

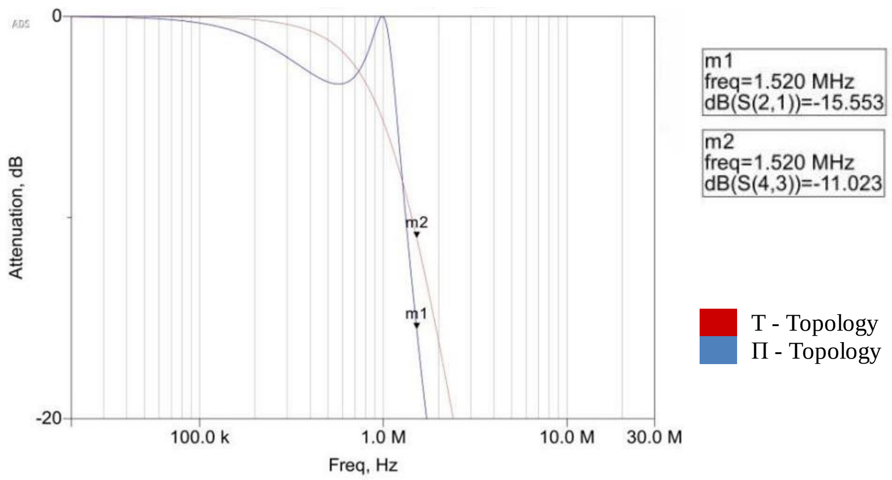


**Figure 4: S[2,1] responses for π and T topologies for the Chebyshev low-pass filter (Adamczyk & Timmerman, 2024).**

### 3.3 Chebyshev Type Design

Chebyshev Types I and II low-pass filters exhibit distinct characteristics that differentiate their performance. Figure 5 is generated using the ADS simulation software, with the 11th number of orders. It is observed that the Chebyshev Type I filter has equal ripple behaviour in the pass-band. In contrast, the Chebyshev Type II filter has a maximally flat pass-band response. The stop-band response of the Type I filter is flat as compared to the Type II, which allows for the effective elimination of interference beyond the cut-off frequency (Laghari *et al*., 2014).

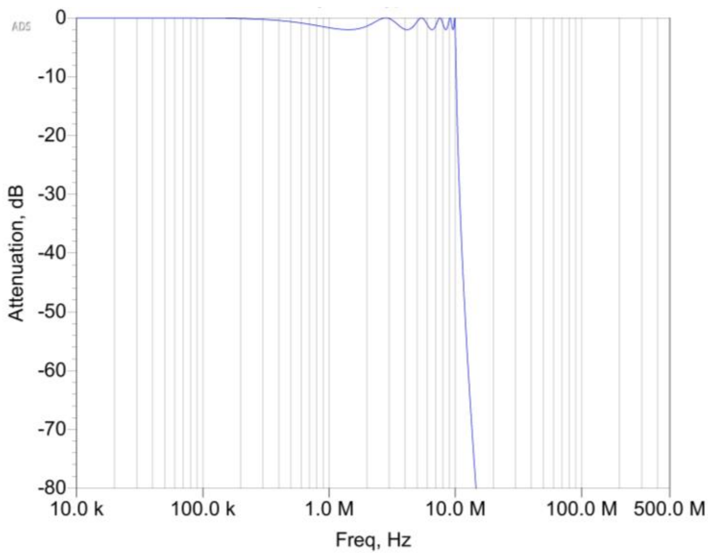


**(a)**

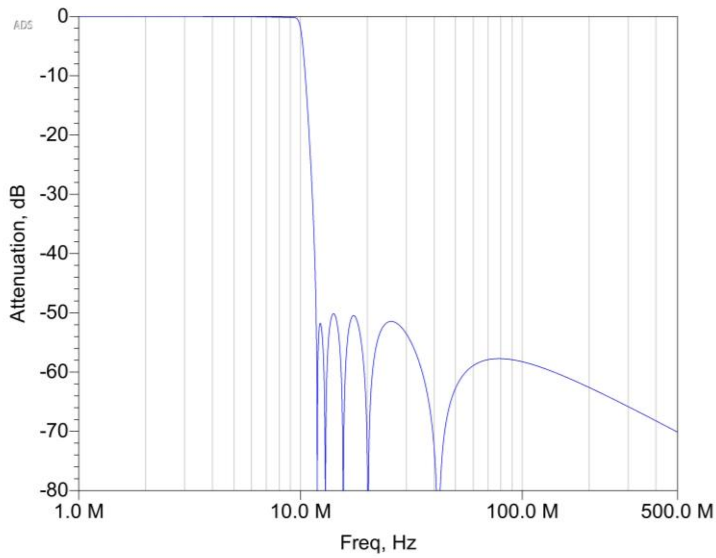


**(b)**

**Figure 5: Comparison between (a) Type I and (b) Type II Chebyshev low-pass filters (Laghari *et al*., 2014).**

### 3.4 Pass-Band Ripple

Chebyshev filters are designed to allow ripple in the pass-band, but steeper roll-off after the cut-off frequency (Mei, 2022). From Figure 6 (a), for S[2,1] for a cut-off of 29.5 MHz, the response shows that the higher the pass-band ripple, the steeper the cut-off. However, for this design, less insertion loss at the pass-band region is needed to ensure there is no significant loss when transmitting or receiving the signal through the tactical radio. Another parameter that needs to be considered in designing an RF filter is S[1,1], which measures the amount of power reflected from the filter's input, indicating how well the filter matches its input impedance. A low S[1,1] value signifies good impedance matching, meaning most of the input power is passing through the RF filter (Kiouach *et al*., 2023). The S[1,1] response in Figure 6 (b) shows that a lower pass-band ripple gives better return loss than a high pass-band ripple. In this design, a lower pass-band ripple is needed due to its minimal insertion loss at the pass-band with better return loss.

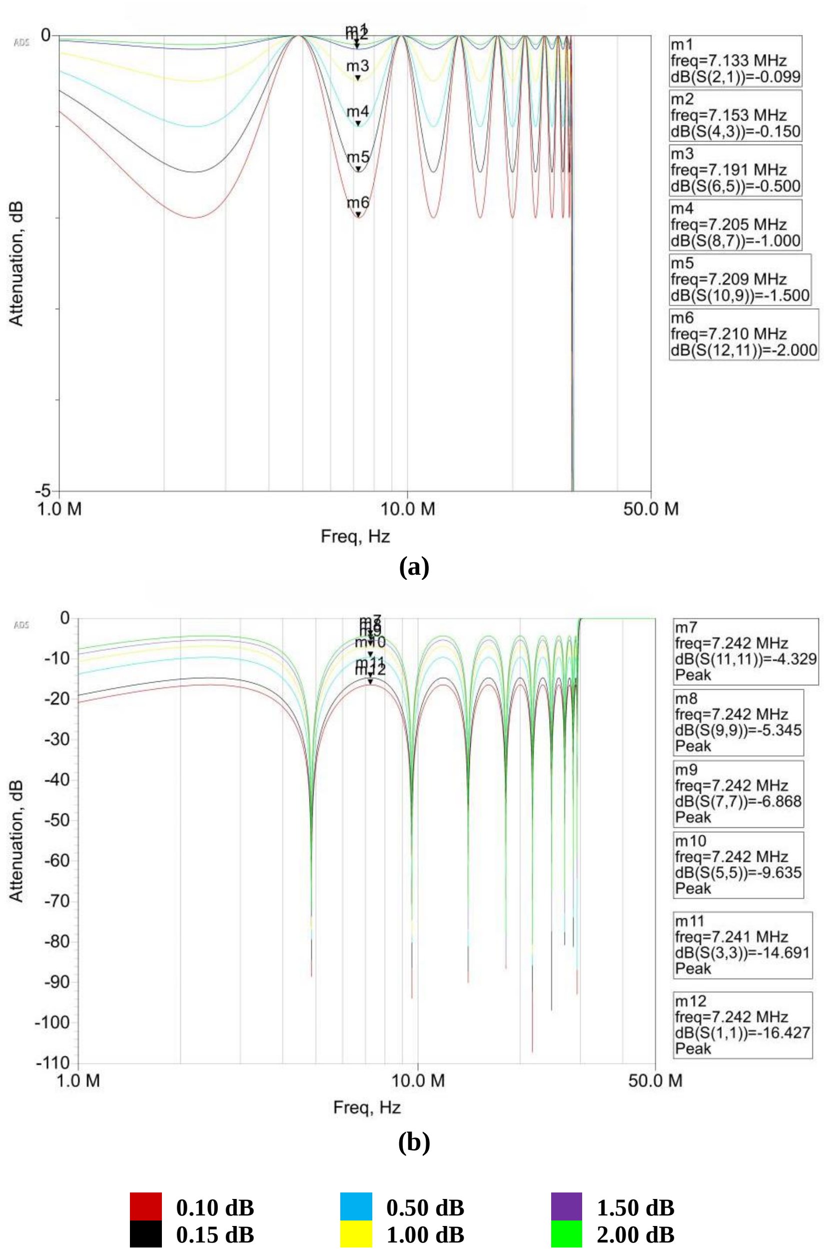


**Figure 6: (a) S[2,1] and (b) S[1,1] parameter responses for various passband ripples.**

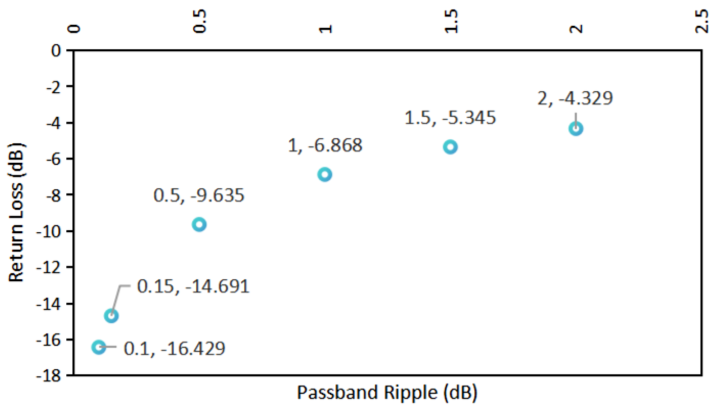


**Figure 7: Graph of return loss versus pass-band ripple.**

Figure 7 is a graph that represents pass-band ripple over return loss, and the data is extracted from S[1,1] from Figure 6 (b). From Figure 7, it can be observed that as the pass-band ripple increases, the return loss decreases. This indicates that the power reflected is higher, which is undesirable if the filter is used in radio communication. The return loss that needs to be achieved is below -10 dB, which, according to the graph, occurs at passband ripples of 0.10 and 0.15 dB, with return losses of -16.429 and -14.691 dB respectively. Additionally, the fabrication of the filter needs to be considered, as fabricating a filter with passband ripple of 0.10 dB is significantly more complex as compared to pass-band ripple of 0.15 dB. Therefore, pass-band ripple of 0.15 dB has been selected for the RF filter design. Moreover, RF filters should have small insertion loss and large return loss (less than -10 dB) for good impedance matching with interconnecting components, and high-frequency selectivity to prevent interference and ensure high performance (Saleh *et al*., 2018).

## 4. PROPOSED DESIGN AND DISCUSSION

The overall design consists of two parts: a low-pass filter and a high-pass filter. When designing a RF filter using the insertion loss method, the low-pass filter must first be designed according to the specified requirements.

### 4.1 Chebyshev Low-Pass Filter

For this design, the Chebyshev low-pass filter is designed with cut-off frequency ($f_o$) of 29.5 MHz, stop-band frequency ($f_s$) of 40 MHz, passband ripple ($L_a$) of 0.15 dB and stop-band attenuation of -113 dB. The equations for determining the number of orders are as follows:

$$\omega_p = 2\,\pi\, f_o \tag{1}$$

$$\omega_p = 2\,\pi\, f_s \tag{2}$$

$$n = \frac{cosh^{-1}\left(\sqrt{\frac{10^{\frac{A_S}{10}}-1}{10^{\frac{A_p}{10}}-1}}\right)}{cosh^{-1}\left(\frac{\omega_S}{\omega_p}\right)} \tag{3}$$

By using these equations, the number of orders is computed as follows:

$$n \approx 18.7407$$

$$\therefore n = 19$$

whereby 19[th] order indicates that 19 elements are used in this design. In order to identify the value of the elements, the coefficients of the Chebyshev filter with passband ripple of 0.15 dB are verified using the following equations:

$$\beta = \ln\left[\coth\left(\frac{L_a}{17.37}\right)\right] \tag{4}$$

$$\gamma = \sinh\left(\frac{\beta}{2n}\right) \tag{5}$$

$$b_k = \gamma^2 + \sin^2\left(\frac{k\pi}{n}\right) \quad , \quad \mathrm{k} = 1,2\ldots,\mathrm{n} \tag{6}$$

$$a_k = \sin\left[\frac{(2k-1)\pi}{2n}\right] \quad , \quad \mathrm{k} = 1,2\ldots,\mathrm{n} \tag{7}$$

$$g_0 = 1 \quad , \quad g_1 = \frac{2a_1}{\gamma} \quad , \quad g_k = \frac{4a_{k-1}a_k}{b_{k-1}g_{k-1}} \quad , \ \mathrm{k} = 2{,}3\ldots,\mathrm{n} \tag{8}$$

$$g_{n+1} = \begin{Bmatrix} 1 & n\ odd \\ \coth^2\left(\frac{\beta}{4}\right) & n\ even \end{Bmatrix} \tag{9}$$

where:

- $n$ is the order of the filter
- $\beta$ is the filter's magnitude response in dB
- $L_a$ is the passband ripple dB.

For this low-pass filter, a passive lumped element is used to create a Chebyshev low-pass filter. The passive lumped element consists of a capacitor (C) and an inductor (L). The following equations are used to determine the values of these components:

$$L'_r = \frac{Z_0 g_r}{\omega_c} \tag{10}$$

$$C'_r = \frac{g_r}{Z_0 \omega_c} \tag{11}$$

where:

- $L'_r$ and $C'_r$ are element values
- $g_r$ is the Chebyshev coefficient
- $Z_0$ is the impedance for impedance matching.

Using Equations 4 to 11, the coefficients for the Chebyshev filter with pass-band ripple of 0.15 dB and the element values for the 19th order are listed in Table 2, which shows that the coefficient and element value of the low-pass filter are symmetrical between ports 1 and 2. These symmetrical element values are due to the low-pass filter circuit being designed with impedance matching ($Z_0$) of 50 Ω at port 1 (HF radio) and port 2 (ATU). This ensures maximum power transfer from the HF radio to the ATU with minimal return loss, thereby maintaining the performance and quality of the HF radio signal. Based on Section 3.2, this design implements the π topology for the Chebyshev low-pass filter. Therefore, the elements are started with the grounded capacitor, $C_1$, then the shunt inductor, $L_1$, and repetitively continued until the grounded capacitor, $C_{19}$, as shown in Figure 8.

**Table 2: Chebyshev coefficients with passband ripple of 0.15 dB and element values for 19th order.**

| Number of Coefficient | Chebyshev Coefficient Value | Number of Element | Element Value for Low-Pass Filter |
|---|---|---|---|
| $g_1 = g_{19}$ | 1.3173 | $C_1 = C_{19}$ | 142.14 pF |
| $g_2 = g_{18}$ | 1.4379 | $L_2 = L_{18}$ | 387.87 nH |
| $g_3 = g_{17}$ | 2.2644 | $C_3 = C_{17}$ | 244.33 pF |
| $g_4 = g_{16}$ | 1.6022 | $L_4 = L_{16}$ | 432.19 nH |
| $g_5 = g_{15}$ | 2.3534 | $C_5 = C_{15}$ | 253.94 pF |
| $g_6 = g_{14}$ | 1.6309 | $L_6 = L_{14}$ | 439.93 nH |
| $g_7 = g_{13}$ | 2.3755 | $C_7 = C_{13}$ | 256.33 pF |
| $g_8 = g_{12}$ | 1.6394 | $L_8 = L_{12}$ | 442.24 nH |
| $g_9 = g_{11}$ | 2.3824 | $C_9 = C_{11}$ | 257.06 pF |
| $g_{10}$ | 1.6415 | $L_{10}$ | 442.80 nH |

The ADS software is employed to simulate the S[1,1] and S[2,1] parameters of the designed circuit, as shown in Figure 8. The simulation is conducted over a frequency range from 20 MHz to 1 GHz with stepping frequency of 1 kHz. Terminations with value of 50 Ω are used for both ports 1 and 2 of the low-pass filter circuit to match the simulation port impedance of the HF radio and ATU.

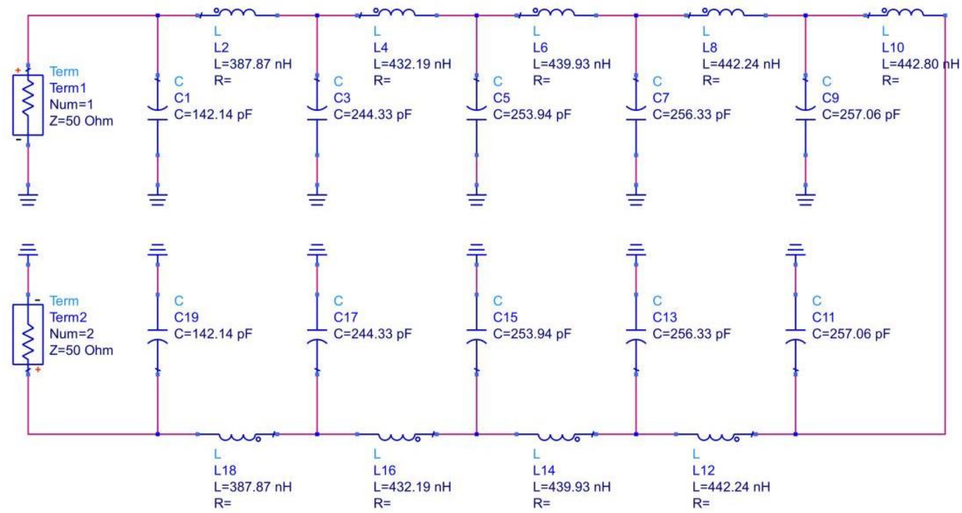


**Figure 8: 19th order Chebyshev low-pass filter schematic with the calculated elements.**

Based on the S[2,1] data shown in Figure 9, the 19th order low-pass filter design has a cut-off frequency of 29.73 MHz at -3.00 dB. This slight deviation from the calculated value of 29.5 MHz is within acceptable limits. The stop-band attenuation from S[2,1] is -114.83 dB at 40.00 MHz, which exceeds the design requirement of -113 dB. Furthermore, the S[1,1] measurement indicates return loss of -14.7 dB at 23.28 MHz, signifying minimal reflection at port 1. This result implies that less than 10% of the power is reflected, which is generally acceptable for this design application. This indicates that the filter effectively suppresses unwanted signals from the VHF band, thereby ensuring high signal integrity of the HF band. In addition, it also indicates that the designed low-pass filter exhibits good impedance matching.

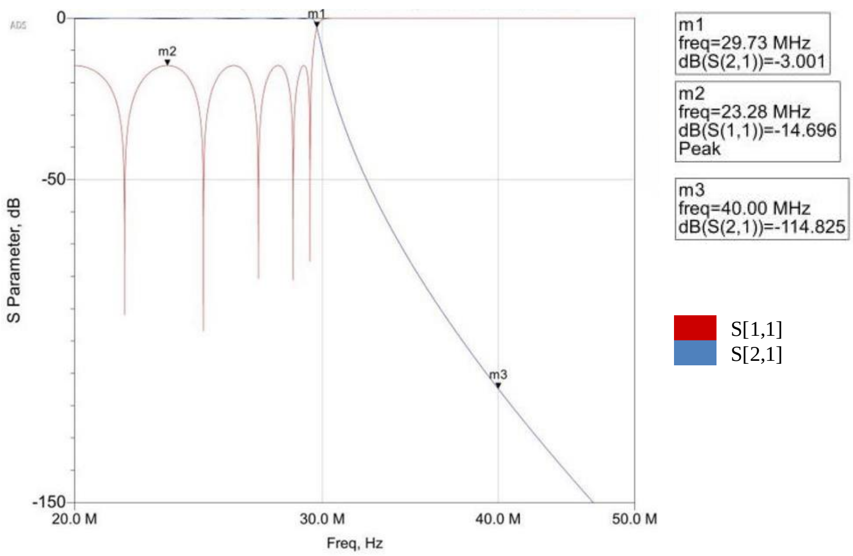


**Figure 9: Simulated frequency response for 19th order Chebyshev low-pass filter.**

Figure 10 illustrates the roll-off performance for filters with different numbers of orders, showing that the 19th order Chebyshev low-pass filter provides better roll-off steepness. As the number of orders increases, the roll-off becomes steeper, resulting in a sharper transition band and improved stopband attenuation. Therefore, this design demonstrates excellent performance in terms of roll-off transition.

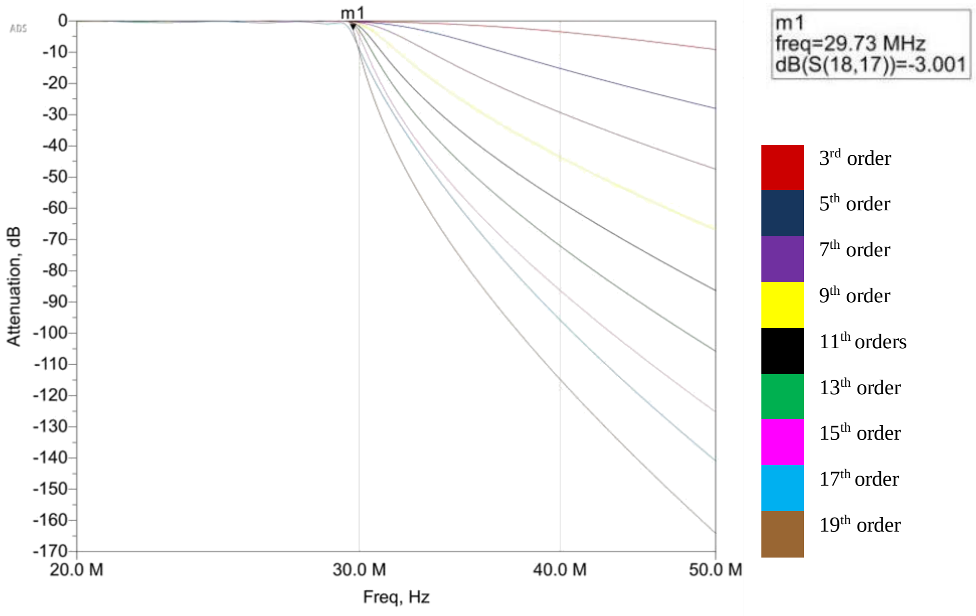


**Figure 10: Simulated frequency response from 3rd to 19th order Chebyshev low-pass filter.**

## 4.2 Chebyshev High-Pass Filter

For the high-pass filter design, the low-pass filter design in Figure 8 is transformed into a high-pass filter by using the following transformation equations:

$$L'_{HPF} = \frac{Z_0}{\omega_c C_r} \tag{13}$$

$$C'_{HPF} = \frac{1}{\omega_c L_r Z_0} \tag{14}$$

where:

- $L'_{HPF}$ and $C'_{HPF}$ are high-pass filter elements
- $L_r$ and $C_r$ are low-pass filter elements
- $Z_0$ is the impedance for impedance matching

The high-pass filter is designed using the filter transformation method from the low-pass filter. Therefore, it also has an impedance matching of 50 Ω at ports 1 and 2, which is the same as the low-pass filter. This is due to the 50 Ω requirement of the existing VHF radio and antenna. Since the value of the high-pass filter elements is determined from the low-pass filter elements by using Equations 13 and 14, therefore the symmetrical characteristics of the elements are the same

The ADS software is used to simulate the S[1,1] and S[2,1] parameters of the designed high pass filter, as shown in Figure 11. The high-pass filter is simulated starting from 20 MHz until 1 GHz with a 1 kHz stepping frequency. Terminations with a value of 50 Ω also are used for both ports 1 and 2 of the circuit.

**Table 3: Element value for 19th orders of high-pass filter.**

| Number of Element | Element Value for High-Pass Filter |
|---|---|
| $L_1 = L_{19}$ | 204.78 nH |
| $C_2 = C_{18}$ | 75.04 pF |
| $L_3 = L_{17}$ | 119.13 nH |
| $C_4 = C_{16}$ | 67.35 pF |
| $L_5 = L_{15}$ | 114.62 nH |
| $C_6 = C_{14}$ | 66.16 pF |
| $L_7 = L_{13}$ | 113.55 nH |
| $C_8 = C_{12}$ | 65.82 pF |
| $L_9 = L_{11}$ | 113.23 nH |
| $C_{10}$ | 65.73 pF |

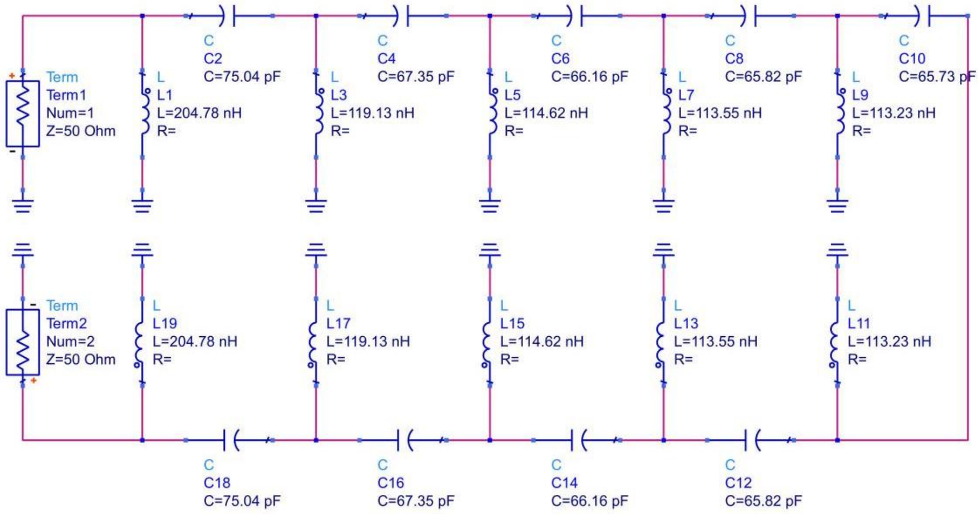


**Figure 11: 19th order Chebyshev high-pass filter schematic with the calculated elements.**

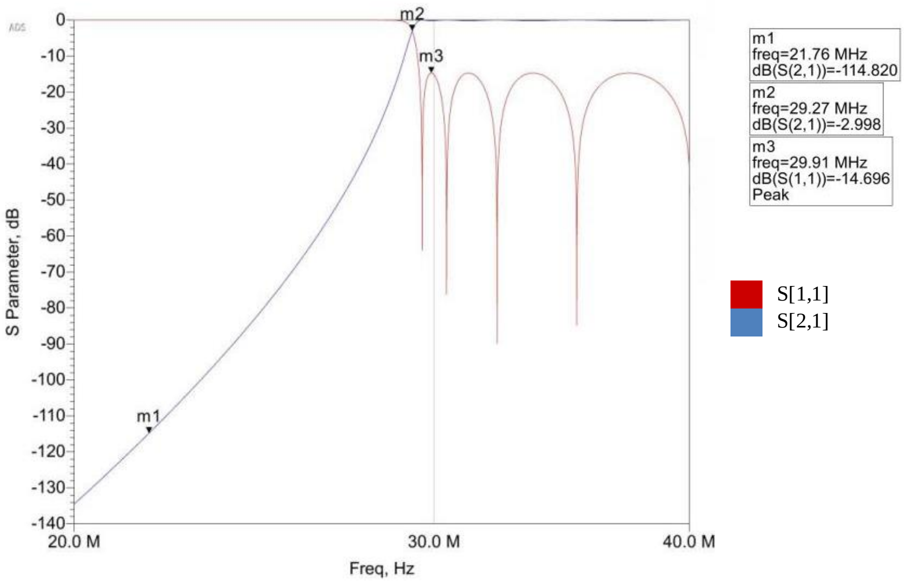


**Figure 12: Simulated frequency response for 19th order Chebyshev high-pass filter**

Based on the S[2,1] response in Figure 12, the filter design has a cut-off frequency of 29.27 MHz at -3.00 dB. The difference from the calculated 29.5 MHz is 0.23 MHz, which is still within acceptable limits. Other than that, the stop-band attenuation based on S[2,1] is -114.82 dB at 21.76 MHz, which is much better as compared to the design requirement parameter of -113 dB. From the S[1,1] response, the return loss is -14.70 dB at 29.91 MHz. This return loss of better than -10 dB is generally considered a good target for this type of filter design. The filter also has less than 10% of reflected power, proving good impedance matching at ports 1 and 2.

## 5. CONCLUSION

In conclusion, both the low- and high-pass filters have been successfully designed using 19$^{th}$ order Chebyshev and simulated to mitigate co-location interference between HF and VHF tactical radios used in military ground vehicles. The low-pass filter achieved a cut-off frequency of 29.73 MHz at -3.00 dB, stop-band attenuation of -114.83 dB at 40 MHz and return loss of -14.7 dB. As for the high-pass filter, it achieved a cut-off frequency of 29.27 MHz at -3.00 dB, stop-band attenuation of -114.82 dB at 21.76 MHz and return loss of -14.7 dB. Overall, the return loss characteristics shown in the plots suggest that this design has achieved a good level of impedance matching, which is important for efficient power transfer and minimising reflections in the system. The low return loss values at the two highlighted frequencies indicate that the design has been optimised to provide a good match across those operating frequencies. Comparing these return loss values to the typical design targets for a Chebyshev low-pass filter, the return loss levels shown in this plot can be considered as exemplary.

## 6. REFERENCES


Adamczyk, B. & Timmerman, J. (2024). *Correlation Between Insertion Loss and Input Impedance of EMC Filters, Part 2: Π and T Filters.* Available online at: https://incompliancemag.com/correlation-between-insertion-loss-and-input-impedance-of-emc-filters-part-2-%cf%80-and-t-filters/ (Last access date: 23 August 2024).

Afzal, U., Channa, B. A., Anjum, U., M. H. Chishti, M.H., Arshad, S. & Hussain, I. (2020). Co-site antenna interference analysis on aerial platform. *23rd Int Multitopic Conf. (INMIC 2020)*, 5-7 November 2020, Bahawalpur, Pakistan.

Bharathy, G.T., Bhavanisankari, S., Tamilselvi, T. & Bhargavi, G. (2020). Analysis and design of RF filters with lumped and distributed elements. Int. J. Rec. Tech. Eng., **8**: 38-42.

Carr, J. J. (2001). *Practical Antenna Handbook*. McGraw-Hill, New York, US.

Chan, K., Chong, P. & Johnsen, F. (2021). Military communications and networks. *IEEE Commun. Mag.,* **60**: 58.

Chen, W. (2013). *RF and Microwave Circuit Design for Wireless Communications, 2nd Ed.*. Artech House, Boston, Massachusetts, US.

Karlsson, S., Grenvall, M., Kvick, Å., Eugensson, L., Grahn, F., & Pettersson, L. (2013). Co-site interference analysis and antenna system integration on a Swedish combat vehicle platform. *2013 IEEE Milit. Commun. Conf. (MILCOM 2013)* , 8-20 November 2013, San Diego, California, US.

Kiouach, F., Aghoutane, B. & Ghzaoui, M. E. (2023). Novel microstrip bandpass filter for 5g mm-wave wireless communications. *Adv. Electr. Eng. Electron. Ener.*, **6**, 100357.

Laghari, W.M., Baloch, M.U., Mengal, M.A. & Shah, S.J. (2014). Performance analysis of analog Butterworth low pass filter as compared to Chebyshev Type-I filter, Chebyshev Type-II filter and elliptical filter. *Circ. Syst..*, **5**: 209-216.

Langhammer, L., Sotner, R. & Theumer, R. (2023). Various-order low-pass filter with the electronic change of its approximation. *Sensors*., **23**: 8057.

Lee, T.-H., Lee, B., Kim, Y.-S., Wu, K. & Lee, J. (2019). Higher order lumped element absorptive low-pass and bandpass filter structures. *IET Microw. Antennas Propag*., **13**: 1166-1173.

Mei, A. (2022). The design and simulation of a fifth-order Chebyshev low-pass filter. *J. Phys.*, **2386**: 012066.

Murthy, U.D.V.B. & C. J. Reddy (2020). Co-site interference analysis on aerospace platforms using advanced simulation tools. *2022 Antenna Meas. Tech. Assoc. Symp. (AMTA)*, 9-14 October 2022, Denver, Colorado, USA.

Polak, R. (2020). Determination of co-site work conditions of selected wideband radio station by measurement method. *Proc. SPIE*, **11442**: 114421E

Pozar, D. M. (2012). *Microwave Engineering*. Wiley, Hoboken, New Jersey, US.

Salama, S., Battah, Y. & Abuelhaija, A. (2022). Design of a microstrip maximally flat 7$^{th}$ order lowpass filter using ads simulation. *J. Eng. Sci. Tech.*, **17:** 895 - 905.

Saleh, E.J., Mohamad, A.J., You, K.W & Jose, R. (2018). A high return loss of microwave bandpass filter using superconducting electrospun YBCO nanostructures. *Prog. Electromagn. Res.*., **81:** 63-75.

Sarris, C.D., Thiel, W., Koh, I.S., Sarabandi, K., Katehi, L.P.B. & Perlman, B.S. (2002). Hybrid time-domain performance analysis of multi-antenna systems on vehicular platforms. *32$^{nd}$ Eur. Microw. Conf.*, 23-26 September 2002, Milan, Italy.

Tomar, P. S., & Parihar, M. S. (2023). The design and investigation of the low-pass filter with high selectivity and ultra-wide stopband. *IETE J. Res.*, **70**: 2366-237.

Yang, K., He, C., Fang, J., Cui, X., Sun, H., Yang, Y. & Zuo, C. (2023). Advanced RF filters for wireless communications. *Chip.*, **2**: 100058.

Zedníček, T. (2023). *Lumped Element L-C Filters Design and Characteristics*. Available online at: https://passive-components.eu/lumped-element-l-c-filters-design-and-characteristics (Last access date: 23 August 2024).

# ALTITUDE EFFECTS ON CELLULAR-CONNECTED UAV PERFORMANCE AND VIDEO TRANSMISSION EFFICIENCY: EMPIRICAL ANALYSIS AND RECOMMENDATIONS

Ahmad Muhaimin Mahadi, Nadhiya Liyana Mohd Kamal*, Alshalabi Omran, Zulhilmy Sahwee, Nurhakimah Norhashim & Shahrul Ahmad Shah

Unmanned Aerial System Research Cluster, Avionics Section, Malaysian Institute of Aviation Technology (MIAT), Universiti Kuala Lumpur (UniKL), Malaysia

*Email: nadhiyaliyanamk@unikl.edu.my

## ABSTRACT

*Unmanned aerial vehicles (UAVs) are widely used nowadays, as numerous applications in various fields can take advantage of UAVs. Wireless communication has received a lot of attention in recent years, as it is one of the most critical enabling technologies for UAVs. Direct link technology, commonly used for UAV communication, can constrain the UAV's operational range and hinder applications in environments with low probability of line-of-sight (LoS). Due to these limitations, simple direct link communication cannot be a scalable solution for future large-scale UAV deployment. Cellular networks are the answer for future development of UAV communication technology, especially with the forthcoming 5G cellular network. It is thought that cellular-enabled UAV communication will provide high-rate and delay-sensitive communication for UAV applications in real-time scenarios. However, despite the promising advantages of cellular-enabled UAVs, the network coverage for UAVs differs slightly from the conventional 2D range for terrestrial users. UAVs operate at high altitudes and speeds, necessitating cellular base stations to provide 3D aerial coverage for UAV users instead of 2D range for terrestrial users. In this paper, the performance of cellular-connected UAVs is investigated by identifying the effects of altitude on the performance of cellular-connected UAVs and video transmission efficiency of cellular-connected UAVs at various video resolutions. This study evaluates UAV performance by obtaining the rate of received signal (Rx), rate of transmit signal (Tx) and latency based on received signal strength indicator (RSSI) values at various altitudes obtained from a previous study. The UAV Cast-Pro software was used to collect data consisting of Rx, Tx and latency values at different video resolutions of 640 x 480, 1,280 x 720, 1,640 x 922 and 1,920 x 1,080 p. The results show that cellular-connected UAVs with reliable cellular network can produce good quality video streaming for various video resolutions at operational altitude of 50 m.*

**Keywords:** *Cellular-connected unmanned aerial vehicles (UAVs); altitude; received signal strength indicator (RSSI); throughput and latency; video quality.*

## 1. INTRODUCTION

An unmanned aerial vehicle (UAV) or drone is an aircraft that is guided autonomously without pilots on board via computerised systems from ground-based stations (Lutkevich, 2021). In recent years, UAVs have seen widespread use in civilian applications, such as construction, commercial, agriculture, transportation, surveillance, monitoring and military. The Royal Malaysian Air Force (RMAF) recently announced the formation of a squadron dedicated to UAV applications at the RMAF base in Gong Kedak, Terengganu, demonstrating the country's profound interest in the technology. In addition, Tenaga Nasional Bhd (TNB) already uses UAVs for power line surveillance; Telekom Malaysia (TM) uses it to supervise telecommunication towers and applications; PETRONAS uses it to monitor oil and gas pipelines; highway authorities use it to assist with traffic management; while railway corporations use it to monitor tracks (David, 2020). This shows that UAVs are now an essential part of our daily lives, owing to advancements in UAV manufacturing technologies and lower costs, making them more affordable to the general public. Due to their numerous and diverse applications, UAVs come in various shapes and sizes in practice. While there is no single standard for UAV classification, UAVs can be classified into multiple categories based on numerous criteria, such as functionality, endurance, wing type and control methods. Different characteristics and specifications of UAVs are crucial for accomplishing their mission efficiently. Although there are various UAVs, they all require the same critical technology, which is wireless communication. Wireless communication is a vital enabler technology for UAVs to exchange essential safety information with various parties, such as remote pilots, nearby aerial vehicles and air traffic controllers, to ensure safe, dependable and efficient flight operations (Zeng *et al*., 2019; Alshalabi *et al*., 2022; Mohd Kamal *et al*., 2024).

Existing UAVs rely on direct link technology, which is simple point-to-point communication with ground nodes. It uses a small and restricted bandwidth, with the 2.4 GHz band commonly used for commercial UAVs connected to ground nodes, which can either be a remote controller or ground station (Fotouhi *et al*., 2019). Direct link technology is usually limited to line-of-sight (LoS) communication, which can constrain the operation range especially in complex propagation environments (Mohd Kamal *et al*., 2024). A UAVs' communication can easily be blocked by tall buildings and trees, especially in areas with low-reliability rate. Therefore, simple direct link communication cannot be a scalable solution, especially for supporting large-scale UAV deployment in the future as the demand for UAV applications increases (Mohd Kamal *et al*., 2024).

As a result, there has recently been a significant increase in interest in utilising existing and future-generation cellular networks to enable UAV-ground communications. Cellular-connected UAVs are aerial user equipment integrated into current and future cellular networks, making them more reliable than direct link UAVs. Cellular technologies employ a complex two-way radio system between the unit and wireless network, utilising the frequency reuse concept, allowing radio frequencies to be used repeatedly. Cellular networks provide global coverage as well as high-speed optical backhaul and advanced communication technologies (Zeng *et al*., 2019; Ali *et al.*, 2022; Alshalabi *et al*., 2022; Mohd Kamal *et al*., 2024).

This study contributes to the field by investigating the effects of altitude on the performance of cellular-connected UAVs and video transmission quality, aiming to recommend optimal operational altitudes for UAV operators. The paper starts with a brief background on the integration of UAVs with cellular networks and performance metrics describing connectivity performance. It further explains the hardware setup used to collect RSSI data, throughput, and latency, with subsequent observation of video transmission quality performance and its relation to the aforementioned metrics.

## 2. BACKGROUND

### 2.1 Cellular Networks

Appropriate wireless technologies are required to achieve seamless connectivity and high reliability of throughput for both air-to-air and air-to-ground wireless communications, as well as meet the UAV applications' control and non-payload (CNPC) and payload communications requirements. There are four types of UAV communication technologies: direct link technology, ad-hoc network, satellite and cellular network technology (Zeng *et al*., 2019; Javaid *et al*., 2023; Wang *et al*., 2023). This research focuses on cellular network technology.

There has been a lot of interest in integrating UAV communication systems into existing and future cellular networks in recent years (Geraci *et al*., 2022). By enabling UAV communication via cellular infrastructure and technologies, the cellular network can provide nearly ubiquitous coverage globally through its high-speed optical backhaul and advanced communication technologies. The current 4G long-term evolution (LTE) cellular network uses a scheduling-based channel access mechanism, which allows multiple users to be served concurrently by assigning them orthogonal resource blocks (RBs) (Mohd Kamal, Sowerby *et al*., 2020). In addition to the traditional satellite-based Global Positioning System (GPS), cellular-based localisation services can provide UAVs with a new and complementary means of achieving more robust and enhanced UAV navigation performance. Cellular-connected UAVs are a cost-effective solution because they reuse millions of cellular base stations worldwide without the need for new infrastructure dedicated to UAVs only (Zeng *et al*., 2019; Mohd Kamal *et al*., 2024).

Cellular networks make use of cellular frequency reuse, which uses the same radio frequencies within a given area separated by a significant distance to establish communication with minimal interference in a regular pattern of areas known as cells. Each of the cells is covered by a single base station with its antenna for transmitting the signal. These cells are typically hexagonal in mobile phone networks. Adjacent cells use different frequencies to keep mutual interference between users to a safe level. These frequencies can be reused in cells that are far enough apart to prevent interference with each other (Fotouhi *et al*., 2019; Alibraheemi *et al*., 2023; Trabelsi *et al*., 2024).

## 2.2 Important Terms

### 2.2.1 Received Signal Strength Indicator (RSSI)

RSSI is a relative index to measure the relative quality of a received signal to a device. It is a metric that measures the power level received by the receiving radio after antenna and cable loss. As a result, the stronger the received signal, the higher the RSSI value. Receivers using different chipsets of equal distance from the transmitter with no interference or blockage will often have different RSSI values for the same signal (Alshalabi *et al*., 2022; Mao *et al*., 2023).

In a previous study conducted by Mohd Kamal *et al*. (2020), investigation work was conducted to predict the throughput performance for both terrestrial and aerial users in a typical Malaysian sub-urban environment using real-time measurements of RSSI. The findings reveal that UAV connection to the current cellular network is reliable when the operational height of the UAV is less than 40 m. If the number of UAV users is maintained to a minimum, stable connection and throughput performance may be accomplished for UAVs at altitudes ranging from 40 to 60 m.

### 2.2.2 Signal-to-Interference Noise Ratio (SINR)

SINR is a wireless communication metric used to assess the quality of wireless connections. It quantifies the ratio of signal power to the combined interference and noise power, with higher values indicating better signal quality relative to interference and noise. The energy of a signal in a wireless network typically fades with distance, which is referred to as path loss (Mao *et al*., 2023). As the energy of a signal decreases with distance, it can lead to smaller SINR values due to the reduced signal power relative to interference and noise. This highlights the challenge of maintaining adequate signal strength over longer distances in wireless communication systems (Dahri *et al*., 2023).

### 2.2.3 Throughput

Throughput refers to the amount of data that can be transferred and received from source and destination within a given timeframe (DNSstuff, 2019). In order to have a high-performance network, many data packets need to passed through and arrive at their destination successfully. Throughput can be measured in bits per second (bps) and data per second (DPS). It can be optimised by minimising network latency that results in poor network performance. For this paper, the rate of received signal (Rx) and rate of transmit signal (Tx) are the throughput values that need to be collected to measure the performance of cellular-connected UAVs.

### 2.2.4 Latency

Latency is measured in milliseconds (ms) and is used to indicate delays in network communication. In networking, latency is defined as the length of time it takes for a packet of data to be collected, transferred, processed by several devices, and then received and decoded at its destination. Long delays in high-latency networks cause communication bottlenecks. This can be overcome by increasing network stability and accuracy by minimising needless overheads and network latency, and by adopting various design features with minimal resource restrictions to dramatically decrease network overheads, as well as improve packet delivery ratio and network latency (Bhandari *et al.*, 2020).

## 3. METHODOLOGY

### 3.1 Hardware Consideration

Five main hardware products were chosen to be used in this research, which were Raspberry Pi 4, Pixhawk, 5V 13A battery, Pi Cam and an internet modem. Raspberry Pi 4 supports the LTE-based control system for the UAV. It is a tiny computer that is roughly the size of a deck of cards. It employs a system on a chip, which combines the central processing unit (CPU) and graphics processing unit (GPU) onto a single integrated circuit, with the random access memory (RAM), universal serial bus (USB) ports and other components soldered onto the board for all-in-one packaging. Pixhawk is an independent open-hardware project providing readily-available, low-cost and high-end autopilot hardware designs to the academic, hobby and industrial communities (PX4DevTeam, 2020). The battery is used to power up the Raspberry Pi and other devices. The Pi Cam supports the Raspberry Pi and can record video. The internet modem is used to establish a network connection to the Raspberry Pi. The connections between these components are illustrated in Figure 1.

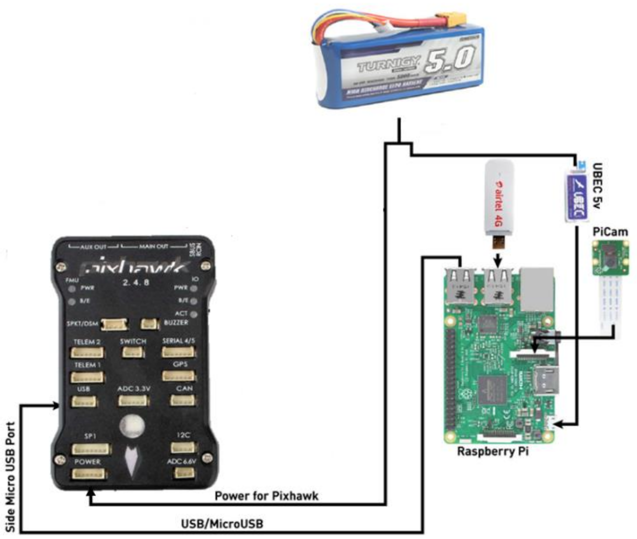


**Figure 1: Illustration of the connection between the components.**

### 3.2 Software Setup

Two main applications were used to accomplish this research. First, Coiler's Site Survey Applications (SSA) Outdoor is a line of tools designed to measure and log signal quality directly on Android smartphones. SSA Outdoor provides test reports that include the exact RSSI values and average RSSI data. Before starting the simulation test, it was essential to ensure that the smartphone was connected to the internet modem for the Raspberry Pi and that the application could detect the device's location. The SSA Outdoor was used to locate spots with desired RSSI values by moving the mobile device. Once identified, the Raspberry Pi unit was placed accordingly. SSA's visualisations made it handy for pinpointing RSS distribution across the region, from which the corresponding data transmission rate from UAVCast-Pro was then obtained.

Second, the UAVCast-Pro application helps the process to communicate with the flight controller over a mobile LTE network. UAVCast-Pro was used to investigate cellular-connected UAV video transmission efficiency by directly collecting Rx, Tx and latency values for four video resolutions, which are 640 x 480, 1,280 x 720, 1,640 x 922 and 1,920 x 1,080 p. Various applications, including Mission Planner, PuTTY, Raspberry Pi Imager and Navio Flight Controller, were installed and integrated for UAVCast-Pro to function well.

### 3.3 Classification of Video Quality

Mission Planner was used to allow the monitoring of the live video transmission quality. The quality of the live video streaming was classified into three categories: good, fair and poor (Figure 2). The video quality must be clean and flicker-free to fall into the good category. Next, the fair category was determined when the video's quality was slightly flickering and grainy. Finally, the poor category was indicated by the presence of white shadows and lagging video.


**(a)**

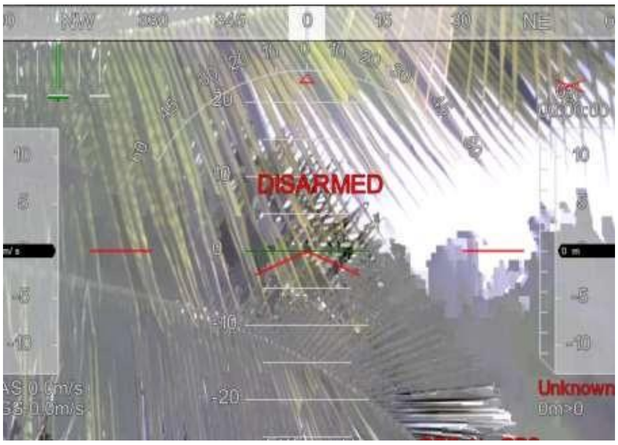



**(b)** **(c)**

**Figure 2: Categories of the video streaming quality: (a) Good (b)Fair (c) Poor.**

## 4. RESULTS & DISCUSSION

In this section, the data acquired from the test is analysed to provide insight into how the cellular-connected UAV's performance and video transmission efficiency are affected by the its flying altitude. The RSSI values in proportion to the altitudes of the UAV, which was obtained from Mohd Kamal *et al*. (2020) using the same SSA Outdoor tool was utilised to measure Rx, Tx and latency values. The data was recorded in proportion to the varying video quality given. Rx indicates the power of the received signal per second by the Raspberry Pi, which received directives from the ground station. Meanwhile, Tx indicates the power of the transmit signal transmitted per second, which provides video live streaming through the Pi Cam and telemetry data to the ground station's Mission Planner.

Latency relates to the time taken for a signal to be transmitted from the Raspberry Pi to the ground control station and back. The Rx, Tx and latency values relative to different resolutions of video qualities of 640 x 480, 1,280 x 720, 1,640 x 922 and 1,920 x 1,080 p were directly obtained from UAVCast-Pro. Meanwhile, the video live streaming quality was monitored using Mission Planner and classified into three categories: good, fair and poor. With the RSSI, Rx, Tx, latency and values, as well as the quality of live video streaming, the results of this simulation indicate if cellular-connected UAVs can provide high performance and high-quality video transmission at high altitudes.

### 4.1 Received Signal Strength Indicator (RSSI) at Various Altitudes

The trend of the RSSI values of cellular-connected UAVs at various altitudes based on Mohd Kamal *et al*. (2020) is shown in Figure 5. As the altitude of the aircraft increases, the RSSI value decreases. The UAV has the highest RSSI value at altitude of 1 m or during take-off, which is -58 dBm, and the lowest value at altitudes of 60, 80 and 90 m at -78 dBm**.** RSSI dropped from -58 to -78 dBm as the UAV approached altitude of 60 m altitude due to the ground transmission antenna being tilted downwards for the use of terrestrial users, which results in decrease of RSSI as the altitude increases. As the UAV altitude increases from 90 to 120 m, RSSI increases potentially due to the side lobes of the ground transmission antenna that transmit increased radiation level to the UAV. The data collected for this study was for up to altitude of 120 m as this is the maximum altitude permitted by the Civil Aviation Authority of Malaysia (CAAM) (CAAM, 2016).

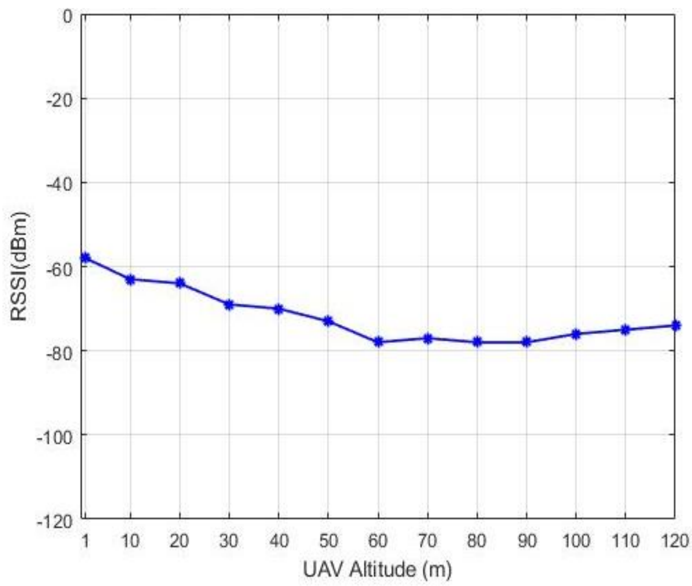


**Figure 3: Graph showing change of RSSI values as the altitude of the UAV increases.**

### 4.2 Video Transmission Performance at Various Altitudes

The data, which consists of Rx, Tx and latency values, was collected directly from UAVCast-Pro at various RSSI values for video resolutions of 640 x 480, 1,280 x 720, 1,640 x 922 and 1,920 x 1,080 p. The data is illustrated in Figures 4 to 6 to facilitate monitoring of the UAV performance trend as the UAV altitude increases. Additionally, for each of the recorded values, the video quality was monitored through using Mission Planner.

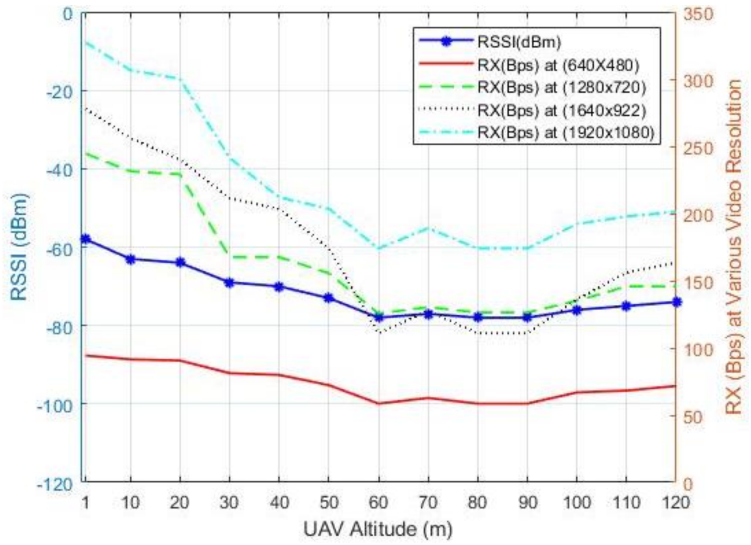


**Figure 4: The UAV Rx performance at different altitudes for various video resolutions.**

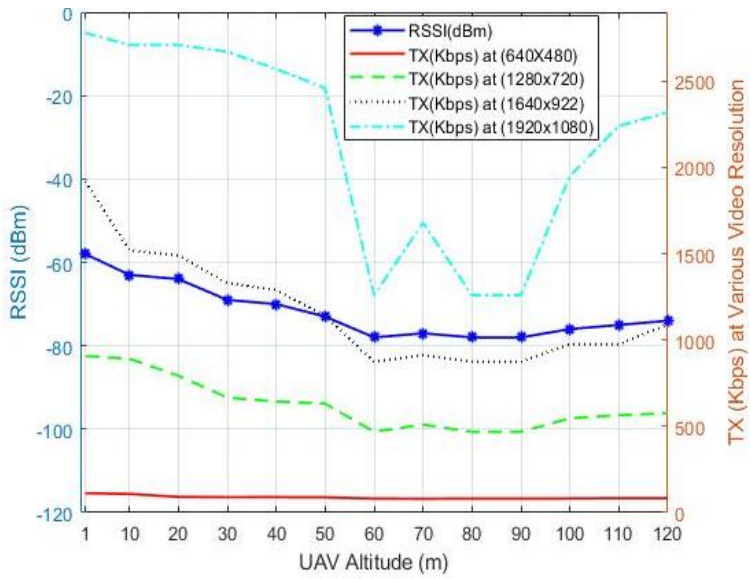


**Figure 5: The UAV Tx performance at different altitudes for various video resolutions.**

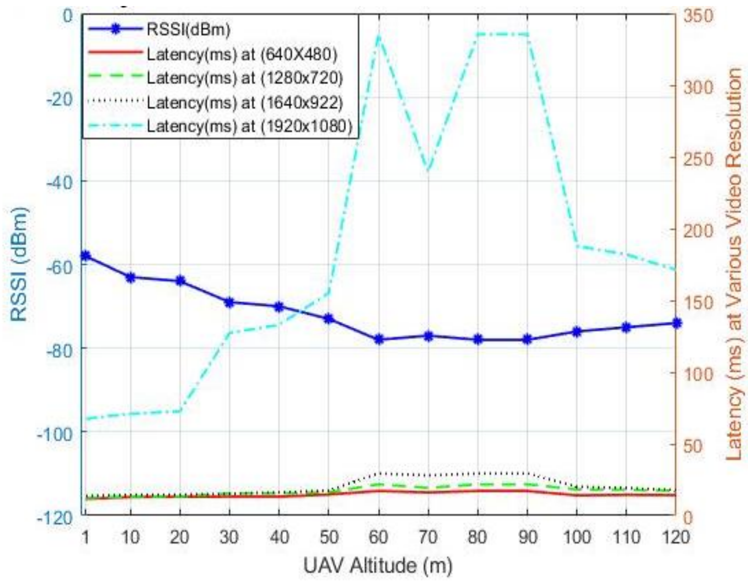


**Figure 6: UAV latency Performance at different altitudes for various video resolutions.**

Figures 4, 5 and 6 illustrate the impact of altitude on Rx, Tx and latency values across various video resolutions. As altitude increases, both Rx and Tx values decrease due to the down-tilted ground transmission antenna reducing the RSSI. The maximum Rx value is observed at an altitude of 1 m, while the minimum Rx value occurred at altitudes of 60 and 80 m. This trend is consistent across different video resolutions, with higher resolutions requiring higher Rx and Tx values due to the larger data transfer demands. Similarly, latency increases with altitude as RSSI decreases, with the lowest latency observed at 1 m altitude and the highest at 60 and 80 m. High video resolutions, particularly 1920 x 1080 p, significantly increase latency, especially at higher altitudes, indicating video transmission lag. These observations highlight how the increasing altitude adversely affects RSSI, Rx, Tx and latency, with the impact being more pronounced at higher video resolutions

### 4.3 RSSI Value, Altitude and Video Quality

As shown in Table 1, the video quality degrades for all the video resolutions as the UAV's altitude increases and RSSI decreases. For video resolution of 640 x 480 p, the video quality remained within an acceptable range as the quality degraded from altitude of 60 to 120 m. For video resolutions of 1,280 x 720 and 1,640 x 922 p, when the altitude exceeds 60 m and the RSSI value approaches -78 dBm, the video quality degrades significantly until the RSSI value increases slightly to -75 dBm, allowing for better video transmission quality. For video resolution of 1,920 x 1,080 p, the video quality degrades as the altitude increases and RSSI decreases. Poor video quality occurs once the UAV reaches altitude of 60 m and the RSSI value drops to -78 dBm. Even as the RSSI increases with altitude, the quality at this resolution remains poor as compared to lower resolutions. This is because higher video resolutions demand larger RSSI to fulfil the data rate requirement, posing a challenge for maintaining satisfactory quality even with improved signal strength.

**Table 1: RSSI values and video qualities for various UAV altitudes.**

| Altitude (m) | RSSI Value (dBm) | Video Quality | | | |
|---|---|---|---|---|---|
| | | 640 x 480 p | 1,280 x 720 p | 1,640 x 922 p | 1,920 x 1,080 p |
| 1 | -58 | Good | Good | Good | Good |
| 10 | -63 | Good | Good | Good | Good |
| 20 | -64 | Good | Good | Good | Good |
| 30 | -69 | Good | Good | Good | Good |
| 40 | -70 | Good | Good | Good | Fair |
| 50 | -73 | Good | Good | Good | Fair |
| 60 | -78 | Fair | Poor | Poor | Poor |
| 70 | -77 | Fair | Poor | Poor | Poor |
| 80 | -78 | Fair | Poor | Poor | Poor |
| 90 | -78 | Fair | Fair | Poor | Poor |
| 100 | -76 | Fair | Fair | Fair | Poor |
| 110 | -75 | Fair | Fair | Fair | Poor |
| 120 | -74 | Fair | Fair | Fair | Poor |

### 4.4 Recommendations for UAV Operators

According to the data gathered, the quality of video transmission for a cellular-connected UAV decreases as the altitude of the UAV increases. UAV operators who use cellular-connected UAVs for live video streaming are advised to fly at a vertical height of 50 m to provide good video streaming experience. This is due to the down-tilted ground transmission antenna for terrestrial users, resulting in decreased RSSI values as altitude increases. With decreased RSSI values, the cellular-connected UAV's Rx and Tx values decrease. Using the data gathered, this work can provide UAV operators with an understanding of how to use different video resolutions at different altitudes to offer the greatest performance of the cellular-connected UAV in delivering videos effectively.

The data received from the UAVCast-Pro was immediately gathered and displayed the precise throughput values, which are Tx, Rx and latency values of the cellular-connected UAV. The higher the Tx value, the more data is sent per second, while the lower the latency value, the shorter the delay in transmitting or receiving the signal. High Tx and low latency values are recommended to get the highest video transmission efficiency.

Different altitudes are recommended for UAV pilots while running various video resolutions for live-streaming footage. For video resolution of 640 x 480 p, flying at altitude of 50 m or below is advice for good video transmission with high transmit signal value and low latency value. However, for this resolution, when the altitude increases up to 120 m, the UAV can still generate reasonable video quality, with minor graininess predicted. For video resolutions of 1,280 x 720 and 1640 x 922 p, it is advised to fly the UAV at altitude of 50 m or below for high-quality video with low latency value. The video quality steadily degrades as the altitude increases, resulting in white shadowing images and significant flickering of the transmitted video. Based on the data acquired, for video resolution of 1,920 x 1,080 p, the UAV produces exceptional video quality while flying at altitude of 30 m and below, and fair quality of video when flying at altitude between 30 and 50 m. As the altitude exceeds 50 m, the video quality degrades. While the values obtained in this study are specific to the hardware used, the trends observed may remain consistent across different hardware configurations.

## 5. CONCLUSION

This paper investigated the effect of altitude on the performance of cellular-connected UAVs and video transmission. According to the acquired data, as the altitude of cellular-connected UAVs increases, the RSSI value drops, resulting in reduced signal strength and hence decreased cellular-connected UAV performance, in particular reduced Tx and Rx values, and increased latency values. This causes decreasing video transmission quality for all the video resolutions.

The data accumulated in this study can help UAV operators evaluate the effectiveness of cellular-connected UAV video transmission at different altitudes and RSSI values. This can then be used to determine optimum operational altitude for UAV operators when flying a cellular-connected UAV with the highest video quality for various video resolutions.

## REFERENCES


Ali, S., Abu Samah, A., Abdullah, N.F. & Mohd Kamal, N.L. (2022). A review of 6G enabler: vertical heterogeneous network (v-HetNet). *2022 IEEE 20th Student Conf. Res. Dev. (SCOReD 2022),* 7-8 November 2022, Bangi, Selangor, Malaysia.

Alibraheemi, A.M.H., Hindia, M.N., Dimyati, K., Izam, T.F.T.M.N., Yahaya, J., Qamar, F. & Abdullah, Z.H. (2023). A survey of resource management in D2D communication for B5G networks. *IEEE Access*, **11**: 7892–7923.

Alshalabi, O., Kamal, N.L.M., Sahwee, Z., Norhashim, N. & Shah, S.A. (2022). Feasibility of LTE-connected unmanned aerial vehicle. *IEEE Symp. Future Telecomm. Tech. (SOFTT 2022),* Johor Bahru, Johor, Malaysia.

Argrow, B. (2016). Unmanned aircraft system design. *In* Barnhart, R.K., Marshall, D.M., Shappee, E. & Most, M.T. (Eds.). *Introduction to Unmanned Aircraft Systems.* CRC Press, Boca Raton, Florida, US, pp. 159-172.

Bhandari, S., Wang, X. & Lee, R. (2020). Mobility and location-aware stable clustering scheme for UAV networks. *IEEE Access,* **8**:106364–106372.

CAAM (Civil Aviation Authority of Malaysia) (2016). *Malaysian Civil Aviation Regulation*. Available online at: https://www.caam.gov.my/legislation-regulations/general/regulations (Last access date: 31 May 2024).

Dahri, S. A., Shaikh, M. M., Alhussein, M., Soomro, M. A., Aurangzeb, K. & Imran, M. (2023). Multi-slope path loss model-based performance assessment of heterogeneous cellular network in 5G. *IEEE Access,* **11**: 30473–30485.

David, A. (2020). *Demand for unmanned aerial systems*. Available online at: https://www.nst.com.my/news/nation/2020/07/604968/demand-unmanned-aerial- systems (Last access date: 1 January 2024).

DNSstuff. (2019, September 19). *What Is Throughput in Networking? Bandwidth Explained.* Available online at: https://www.dnsstuff.com/network-throughput-bandwidth#:~:text=Again%2C%20 network%20throughput%20refers%20to,measured%20in%20data%20per%20second (Last access date: 1 January 2024).

Fotouhi, A., Qiang, H., Ding, M., Hassan, M., Giordano, L.G., Garcia-Rodriguez, A. & Yuan, J. (2019). Survey on UAV cellular communications: practical aspects, standardization advancements, regulation, and security challenges. *IEEE Commun. Surv. Tut.*, **21**: 3417–3442.

Geraci, G., Garcia-Rodriguez, A., Azari, M. M., Lozano, A., Mezzavilla, M., Chatzinotas, S., Chen, Y., Rangan, S. & Renzo, M.D. (2022). What will the future of UAV cellular communications be? A flight from 5G to 6G. *IEEE Commun. Surv. Tut.*, **24:** 1304–1335.

Javaid, S., Saeed, N., Qadir, Z., Fahim, H., He, B., Song, H. & Bilal, M. (2023). Communication and control in collaborative UAVs: Recent advances and future trends. *IEEE T. Intell. Transp.*, **24**: 5719–5739.

Lutkevich, B. (2021). *Drone (UAV)*. Available online at: https://www.techtarget.com/iotagenda/definition/drone (Last access date: 1 January 2024).

Mohd Kamal, N.L., Sahwee, Z., Norhashim, N., Lott, N., Abdul Hamid, S., & Hashim, W. (2020). Throughput performance of 4G-based UAV in a sub-urban environment in Malaysia. *8th Annual IEEE Int. Conf. Wireless Space Extreme Environ. (WiSEE 2020)*, Vicenza, Italy.

Mohd Kamal, N. L., Sahwee, Z., Norhashim, N., Ahmad Shah, S. & Hashim, W. (2024). Throughput performance of cellular-connected UAV coexisting with terrestrial users. *Unmanned Syst.*, In press.

Mohd Kamal, N.L., Sowerby, K.W. & Neve, M.J. (2020). On the influence of the propagation environment on throughput performance in indoor wireless network. *Wireless Netw.*, **26**: 865–878.

Mao, J., Zhao, Y., Xia, Y., Yang, Z., Xu, C., Liu, W. & Huang, D. (2023). Revisiting link quality metrics and models for multichannel low-power lossy networks. *Sensors*, **23**:1303.

PX4DevTeam. (2020). Pixhawk Series. Available online at: https://docs.px4.io/v1.9.0/en/flight_controller/pixhawk_series.html (Last access date: 31 May 2024).

Trabelsi, N., Chaari Fourati, L. & Chen, C.S. (2024). Interference management in 5G and beyond networks: A comprehensive survey. *Computer Netw.*, **239**: 110159.

Wang, Q., Li, W., Yu, Z., Abbasi, Q., Imran, M., Ansari, S., Sambo, Y., Wu, L., Li, Q. & Zhu, T. (2023). An overview of emergency communication networks. *Remote Sens.*, **15**: 1595.

Zeng, Y., Wu, Q. & Zhang, R. (2019). Accessing from the sky: A tutorial on UAV communications for 5G and beyond. *Proc. IEEE,* **107** :2327–2375.

# AN INITIAL CELLULAR COMMUNICATION STUDY FOR eVTOL OPERATIONS IN MALAYSIA FOR UAM ESTABLISHMENT

Zulhilmy Sahwee*, Nurhakimah Norhashim, Nadhiya Liyana Mohd Kamal, Shahrul Ahmad Shah & Mohammad Khir Harun
Unmanned Aerial System Research Laboratory, Avionics Section, Malaysian Institute of Aviation Technology, Universiti Kuala Lumpur, Malaysia

*Email: zulhilmy@unikl.edu.my

**ABSTRACT**

*Urban air mobility (UAM) using electric vertical take-off and landing (eVTOL) technology can revolutionise travel in congested urban areas by reducing cost and time. Implementing UAM in Malaysia requires a collaborative framework involving aviation authorities, local governments and technology providers to establish standardised protocols. Cellular networks used in UAM are crucial for beyond visual line of sight (BVLOS) operations due to their extensive range and seamless transitions. This study examines cellular data quality in selected rural areas to enable the adaptation and scaling of technologies to urban settings, providing a framework for UAM deployment. The research involves evaluating signal strength and quality at altitudes of 0, 50, and 100 m for three network providers (Digi, Celcom, and Maxis). The results show that while signal strength increases with altitude due to reduced line-of-sight blockage, signal quality can decrease due to interference. Specifically, Digi performed best at the ground level, Maxis at 50 m, and Celcom at 100 m. These insights into performance variations and limitations in rural areas allow for optimised adaptations in urban environments. The study demonstrates acceptable network handovers and overall network performance, supporting further exploration of cellular network technology for UAM operations in Malaysia.*

**Keywords:** *Urban air mobility (UAM); unmanned aerial vehicle (UAV); cellular communication; reference signal reception quality (RSRQ); altitude.*

## 1. INTRODUCTION

Efforts to establish an urban air mobility (UAM) framework present an opportunity to address urban transport issues, promote economic growth and drive technological innovation. The Malaysian government has identified that medical transport, tourism and urban logistics are among the potential use cases for UAM and has identified these to create a regulatory framework. Unmanned aerial vehicle (UAV) networks are one of the principal technologies used in smart city applications (Yun *et al*., 2021). Due to congestion caused by both traffic and accelerated urbanisation that makes urban travel more difficult, efforts are being made to introduce vertical movement of individuals and goods in urban areas. In this respect, UAVs enable the development of effective and sustainable urban transportation systems (Rozenberg *et al*., 2020). Electric vertical take-off and landing (eVTOL) is a new class of lightweight aircraft that uses electric power to lift off, hover and land vertically. It has become an integral part of meeting modern transportation requirements in and around urban areas. With eVTOLs, it is possible to transport people in urban areas while minimising traffic congestion on the ground (Trock & Matthews, 2022).

UAVs, commonly referred to as unmanned aerial systems (UAS) or drones, are employed nowadays in civilian applications such as recreation (Liu *et al*., 2015), traffic monitoring (Sutheerakul *et al*., 2017), mapping (Besada *et al*., 2018) and agriculture (Norhashim *et al*., 2023). In recent years, the use of UAVs has consistently increased across numerous industries, with the UAM industry among the most promising.

The current air traffic management (ATM) system's inability to control urban airspace is the primary obstacle to the development of urban air transportation (Vascik & John Hansman, 2017). These obstacles place a strain on the current air traffic control (ATC) system and indicate the need for substantial system modifications. Each airspace class has a set of rules that specify how aircrafts should fly and how ATC should deal with such aircrafts. As a result, the International Civil Aviation Organization (ICAO) defines each airspace class based on the type of flights it services, provided separations, type of air traffic service, speed and altitude limitations, radio communication requirements, as well as ATC clearances (Bauranov & Rakas, 2021).

UAM aircrafts travel at low altitudes and frequently pass near to structures and other obstructions, making it challenging for conventional ATC systems to control and track them. As a result, new techniques and technologies might be required to guarantee the safe and effective operation of UAM vehicles. Wireless communication networks are essential for modern ATC systems, ensuring safe management of aircrafts in real-time. Wireless networks offer the critical advantage of mobility, ensuring uninterrupted communication from the point of departure to the point of arrival. These networks allow for instantaneous data exchange between control towers and the aircrafts, facilitating timely and accurate instructions for take-off, landing and in-flight adjustments. Given that aircrafts are highly agile vehicles that covering vast distances at high speeds, a fixed-line communication system would be impractical (Kagawa *et al*., 2018), thus wireless communication utilising other methods such as cellular networks is a good option (Mohd Kamal *et al.* , 2019, 2020; Sahwee *et al*., 2020).

Urban and suburban areas pose unique challenges for UAM network management. In densely populated urban regions, line-of-sight blockage from buildings, as well as interference from electronic devices and other wireless signals can be significant. This complicates the task of managing communication networks for UAM (West & Sherry, 2020).

This paper discusses on cellular network signal quality in the rural areas, where interference may be less of an issue due to lower population density. However, network coverage can still become a challenge, and ensuring reliable communication over vast, sparsely populated regions is crucial. Rural areas often lack the necessary communication infrastructure, such as ground-based communication stations and high-speed internet access, which are readily available in urban and sub-urban environments. While there may be less air traffic in rural areas, coordinating UAM operations with other airspace users, such as agricultural aircrafts and general aviation, remains vital to prevent conflicts and ensure safe and efficient operations in these less densely populated regions. Therefore, the data obtained in rural areas can be a good indication in scaling and adapting technologies for urban and suburban environments. By understanding the capabilities and limitations of the tested cellular communication technology in rural areas, adjustments can be made to maximise performance in urban settings (Solomitckii *et al*., 2018).

In addition, the data collected in this study is crucial for assessing the feasibility of using existing cellular networks to support eVTOL operations. By comparing different network providers (Digi, Celcom and Maxis), the study identifies which provider offers the best coverage and quality at different altitudes. This study focuses on the investigation of reference signal reception quality (RSRQ) performance. Although actual data rate performance and connectivity are influenced by the signal-to-interference-plus-noise ratio (SINR), the necessary data on interference levels to analyse SINR and actual data rates are not available. Despite this limitation, RSRQ remains a crucial parameter for evaluating network performance as it provides valuable insights into the quality and reliability of the received signal. By analysing RSRQ, overall network performance can be inferred and potential areas with weak signal reception can be identified, which is critical for optimising and troubleshooting cellular networks.

## 2. METHODOLOGY

In this study, RSRQ data was collected at a rural area in Sungai Besar, Selangor, Malaysia. The tests were conducted near a cell tower located in a rice field area. Figures 1 shows the test site views from Cell Mapper for Digi, Celcom and Maxis. The effectiveness of the long-term evolution (LTE) networks was evaluated using the RSRQ parameter, which measures the quality of reference signals. User equipment (UE) for cellular communications continuously tracks signals from all neighbouring cell towers to connect to the one with the strongest signal. Standard reference signals are an integral feature of LTE technology, allowing UEs to assess the quality of their connection to a specific cell tower. RSRQ, calculated using the reference signal, represents the ratio between carrier and interference powers (Alshalabi *et al*., 2022).

A fixed-wing UAV was employed to collect data and carry the necessary sensors for the study. Three smartphones, each with an active mobile connection and mobile data access through Digi, Maxis and Celcom, were used simultaneously during the experiment. Each network provider operates within allocated frequency bands to prevent overlap with neighbouring providers. This frequency planning, governed by national regulatory standards, guarantees that every base station and mobile device operates on unique frequencies, significantly reducing the potential for interference (Chen *et al*., 2023). When measuring received signal strength, the assessment predominantly captures the signal level received at the physical layer, originating from the nearest base station operating within its designated spectrum (Ayman *et al*., 2023).

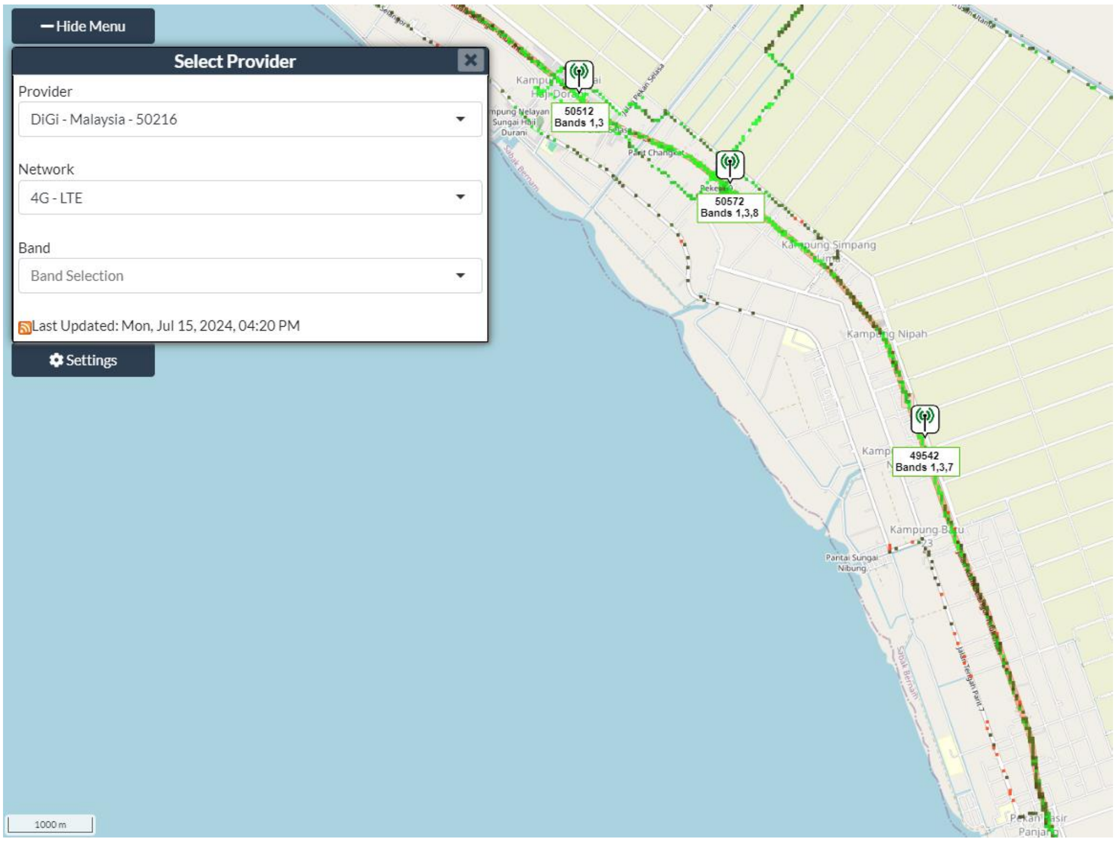


**(a)**

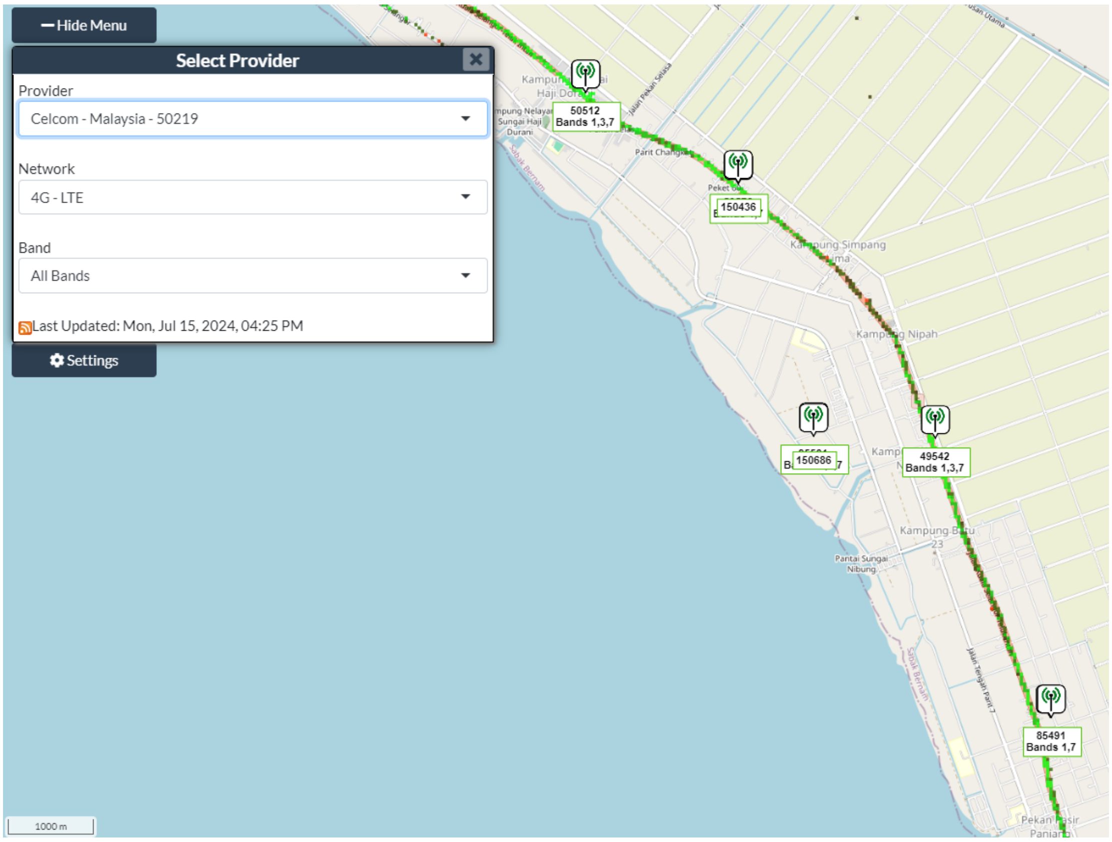


**(b)**

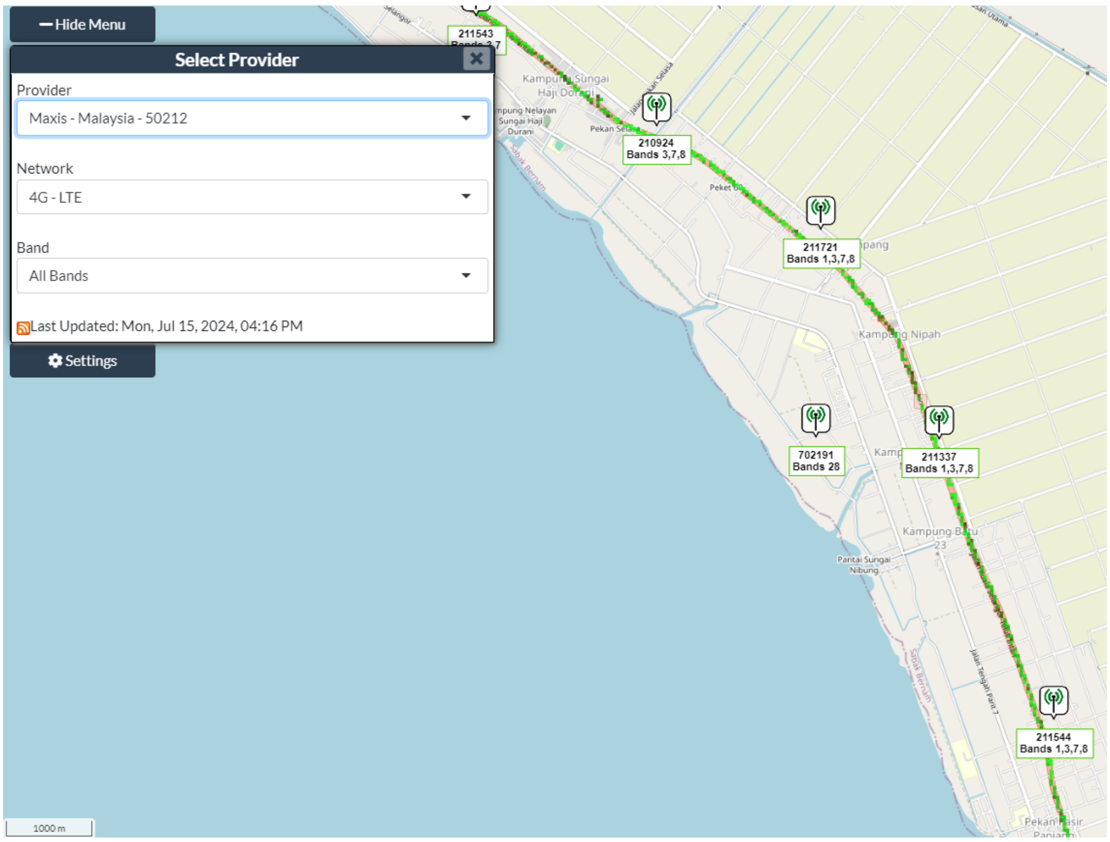


**(c)**

**Figure 1: Locations of cell towers for: (a) Digi (b) Celcom (c) Maxis.**

The UAV's route was mapped using three distinct checkpoints as shown in Figure 2. The ground station served as Checkpoint 1, followed by a right turn manoeuvre at Checkpoint 2. The UAV then proceeded to Checkpoint 3, where it turned around and returned to Checkpoint 1. The UAV had a total flight range of approximately 14 km.

The data and telemetry links for the UAV were established using a 2.4 GHz remote control and a 915 MHz telemetry system. The Mission Planner software, which functions as the UAV's ground station, was utilised to plan and monitor the flight path. The UAV was flown at two different altitudes, 50 and 100 m, and a reference test was conducted on the ground following the route mapped by Mission Planner.

The data collected with the Altimeter App and Net Monitor Lite App was used to verify the UAV's flight path and RSRQ data from the network providers. In addition, MATLAB was used to analyse and visualise the data collected by the applications on the smartphones. The results were visualised using MATLAB and divided into three categories: the data from the ground test, 50 m flight altitude test and 100 m flight altitude test. Geoscatter-style plots were created by sampling the length of the data. The plots display the RSRQ data for each of the three network operators in relation to the latitude and longitude of the UAV.

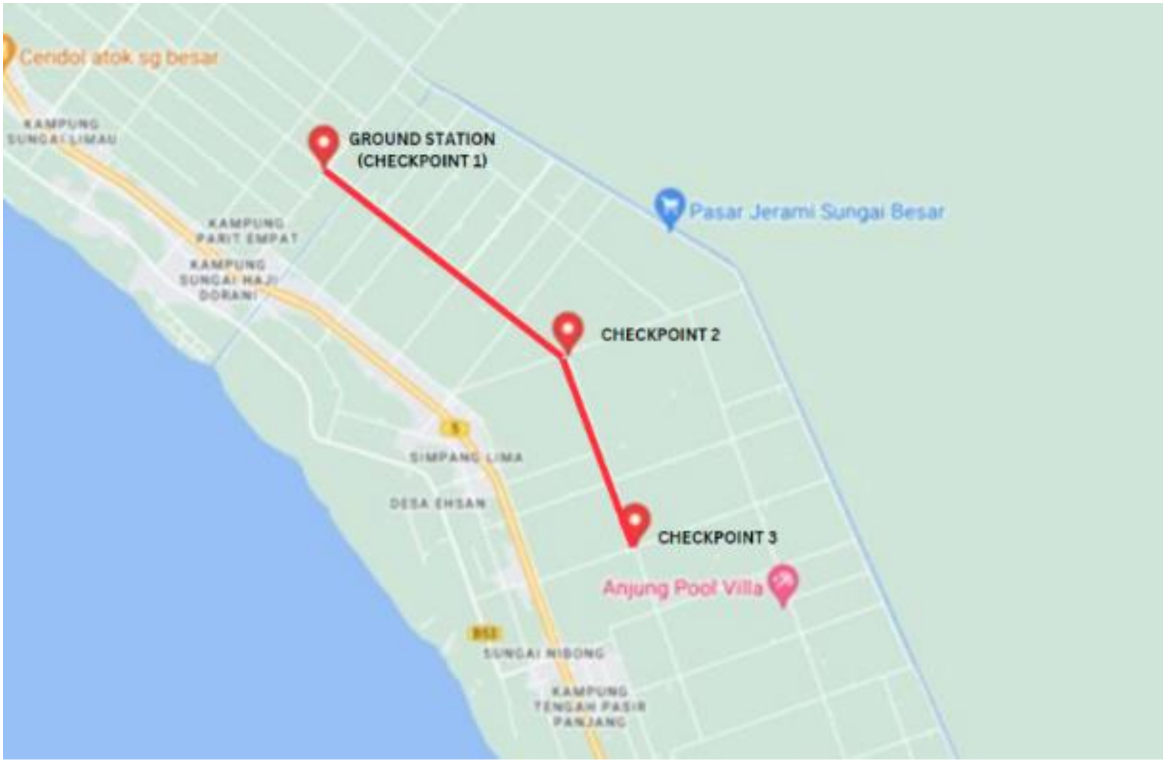


**Figure 2: Checkpoints for the flight test.**

## 3. RESULTS & DISCUSSION

Figures 3 to 5 show the RSSQ values along the route at the test area for the three different altitudes (0, 50 and 100 m) and three different network providers (Digi, Celcom and Maxis). The RSRQ measurements for Celcom, Digi and Maxis at ground level reveal distinct signal quality patterns as shown in Figure 3. The colour bar ranges from 0 to -20 dB, with lighter colours (yellow to green) indicating better signal quality and darker colours (blue to dark blue) indicating poorer signal quality. Digi maintains the most consistent and reliable signal quality, with fewer weak spots and a uniform distribution between -6 and -12 dB. Celcom shows a similar range but includes notable weak areas between -14 and -16 dB. Maxis exhibits the most variability, with frequent poor signal spots below -14 dB, making it less reliable overall. Overall, Digi provides the best RSRQ performance at ground level in the surveyed area, followed by Celcom and then Maxis.

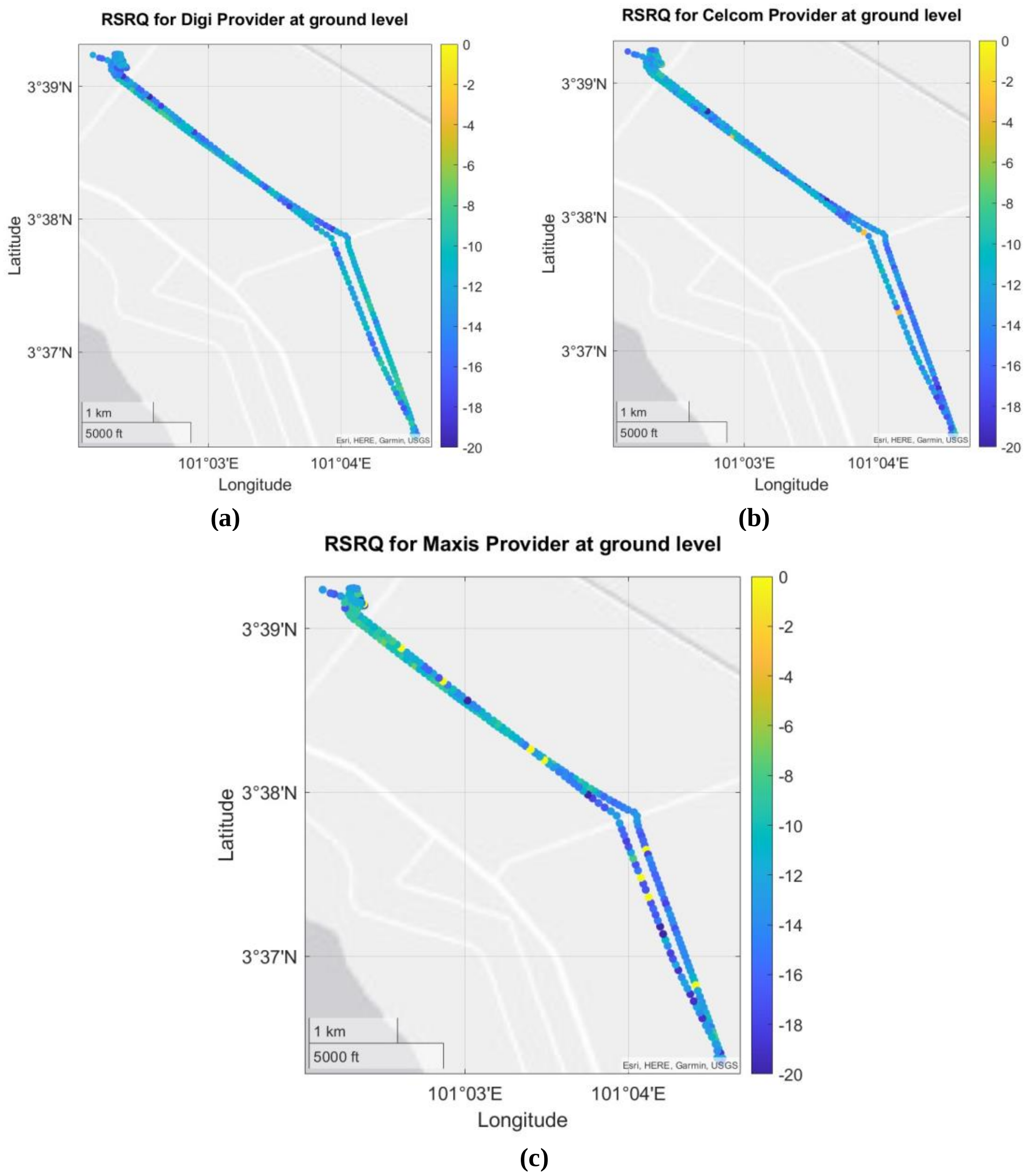


**Figure 3: RSRQ data at ground level (0 m) for: (a) Digi (b) Celcom (c) Maxis.**

Based on the analysis of RSRQ values of the network providers at altitude of 50 m (Figure 4), Celcom exhibits varying signal quality with sporadic high-quality regions but lacks consistency. Digi provides a more consistent, moderate signal quality throughout the route but lacks high-quality areas. Maxis shows significant variability, with both high and very low-quality regions dispersed along the route. Overall, Celcom offers the best performance due to occasional high-quality pockets, while Digi provides the most consistent signal quality at a moderate level.

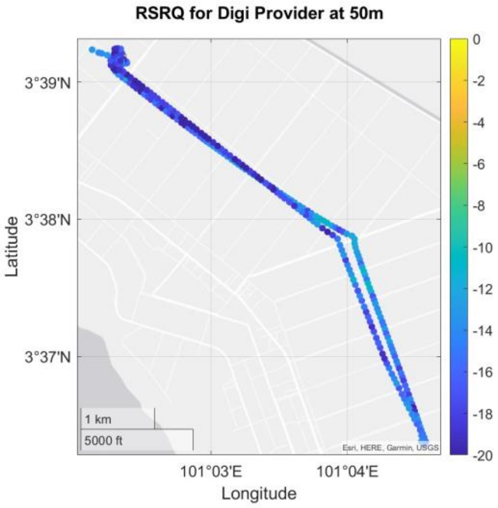


**(a)**

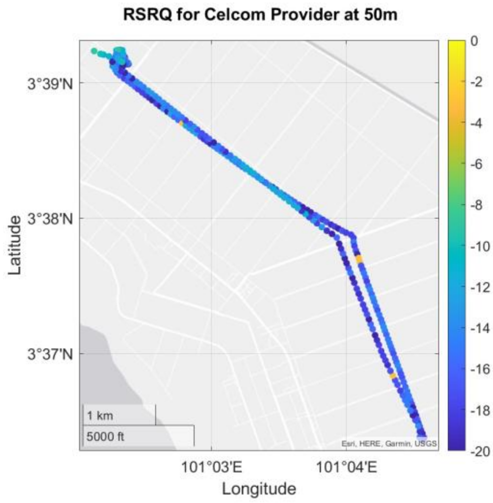


**(b)**

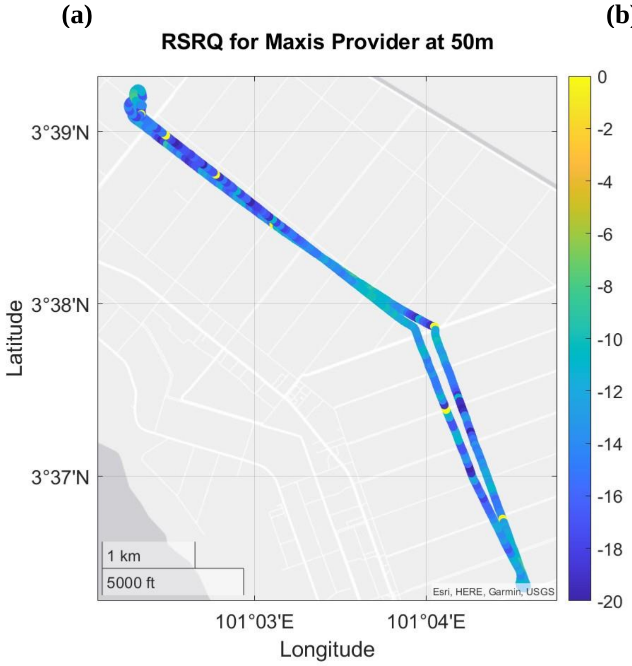


**(c)**

**Figure 4: RSRQ data at altitude of 50 m for: (a) Digi (b) Celcom (c) Maxis.**

At altitude of 100 m (Figure 5), the findings indicate that Celcom and Maxis offer relatively better RSRQ performance as compared to Digi. Celcom's coverage shows a balanced distribution of RSRQ values with both good and poor signal quality areas, while Maxis exhibits slightly better consistency with more green and yellow areas, indicating superior signal quality. Conversely, Digi demonstrates the poorest performance, predominantly displaying blue shades that correspond to lower RSRQ values and suggesting inferior signal quality. Thus, Maxis and Celcom are preferable for users seeking better network performance at elevated altitudes, with Digi lagging behind.

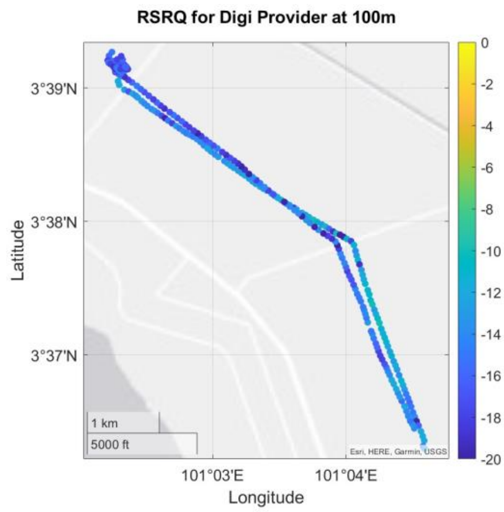


(a)

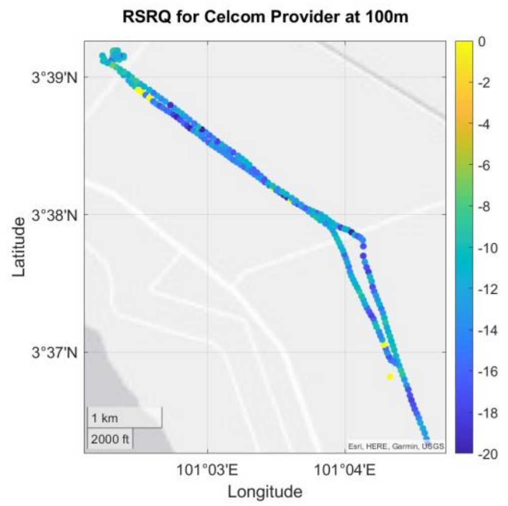


(b)

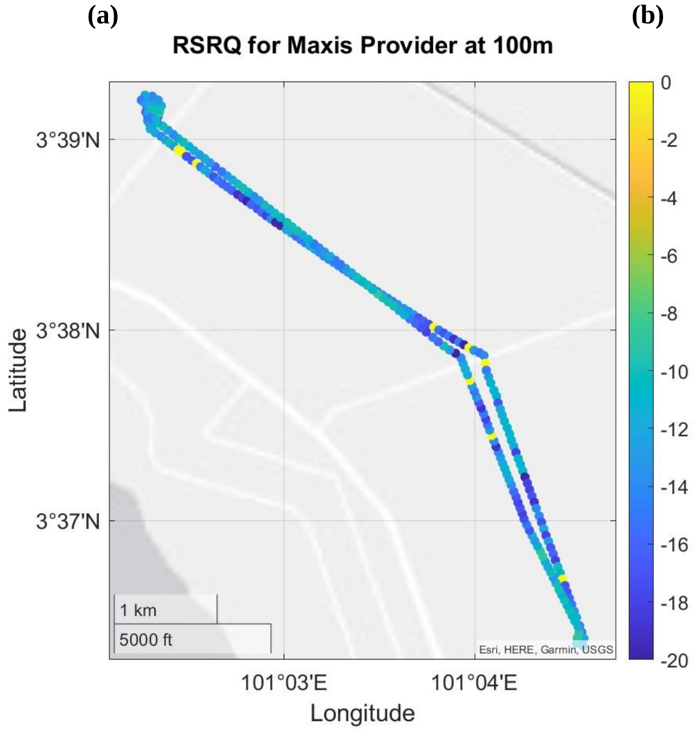


(c)

**Figure 5: RSRQ data at altitude of 100 m for: (a) Digi (b) Celcom (c) Maxis.**

The average RSSQ values for the different altitudes are shown in Figure 6. It is found that Digi (-12.63 dBm) performed better at the ground level as compared to Maxis (-12.89 dBm) and Celcom (-12.91 dBm). Maxis (-12.09 dBm) performed better than Celcom (-13.67 dBm) and Digi (-15.80 dBm) at altitude of 50 m, while Celcom (-11.80 dBm) performed better than Maxis (-11.83 dBm) and Digi (-15.19 dBm) at altitude of 100 m. The data also shows that the signals from all three providers can be reached from both the flight altitudes.

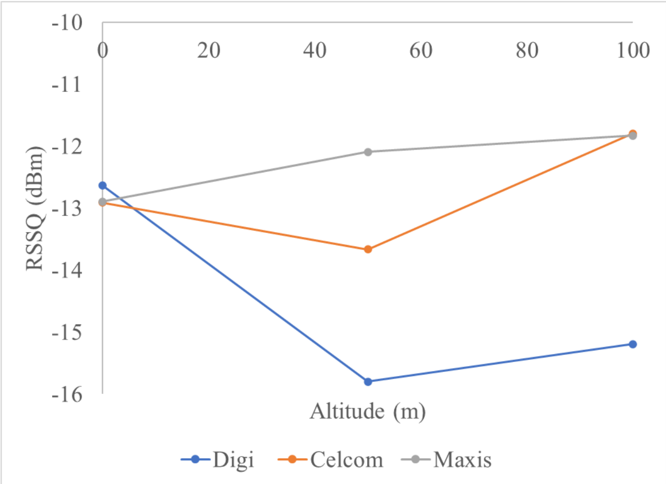


**Figure 6: Mean RSSQ values for the different altitudes.**

One observed trend is that the signal is stronger at higher altitudes but of lower quality. At higher altitudes, there is generally less obstructions (e.g., buildings and trees), leading to stronger signal reception due to clearer line-of-sight to the cell towers, reducing signal attenuation and loss. However, the distance between the UAV receiver and cell tower increases, reducing signal strength based on the free space path loss model. Despite stronger signals, the quality may decrease at higher altitudes due to factors such as increased interference from multiple cell towers and reduced signal-to-noise ratio. Higher altitudes might also expose the UAV to overlapping coverage areas of different towers, leading to more interference, as predicted by the multipath propagation theory. This phenomenon indicates that while the received signal power increases, interference from signals reflected off surfaces and arriving at different times degrades the overall quality (Zulkifley *et al*., 2021).

The three cellular network providers' performance varied at different altitudes. At the ground level, Digi had the highest average RSSQ value of -12.63 dBm, which could be due to better tower placement and optimised coverage for ground-level communication. This might be influenced by the strategic positioning of Digi's cell towers to minimise obstacles and maximise direct signal paths. At altitude of 50 m, Maxis had the highest average RSSQ value of -12.09 dBm, which suggests that Maxis has invested in tower placements and configurations that reduce signal degradation at medium heights. At altitude of 100 m, Celcom had the highest average RSSQ value of -11.80 dBm, which could indicate that their network is optimised for higher altitudes, with potentially better handling of interference and signal management at these heights.

The ability of all three providers to maintain signal reception at various altitudes demonstrates the robustness of Malaysia's cellular infrastructure. This is promising for eVTOL operations, indicating that the current networks could be adapted for UAM with appropriate adjustments and enhancements. The findings suggest that while existing networks can support eVTOL operations, further optimisation might be necessary, especially for handling higher altitudes and ensuring consistent signal quality. This could involve deploying more cell towers, especially small cells and microcells, to enhance coverage and reduce interference. Collaborating with network providers to enhance coverage and quality at different altitudes can help in creating a more reliable communication framework for UAM. Moreover, the study underscores the need for regulatory bodies to consider cellular communication performance in their safety protocols for eVTOL operations, ensuring that communication reliability meets the stringent safety standard.

## 4. CONCLUSION

In summary, the data gathered and observed trends highlight the complex interplay between signal strength, quality and altitude. They provide valuable insights into the current capabilities and limitations of cellular networks for supporting emerging UAM solutions. This information is critical for planning the infrastructure needed to support the safe and efficient operation of eVTOLs, ensuring that UAM becomes viable and reliable.

Based on the data from this study, which includes handover of networks from one cell tower to another and its stability at three different altitudes, the beyond visual line of sight (BVLOS) operation of UAMs over LTE networks proved to be viable for up to altitude of 100 m. Future studies should focus on the development of interference management strategies specifically tailored to Malaysia, such as the development of intelligent systems capable of dynamically changing communication parameters in response to real-time assessments of the country's topography and atmospheric conditions. In addition, extensive rural testing and validation programmes are required in various Malaysian regions to ensure the reliability and consistency of UAM communication systems. The successful deployment of UAM will be greatly aided by these research efforts, which will also contribute to the advancement of technological and infrastructural capabilities by providing safe and efficient air transport solutions that can benefit the country's urban and rural areas.

## REFERENCES


Alshalabi, O., Mohd Kamal, N. L., Sahwee, Z., Norhashim, N. & Ahmad Shah, S. (2022). Feasibility of LTE-connected unmanned aerial vehicle. *2022 IEEE Symp. Future Telecommun. Tech. (SOFTT 2022)*, 14-16 November 2022, Johor, Malaysia.

Ayman A.E.S, Abdulraqeb, A., Ibraheem, S., Wan Haslina, H., Mohamed Shaik, H. & Yousef, I.D. (2023). Measurement analysis and performance evaluation of mobile broadband cellular networks in a populated city. *Alexandria Eng. J.*, **66**: 927-946.

Bauranov, A. & Rakas, J. (2021). Designing airspace for Urban Air Mobility: A review of concepts and approaches. *Prog. Aerospace Sci.*, **125**: 100726

Besada, J.A., Bergesio, L., Campaña, I., Vaquero-Melchor, D., López-Araquistain, J., Bernardos, A. M. & Casar, J.R. (2018). Drone mission definition and implementation for automated infrastructure inspection using airborne sensors. Sensors, **18**: 1170.

Chen, S., Hu, J., Zhao, L., Zhao, R., Fang, J., Shi, Y. & Xu, H. (2023). Spectrum needs and planning. *In* Chen, S., Hu, J., Zhao, L., Zhao, R., Fang, J., Shi, Y. & Xu, H. (Eds.), *Cellular Vehicle-to-Everything (C-V2X)*. Springer, Singapore.

Kagawa, T., Ono, F., Shan, L., Takizawa, K., Miura, R., Li, H.B. & Kato, S. (2018). A study on latency-guaranteed multi-hop wireless communication system for control of robots and drones. *20th Int. Symp. Wirel. Pers. Multim. Comm.* (*WPMC 2017)*, 17-20 December 2017, Bali, Indonesia

Liu, Z., Li, Z., Liu, B., Fu, X., Raptis, I. & Ren, K. (2015). Rise of mini-drones: Applications and issues. *2015 Worksh. Priv.-Aware Mobile Comput. (PAMCO 2015)*, 22 June 2015, Hangzhou, China

Mohd Kamal, N.L., Sahwee, Z., Abdul Hamid, S., Norhashim, N. & Lott, N. (2019). Cellular network and its relevance for unmanned aerial vehicle application in Malaysia. *5th Int. Conf. Man Mach. Syst.*, 26–27 August 2019, Pulau Pinang, Malaysia

Mohd Kamal, N.L., Sahwee, Z., Norhashim, N., Lott, N., Abdul Hamid, S. & Hashim, W. (2020). Throughput performance of 4G-based UAV in a sub-urban environment in Malaysia. *8th Ann.*

*IEEE Int. Conf. Wirel. Space Extreme Environ.*, 12-14 October 2020, Vicenza, Italy.
Norhashim, N., Kamal, N.L.M., Shah, S.A., Sahwee, Z. & Ruzani, A.I.A. (2023). A review of unmanned aerial vehicle technology adoption for precision agriculture in Malaysia. *Unmanned Syst.*, **12**: 707-725.

Rozenberg, R., Szabo, S., Polishchuk, V., Nemethova, H., Jevcak, J., Choma, L. & Vukovic, D. (2020). Information model for evaluation and selection of instructor pilots for smart city urban air mobility. *5th Int. Conf. Smart Sustain. Technol. (SpliTech 2020)*, 23-26 September 2020, Split, Croatia.
Sahwee, WH Z., Mohd Kamal, N.L. & Abdul Hamid, S. (2020). Study on channel propagation of cellular-to-UAV in a typical sub-urban environment in Malaysia. *Int. J. Adv Sci. Tech.*, **29**: 1394-1400
Solomitckii, D., Gapeyenko, M., Semkin, V., Andreev, S. & Koucheryavy, Y. (2018). Technologies for efficient amateur drone detection in 5G millimeter-wave cellular infrastructure. *IEEE Comm Mag.*, **56**: 43–50.
Sutheerakul, C., Kronprasert, N., Kaewmoracharoen, M. & Pichayapan, P. (2017). Application of Unmanned Aerial Vehicles to pedestrian traffic monitoring and management for shopping streets. *Transp. Res. Procedia*, **25**: 1717–1734.
Trock, J. & Matthews, A.E. (2022). *Regulation and Certification of Electric Vertical Take-Off and Landing (eVTOL) Aircraft.* Available online at: https://www.lexology.com/library/detail.aspx?g=158fa911-d418-4396-a5af-9ffeae3832e7 (Last access date: 1 May 2024).
Vascik, P.D. & John Hansman, R. (2017). Constraint identification in on demand mobility for aviation through an exploratory case study of Los Angeles. *17th AIAA Aviat. Technol. Integr. Oper. Conf.*, 5-9 June 2017, Denver, Colorado, US .
West, J. & Sherry, L. (2020). Agent-based simulation of metropolitan area evacuation by unmanned air mobility. *2020 Integr. Comm. Nav. Surveillance Conf.* (ICNS 2020), 8-10 September 2020, Herndon, Virginia, US.
Yun, W. J., Ha, Y. J., Jung, S., & Kim, J. (2021). Autonomous aerial mobility learning for drone-taxi flight control. *2021 Int. Conf. Inf. Commun. Technol. Converg. (ICTC)*, 20-22 October 2021, Jeju Island, Republic of Korea
Zulkifley, M.A., Behjati, M., Nordin, R. & Zakaria M.S. (2021). Mobile network performance and technical feasibility of LTE-powered unmanned aerial vehicle. *Sensors*. **21**: 2848.

# EVALUATION OF MULTI-GNSS ADJACENT BAND COMPATIBILITY VIA GNSS SIMULATION

Dinesh Sathyamoorthy

Science & Technology Research Institute for Defence (STRIDE), Ministry of Defence, Malaysia

*Email: dinesh.sathyamoorthy@stride.gov.my

**ABSTRACT**

*This study is aimed at evaluating the adjacent band compatibility of single frequency multi-Global Navigation Satellite System (GNSS), consisting of the Global Positioning System (GPS) L1 coarse acquisition (C/A) and Galileo E1 open service (OS) signals. The study is conducted using GNSS simulation, which allows for the tests to be held with various repeatable conditions, as defined by the users. It is found that the factors that affect the level of disruption from adjacent band interference include GNSS receiver parameters, as well as carrier frequency and bandwidth of interference signals. GNSS receivers with lower receiver sensitivity and higher receiver noise would be more susceptible to adjacent band interference. Moving the carrier frequency of interference signals away from the frequency of the GNSS L1 / E1 band (1575.42 MHz) as well as increasing their bandwidths increase the power levels that affect GNSS performance. The GPS + Galileo mode has slightly improved performance against interference as compared to the GPS only mode due to the alternative binary offset carrier (AltBOC) modulation that is employed for the Galileo E1 OS signal, which is improves its robustness.*

**Keywords:** *Adjacent band compatibility; Global Navigation Satellite System (GNSS) simulation; GPS L1 coarse acquisition (C/A) and Galileo E1 open service (OS) signals; estimate probable error (EPE); degradation of accuracy and location fix loss.*

## 1. INTRODUCTION

Adjacent band signals at frequencies close to Global Navigation Satellite System (GNSS) signal bandwidths can disrupt the performance of GNSS receivers, in particular those that incorporate poor filtering design to achieve a low-cost product. Every signal, even though it operates in a specific portion of the spectrum, introduces interference into adjacent portions of the spectrum. The amount of interference that is permissible to seep over into adjacent spectrums is controlled in many countries by their respective communications commissions, but it is not possible to eliminate it completely. The higher the transmission power used, the higher the interferences will be in adjacent portions of the spectrum. The number of systems that make use of the radio frequency (RF) spectrum has significantly increased in recent years and the number of users increases daily. This development has crowded the RF spectrum significantly, resulting in increased occurrences of adjacent band interferences for GNSS receivers (DOT, 2018; Drocella *et al.*, 2020; Hegarty *et al.*, 2020; Buesnel, 2021). To this end, various studies have been conducted to evaluate GNSS adjacent band compatibility, with the aim of developing new GNSS spectrum interference standards to ensure that future proposals for use of spectrum bands adjacent to GNSS signals will not compromise GNSS performance, in particular for vital applications such as public safety, navigation and time synchronisation (Zdunek, 2016; Uhrich *et al.*, 2019; Setlak & Kowalik, 2021; Sokolova *et al.*, 2022).

Dinesh *et al.* (2017) evaluated adjacent band power levels that can be tolerated by the Global Positioning System (GPS) L1 coarse acquisition (C/A) signal and the extent to which such power levels impact GPS performance. It was conducted using GNSS simulation, which allowed for the tests to be conducted with various repeatable conditions, as defined by the users. As the tests were conducted in controlled laboratory environments, they were not be inhibited by unintended signal interferences and obstructions (Pozzobon *et al*., 2013; Arul Elango & Sudha, 2016; Bi & Yuan *et al*., 2021; Emerick, 2022).

In this paper, the study is extended to evaluate the adjacent band compatibility of single frequency multi-GNSS, consisting of the GPS L1 C/A and Galileo E1 open service (OS) signals. The study is conducted using GNSS simulation for a GPS receiver, Garmin GPSMAP 60CSx (Garmin, 2007) (Receiver R1), and a multi-GNSS receiver, Garmin GPSMAP 66sr (Garmin, 2021) (Receiver R2).

## 2. METHODOLOGY

The apparatus used in the study are an Aeroflex GPSG-1000 GNSS simulator (Aeroflex, 2010), a Spectran HF-60105 spectrum analyser (Aaronia, 2015), an IFR 2023B signal generator (IFR, 1999), a Hyperlog 60180 directional antenna (Aaronia, 2009) and a notebook running GPS Diagnostics v1.05 (CNET, 2008). The study is conducted in STRIDE's semi-anechoic chamber (A. Faridz, 2010) to avoid external interferences signals and multipath errors. The test setup employed is as shown in Figure 1. Simulated GNSS signals are generated using the GNSS simulator and transmitted via the coupler, while interference signals are generated using the signal generator and transmitted via the directional antenna. The tests are conducted with the assumption that there are no ionospheric and troposheric delays, GNSS satellite clock and ephemeris errors, obstructions and multipath, as well as unintended interference signals.

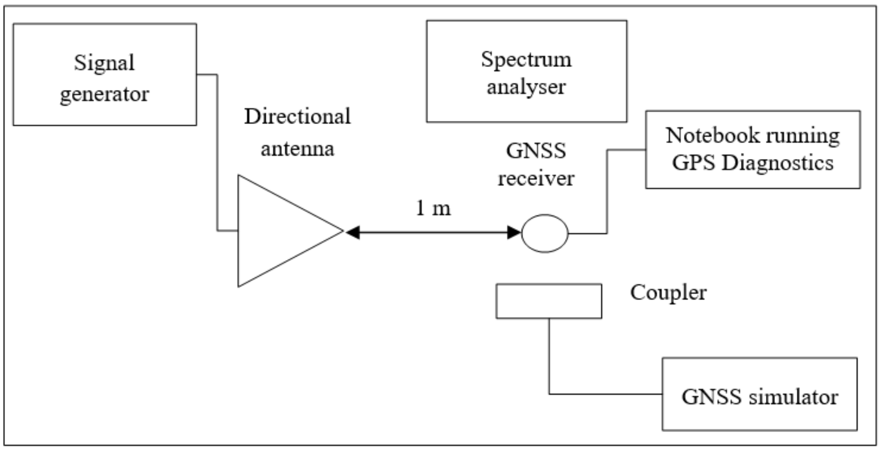


**Figure 1: The test setup employed for the study.**

The test procedure is conducted for coordinated universal time (UTC) of 0000 at Kajang, Selangor, Malaysia (N 2° 58', E 101° 48') and GNSS signal power level of -130 dBm. The almanac data for the periods is downloaded from the US Coast Guard's web site (USCG, 2023) and imported into the GNSS simulator.

Based on the functionalities of the GNSS simulator, this study is conducted for the GPS L1 C/A and Galileo E1 OS signals. The GPS L1 C/A signal is an unencrypted civilian GPS signal that is widely used by various GPS receivers. The signal has fundamental frequency of 1,575.42 MHz and code structure that modulates the signal over a 2 MHz bandwidth (USACE, 2011; Kaplan & Hegarty, 2017; DOD, 2020). The Galileo E1 OS signal also has fundamental frequency of 1,575.42 MHz, with code structure that modulates the signal over a 4 MHz bandwidth (Kaplan & Hegarty, 2017; Povero, 2019; ESA, 2021). For Receiver R2, the tests are conducted for two conditions: 1) GPS only with 12 satellites (R2-GPS); 2) GPS with six satellites and Galileo with six satellites (R2-GPS-GAL).

Once a location fix is obtained with the GNSS receiver, the estimate probable error (EPE) is recorded using GPS Diagnostics. The interference signal used is a frequency modulated (FM) signal with information frequency of 5 kHz, and bandwidths of 2, 4, 8 and 16 MHz. The carrier frequency is varied from 1,550 to 1,600 MHz at intervals of 5 MHz. Interference signal transmission is started at power level of -140 dBm. The power level is increased by increments of 3 dBm and the corresponding EPE values are recorded.

## 3. RESULTS & DISCUSSION

For the tests conducted, the power levels at which the first degradation of accuracy occurs and the location fix is lost are shown in Figures 2 and 3 respectively. It is observed that interference signal power levels required to affect Receiver R1 are lower as compared to Receiver R2. This is as Receiver R1 has lower receiver sensitivity and higher receiver noise, which results in reduced carrier-to-noise density ($C/N_0$) levels for GNSS satellites tracked by the receiver, which is the ratio of received GNSS signal power level to noise density. Lower $C/N_0$ levels result in increased data bit error rate when extracting navigation data from GNSS signals, and hence, increased carrier and code tracking loop jitter. This, in turn, results in more noisy range measurements and thus, less precise positioning (Petovello, 2009; USACE, 2011; Kaplan & Hegarty, 2017; DOD, 2020).

For Receiver R2, it is found that interference signal power levels required to affect the GPS + Galileo mode are higher as compared to the GPS only mode. This could be as the Galileo E1 OS signal makes use of alternative binary offset carrier (AltBOC) modulation, which improves its robustness against various sources of interferences (Kaplan & Hegarty, 2017; Povero, 2019; ESA, 2021).

It is also found that as the carrier frequency of the interference signal moves away from the frequency of the GNSS L1 / E1 band (1575.42 MHz), the interference signal power levels required to affect GNSS performance increase. Increasing bandwidth of interference signals also increases the power levels that affect GNSS signal, as the interference signal's strength is dispersed over a wider bandwidth.

It is observed that interference signal power levels required to affect GNSS performance are significantly high as compared to the corresponding GNSS signal power levels. The noise-like GPS C/A and Galileo OS code structures, which modulate the L1 and E1 signals over 2 and 4 MHz bandwidths respectively, allow for the signals to be received at low levels of interferences. The GPS precision (P(Y)) and Galileo public regulated service (PRS) codes (restricted codes) have more robust structures, modulating the L1 and E1 signals over 20 and 24 MHz bandwidths respectively, and thus have better resistance to interference. The absence of other error parameters, including ionospheric and tropospheric delays, GNSS satellite clock and ephemeris errors, obstructions and multipath, as well as unintended interference signals, results in the required minimum jamming power levels in this study to be significantly higher as compared to field evaluations conducted in Dinesh *et al.* (2010, 2023) and Ahmad Norhisyam *et al*. (2013).

The tests conducted in this study employed GNSS signal power level of -130 dBm. Usage of lower GNSS signal power levels would result in reduced $C/N_0$ levels and hence, interference signal power levels required to affect the GNSS receivers would be lower.

A limitation faced in this study is that while the GNSS simulator employed can transmit GPS L1 / Galileo E1 and GPS L5 / Galileo E5 signals, this cannot be done simultaneously. Furthermore, the settings of the Receiver R2's chip seem to ensure that readings can only be taken when the GPS L1 signal is available. Hence, this study could only be conducted for modes of GPS L1 only and GPS L1 + Galileo E1. In this regard, the scope for future work includes procurement of a GNSS simulator that transmits multifrequency GNSS signals to allow for evaluation of adjacent band compatibility of multifrequency GNSS. In addition, a wider range of GNSS receivers, in particular multifrequency receivers, should also be evaluated.

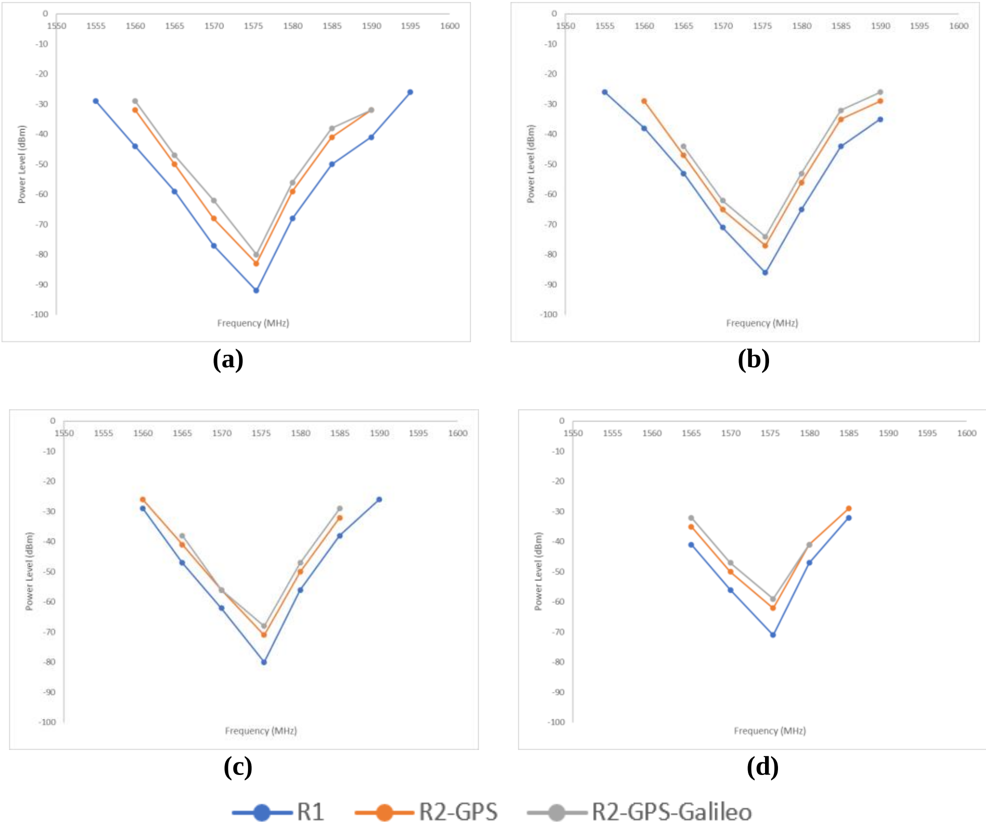


**Figure 2: Interference signal power levels at which first degradation of accuracy is noticed for interference signal bandwidths of: (a) 2 MHz (b) 4 MHz (c) 8 MHz (d) 16 MHz.**

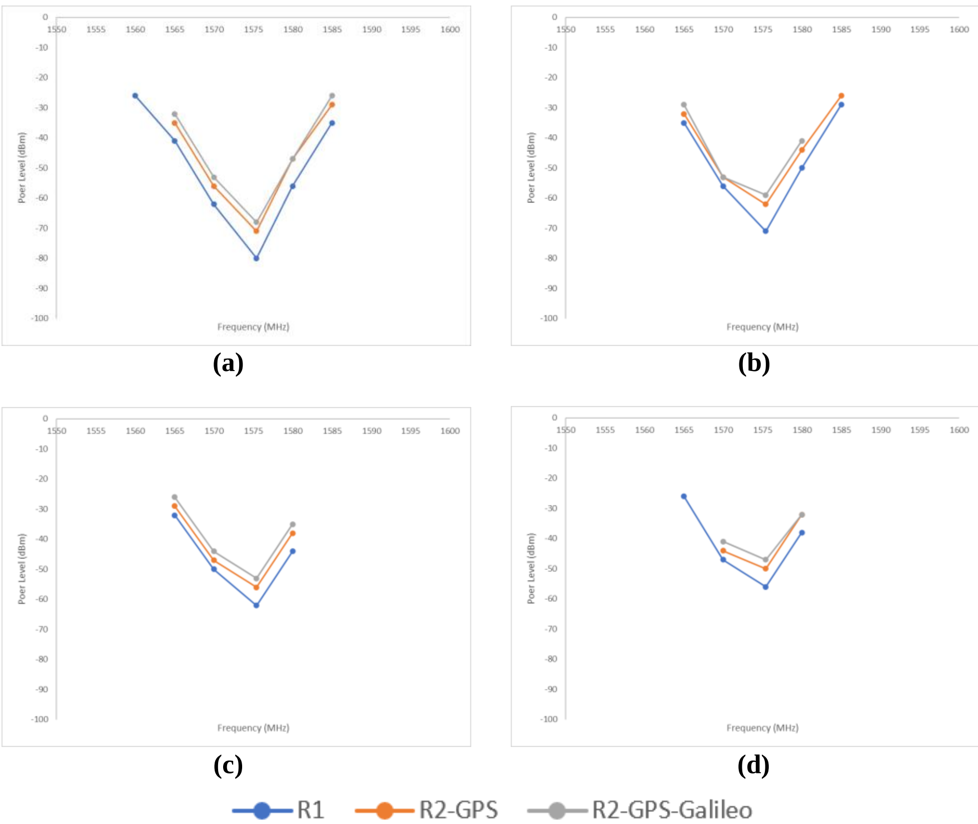


**Figure 3: Interference signal power levels at which location fix is lost for interference signal bandwidths of: (a) 2 MHz (b) 4 MHz (c) 8 MHz (d) 16 MHz.**

## 4. CONCLUSION

This study has demonstrated that the GPS L1 C/A and Galileo E1 OS signals are susceptible to adjacent band interference. It is found that the factors that affect the level of disruption include GNSS receiver parameters, as well as carrier frequency and bandwidth of interference signals. GNSS receivers with lower receiver sensitivity and higher receiver noise would be more susceptible to adjacent band interference. Moving the carrier frequency of interference signals away from the frequency of the GNSS L1 / E1 band (1575.42 MHz) as well as increasing their bandwidths increase the power levels that affect GNSS performance. For Receiver R2, the GPS + Galileo mode slightly improves performance against interference due to the AltBOC modulation that is employed for the Galileo E1 OS signal, which is improves its robustness. Further studies are required using a wider range of GNSS receivers, in particular multifrequency receivers, in order to develop appropriate GNSS spectrum interference standards.

## REFERENCES


A. Faridz, A.G., M. Razali, M.Y. & W. Salwa, W.H. (2010). STRIDE's 3 meters EMC semi-anechoic chamber: Design considerations and compliance to standards. *2010 IEEE Asia-Pacific Conf. Appl. Electromagnetics (APACE 2010)*, 9-11 November 2010, Port Dickson, Negeri Sembilan, Malaysia.

Aaronia (2009). *Precompliance Test Antenna Series HyperLOG® 60xxx: Span 680 MHz to 18 GHz*. Aaronia AG, Strickscheid, Germany.

Aaronia (2015). *Handheld Spectrum Analyzer Spectran V4*. Aaronia AG, Strickscheid, Germany.

Advantest (2009). *U3741/3751 Spectrum Analyzers*. Advantest Corporation, Chiyoda-ku, Tokyo.

Aeroflex (2010). *Avionics GPSG-1000 GPS / Galileo Portable Positional Simulator*. Aeroflex Inc., Plainview, New York.

Ahmad Norhisyam, I., Dinesh, S. & Azman, M.S., 2013. Effect of radio frequency interference (RFI) on the performance of Global Positioning System (GPS) static observations. *9$^{th}$ IEEE Colloq. Signal Process. Appl. (CSPA 2013)*, 8-10 March 2013, Kuala Lumpur.

Arul Elango, G. & Sudha, G.F. (2016). Design of complete software GPS signal simulator with low complexity and precise multipath channel model. *J. Electr. Syst., Inform. Tech.*, **3**: 161-180.

Bi. Y. & Yuan, J. (2021). A portable GPS signal simulator design based on ZYNQ. *2$^{nd}$ Int. Symp. Comp. Eng. Intell. Comm. (ISCEIC 2021)*, 6-8 August 2021, Nanjing, China.

Buesnel, G. (2021). *Ligado Controversy Highlights Risk of Adjacent Band Interference to GPS Receivers*. Available online at: https://www.spirent.com/blogs/ligado-controversy-highlights-risk-of-adjacent-band-interference (Last access date: 7 December 2023).

CNET (2008). *GPSDiag 1.0*. Available online at: https://download.cnet.com/GPSDiag/3000-2130_4-10055902.html (Last access date: 9 June 2022).

Dinesh , S., Wan Mustafa, W.H., Mohd Faudzi., M., Kamarulzaman, M., Hasniza, H., Nor Irza Shakhira, B., Siti Robiah, A., Shalini, S., Jamilah, J., Aliah, I., Lim, B.T., Zainal Fitry, M.A., Mohd. Rizal, A.K., Azlina, B. & Mohd. Hasrol, H.M.Y. (2010). Evaluation of the effect of radio frequency interference (RFI) on Global Positioning System (GPS) accuracy. *Defence S&T Tech. Bull.*, **3**: 100-118.

Dinesh, S., Zainal Fitry, M.A. & Shahrudin, A.H. (2017). Evaluation of Global Positioning System (GPS) adjacent band compatibility via GPS simulation. *Defence S&T Tech. Bull.*, **10**: 229 – 235.

Dinesh, S., Hafizah, M.Y., Ahmad Firdaus, A.K., Mohd Zuryn, M.D. & Maizurina, K. (2023) Evaluation of the effect of radio frequency interference (RFI) on dual-frequency Global Navigation Satellite System (GNSS). *Defence S&T Tech. Bull.*, **16**: 228-237.

DOD (Department of Defence) (2020). *Global Positioning System Standard Positioning Service Performance Standard, Command, Control, Communications, and Intelligence, 5$^{th}$ Ed.* Department of Defence (DOD), Washington D.C.

DOT (Department of Transportation) (2018). *Global Positioning System (GPS) Adjacent Band Compatibility Assessment*. Department of Transportation (DOT), Washington DC, US.

Drocella, E., Wang, C.W. & LaSorte, N. (2020). *Assessment of Compatibility Between Global Positioning System Receivers and Adjacent Band Base Station and User Equipment Transmitters*. National Telecommunications and Information Administration (NTIA), Washington DC, US.

Emerick, M. (2022). *EUSPA to hold GNSS Signal Simulator Manufacturers Forum in December*. Available online at: https://www.gpsworld.com/euspa-to-hold-gnss-signal-simulator-manufacturers-forum-in-december (Last access date: 23 November 2022).

ESA (European Space Agency) (2021). *European GNSS (Galileo) Open Service Signal-in-Space Interface Control Document*. European Space Agency (ESA), Paris, France.

Garmin (2007). *GPSmap 60CSx Owner's Manual*. Garmin International Inc., Olathe, Kansas.

Garmin (2021). *GPSMAP 66 Owner's Manual*. Garmin International Inc., Olathe, Kansas.

Hegarty, C.J., Bobyn, D., Grabowski, J. & Dierendonck, A.J. (2020). An overview of the effects of out-of-band interference on GNSS receivers. *Nav.*, **67**: 143-161.

Kaplan, E.D. & Hegarty, C.J. (2006). *Understanding GPS: Principles and Applications*. Artech House, Norwood, Massachusetts.

Osechas, O., Fohlmeister, F., Dautermann, T. & Felux, M. (2022). Impact of GNSS-band radio interference on operational avionics. *Nav.*, **69**: 2.

Petovello, M. (2009). Carrier-to-noise density and AI for INS / GPS integration. *Inside GNSS*, **4**: 20-29.

Povero, G. (2019). *GNSS Signals Introduction*. Links Foundation, Torino, Italy.

Pozzobon, O., Sarto, C., Chiara, A.D., Pozzobon, A., Gamba, G., Crisci, M. & Ioannides, R. (2013). Developing a GNSS position and timing authentication testbed: GNSS vulnerability and mitigation techniques. *Inside GNSS*, **8**: 45-53.

Setlak, L. & Kowalik, R. (2021). Study and analysis of interference signals of the LTE system of the GNSS receiver. *Sensors*, **21**: 4901.

Sokolova, N., Morrison, A. & Diez, A. (2022). Characterization of the GNSS RFI threat to DFMC GBAS,signal bands. *Sensors*, **22**: 8587.

Uhrich, P., Abgrall, M., Riedel, F., Chupin, B., Achkar, J. & Rovera, G.D. (2019). A powerful signal nearby L1 frequency band jamming GNSS stations in Observatoire De Paris. *ITU J.*, **2**: 1

USACE (US Army Corps of Engineers) (2011). *Engineer Manual EM 1110-1-1003: NAVSTAR Global Positioning System Surveying*. US Army Corps of Engineers (USACE), Washington D.C.

USCG (US Coast Guard) (2023). *GPS NANUs, Almanacs, & Ops Advisories*. Available online at: https://www.navcen.uscg.gov/gps-nanus-almanacs-opsadvisories-sof (Last access date: 12 December 2023).

Zdunek, K. (2016). GPS and adjacent band co-existence study: Summary of method and results. *17th Space-Based PNT Advisory Board Meet.*, 18-19 May 2016, National Harbor, Maryland.

# STRENGTHENING HUMAN CAPABILITY THROUGH DEFENCE OFFSET AND INDUSTRIAL COLLABORATION RESOURCES

Kogila Balakrishnan[1*], Khalifah Badia[2] & Ananthan Subramaniam[3]

[1]WMG, University of Warwick, UK
[2]General Authority for Military Industries (GAMI), Kingdom of Saudi Arabia
[3]National Defence University of Malaysia (NDUM), Malaysia

[*]Email: Kogila.Balakrishnan@warwick.ac.uk

## ABSTRACT

*This paper proposes a policy framework for using offset and industrial collaboration (IC) to develop human capability in the defence and security sector, focusing on Malaysia. It underscores the importance of integrating human capital development with traditional defence spending. Key challenges and success factors in executing offset policies for human capability enhancement are identified. The introduced 'MINERVA' framework includes elements such as a clear vision for human capital development, capability gap analysis, knowledge transfer incentives, credible partners, governance frameworks, stakeholder engagement, efficient project implementation, and assessing absorptive capacity. Through qualitative analysis of Malaysian case studies, the paper highlights optimising defence budgets for skills, education and training. The paper argues that the alignment of international defence procurement with offset policies focused on human capital development can enhance indigenous defence capabilities, military potential, job creation, regional clusters and exports. This alignment bolsters national security and resilience against challenges such as digitalisation and pandemics.*

**Keywords:** *Offset; industrial collaboration; defence and security; human capital development; MINERVA framework.*

## 1. INTRODUCTION

Offset or industrial collaboration (IC) is a policy tool used by importing nations to encourage investment, technology transfer and human capital development in domestic industries through international defence procurement contracts (Balakrishnan & Matthews, 2009, Matthews & Anicetti, 2022). Unlike mainstream economic policies such as investment incentives and trade policies (Zeiler, 1998), offset are primarily used to enhance national security by reducing dependence on external sources and building indigenous defence capabilities (Balakrishnan, 2018, Balakrishnan, 2022). The state has a strong interest in entering into an offset agreement with foreign contractors to build indigenous defence industrial capability, as well as enhance military potential, jobs, regional clusters and exports (Balakrishnan, 2018, Maharani *et al.*, 2023). Despite its benefits, the secretive nature of the defence sector makes it challenging to publicly justify the relevance of offsets as a constructive policy tool (Malm *et al.*, 2016; Balakrishnan, 2018, Anicetti, 2024).

Empirical studies have shown that offset contribute to economic and industrial growth, particularly in building defence industrial bases (Martin, 1996; Brauer & Dunne, 2004). These studies often focus on macroeconomic impacts and organisational improvements in quality, processes, systems and technology (Balakrishnan & Matthews, 2009; Situmeang *et al.*, 2020; Matthews & Maharani, 2021). However, there is a lack of research on how offset enhance human capability through skill and knowledge development, largely due to the confidentiality of defence data.

This paper addresses this gap by exploring how defence offset can develop human capability. Despite 30% of global defence budgets being allocated to offset (SIPRI, 2022), research on their impact on human capability development is limited. The proposed MINERVA policy framework aims to provide adaptable guidelines for governments, defence ministries and multinational corporations involved in offset and IC.

Human capital development is increasingly critical for economic growth, social mobility and global competitiveness. The UN's Fourth Sustainable Development Goal and UNESCO's Education for Sustainable Development framework highlight the importance of lifelong learning and skill development (UN, 2023; UNESCO, 2023, OECD, n.d.). National offset policies often include elements such as technology transfer and job creation, which are crucial for building capability (Nam & Joon, 2004; Maniar, 2018). However, unclear funding stipulations can hinder these objectives.

The defence sector's evolving demands, driven by geopolitical tensions and rapid technological advancements, necessitate significant investment in training personnel in emerging technologies (UK Parliament, 2023). Traditional defence spending prioritises equipment and infrastructure over training and education. The rapid advancement of emerging technologies in artificial intelligence (AI), cyber, robotics and advanced manufacturing, primarily originating from the commercial sector, must be adapted for defence applications. This adaptation requires significant funding to train personnel in these areas. The capabilities needed by companies and the methods for building these skills have evolved. Rapid technological progress and the introduction of disruptive technologies have created an urgent demand for new human capabilities within the defence sector. Unlike more agile sectors, the defence industry struggles to rapidly acquire new capabilities to meet evolving demands. RAND Europe, commissioned by the European Defence Commission, has undertaken major projects to study how to build skills for the defence sector (Galai *et al.*, 2023). Additionally, the demand for skill development has been intensified by the war resulting from Russia's invasion of Ukraine (Antinozzi, 2023). The Lowy Institute's Asia Power Index mentioned that countries such as the US, South Korea and Singapore invest significantly in training to maintain military capabilities (Lowly Institute, 2023).

This research aims to develop an enhanced offset policy framework to nurture human capability in the defence sector. It identifies critical success factors for leveraging offset funding and explores challenges in building human capability. Using Malaysia as a case study, the research defines "capability" as skills, expertise and technological prowess.

The paper is structured into five sections: the Introduction establishes the study's context; the Literature Review provides an overview of offset and their role in defence industry development; the Research Methodology details the study's approach; the Data Analysis and Findings section discusses the results; while the Conclusion offers a policy framework and acknowledges study limitations.

## 2. OFFSETS AND HUMAN CAPABILITY

### 2.1 Theory of Offset

The primary aim of a procurement strategy utilising offset is to ensure nations build indigenous defence and security industry capabilities, reducing dependence on foreign sources, as well as promoting self-sufficiency (Brauer & Dunne, 2004). Offsets enable importing nations to gain economic, industrial and technological benefits beyond the procurement itself. Although precise global data is lacking, offsets are estimated to constitute around 30% of global military spending, approximately $672 billion in 2022 (SIPRI, 2022). Offset are known by various terms such as industrial participation, collaboration and engagement (Brauer & Dunne, 2004). Some countries have adopted more competitive policies to sustain their defence industries. For instance, Canada refers to offsets as "industrial and technological benefits" (Government of Canada, 2022), Australia as the "Australian Industrial Capability Programme"

(Australian Government, 2016), and the UK as "Capability, Skills and Prosperity" requirements. The US employs offsets through the "Buy America Act," "Defence Production Act," and "Small Business Act" (Zeiler, 1998).

While often considered a modern practice, offset trace their roots to ancient times when technology transfer occurred through trade, conquest and diplomacy (Trigger, 2003). A notable 19$^{th}$ century example is Japan's Meiji era, during which Western technologies were adopted through engagement with foreign experts (Huffman, 2010). Modern offsets emerged in the 21$^{st}$ century, evolving from post-World War II efforts aimed at rebuilding Europe's defence industry and integrating American equipment for interoperability. By the 1990s, offsets were formalised in procurement policies and tenders (Balakrishnan, 2018). Globalisation has since increased the complexity of offset, balancing multinational supply chains and government mandates to protect national security and retain industrial benefits locally (Brauer & Dunne, 2010; Balakrishnan, 2018). Examples include Saudi Arabia's Industrial Participation Policy, UAE's Economic Vision 2030 (Government of Abu Dhabi, 2023), and Malaysia's Industrial Collaboration Policy (ICP) (TDA, 2022), focusing on innovation, technology transfer, skills development and strategic alliances.

Offsets are driven by commercial and geopolitical interests. Defence contractors view offset as opportunities for international growth and compliance, transforming what was once seen as a burden (Dehoff *et al.*, 2014). Geopolitically, technology transfer fosters platform commonality and interoperability among allied nations, exemplified by the AUKUS alliance and Saudi Arabia's drone purchase from Turkey, which emphasises long-term industrial partnerships (Savoy & Staguhn, 2022; Dutton, 2023). National aspirations to establish a sustainable defence industrial base motivate the attraction to offset. These aspirations include military capability support, economic development, innovation and human capital development, crucial for a skilled workforce capable of sustaining a resilient defence industry (Hartley & Martin, 1995; Balakrishnan & Matthews, 2009).

Critics argue that offset inflate procurement costs and complicate delivery due to supply chain disruptions, intellectual property risks and regulatory compliance issues (Goodman, 2024). Despite many countries emphasising human capability in offset policies, resource allocation remains debated. The next section explores offsets' contribution to capability building.

## 2.2 Offset and Capability-Building

"Capability" refers to the power or ability to achieve specific tasks or goals at individual, organisational, and systemic levels (Vincent, 2008). This paper aligns with endogenous growth theory, emphasising the link between technology, human capital, innovation and knowledge for enhanced productivity and economic growth (Romer, 1986; Lucas, 1988). As technology evolves, so do skill requirements, necessitating investments in education, research and innovation-friendly regulations. Capabilities, which combine knowledge, skills, expertise and technology, should yield competitive advantages and contribute to organisational survival and prosperity (Winter, 2000; Oppat, 2008; Ogunade, 2011).

In the defence sector, capability development focuses on military capability, with offset historically used to enhance defence industrial capacity. This includes research, manufacturing, supply chains, infrastructure, technology bases, partnerships, exports, innovation, quality control and testing. This paper emphasises the importance of linking technology to human capital, fostering a more productive workforce and sustained economic growth. As nations advance technologically, the demand for high skills increases, highlighting the need for robust education, R&D support and a regulatory environment that promotes innovation (Lucas, 1988).

Organisational capability, influenced by dynamic capability (Teece, 1997) and absorptive capacity (Cohen & Levinthal, 1990; Argote *et al*., 2003; Argote & Miron-Spektor, 2011), involves an organisation's ability to adapt and reconfigure competencies in a changing environment. Offsets in the defence sector are crucial for developing these capabilities, ultimately contributing to national prosperity. Many countries, including India, Saudi Arabia, the UAE, Turkey, South Korea, Brazil and South Africa, use offsets to build their defence industrial and technological capabilities. These policies mandate that a portion of procurement contracts supports diversification, technology transfer, local manufacturing, job creation and skills development to enhance indigenous defence capabilities (Hartley & Martin, 1995; Brauer & Dunne, 2004; Bitzinger & Kurç, 2019). Empirical studies, particularly case studies, have evaluated these activities' success in developing organisational-level defence capabilities, focusing on technological advancements, system innovations, economic impacts, job creation and higher local salaries. However, the term "capability" is rarely explicitly mentioned in offset policies, except in Australia and the UK, where it is linked to building defence industrial capability through procurement (Australian Government, 2001, 2016, 2020; UK Defence Capability Framework, 2022).

### 2.3 Human Capital Development for Delivering Human Capability

Nevertheless, people and their skills are crucial for building defence capabilities. This paper emphasises the necessity of allocating adequate resources for human capital development to create a sustainable and resilient defence industrial base. It distinguishes between human capital and human capability. Human capital includes tangible qualities such as knowledge, skills and expertise gained through education, training, work experience and personal development. This encompasses technical skills, problem-solving abilities, and interpersonal skills. On the other hand, human capability extends beyond these tangible qualities, encompassing the broader potential and capacity for individuals and groups to perform tasks, solve problems and adapt to change. In the current context, human capability involves investing offsets resources into human capital development to enhance skills, knowledge and productivity (Malm *et al.*, 2016). Building human capability through offsets involves the transfer of know-how from foreign institutions to individual knowledge recipients. Success hinges on the credibility and competency of the foreign institution and the technology recipient's ability to absorb and apply the knowledge (Balakrishnan & Lazar, 2022).

However, there is a lack of explicit mention of human capital development in most offset policies. Some aspects of policies may indirectly contribute to skills enhancement and workforce development. Some countries do recognise the importance of developing human capability and have introduced policies to support this vision. Countries such as the UAE, Oman, Türkiye and South Korea have encouraged human capital development using offsets resources.

Malaysia started with a structured offset policy primarily for the defence sector in 2005. The policy was further enhanced to become the National Offsets Policy in 2010(Balakrishnan, K, 2007). The policy subsequently evolved to become the Industrial Collaboration Policy in 2015 and had been reviewed several times under the leadership of the Ministry of Finance (MOF) (TDA, 2022). All the mentioned policies had explicitly focused on human capability through various HCD programmes for the defence, dual-use and commercial sectors. In the past, OEMs have been incentivised with huge offset credits to support with developing local talents and skills for the various industrial sectors. MOF together with the Defence Industry Division (DID) at the Ministry of Defence continue to focus on utilisation of offset and ICP for human capital development. Malaysia however does not have specific policy framework dedicated to human capital development although there are mentions of the importance of HCD in the Twelfth Malaysia Plan (2012 – 2025) (Ministry of Economy, 2021) and specific tools such as the national training index have been created by the Human Resource Development Fund (HRDF) ( HRM Asia, 2024).

However, the Kingdom of Saudi Arabia is an interesting example of a country that is driving forward the human capital development agenda through offset and defence procurement but more widely through its Vision 2030 Policy (Bilal, 2013; Kingdom of Saudi Arabia, 2023; Gulf Research Center, 2023). The General Authority for Military Industry (GAMI) created the National Military Industry Human Capital Development (NMIHCD), a dedicated department that is currently implementing key human capital development (HCD) strategies and initiatives (Military Industry Human Capital Strategy). The HCD initiatives provide mature services for the military industry sector that are in place to deliver growth and increase the awareness of offset spend through its Industrial Partnership Program (IPP). GAMI's human capital development policy aims to clarify the roles and responsibilities for all stakeholders and articulates how stakeholders interact to deliver qualitative and quantitative growth of Human Capital in the sector, (GAMI Policy and Regulation). The IPP authority within GAMI together with other strategic partners and end-users have taken the initiative to infuse NMIHCD with GAMI in providing clear, mature and tailored opportunities to 'spend' IPP credits based on a win-win-win situation for the Kingdom (Asharq, 2022). For the Kingdom, examples of these services include the Military Industries Scholarship Program, the Military Industries Short Courses Program, and the Academy for Defence Industries (ADI). ADI, the first of its kind in the Kingdom and the region is the dedicated training provider that serves as the leading institute that delivers vocational training, short courses and technical training partnered with original equipment manufacturers (OEMs) locally and overseas (ADI, 2023).

## 2.4 The MINERVA Framework

The MINERVA framework, introduced by the authors in Figure 1, outlines essential components for planning and implementing HCD programmes using offset resources. It identifies critical success factors such as localising HCD programmes, stakeholder engagement, knowledge exchange, effective project management, incentives from offset authorities, and mature relationships among partners. The challenges include difficulties in localising complex technical transfers, managing risks, ensuring governance, and clear roles. The framework is designed to be generalisable for governments and offset management offices, particularly in the defence sector but more generally for national critical infrastructure projects (CNIs). This paper uses the MINERVA model to explore Malaysia's use of offsets to enhance human capability in the defence industry through an international educational partnership between institutions in the UK and Malaysia, investigating the successes and challenges in planning and implementation stages. The framework is designed to be generalisable and can assist governments considering the use of offset or other Government-to-Government (G-to-G) funding for HCD projects. It is applicable to offset management offices (OMOs), and Ministries of Defence and Finance by helping to guide their HCD project planning. Additionally, academics can use this framework to critically examine the factors influencing HCD programmes and identify gaps for further research in this field, particularly in the defence and security sectors.

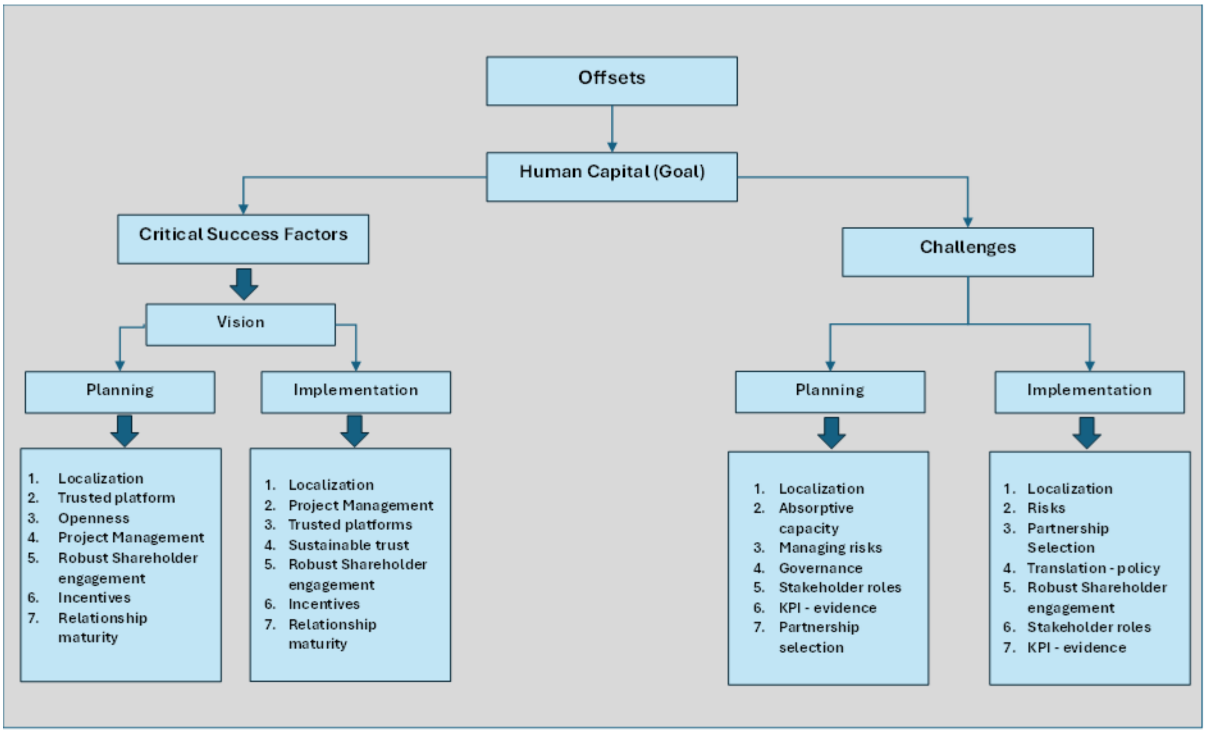


**Figure 1: The Minerva framework.**

Malaysia has explicitly integrated HCD into its ICP, leveraging offset resources to enhance capabilities in the military, defence, security and dual-use sectors. This approach is evident in major procurement contracts, which include HCD projects. Using the MINERVA framework, this paper examines how Malaysia, with a defence budget of 1.5% of its gross domestic product (GDP), has utilised offsets to improve its defence industry's human capability. The research focuses on an international educational partnership formed through an offset agreement between academic institutions in the UK and Malaysia, analysing the successes and challenges during the planning and implementation stages of these educational programmes.

## 3. RESEARCH METHODOLOGY

This exploratory research delves into the practical challenges of using offsets funding for HCD to enhance human capability within the defence industry. The study addresses the research question of how offset funding can effectively build human capacity were measuring the impact of HCD within offset policy framework is difficult due to a lack of specific indicators. Focusing on a Malaysian HCD programme funded through offset, this paper uses the MINERVA model to assess success factors and challenges. The research aims to develop a policy framework for effectively delivering HCD initiatives and building human capability using offset resources (Yin, 2018; Abdullah, 2019). Insights are drawn from the author's direct involvement in shaping offset policies and HCD, as well as their experiences in planning and implementing HCD projects. Theoretical perspectives are based on observations, participation in meetings, and reflections (Glaser & Strauss, 1967). The study employs both deductive and inductive methods (Saunders *et al.*, 2019) through a mixed-method approach, emphasising actionable outcomes for stakeholders. By combining qualitative and quantitative data, the research identifies patterns, theories and relationships, confirming deductive practices from the literature (Creswell & Poth, 2018). The aim is to bridge theory and practice by reviewing the literature on offset, defence industry capability and HCD, alongside practical experiences from policymaking, implementation and stakeholder engagement (Saunders *et al.*, 2019).

Data collection includes primary sources such as company and university project reports, and semi-structured interview questionnaires, as well as secondary sources such as scholarly articles, books, policy documents and government reports (Creswell & Poth, 2018; Abdullah, 2019). The semi-structured questionnaire comprises predetermined questions about the respondents' prioritised factors, identified through both deductive and inductive approaches, and includes open-ended questions for additional insights.

The units of analysis relate to the specific HCD programme for this research. This specific programme has been chosen as the case study considering the authors were directly involved in formalising the educational partnerships besides the planning and implementation of the projects throughout the 12-years period. Furthermore, this advantage enabled the authors to get access to the data and access to participants who were directly involved in the project. The programme consists of an academic partnership between University A in Malaysia and University B in the United Kingdom. The research was focused on three projects worth approximately GBP 4.5 million delivered through this partnership between 2012 and 2024. The respondents were from these three stakeholder groups being the government, industry players and academia. A total of 25 interviewees were identified from a pool of potential stakeholders who were directly involved in the three identified projects being Projects 1, 2 and 3. The participants were individuals operating at strategic and decision-making levels, senior management who had substantive knowledge and experience in offsets policy, as well as academics who were directly involved in the knowledge transfer programme (Lavrakas, 2008). The questionnaire was sent out via email to all the respondents with clear instructions and notes explaining the research background and what was expected of them, along with a request for interview slots with prospective participants. Out of the 25 participants, 18 (75%) responded. Table 2 describes the participants and their roles.

The researchers obtained prior written approval from the participants to record and transcribe interviews for accuracy. An email with a consent note outlining ethical processes and researchers' responsibility to safeguard identities was sent, anonymising respondents' identities to comply with the General Data Protection Regulation (GDPR) and data protection. Participants were assured of confidentiality and transcripts would be destroyed post-publication.

The 18 respondents were successfully interviewed, acknowledging limitations in participant number, especially from government and OEM sectors. Despite potential biases, rich input from participants compensated for the limited responses. The researchers, as practitioners, used a pragmatic inductive participatory observation approach to ensure data reliability.

**Table 1: Roles of interview participants.**

| Stakeholder Segment | Description of Required Role | Code |
|---|---|---|
| Academic | Academic Project Lead for UK University | R1 |
| OEM | Offsets Manager | R2 |
| Government | Principal Assistant Secretary, Offsets Authority, Ministry of Defence | R3 |
| Academic | Academic Project lead from Malaysian University | R4 |
| OEM | Offsets manager, local office Malaysia | R5 |
| Academic | Academic Project lead from Malaysian University | R6 |
| Academic | Tutor | R7 |
| Academic | Academic Project Lead for UK University | R8 |
| Senior management | Senior Programme Director for Malaysian University | R9 |
| Project lead | OEM | R10 |
| Academic | Senior Programme Director for Malaysian University | R11 |
| Senior Management | Deputy Vice-Chancellor Malaysian University | R12 |
| Business Development | OEM | R13 |
| Academic | Tutor UK | R14 |
| Academic | Tutor Malaysia | R15 |
| Academic | Tutor Malaysia | R16 |
| Academic | Tutor UK | R17 |
| Academic | Academic Project lead from Malaysian University | R18 |

Thematic analysis was conducted for methodically examined literature and documents, with thematic coding of keywords such as HCD, challenges and policy suggestions. Content analysis of interview findings identified themes to standardise data for relationship identification (Seidman, 1998; Braun & Clarke, 2006). Excel spreadsheets tabulated ranked factors, providing quantitative measures for success factors and challenges hierarchy.

## 4. Results and Discussion

This section outlines the results from the data collection and discusses the outcome based on the research questions. The section is divided into six sub-sections. Section 4.1 illustrates the relevance of HCD to the Malaysian offset policy while Section 4.2 sets the background to the three individual projects and outcomes. Section 4.3 critically analyses the success factors for enabling the educational projects, while Section 4.4 discusses the challenges faced in planning and delivering the projects using offset resources. Section 4.5 then discusses the relevance of offset for HCD, while Section 4.6 provides recommendations from respondents on how to enhance the policy by incorporating HCD for building human capability for the defence industry sector.

### 4.1 The Malaysian Offsets Policy and the HRD Offsets Programme Background

Malaysia's ICP 2015 emphasises on human capital development within the offset framework, allowing recipients to enhance skills relevant to procurement. The policy includes provisions for industrial training and skills expansion (PMO, 2019). Universities such as the Malaysian National Defence University (NUDM), University Kuala Lumpur (UniKl), Universiti Teknologi Malaysia (UTM) and Universiti Malaysia Terengganu (UMT) have benefited from offset by offering various educational programmes. A government-to-government agreement established a partnership between Malaysian and UK universities, focusing on defence industry excellence and localising programme delivery.

Table 2 lists the academic projects funded through the offset programmes, with further details provided in the next section.

**Table 2: Summary of project outcome and funding.**

| Project | Partnership | OEM | Number of students (total) | Number of students who graduated | Total graduated for each programme | Shadow tutors trained | Total Funding (GBP) |
|---|---|---|---|---|---|---|---|
| MSC in Engineering Business Management (Defence and Security) | Malaysian University (A) and UK University (B) and UK University (C) | OEM (France) | 2012 - 20<br>2013 – 24<br>2014 – 23<br>2015 - 19 | 2012 -18<br>2013 – 21<br>2014 – 21<br>2015 - 18 | 78 | 7 | 1.1 million |
| MSC in Cyber Security and Management | Malaysian University (A) and UK University (B) | OEM (Sweden) | 2016 – 18 (2 terminated)<br>2018 – 6<br>2019 – 18 | 2016 – 15<br>2018 – 5<br>2019 - 15 | 35 | 4 | 1.2 million |
| MSC in International Technology Management for Defence and Security | Malaysian University (A) and UK University (B) | OEM (UK) | 2019 -13<br>2022 – 9<br>2023 - 20 | 2019 – 11<br>2022 – 0<br>2023 - 0 | 11 to date | 10 | 1.2 million |

***Source: University A***

### 4.2 Project Background and Outcome

#### 4.2.1 Project 1: MSc in Engineering Business Management (Defence and Security)

Project 1, a MSc programme in Engineering Business Management (EBM) for Defence and Security, was funded by the offsets from the Scorpene submarine procurement from DCNS France (2000-2008). This four-year, GBP 1.1 million project aimed to integrate business management into engineering and technology for the Malaysian Armed Forces (MAF), Ministry of Defence and defence industry professionals. It included a localisation component for training University A academics in Malaysia and the UK to eventually deliver the programme locally. Led by University B with support from Universities A and C, the content and curriculum were developed through need analysis workshops.

From 2012 to 2015 (Table 4), 85 students were enrolled, and 78 graduated with an MSc in Engineering Business Management for defence and security. Seven University A academics were trained in module delivery, while 15 tutors were trained in MSc project supervision. A workshop in March 2013 familiarised supervisors with Universities B and C's dissertation supervision processes procedures and norms for dissertation supervision.

### 2.2 Project 2: MSc in Cyber Security and Management (Defence and Security)

Project 2 involved a three-year MSc programme in Cyber Security and Management funded by GBP 1.2 million from the offsetf programme associated with the 155 mm gun procurement for the littoral combat ship for the Royal Malaysian Navy (RMN) (SIPRI, 2023). This initiative, part of the 10$^{th}$ Malaysia Plan, aimed to enhance information and communications technology (ICT) capabilities for economic transformation while addressing cyber risks (Economic Planning Unit, Prime Minister's Office, Malaysia, 2010). The Defence White Paper 2020 highlighted cybercrime as a major threat, necessitating the development of a robust industrial base to support the cyberforce (MOD, 2020). The programme, delivered by University B in partnership with University A, capitalised on strong UK-Malaysia cyber-intelligence cooperation (EITN Malaysia, 2016). The curriculum covered network security, computer security, information security, encryption, intrusion detection, penetration testing, access control, digital forensics, risk management, and security governance. Between 2016 and 2019, 36 students enrolled in the programme, and 35 graduated with an MSc in Cyber Security Management. However, only four of the 10 University A academics completed their training under the localisation programme during this period, due to disruptions from the COVID-19 pandemic and budget implications.

### 4.2.3 Project 3: MSc in International Technology Management for Defence and Security

Project 3 involved a MSc in International Technology Management (ITM) for Defence and Security, funded by GBP 1.2 million from the offsets programme for the short-range missile systems (SHORAD) procurement for the Malaysian Army. Launched in 2019, this programme addressed the Ministry of Defence's requirement to integrate emerging technology management into the defence sector, following the 2010 Defence Industrial Blueprint's focus on skills in hard technology and management (MOD, 2010). Universities A and B collaborated to deliver the ITM programme, offering modules in technology management, strategy, systems thinking, international defence acquisition, project management, finance, and leading change. As of 2024, 42 students enrolled, 13 have graduated and 20 are expected to graduate soon. A total of ten academics were trained for future module delivery, with University A receiving intellectual property rights for the course material. However, the project faced delays due to COVID-19, extending from 2019 to 2024.

## 4.3 Critical Success Factors (CSF) That Had Enabled the Success of HCD Programmes at the Planning and Implementation Stages

### 4.3.1 Planning and Implementation

The quantitative survey results were analysed using ranking to determine the critical success factors (CSFs) (Figure 2). The results reveal that localisation (1) was the most crucial consideration during the planning stage. This was followed by establishing a trusted platform (2), openness in knowledge exchange (3), effective project management (4), robust stakeholder engagement (5), relationship maturity (6), pragmatic policy (7), and sustainable trust (8).

Figure 3 identifies localisation (1) as the most critical factor during the implementation stage, followed by effective project management (2), sustainable trust (3), a trusted platform (4), openness in knowledge exchange (5), pragmatic policy (6), stakeholder engagement (7), and relationship maturity (8).

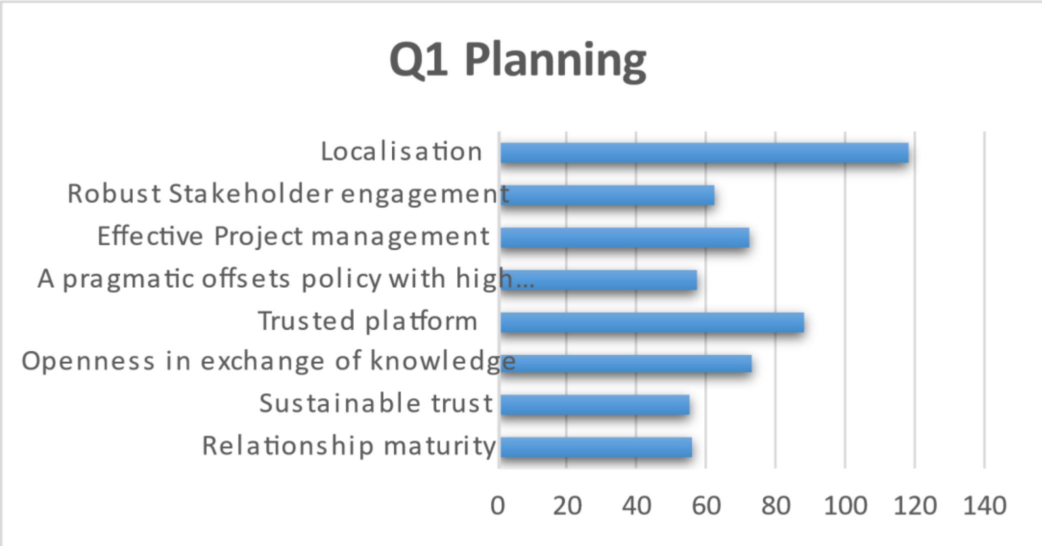


**Figure 2: CSF for planning of HCD programmes using offset resources.**

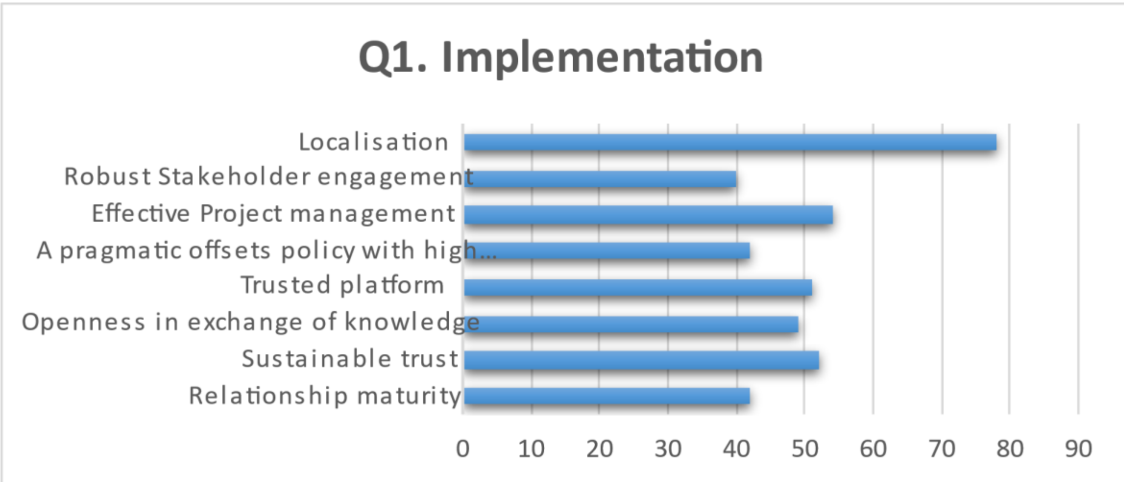


**Figure 3: CSF for implementation of HCD programmes using offset resources.**

### 4.3.2 Analysis of Factors Critical for Using Offset Resources for HCD Programmes

During the interviews, several other factors for success emerged as illustrated in Table 3. The synthesis approach through merging of quantitative and qualitative data identified several key themes and conclusions for prioritising critical factors at both the planning and delivery stages of offset projects. The analysis highlighted several essential points. Firstly, critical factors differed between the planning and implementation stages. During planning, localisation, trusted platforms for engagement and knowledge exchange were prioritised, followed by effective project management. In the implementation phase, localisation remained crucial, followed by effective project management, sustainable trust and trusted platforms. Sustainable trust was deemed least important at the planning stage, while relationship maturity was least important during implementation. Localisation emerged as the most critical factor for success in utilising offset resources for capability building (R1, R2, R9, R12, R14 and R16). Trust also scored highly at both stages, reflecting the necessity of mutual trust among stakeholders for effective knowledge exchange. Project management was critical for systematic project planning, implementation and monitoring.

**Table 3: Qualitative results from the interview.**

| CSF | Explanation | Respondents |
|---|---|---|
| Vision | Vision as a driving force for carrying through the programme difficulties. | R2, R5, R9 and R16 |
| Team | Ensuring that the right people are on the team, in the right roles, with the right skills. | R2 |
| Skill sets | Different skills required to plan from those delivering | R2 |
| Project management | Consistency across the programme schedule | R2, R4 and R9 |
| Partner selection | Importance of selecting competent, capable and ambitious partners | R2 |
| Product and services | Availability of good product and services | R2 |
| Localisation | • Local tutors using material to feed into their own modules<br>• Secondment and shadow tutoring<br>• Placement at partner institutions | R1, R2, R9, R12, R14 and R16 |
| Relationship maturity | • Strong engagement with the student's post-graduation for continuous education<br>• Good understanding between the partners and other stakeholders | R1,R5, R10, R11, R15 and R17 |
| Inter-cultural understanding | • Knowledge and understanding in both of different culture and environment. | R11 |

Secondly, policy content and incentives were not seen as critical for success at either the planning (ranked 7$^{th}$) or implementation (ranked 6$^{th}$) stages. However, qualitative data suggested that pragmatic policies and higher multipliers could attract better HCD projects. Thirdly, quantitative data indicated that relationship maturity was less prioritised as compared to other factors at the planning (6$^{th}$) and implementation (8$^{th}$) stages. This contrasted with qualitative findings that emphasised robust partnerships as crucial for success (R1, R5, R10, R11, R15 and R17). Fourthly, qualitative analysis revealed additional themes critical for success, including setting clear project visions (R2, R5, R9 and R16), selecting skilled partners, fostering teamwork, ensuring product and process quality, as well as promoting intercultural communication. Overall, there was a strong emphasis on localising projects, with the Ministry of Defence keen on transferring know-how to local institutions. Building trust and long-term relationships with academic and foreign partners was also crucial. Despite a more distant relationship with the armed forces, continuous engagement was emphasised to secure their buy-in and programme input.

## 4.4 Challenges in the Planning and Implementation of the HCD Programme

### 4.4.1 Planning and Implementation

During the programme planning stage, several challenges were identified. As illustrated in Figure 4, localisation was the most challenging aspect (ranked 1$^{st}$), followed by absorptive capacity (2$^{nd}$), risk management (3$^{rd)}$, evidence of key performance indicators (KPIs) (4$^{th}$), governance (5$^{th}$), stakeholder roles (6$^{th}$), partnership selection (7$^{th}$), and translation of the policy (8$^{th}$).

At the implementation stage, as illustrated in Figure 5, localisation remained the most challenging aspect (ranked 1st). This was followed by risk management (2nd), partnership selection (3rd), stakeholder engagement (4th), translation of policy (5th), absorptive capacity (6th), KPI outcomes (7th), and governance (8th).


**Figure 4: Challenges faced at the planning stages of the offset programme.**

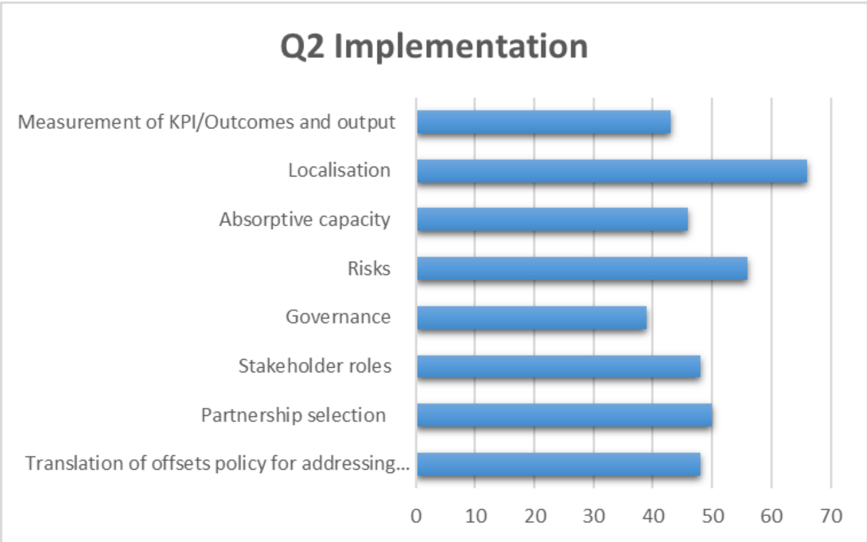


**Figure 5: Challenges faced at the implementation stages of the offset programme.**

### 4.4.2 Analysis of the Challenges in Delivering HCD Programmes

During the interviews, several other challenges emerged as illustrated in Table 4. The analysis of challenges in delivering critical priorities at the planning and delivery stages of offset projects highlighted several key themes and conclusions. First, challenges differed between the planning and implementation stages. At the planning stage, localisation, absorptive capacity and risk management were key. On the other hand, implementation focused on localisation, risk management and partnership selection.

Table 4: **Other challenges in implementation.**

| Challenges | Explanation | Respondent |
|---|---|---|
| Curriculum and module changes | Changing focus of module content and curriculum needed to be aligned to the changing landscape | R7 |
| Contracting and funding mechanism | • Clear identification of the partners commercial responsibilities and liabilities are essential along with transparent and performance-based funding mechanisms in place at the outset.<br>• Lack of understanding to finances in delivery of the programme and constraints involved such as project implementation costs, | R2 |
| Stakeholder alignment | Alignment of competing requirements of Government, Industry and Academic stakeholders needs to be carefully managed. | R3 |
| Data sharing | Sharing all the necessary information to allow good decision making - schedule of student availability and all the costs associated with delivering a programme. | R2 |
| Planning and implementation gap | People at the planning and implementation stage had different skills and lacked a seamless transition | R2 |
| Offsets mechanism for approval and implementation of HCD at MOD | • The lack of an official and efficient mechanism for approving and implementing educational projects within offset agreements.<br>• Bureaucratic hurdles, unclear processes, and inadequate coordination between relevant stakeholders, which made it challenging to align stakeholders' interests and ensure seamless collaboration throughout the project lifecycle. | R3 |
| Size of the offset programme | Experience in using earned value management on a small project is costly not more than 100,000 not useful since the amount of data for perception is too small (the result will not be reliable). | R10 |

The scores indicate that localisation was the primary challenge. Concerns stemmed from OEMs' lack of commitment to content development, which is crucial for programme success due to their industrial expertise. In some cases, OEMs were minimally involved or reluctant, leading to disagreements between academic staff and company officials. Some tutors lacked sector-specific understanding, which impacted module quality, while others lacked industry experience, essential for real-world relevance, hindering trust between parties. Local institutions' commitment to localisation posed significant challenges, including deficiencies in plans, unclear KPIs, implementation gaps, difficulties in identifying tutors, and stakeholder buy-in issues. Local tutors lacked incentives and awareness of project objectives, viewing the assignment as an additional burden.

Partnership selection posed fewer challenges at the planning stage, but it became significantly more difficult during implementation. The ICP policy facilitated government-to-government partnerships, bypassing competitive bidding for university selection. University A was chosen for its specialisation in defence and security education, despite being relatively new, aiming to enhance its future programme offerings. University B, selected for its expertise in industry-oriented education, lacked strength in defence and security. Initially, the partnership thrived with strong engagement and leadership buy-in for five years, involving active participation from both institutions' academic and faculty members. In several projects, a notable lack of trust existed among stakeholders at the operational level. Both the

Ministry of Defence and overseas defence contractors, acting as offset sponsors, often remained passive and showed minimal interest in monitoring project progress. The contracts lacked clarity regarding the responsibilities of each delivery partner, resulting in convoluted decision-making processes and mutual blame for project setbacks.

A major governance issue within the programme and its partnerships was the inconsistency in contracts regarding the structure and roles of two-level committees. Sometimes, the OEM co-chaired committees, while at other times, either the overseas or local university partner chaired them. This inconsistency caused confusion and lack of clear responsibilities. Appointing an independent chair with relevant expertise could have ensured more consistent decision-making. Mid-project, the local partner's educational regulatory body revised its rules, demanding additional documentation from the overseas university regarding standards. Absorptive capacity posed a significant challenge during planning and remained low during implementation. The transfer of knowledge to students was hindered by issues with student selection and tutor choice. Deviations from student intake criteria impacted some students' ability to grasp module content and affected their performance. Furthermore, varying levels of English proficiency also influenced project quality.

The teaching and learning context were major issues, with many key project individuals lacking experience. The lead at University A, responsible for project planning, initially lacked sufficient expertise in defence and security content. This led to difficulties with student selection criteria, marketing and programme communication, as well as a lack of clear objectives and defined performance measurements such as key performance indicators. Insufficient emphasis on metrics and evaluation methods during programme design made it difficult to later capture project performance data. The ICP incorporated HCD but lacked clear implementation guidelines. Projects were chosen ad-hoc instead of using an evidence-based skills matrix. Guidance from the Ministry of Defence and local partners on skill gaps was lacking, with minimal industry engagement to develop a skills matrix. The programme's long-term vision was undefined, starting as a pilot and evolving without a clear direction. The strategic planning involved only a few senior officials, leaving others uninformed and fostering scepticism among stakeholders. Qualitative analysis revealed challenges, including the programme's failure to adapt content to technological advancements and issues with contract establishment, funding execution, as well as management between partners. Inadequate mechanisms for sharing data on materials, funding and processes were identified. In conclusion, delivering HCD projects through offsets faced challenges in localisation, risk management, absorptive capacity and governance. Addressing these issues requires clearer guidelines, better strategic planning and improved stakeholder engagement.

### 4.5 Views on Using Offset Resources for Building Human Capability

As indicated in Table 5, most respondents emphasised on the significance of using offset resources for industry-focused education and training projects that aim to solve real-world problems and enhance industry capabilities. Additionally, the respondents emphasised the need to maintain a balance between offering short-term skills courses through workshops and seminars, and providing long-term educational programmes that foster sustainable capabilities. The feedback also highlighted the greater value of intangible outcomes such as the transfer of know-how and knowledge through HCD projects, given their long-term impact on building sustainable human capabilities.

### 4.6 Suggestions on Enhancing Human Capability Through Offsets

The qualitative survey in Table 7 provides recommendations for enhancing human capability through offsets. Firstly, it stresses the need for defining success and establishing key performance indicators (KPIs). Secondly, it suggests implementing clear offset management processes guided by the Offset Management Office (OMO) at the planning and implementation stages. Evaluating foreign contractors' capabilities in delivering HCD projects and selecting partners with relevant skills and experience in defence are crucial. Intangible values such as sustainability, trust and relationships should also be included in KPIs. Recommendations extend to using offset funding for short courses covering technical areas and defence business topics, alongside transferable skills development.

**Table 5: Summary of respondents' main viewpoints.**

| Viewpoints on offsets usage | Explanation | Respondent |
|---|---|---|
| Cross cultural exposure | Offset to be used for cross-cultural experiences and exposure to emerging technologies and industry of buyer countries | R1 and R4 |
| Education versus training | Offset creating a balance on prioritisation between meeting short-term skills focus with long-term education and capability building focus | R6, R9 and R12 |
| Industry focussed | Offset to focus on industry combined education programme for capability R&D and secondment.<br>Investment into scholarship and TVET programme, workshops and STEM related projects | R3, R4, R2, R10 and R13 |
| Risks plan and mitigation | Ensuring Offset planning considers a risk plan and mitigation | R2 and R3 |
| Stakeholder engagement and leadership | Strong Leadership in managing stakeholders and buy-in | R3, R10 and R11 |
| Sustainable knowledge management | Using academic and research institutions to deliver HCD projects rather than implementation through indexical companies which is short-term and lacks continuity | R5 |
| Vision | Vision in what is to be achieved | R2 and R9 |
| Incentives | Higher multiplier as incentives for transfer of soft knowledge – education and training/skills | R2, R4, R5 and R9 |
| Capability gap | Identifying capability gaps and delivering in those areas | R6, R8 and R18 |

**Table 6: Summary of respondents' suggestions for human capability using offsets funding.**

| Suggestions | Explanation | Respondent |
|---|---|---|
| Review KPI and Success | Offset policy need to define success and determination of KPI | R1 |
| Offset management | Clear planning, process and implementation of how offset is used for HCD | R2, R10 and R17 |
| Foreign contractor capability and track record | OEM with a good track record of HCD delivery and capability of execution<br>Export focus on promoting HSC to support supply chain and life cycle management | R2 and R5 |
| Short courses and training certification | Offset to be used to plan and deliver short courses | R4, R7 and R12 |
| Centre of Excellence (COE) | Offset to be used as catalyst for the formation of COEs, research centres, MRO centres, Centre of Innovation and Data management centre | R4, R7, R9, R12 and R18 |
| Values | Offset and procurement decision making to consider sustainability, trust, and relationship for 'out of the box' thinking. | R9 and R13 |
| Transferable skills | Offset is also to be used for developing transferable skills such as coaching, mentoring, community teambuilding and training | R14 and R15 |
| Partner selection | Selection of partners with appropriate skills, knowledge, and experience in the defence sector | R2, R9, R10 and R16 |

## 5. CONCLUSION

In conclusion, this paper examined how offsets and IC enhance human capability in Malaysia's defence and security sector using the MINERVA framework. It identified critical success factors such as clear planning, robust stakeholder engagement and localisation to facilitate knowledge transfer essential for defence industries. The study suggested that with targeted policy adjustments and clear, measurable objectives, offset can significantly contribute to building a resilient defence workforce, aligning with national educational and industrial goals to enhance defence spending efficacy.

The authors, leveraging their extensive experience in offsets and HCD for the industrial sector, presented key recommendations. They emphasised that building HCD should not solely be the responsibility of the government but should involve a collaborative public-private partnership. Efforts to enhance capabilities in the defence industry and related sectors should extend beyond offset funding and should not be viewed as one-off activities. Success in this area requires a holistic and robust HCD strategy, supported by careful planning and execution. Moreover, it is crucial to identify skill gaps and develop specific guidance and tools to establish human capability effectively. Nations should explore various funding sources and policy mechanisms through broader public sector regulators and in collaboration with the private sector to ensure continuous HCD programmes that foster sustainable human capability building. The key is to align the HCD offset objectives of the key stakeholders the buyer government with the OEMs' long-term strategic objectives.

Regarding offsets, it is insufficient to merely offer higher incentives for HCD programmes. There is a need for clarity, detailed planning and an implementation roadmap that funders should be able to readily access. The current offset models are often ad-hoc or reactive, leading to ineffective and short-term outputs. Instead, a proactive offsets policy with a clearly defined strategic intent will deliver long-term HCD strategies and significant impacts. For this, the offset policy should also align with the national HCD plan. Emerging evidence highlights the positive impact of offset spending in the Kingdom of Saudi Arabia through the advanced implementation of a mature HCD model. As a result, opportunities to earn offset credits through training and education are identified at the earliest stages of procurement. These opportunities are then incorporated into proposals and contracts, leading to tailored support that delivers optimal human capital outcomes for companies. This integration ensures that human capital considerations are embedded into contracts from the outset. It fosters the transfer of knowledge and skills, while also promoting the localisation of education and training. This approach incentivises specific behaviours and addresses human capital barriers to investment. By adopting this proactive HCD model alongside the offset or IPP model, the Kingdom is positioning itself as an attractive investment destination.

However, the research has limitations. The concept of capability, especially human capability for sustainability, requires further exploration in the defence and security context. The model itself needs testing with different empirical data sets, as it was developed primarily using Malaysia, a middle-income country with modest defence spending. Access to stakeholders was limited, affecting the sample population. Detailed empirical analyses from a larger dataset would validate the MINERVA framework. Cross-case analysis comparing different projects is also needed but accessing sensitive data across diverse defence sectors poses challenges. Nonetheless, as the first study on using offsets for HCD, specific country case studies can refine the model for broader applicability. Further research and policy refinement are essential to ensure offset support sustainable HCD, enhancing national security in a complex global environment (Eisenhardt, 1989; Yin, 2018).

## REFERENCES


ADI (Academy of Defence Industries). (2023). *Our Programs*. Available online at: https://adi.edu.sa/en/our-programs (25 June 2024).

Anicetti, J. (2024). *Defence Offset and Global Arms Trade: Explaining Cross-National Variation*. Routledge, Abingdon 2024

Antinozzi, I. (2023). *Written Evidence: Implications of Russia's Invasion of Ukraine for UK-EU Relations*. Royal United Services Institute (RUSI), London, UK

Asharq, A.A. (2022). *GAMI Establishes Human Capital Roadmap in Saudi Military Industries*. Available online at: https://english.aawsat.com/home/article/3460661/gami-establishes-human-capital-roadmap-saudi-military-industries (Last access date: 25 June 2024).

Argote, L. & Miron-Spektor, E. (2011). Organizational learning: From experience to knowledge. *Organ. Sci.*, **22**: 1123-1137.

Argote, L., McEvily, B. & Reagans, R. (2003). Managing knowledge in organizations: An integrative framework and review of emerging themes. *Manage. Sci.*, **49**: 571-582.

Australian Government. (2001). *DCP Defence Capability Plan 2001-2010*. Available online at: http://repository.jeffmalone.org/files/defence/dcp01.pdf (Last access date: 12 July 2024)

Australian Government. (2020). *Centre for Defence Industry Capability Review*. Available online at: https://www.defence.gov.au/about/reviews-inquiries/centre-defence-industry-capability-review (Last access date: 12 July 2024)

Australian Government. (2016). *Australian Industry Capability Program*. https://www.defence.gov.au/business-industry/industry-capability-programs/australian-industry-capability-program (Last access date: 12 July 2024)

Balakrishnan, K. (2023). Generating value through offsets in International Defence Procurement. *In* Cleary, L & Darby, R (Ed)., Managing Security: Concepts and Challenges. Routledge, Abingdon, UK.

Balakrishnan, K. (2018). Technology offsets in international defence procurement. Routledge. Abingdon, UK

Balakrishnan, K. & Lazar, Z. (2022). The challenges in buyer-supplier relationship for technological absorption capability in international defence acquisition: The case of Southeast Asia. *Defense Secur. Anal.*, **38**: 317-335.

Balakrishnan, K. & Matthews, R. (2009). The role of offsets in Malaysian Defence Industrialisation. *Defence Peace Econ.*, **20**: 341-358.

Balakrishnan, K. (2007). Evaluating the effectiveness of offsets as a Mechanism for promoting Malaysian Defence Industrial and technological development, PhD thesis, *Cranfield University,UK*

Bilal, S. Y. (2013). *The Gulf Rising: Defense Industrialization in Saudi Arabia and the UAE*. Atlantic Council, Washington, DC, US.

Bitzinger, R., & Kur, C. (2019). Defense industries in the 21st century: A comparative analysis. Comparat. Strategy, **37**: 255-259.

Brauer, J. & Dunne, P. (2004). *Arms Trade and Economic Development*. Routledge, Abingdon, UK.

Brauer, J. & Dunne, P. (2010). *Arming the South: The Economics of Military Expenditure, Arms Production and Arms Trade in Developing Countries*. Macmillan Publisher, London, UK.

Cohen, W. M., & Levinthal, D. A. (1990). Absorptive capacity: A new perspective on learning and innovation. *Admin. Sci. Quart.*, **35**: 128-152.

Creswell, J.W. & Poth, C.N. (2018). *Qualitative Inquiry and Research Design: Choosing Among Five Approaches*. Sage Publications, Los Angelas, US.

Dehoff, K., Dowdy, J. & Kwon, O.S. (2014). *Defense Offsets: From Contractual Burden to Competitive Weapon. McKinsey and Company* Available online at: https://www.mckinsey.com/industries/public-sector/our-insights/defense-offsets-from-contractual-burden-to-competitive-weapon (Last access date: 13 July 2024)

Dutton, J. (2023). *Saudi Arabia Agrees to Produce Turkey's Baykar Drones*. Available online at: https://www.al-monitor.com/originals/2023/08/saudi-arabia-agrees-produce-turkeys-baykar-drones (Last access: 13 July 2024)

Eisenhardt, K.M. (1989). Building theories from case study research. The Academy of Management Review, **14**: 532-550.

EITN Malaysia. (2016). Malaysian UK Trade Mission strengthens ties between the two nations' technology sectors. Available online at: https://www.enterpriseitnews.com.my/malaysian-uk-trade-mission-strengthens-ties-between-the-two-nations-technology-sectors (Last access: 13 July 2024)

Galai, K., Retter, L., Muravska, J., Kepe, M., Lynch, A., Knack, A., Bellasio, J., Ward, A., Meranto, A.S., & Maistro, D. (2023). *Understanding Skills Gaps in the European Defence Sector*. RAND Europe, Cambridge, UK .

GAMI (General Authorities for Military Industries) (2023). *Military Industry Human Capital Strategy*. Available online at: https://www.gami.gov.sa/en/human-capital-strategy. (Last access date: 14 July 2024).

GAMI (General Authorities for Military Industry (GAMI)(2024). *Policies and Regulation*. Available online at: https://www.gami.gov.sa/en/policies-and-regulations. (Last access: 12 July 2024).

Glaser, B., & Strauss, A. (1967). *The Discovery of Grounded Theory: Strategies for Qualitative Research*. Sociology Press, California, US.

Goodman, C. (2024). *Blissfully Blind: The New US Push for Defense Industrial Collaboration With Partner Countries and Its Corruption Risks*. Transparency International US, Washington DC, US.

Government of Abu Dhabi (2023). *Abu Dhabi Economic Vision 2030*. Available online at: https://u.ae/en/about-the-uae/strategies-initiatives-and-awards/strategies-plans-and-visions/finance-and-economy/abu-dhabi-economic-vision-2030 (Last access: 13 July 2024)

Government of Canada (2022). *Industrial and Technological Benefits Policy: Value Proposition Guide*. Available online at: https://ised-isde.canada.ca/site/industrial-technological-benefits/sites/default/files/attachments/2022/ISED_VPGuide_eng.pdf (Last access: 13 July 2024)

Gulf Research Center. (2023). *The Military and Defense Industries Sector in the Kingdom of Saudi Arabia: Opportunities and Challenges*. Available online at: https://www.grc.net/publication/556 (Last access: 13 July 2024)

Hartley, K. & Martin, S. (1995). Defense equipment, exports and offsets: The UK experience. *Defense Anal.*, **11**: 21-30.

HRM Asia. (2024). Elevating human capital development in Malaysia, Available online at: https://hrmasia.com/elevating-human-capital-development-in-malaysia/ (( Last access: 9 August 2024)

Huffman, J.L. (2010). *Modern Japan*. Oxford University Press, Oxford, UK.

Kingdom of Saudi Arabia. (2023). *Vision 2030*. Available online at: https://www.vision2030.gov.sa/en/ (Last access: 13 July 2024)

Lowy Institute. (2023). *Network Power: Asia Power Index 2023 Edition*. Available online at: https://power.lowyinstitute.org/network-power (Last access date: 16 July 2024).

Lucas, R.O. (1988). On the Mechanics of Economic Development. *J. Monetary Econ.*, **22**: 3-42

Malm, A., Fredriksson, A. & Johansen, K. (2016). Bridging capability gaps in technology transfers within related offsets. *J. Manuf. Tech. Manage.*, **27**: 640-661.

Maniar, K. (2018). *Understanding India's Offset Policy*. Available online at: https://elplaw.in/wp-content/uploads/2018/09/ELP-Trade-Security-Journal.pdf (Last access: 12 July 2024)

Martin, S. (1996). *The Economics of Offsets: Defence Procurement and Countertrade*. Routledge, Abingdon, UK.

Matthews, R. & Maharani, C. (2023). The role of offset in the enduring gestation of Indonesia's strategic industries. *Defence Peace Econ.*, **34**: 1-22.

Matthews, R. & Anicetti, J. (2022). Offset in a post-Brexit world. *RUSI J.*, **166**: 50-62.

Ministry of Defence UK (2022), Defence Capability Framework, United Kingdom,

MOD (Ministry of Defence) (2010). *Defence Industry Blueprint*. Ministry of Defence, Malaysia.

MOD (Ministry of Defence) (2020). *Defence White Paper*. Ministry of Defence, Malaysia.

Ministry of Economy, (2006-2010). *Ninth Malaysia Plan*, Malaysia

Ministry of Economy ( 2021-2025) *Twelfth Malaysia Plan,* Malaysia

Nam, S.H. & Joon, S.P. (2004). The defense offset policy in South Korea. *KIDA Papers*, **4**: 1-15.

OECD. (n.d.). *Productivity, Human Capital and Educational Policies*. OECD.org. Available online at: https://www.oecd.org/economy/human-capital (Last access: 14 July 2024).

Ogunade, A. O. (2011). *Human Capital Investment in the Developing World: An Analysis of Praxis*. Seminar Research Paper Series. Paper 38, University of Rhode Island, Rhode Island, US.

Oppat, K. (2008). *Disseminative Capabilities A Case Study of Collaborative Product Development in the Automotive Industry*. Springer, Wiesbaden, Germany.

PMO (Prime Minister's Office) (2019). *Malaysia's National Defence Policy*. Available online at: https://www.pmo.gov.my/wp-content/uploads/2019/07/National-Defence-Policy.pdf. (Last access: 14 July 2024)

Romer, P. M. (1986). Increasing returns and long run growth. *J. Polit. Econ.,* **94**: 1002-1037.

Saunders, M. N., Lewis, P. & Thornhill, A. (2019). *Research Methods for Business Students*. Pearson, London, UK.

Savoy, C. M., & Staguhn, J. (2022). *Global Development in an Era of Great Power Competition*. Center for Strategic and International Studies, Washington DC, US. (Last access: 12 July 2024).

Sen, A. (1999). *Development as Freedom*. Alfred A. Knopf, New York City, US.

SIPRI (Stockholm International Peace Research Institute) (2022). *Trends in World Military Expenditure, 2022*. Stockholm International Peace Research Institute (SIPRI), Stockholm, Sweden.

SIPRI (Stockholm International Peace Research Institute) (2023). *SIPRI Arms Transfer Database*. Stockholm International Peace Research Institute (SIPRI), Stockholm, Sweden.

Situmeang, F., Suyudi, I. & Susilo, A. K. (2020). Defense offset strategy for development of the national defense industry in Indonesia. *J. Defense Resour. Manage.*, **11**: 108-123.

TDA (Technology Depository Agency) (2022). *Policy and Guidelines on Industrial Collaboration Programme (ICP) in Government Procurement*. Technology Depository Agency, Malaysia.

Teece, D. J., Pisano, G. & Shuen, A. (1997). Dynamic capabilities and strategic management. *Strateg. Manage. J.*, **18**: 509-533.

Trigger, B.G. (2003). *Understanding Early Civilizations: A Comparative Study*. Cambridge University Press, Cambridge, UK.

US Department of Defense (2023). *AUKUS: The Trilateral Security Partnership Between Australia, U.K. and U.S.* Available online at: https://www.defense.gov/Spotlights/AUKUS (Last access: 12 July 2024).

UK Parliament (2023). *UK Defence Policy and the Role of the Armed Forces*. Available online at: https://lordslibrary.parliament.uk/uk-defence-policy-and-the-role-of-the-armed-forces (Last access 15 July 2024).

UNESCO (United Nations Educational, Scientific and Cultural Organisation) (2023). *Education Sustainable Development*. Available online at: https://www.unesco.org/en/education-sustainable-development (Last access: 12 July 2024)

UN (United Nations) (2023). *Sustainable Development Goals*. https://www.un.org/sustainabledevelopment (Last access: 15 July 2024)

Vincent, L. (2008). Differentiating competence, capability and capacity. *Innov. Perspective*, **16**: 3.

Winter, S.G. (2000). The satisficing principle in capability learning. *Strateg. Manage. J.*, **XXI**: 981-996. Available online at: https://www.jstor.org/stable/3094423.

World Bank (2020). *COVID-19 Will Hit the Poor Hardest: Here's What We Can Do About It.* Available online at: https://blogs.worldbank.org/voices/covid-19-will-hit-poor-hardest-heres-what-we-can-do-about-it. (Last access date: 14 July 2024).

Yin, R.K. (2018). *Case Study Research*. Sage Publications, Washington DC, US.

Zawya (2022). *Saudi's GAMI Announces Establishing National Academy of Military Industries*. Available online at: https://www.zawya.com/en/economy/gcc/saudis-gami-announces-establishing-national-academy-of-military-industries-xi5x0qph (Last access: 14 July 2024)

Zeiler, T.W. (1998). Managing protectionism: American trade policy in the early cold war. *Diplomatic His.*, **22**: 337-360.